RheinlandPfalz
ZENTRALSTELLE DER FORSTVERWALTUNG

ANALYSIS OF FOREST-SPECIFIC ECOSYSTEM SERVICES WITH REGARD TO WATER BALANCE COMPONENTS: RUNOFF AND GROUNDWATER RECHARGE IN THE FOREST

Mitteilungen aus der Forschungsanstalt für Waldökologie und Forstwirtschaft Nr. 90/23

Landesforsten Rheinland-Pfalz

IMPRESSUM

Herausgeber:
Zentralstelle der Forstverwaltung
Forschungsanstalt für Waldökologie und Forstwirtschaft Rheinland-Pfalz (FAWF)
Hauptstr. 16
D-67705 Trippstadt
Telefon: +49-6131-884-268-0, Telefax: +49-6131-884-268-300
zdf.fawf@wald-rlp.de
www.fawf.wald.rlp.de

Verantwortlich:
Der Leiter der Forschungsanstalt für Waldökologie und Forstwirtschaft Rheinland-Pfalz

Dokumentation:
Mitteilung FAWF, Trippstadt
Nr. 90/23, 205 Seiten

Gestaltung, Grafik und Satz:
Christine Romero, FAWF Rheinland-Pfalz

ISSN 1610-7705 Mitteilungen aus der
Forschungsanstalt für Waldökologie und Forstwirtschaft Rheinland-Pfalz, Nr. 90/23

nur als Download
http://fawf.wald.rlp.de/index.php?id=2601

Titelbild:
Natural retention area in the Palatinate Forest, Stütenhof 2016 (Foto: Prof. Dr. G. Schüler)

EVA VERENA MÜLLER

Department VI Spatial and Environmental Science
at the University of Trier
to obtain the academic degree
Doctor of Science (Dr. rer. nat.)
approved dissertation

ANALYSIS OF FOREST-SPECIFIC ECOSYSTEM SERVICES WITH REGARD TO WATER BALANCE COMPONENTS: RUNOFF AND GROUNDWATER RECHARGE IN THE FOREST

Referee
Prof. Dr. Gebhard Schüler (University of Trier)

Co-referees
Prof. Dr. Tobias Schütz (University of Trier)
Prof. Dr. Nicola Fohrer (University of Kiel)

Date of examination: May, 18th 2022

Trier, May 2022

Landesforsten Rheinland-Pfalz
Zentralstelle der Forstverwaltung
Forschungsanstalt für Waldökologie und Forstwirtschaft
Trippstadt 2023

The most sustainable and best quality fresh water sources in the world originate in forest ecosystems

(Neary et al. 2008)

ACKNOWLEDGEMENT

I have to thank all members of the Institute for forest ecology and forestry (FAWF) in Trippstadt, who were involved in the Ecoserv project, as well as the employees of the Landesforsten, State Office for Geology and Mining, the State Office for Water Management, and the State Office for the Environment of Rhineland-Palatinate, who supported the project with data and council.

Special thanks go to Hans-Peter Ehrhart for giving me the chance to work on the Ecoserv project, Dr. Martin Greve, who was never at a loss for a crucial clue, and Dr. Tilmann Sauer who always had an open ear and good advice.

I have to express my gratitude to the Department of Hydrology of the University Kiel (CAU), especially to Dr. Tibebe Tigabu, who has a large share on this work, and who always supported me the most committed way, but also to Dr. Paul Wagner, and Prof. Dr. Nicola Fohrer for offering me their council, infrastructure and expertise.

The indicator, and supporter in any moment, from animated discussions to struggles and through crisis, is, however, Prof. Dr. Gebhard Schüler. He always offered me his expertise, his enthusiasm for the subject, and, what might be the most important thing, his confidence in me.

Through all this work, one person like no other did not get tired of supporting, and believing in me: My husband Uwe Muschinski. This work couldn´t have happened if it wasn´t for him, so it is clearly dedicated to him and our shared love for the forest.

Mein Dank gilt den Mitarbeitern der Forschungsanstalt für Waldökologie und Forstwirtschaft (FAWF) in Trippstadt, die am Ecoserv-Projekt beteiligt waren, wie auch den Mitarbeitern der Landesforsten, des Landesamts für Geologie und Bergbau (LGB), des Landesamts für Wasserwirtschaft (LfW), sowie des Landesamts für Umwelt (LfU) in Rheinland-Pfalz, die mich in meiner Arbeit unterstützt haben.

Besonderer Dank gilt Herrn Hans-Peter Ehrhart für die Chance, am Ecoserv-Projekt beteiligt sein zu dürfen, Dr. Martin Greve, der nie um einen entscheidenden Hinweis verlegen war, und Dr. Tilmann Sauer, der immer mit offenem Ohr und gutem Rat zur Seite stand.

Großer Dank gebührt der Abteilung für Hydrologie der Universität zu Kiel (CAU), besonders Dr. Tibebe Tigabu, der einen großen Teil an dieser Arbeit trägt und mich zu jeder Zeit engagiert unterstützt hat, sowie Dr. Paul Wagner und Prof. Dr. Nicola Fohrer für ihren fachlichen Rat, die Infrastruktur und Expertise.

Initiator dieser Arbeit und Unterstützer in jeder Lage, von angeregten Diskussionen, durch Zweifel und Krisen, war Prof. Dr. Gebhard Schüler, der mir stets mit seiner Expertise und seinem Enthusiasmus für die Materie zur Seite stand und sein Vertrauen in mich setze.

Während der ganzen Zeit unterstütze mich eine Person wie keine andere: Mein Mann Uwe Muschinski. Diese Arbeit hätte ohne ihn nicht stattfinden können, daher ist sie ihm und unserer gemeinsamen Leidenschaft für den Wald gewidmet.

ABSTRACT

Water-related regulative and provisioning ecosystem services (ES) were examined, aiming at runoff regime and groundwater recharge in the Palatinate Forest Biosphere Reserve in south-western Germany with hydrological modelling using the Soil and Water Assessment Tool (SWAT+). A holistic approach was included with indicators of functional and structural ecological processes assigned to intermediate components of ES. As potential risk factors for the degradation of water-related ES in the forest, soil compaction due to driving with heavy machinery in the course of harvest operations, disrupted areas with rejuvenation, as a result of either silvicultural management practices, or due to windthrow, pests and calamities in the course of climate change, as well as climate change itself as a major stressor for forest ecosystems were analyzed with regard to their impact on hydrological processes. For each of those influencing factors, separate SWAT+ model scenarios were created, and compared to the calibrated baseline model, which represented the current watershed conditions based on field data.

The simulations confirmed the favorable site conditions of the Palatinate Forest for groundwater formation. Related to the high infiltration capacity of the Red Sandstone soil substrates in the catchment area, as well as to the retarding and buffering influence of forest canopy cover on precipitation water, the Palatinate Forest was simulated to exhibit a significant mitigation effect on runoff generation, and a pronounced retention potential concerning spatial and temporal water distribution in the catchment. Nevertheless, elevated amounts of precipitation, exceeding the infiltration capacity of the sandy soils, were found to result in a short circuit drain reaction with pronounced surface runoff peaks. The simulations depicted the sensitive character of forest-water-cycle-interactions, as well as the hydrological impact of age-patterns related to differences in canopy expression, climate change, and deteriorated soil functions.

Future climate projections, simulated using BIAS-adjusted REKLIES and EURO-CORDEX regional climate models (RCM), forecasted a higher evaporative demand, an extension of the vegetation period, and at the same time drought periods to occur more frequently, which was found to shorten the period of groundwater replenishment, resulting in a projected decline in the provisioning ES groundwater formation by the middle of the century. Being strongly correlated to precipitation inputs, all uncertainties in their forecast given, surface runoff generation was projected to be promoted with elevated intensity and duration of precipitation events by the end of the century.
Soil compaction from using heavy forestry machineries was simulated adjusting soil bulk density, and the SCS Curve Number in SWAT+, both derived from driving test data collected in the area. The favorable infiltration conditions, and the relatively low susceptibility for soil compaction of the coarse-textured Red Sandstone were found to dominate the magnitude of impact on watershed level, resulting in moderate signs of deterioration. The simulations furthermore revealed a clear influence of soil type on hydrological responses to soil compaction on skid trails, and thus support the assumption that the vulnerability of soils to compaction increases with the percentage of silt and clay soil particles. The pathway system was found effective in the contribution to elevated amounts of surface runoff at high precipitation inputs.

Disrupted areas with rejuvenation were simulated based on an artificial model within a sub-catchment area, assuming 3 years old tree saplings with a simulation period of 10 years, and compared to mature stocks (30 to 80 years) with regard to selected water balance components. Rejuvenations with undeveloped canopy cover suffer losses in their retarding effect on the water flow regime, which favors the generation of overland flow, and slightly promotes higher leaching in quantitative terms. The hydrological differentiation between closed canopy stands and close to open field stand conditions was found to be governed by the dominant factors atmospheric evaporative impetus, precipitation amounts, and canopy expression, indicating that with higher evaporative demand, but scarce water inputs to the system, the hydrological impact of disrupted forest areas compared to mature stocking structures was the most pronounced the less developed the regrown rejuvenation canopy cover. The results suggest that in the evaluation of enhancement measures for decentralized flood control, critical source areas (CSA) for runoff generation in the forest are recommended to move into focus of forest management. The sensitivity, and thus susceptibility for deterioration of forests to ecosystem conditions allow for the conclusion, that maintenance of the complex structure and intactness of its interrelations, especially with the given challenge climate change, urges for carefully adapted measures of conservation, efforts in the identification of CSA, as well as preservation and reestablishment of the hydrological continuity in forest stands.

ZUSAMMENFASSUNG

Wasserbezogene regulierende und versorgende Ökosystemdienstleistungen (ÖSDL) wurden im Hinblick auf das Abflussregime und die Grundwasserneubildung im Biosphärenreservat Pfälzerwald im Südwesten Deutschlands anhand hydrologischer Modellierung unter Verwendung des Soil and Water Assessment Tool (SWAT+) untersucht. Dabei wurde ein holistischer Ansatz verfolgt, wonach den ÖSDL Indikatoren für funktionale und strukturelle ökologische Prozesse zugeordnet werden. Potenzielle Risikofaktoren für die Verschlechterung von wasserbedingten ÖSDL des Waldes, wie Bodenverdichtung durch Befahren mit schweren Maschinen im Zuge von Holzerntearbeiten, Schadflächen mit Verjüngung, entweder durch waldbauliche Bewirtschaftungspraktiken oder durch Windwurf, Schädlinge und Kalamitäten im Zuge des Klimawandels, sowie der Klimawandel selbst als wesentlicher Stressor für Waldökosysteme wurden hinsichtlich ihrer Auswirkungen auf hydrologische Prozesse analysiert. Für jeden dieser Einflussfaktoren wurden separate SWAT+-Modellszenarien erstellt und mit dem kalibrierten Basismodell verglichen, das die aktuellen Wassereinzugsgebietsbedingungen basierend auf Felddaten repräsentierte. Die Simulationen bestätigten günstige Bedingungen für die Grundwasserneubildung im Pfälzerwald. Im Zusammenhang mit der hohen Versickerungskapazität der Bodensubstrate der Buntsandsteinverwitterung, sowie dem verzögernden und puffernden Einfluss der Baumkronen auf das Niederschlagswasser, wurde eine signifikante Minderungswirkung auf die Oberflächenabflussbildung und ein ausgeprägtes räumliches und zeitliches Rückhaltepotential im Einzugsgebiet simuliert. Dabei wurde festgestellt, dass erhöhte Niederschlagsmengen, die die Versickerungskapazität der sandigen Böden übersteigen, zu einer kurz geschlossenen Abflussreaktion mit ausgeprägten Oberflächenabflussspitzen führen. Die Simulationen zeigten Wechselwirkungen zwischen Wald und Wasserkreislauf sowie die hydrologische Wirksamkeit des Klimawandels, verschlechterter Bodenfunktionen und altersbezogener Bestandesstrukturen im Zusammenhang mit Unterschieden in der Baumkronenausprägung. Zukunfts-Klimaprojektionen, die mit BIAS-bereinigten REKLIES- und EURO-CORDEX-Regionalklimamodellen (RCM) simuliert wurden, prognostizierten einen höheren Verdunstungsbedarf und eine Verlängerung der Vegetationsperiode bei gleichzeitig häufiger auftretenden Dürreperioden innerhalb der Vegetationszeit, was eine Verkürzung der Periode für die Grundwasserneubildung induzierte, und folglich zu einem prognostizierten Rückgang der Grundwasserneubildungsrate bis zur Mitte des Jahrhunderts führte. Aufgrund der starken Korrelation mit Niederschlagsintensitäten und der Dauer von Niederschlagsereignissen, bei allen Unsicherheiten in ihrer Vorhersage, wurde für die Oberflächenabflussgenese eine Steigerung bis zum Ende des Jahrhunderts prognostiziert.

Für die Simulation der Bodenverdichtung wurden die Trockenrohdichte des Bodens und die SCS Curve Number in SWAT+ gemäß Daten aus Befahrungsversuchen im Gebiet angepasst. Die günstigen Infiltrationsbedingungen und die relativ geringe Anfälligkeit für Bodenverdichtung der grob-körnigen Buntsandsteinverwitterung dominierten die hydrologischen Auswirkungen auf Wassereinzugsgebietsebene, sodass lediglich moderate Verschlechterungen wasserbezogener ÖSDL angezeigt wurden. Die Simulationen zeigten weiterhin einen deutlichen Einfluss der Bodenart auf die hydrologische Reaktion nach Bodenverdichtung auf Rückegassen und stützen damit die Annahme, dass die Anfälligkeit von Böden gegenüber Verdichtung mit dem Anteil an Schluff- und Tonbodenpartikeln zunimmt. Eine erhöhte Oberflächenabflussgenese ergab sich durch das Wegenetz im Gesamtgebiet.

Schadflächen mit Bestandesverjüngung wurden anhand eines artifiziellen Modells innerhalb eines Teileinzugsgebiets unter der Annahme von 3-jährigen Baumsetzlingen in einem Entwicklungszeitraum von 10 Jahren simuliert und hinsichtlich spezifischer Wasserhaushaltskomponenten mit Altbeständen (30 bis 80 Jahre) verglichen. Die Simulation ließ darauf schließen, dass bei feh-

lender Kronenüberschirmung die hydrologisch verzögernde Wirkung der Bestände beeinträchtigt wird, was die Entstehung von Oberflächenabfluss begünstigt und eine quantitativ geringfügig höhere Tiefensickerung fördert. Hydrologische Unterschiede zwischen dem geschlossenem Kronendach der Altbestände und Jungbeständen mit annähernden Freilandniederschlagsbedingungen wurden durch die dominierenden Faktoren atmosphärischer Verdunstungsanstoß, Niederschlagsmengen und Kronenüberschirmungsgrad bestimmt. Je weniger entwickelt das Kronendach von verjüngten Waldbeständen im Vergleich zu Altbeständen, je höher der atmosphärische Verdunstungsanstoß und je geringer die eingetragenen Niederschlagsmengen, desto größer war der hydrologische Unterschied zwischen den Bestandestypen.

Verbesserungsmaßnahmen für den dezentralen Hochwasserschutz sollten folglich kritische Bereiche für die Abflussbildung im Wald (CSA) berücksichtigen. Die hohe Sensibilität und Anfälligkeit der Wälder gegenüber Verschlechterungen der Ökosystembedingungen legen nahe, dass die Erhaltung des komplexen Gefüges und von intakten Wechselbeziehungen, insbesondere unter der gegebenen Herausforderung des Klimawandels, sorgfältig angepasste Schutzmaßnahmen, Anstrengungen bei der Identifizierung von CSA sowie die Erhaltung und Wiederherstellung der hydrologischen Kontinuität in Waldbeständen erfordern.

I TABLE OF CONTENTS

II LIST OF FIGURES

III LIST OF TABLES

IV LIST OF ABBREVAIATIONS

a	annual
aa	annual average
aET	Actual evapotranspiration
AEUV	Vertrag über die Arbeitsweise der Europäischen Union
AFD	Annual falling debris
Al	Aluminium
app.	Appendix
approx.	approximately
ArcGIS	Geo information system softwarefrom ESRI
ATKIS	Official Topographic Cartographic Information System
av.	average
AWC	Plant available water capacity
BMU	Federal ministry for the environment
BMVI-ExpN	Expert network of the Federal Ministry for Digital and Transport
BNatSchG	Federal act for the protection of nature
C	Elementary carbon
°C	Degree Celsius
CBD	Convention on Biological Diversity
CCLM	COSMO - CLM simulations
CEC	Cation Exchange Capacity
cf.	compare
CICES	Common International Classification of Ecosystem Services
CLM	Climate Limited-area Modeling Community
cm	centimeters
CO_2	Carbondioxyd
CSA	Critical source areas
CVM	Contingent Valuation Method
DBG	Deutsche Bodenkundliche Gesellschaft
DIN	Deutsches Institut für Normung
DWD	German Meteorolocal Service
ET	Evapotranspiration
et al.	et alii (und andere)
EPIC	Erosion-Productivity Impact Calculator
ES	Ecosystem Services
EU	Europian Union
EURO-CORDEX	Coordinated Downscaling Experiment for Europe
FAWF	Research Institute of Forest Ecology and Forestry
FC	Field capacity
Fe	Elementary iron
Fig.	Figure
GCM	Global climate model
GG	Grundgesetz
GemO	Gemeindeordnung
ha	hectar
HI	Harvest Index
hPa	Hecto pascal
HRU	Hydrological response unit
HYRAS	Hydrometeorological grid datasets

ibid.	In the same place
i.e.	id est (that is)
InterMet	Interpolation of meteorological parameters
IPBES	Intergovernmental Platform on Biodiversity and Ecosystem Services
IPCC	Intergovernmental Panel on Climate Change
JUV	Juvenile stock scenario
kf	Hydraulic conductivity
kg	kilogram
km	kilometers
kPa	Kilo pascal
L	Sandy loam soils
LAI	Leaf area index
LfW	State office for Water Management RLP
LiDAR	Light Detection and Ranging
LGB RLP	State office of geology and mining of Rhineland-Palatinate
LfU RLP	State office of the environment Rhineland-Palatinate
LSU	Landscape unit
LVermGeo RLP	State Office for Surveying and Geospatial Information
LWG	Landeswassergesetz
m	meters
m^2	Square meters
MAT	Mature stock scenario
mm	millimeters
MEA	Millennium Ecosystem Assessment
mamsl.	Meters above mean sea level
MJ	Mega Joule
MPa	Mega Pascal
MPI-CSC-REMO2009	EURO CORDEX 11 regional climate model
N	Elementary nitrogen
NPP	Net Primary Production
NRCS	Natural Resource Conservation Service
NSG	Naturschutzgebiet
NSE	Nash-Sutcliffe efficiency
NST	Nährstoffe
O_2	Oxygen
P	Elementary Phosphorus
PBIAS	Percent bias
pET	Potential evapotranspiration
pH	pondus hydrogenii (weight of hydrogen)
PTF	Pedo Transfer Function
RACMO	KNMI regional atmospheric climate model
RCA4	Rossby Centre regional atmospheric model
RCP	Representative Concentration Pathways
RCM	Regional climate model
REKLIES	Regional climate projections ensemble for Germany
RSR	Root mean square error
RUE	Radiation Use Efficiency
s	seconds

SCS-CN	Soil Conservation Service Curve Number
SL	Loamy sand soils
SOM	Soil organic matter
SPAC	Soil-plant-atmosphere continuum
SRU	Sachverständigenrat für Umweltfragen
SS	Pure sand soils
SU	Silty sand soils
SWAT	Soil and Water Assessment Tool
Tab.	Table
TEEB	The Economics of Ecosystems and Biodiversity
TEV	Total Economic Value
U	Silt soils
UHOH-WRF361H	REKLIES-DE regional climate model
UBA	Federal Environment Agency
UN	United Nations
UNESCO	United Nations Educational, Scientific and Cultural Organization
UNO	United Nations Organisation
U.S.	United States
USDA	Agricultural Research Service of the U.S. Department of Agriculture
VPD	Vapor pressure deficit
WaldIS	Geographic information system of the FOREST INVENTORY
WP	Permanent wilting point
WUE	Water use efficiency

V LIST OF FORMULAS

1 INTRODUCTION

Water is the prerequisite for all life on earth. Its utilization has always formed the basis of human habitat. Its systemic interconnectedness with other spheres, such as soil and vegetation, forms the basis of natural spaces (cf. Wohlrab et al. 1992:18). Forests have a decisive influence on runoff and thus on water supply and material balance of rivers and groundwater in terms of quantitative and temporal dimensions. Due to the storage and retention of precipitation in the canopy, and favorable soil conditions for infiltration and soil water storage, forests have a large water retention capacity and thus contribute to decentralized flood protection (Peck & Mayer 1996; Schüler 2006; Engler 1919, Günther 1979, Schwarz 1985, Hegg et al. 2004 in Nordmann 2011; EEA 2015; Bott 2002). Water retention also ensures a high quantity, and, due to the water-purifying processes in the soil passage, high quality of groundwater formation (Schüler 2006). By reducing surface runoff-erosion the transport of substances into surface waters, and thus the risk of eutrophication, is counteracted (Neary et al. 2009; Wagenbrenner et al. 2010). The underlying processes, functions and structures (in this context referred to as intermediate components) are part of a complex, multi-organismic network of relationships, in which the processes, functions and structures of one bring benefit and dependencies for the other life forms involved (Matyssek & Herppich 2019). Being part of the natural systems and essentially dependent on the usability of natural resources, humans are sensitively linked to ecosystems and their functionality. Their diverse forms of naturally provided material, energetic, spatial, aesthetic and functional resources are the basis for human well-being. The idea of Ecosystem Services (ES) is a recognition of the dependence of humans on nature and their responsibility for preserving its functionality, for their own survival and for maintaining the complex framework in which they live. By deriving the services that the ecosystems provide for human well-being, underlying intermediate components of the natural balance are identified, the conservation requirements of which show necessities for human action. The services derived from the respective abiotic and biotic intermediate components can be differentiated into provisioning, regulating, cultural and supporting services, which are utility-related (use values) or not (non-use values) (MEA 2005). Regulative ES can be considered a prerequisite to other ES, as they basally regulate and control biotic and abiotic factors in natural processes, such as the flow of information, energy and substances and thus the complex interactions of ecosystem elements other ES are based upon (Chicharo et al. 2015; Mace et al. 2011, Puydarieux & Beyou 2017 in Brockerhoff et al. 2017). In connection with water-balance-related ES of the forest, the regulative services must be emphasized, as they correlate closely with the regulation of the water and nutrient cycle. The related intermediate components range from the basic filter, buffer and transformer functions of the soil, and its pronounced biological activity in topsoil and humus layer, to the associated water retention and purification processes, which bring about clean drinking water supply, stabilization of the nutrient cycle, erosion protection, retention potential and regulation of the global climate via carbon sequestration (Keesstra et al. 2012; Dixon et al. 1994; Mueller et al. 2012; Fabiánek et al. 2009; EASAC 2017). With reference to water, the latter is important for the harmonization of the water cycle against the background of changing precipitation patterns associated with climate warming and increased evaporation values due to rising air temperatures. In addition to essential biological dependencies that humans have to recognize in their relationship with nature, monetary aspects of ES of the forest do unfold in a reduced financial outlay concerning flood events or drinking water treatment (Munich RE 2000). Based on the maintenance of intact soil functions as a prerequisite for the processes of water retention and water purification, the protection of water resources in the forest is inextricably linked with soil protection (Schüler et al. 2002; Nordmann 2011; Leuschner 1998, Schäfer et al. 2002).

1.1 Research relevance, framework and objectives

Freshwater resources are not evenly distributed around the world. Its shortage contributes to the emergence of armed conflicts in many parts of the world (UNESCO 2019). Although the trouble spots about the availability of the life-giving resource are predominantly in developing countries and far away parts of the world, a gradual process of deterioration of the water resource is emerging in European countries, too, including Germany. In quantitative terms, the problem is based on increasing water consumption worldwide, associated with population growth, changes in lifestyles and increasing agro-industrial use (UNESCO 2015, 2019). Since the groundwater is integrated into the hydrological cycle in a sensitively responsive manner, climate change has a direct effect on the rate of its new formation (cf. Rosenzweig et al. 2007:90): Climate change induced increases in air temperature lead to higher evaporation rates, and thus might, in combination with altered precipitation patterns and an extended vegetation period, lower the groundwater formation rate. The trend of falling groundwater levels is already documented for areas in Germany through various measurements (cf. HLUG 2015; LfU Bavaria 2008; **fig. 83** app., KLIWA 2017). In addition to quantitative changes, the qualitative pollution of groundwater and drinking water supplies is increasingly moving into the focus of science. The pollution with environmental chemicals from industry, agriculture and households is already causing a shortage of water of good quality in some regions of Germany (Rust 2009; BMU 2008; UBA 2017a). Since around 75% of the drinking water in Germany is fed by groundwater, and its contamination with pollutants cannot be remedied in reasonable time, the protection of this valuable asset is a major social responsibility (BMU 2006, SRU 1998, 2008). Although since the Water Framework Directive (WFD) came into force in 2000, significant improvements in the reduction of pollutant and nutrient inputs from point sources were achieved, diffuse inputs continue to represent a major burden on the water quality benefit. As groundwater also fulfills essential ecological functions in the landscape hydrology for numerous groundwater-dependent biotopes, its importance for biodiversity is no less important (cf. SRU 1998:13), especially with respect to the complexity of interrelationships in the global network of life humans depend upon. With heavy storm events predicted to occur more frequently as climate change advances (Butzen et al. 2014; Reiter et al. 2018), flood events may become a more frequent threat to urban spaces along rivers as well, with aggravating expenditure regarding flood protection and damage management (EU 2014; BMI 2013). In the generation of flood disasters along major rivers, forested areas smaller tributary rivers origin from contribute significantly to the overall water volume of flood generation (Schüler 2006). The assessment of surface runoff generating processes in forests is therefore crucial to improvements of effective water-retention and runoff-delaying measures (Moltschanov 1966, Hibbert 1967, Voronkov et al. 1976, Rosemann 1988, Moeschke 1998, Mendel 2000 in Schüler 2006).
As humans influence the bio-geo-chemical material cycles and thereby bring about changes in the biosphere with complex pathways, pressures from human activities have led to forest loss and degradation (FAO 2015). In the provision of ES of the forest, the anthropogenic degradation of forest ecosystems has long-term effects in the form of reduced resilience to disturbances. Climate extremes or pests and pathogens impair the intermediate components ES are based upon. It is important to gain a better understanding of the complex relationships between intermediate components and ES of the forest in order to enhance quantification and knowledge of nature process interactions linked to human well-being. The goal pursued by visualizing the services forests provide to human society is to challenge conventional notions of value assignments with a still dominating orientation towards economic growth with a more prosperity and well-being oriented economic conceptualization. This is con-

sidered a contribution for a better implementation of the UN Sustainable Development Goals into human societies and actions (Costanza et al. 2017).

In order to achieve both, to comprehend the complex interrelations between intermediate components and ES of the forest, as well as visualizing their value in the context of human society, the European INTERREG project Ecoserv this work was embedded in aimed the detection of water-related ES of the forest, the derivation of strategies and concrete recommendations for action for cross-border forest management, and knowledge transfer related to the detected ecological components in the educational sector in the area of the Palatinate Forest/Northern Vosges Biosphere Reserve (fig.1).

The project "Ecoserv - cross-border improvement of the quality of ecosystem services in protected areas and adjacent regions: recording, instruments, strategies", conducted from 2018 to 2021, was a cooperation between the University of Landau, the Black Forest Biosphere Reserve, the Palatinate Forest Nature Park, the Research Institute for Forest Ecology and Forestry (FAWF), the Hunsrück-Hochwald National Park, the École Nationale du Géinie de l´Eau et de l´Environment de Strasbourg, the Parc naturel régional des Vosges du Nord, the Université de Strasbourg, the Féderation du Bas-Rhin pour la Pêche et la Protection du Milieu and the Center National de la Recherche Scientifique.
This work is dedicated to the contribution that the forest ecosystem can make to water protection, with focus on quantitative water fluxes.

Figure 1: German part of the Biosphere Reserve Palatinate Forest/Northern Vosges (Google Maps-For-Free SRTM3 Webserver, modified by T. Groan (2008)

Therefore, the study aims an impact assessment of human activities on water-related ES of the forest, with special regard to disturbing factors on water retention and water fluxes of surface waters and groundwater in the Palatinate Forest. It therefore aims on regulative (water and nutrient cycle regulation), and provisioning ES (clean drinking water, decentralized flood control) in the area.
In order to meet the challenges facing water protection in the 21st century, integrative overall concepts of environmental protection planning in all areas of society that account for the systemic interrelationships of natural environments appear to be necessary. In this manner, the work aims recommendations for forest management strategies and their medium-term operational planning to support regulative and provisioning ES of the forest. Therefore, the assessment of changes or losses to water related ES that are linked to climate change and human activities is inevitable. Next to fundamental changes in basic environmental conditions induced by climate change, human activities in the course of forest management operations, such as driving on forest soils with heavy machines, or disrupted areas with regrowing rejuvenation, were identified to show effects on water-related ES.

The associated forest functions were analyzed regarding their functional integrity with respect to the elucidated influencing factors via hydrological modelling, using the model SWAT+.

The approach taken here assessed the following aspects:

- Water balance regulation: quantitative groundwater formation in a forested area, and components of the water cycle related to it (flow regimes, loss factors)

- Effects of compaction due to harvest machinery on soil functions, water balance regulation and quantitative groundwater formation in a forested area

- Effects of disrupted areas with rejuvenation, either in the course of management treatments or as climate change related phenomena (windthrow, calamities, drought induced forest die-off, wild fires) on water balance components in a forested area

- Effects of climate change on the development of water balance regulation and groundwater formation in the future

Section **2** is devoted to the fundamental physical processes of groundwater recharge and their influencing factors in the forest. The conditions and special characteristics of the study area are specified in section **3**. Input and evaluation of data as well as the results, and the analysis of the model sequence are reflected in section **4** and **5**. The results are discussed with regard to water-related ES of the forest in section **6**. Section **7** concludes potential contributions forest can make to decentralized flood control and water protection. Derivable recommendations for actions in the field of forest management and politics are discussed. Aiming the focus on ES of the forest is rare in hydrological modeling. Although the number of studies published on the topic of modelling ES has increased rapidly in the past decades (Fisher et al. 2009), SWAT studies conducted in forest ecosystems are still scarce. Also, the effects of soil compaction due to heavy machinery in the course of harvest operations, have not been investigated on macro-scale watershed level by hydrological modeling in Germany so far. To investigate hydrological effects of disrupted areas with regrowing rejuvenation compared to permanent forests, model applications were tested and modified for the purpose of depicting age-related differences in water balance. This, to the best of the author´s knowledge, has never been done before using SWAT+. Furthermore, the SWAT+ model has been analyzed and tested on the purpose of adapting it to the specific conditions of the local tree species. Therefore, the plant parametrization was modified based on monitoring data in the field, the findings of which point to possible model developing potentials with regard to the simulation of forest-specific transpiration factors and growth performance.

1.2 Methodical approach

Hydrological modelling allows for an estimation of quantitative groundwater formation, fluxes of surface waters as well as related disturbances It is a useful tool to assess possible influences of anthropogenic pressures (silvicultural operations, climate change) on the groundwater resource and runoff behavior. It furthermore provides the projection of future developments, and thus can be used to derive recommendations for actions to adapt the forest of the future to the essential issue water.
In this thesis, the model **S**oil and **W**ater **A**ssessment Tools+ (SWAT+) was used to simulate the water balance of the study area. For the requirements of modeling in the specific area, a collaboration with the department of hydrology of the University of Kiel was carried out and executed by Dr. T. Tigabu and Dr. P. Wagner under the direction of Prof. Dr. N. Fohrer.
The physically based model SWAT+ was developed to predict the influence of agricultural processes on water, sediment and chemical loads in long time series in the meso and macroscale range (Arnold et al. 1998). It is therefore primarily used in large catchment areas with different soil types, uses and cultivation methods to forecast how certain interventions in nature will affect the water balance, and to predict water and nutrient fluxes in a watershed under different land use/cover classes. In order to depict the groundwater flow more detailed, the groundwater section of SWAT+ was modified. Although modelling cannot be understood as an empirical foundation, it can be used as a diagnose, control, forecast and decision-making instrument, as it provides the comprehension of selected attributes of complex physical, biological, economic, or social systems (EPA 2009). Watershed modelling provides the quantification of potential shifts in ES and a better understanding of dynamics, non-linear, spatially explicit contributions of nature to the social-ecological system (cf. Kubiszewski et al. 2017 in Costanza et al. 2017).
To feed the model system, an extensive data set of spatial and time-related data on climate, runoff, exposure/terrain, land use and soil/geology is required. The data was provided by various sources (LGB RLP, LFU RLP, FAWF, Forest Inventory), processed for application, parameterized, calibrated and validated using measured reference values. Based on the hydrological model, relevant influencing variables on groundwater recharge and water fluxes were then considered. Important aspects of the soil functions and possible impairments were highlighted. In addition to differentiated stand types for the main tree species (oak, beech, pine, spruce, douglas fir and mixed stands), a simulation of different age patterns and their effect on water balance components was performed. Also, a traffic map representing pathways, skid trails and preloaded areas was incorporated for the assessment of potential soil compaction. In order to visualize the influences of climate change on water-related ES, the simulation of long-term climate scenarios was performed. To determine the potential quantitative effects of climate changes on dynamics in the water balance, high-resolution statistical and dynamic regional models were used based on the BIAS-adjusted REKLIES and EURO-CORDEX simulations RCP2.6 and RCP8.5 over the HYRAS area using downscaling methods (CCLM4.8.17, RACMO22E, RCA4, CLM, UHOH-WRF361H, MPI-CSC-REMO2009).

2 FUNDAMENTALS AND DEFINITIONS

Due to its dipole character water is a very good solvent, which allows the uptake and transport of nutrients vital to plants (Davie 2002). Its natural occurrence in all three phases is a major driver of energy around the globe. The water cycle is closely linked to the energy cycle through the atmospheric circulation by influencing the heat budgets (Anderson & McDonnell 2005; Bauer 2019). When the groundwater reflects the long-term climatological situation due to its long residence times, soil water influences the energy balance at the land surface, partitioning the amount of precipitation into percolation and run-off (Anderson & McDonnell 2005). Evaporation as latent heat flux from the surface to the atmosphere is highly dependent on solar radiation as well as on soil moisture, which makes the actual evapotranspiration driven both atmospherically and hydrologically. This becomes particularly evident in the relation of stomatal closure bound either to the water vapor pressure deficit with increase in temperature or to dryness of soil moisture. The vegetation also influences the surface energy and water balance not only by the transfer of water through their roots from soil to atmosphere, but also in terms of surface albedo, and by intercepting precipitation (ibid.). **Figure 2** shows the global water cycle with its components and fluxes.

A major impact on the formation of precipitation is anthropogenic global warming due to the atmospheric greenhouse effect. It is responsible for alternating precipitation patterns with respect to location, type, amount, frequency, intensity and duration. It enhances evaporation and thus cloud formation, and at the same time accelerates land-surface drying (IPCC 2007; Trenberth 2005). As the water balance remains the same in total amounts, the evaporated moisture gath-

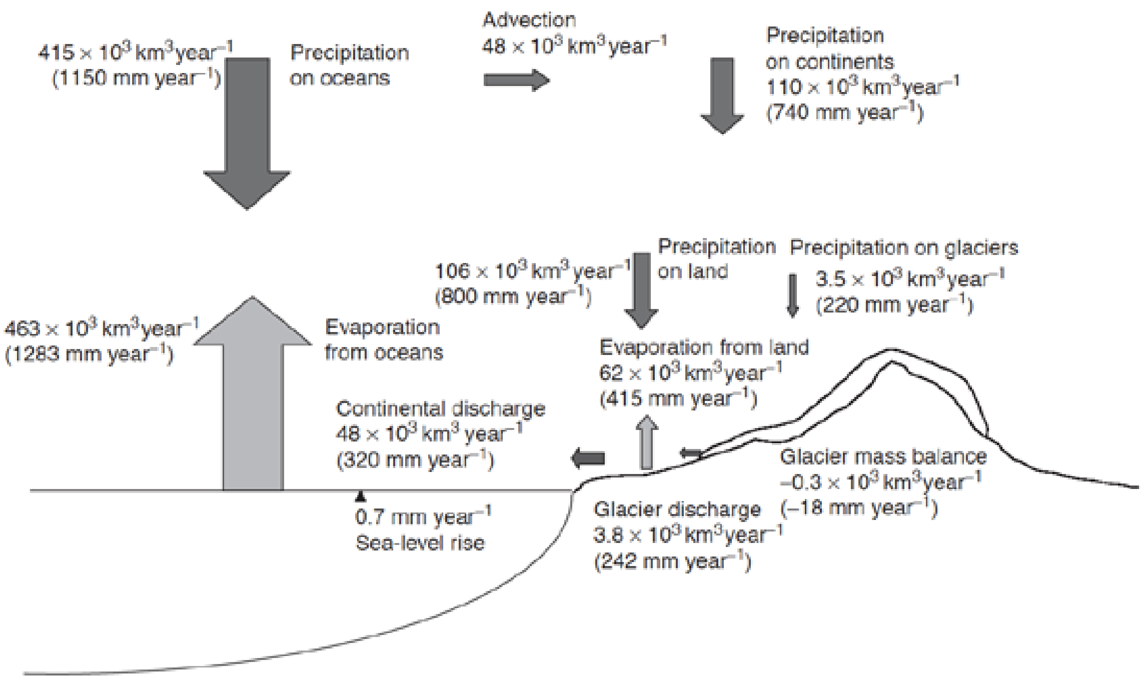

Figure 2: The global water cycle and its components and the fluxes (Anderson & McDonnell 2005:398)

ers and increases the occurrence of heavy storm events, while duration and frequency of precipitation are reduced (cf. Trenberth 2005:2). The IPCC prognoses for Central and Eastern Europe the summer precipitation to decrease, causing higher drought-stress (cf. IPCC 2007:14). Especially within the early vegetation period, drought stress inhibits the development and growth of trees, whereas heavy storm events evoke soil erosion (IPCC 2007:18). Raindrop impact and flow traction promote the detachment of grains of soil and small aggregates. Their deposition on the soil surface contributes to crust formation, which impedes infiltration and increases infiltration excess overland flow (cf. Anderson & McDonnell 2005:55). Globally, deforestation, biomass burning and other changes in land-use practices release CO_2, CH_4, and N_2O into the atmosphere and thus enhance radiative forcing (IPCC 1990). Although nitrogen must be considered a limiting factor for plant growth under natural conditions (Lehn et al. 1995), human activities, such as the intensification of agricultural production, animal feedlot operations, biomass burning (including forest fires), and fossil fuel combustion in industry and transport (Krupa 2002; Godbold & Hüttermann 1994), have increased the proportion of reactive nitrogen compounds massively since the middle of the 19th century[1] . Despite all efforts in the reduction of emissions, critical loads, below which sustainable, stable environmental development is assumed (BnatSchG 2009, BGBL 2004 II p. 885; Nagel & Gregor 1999), are exceeded in many parts of Germany (UBA 2018A,B, UBA 2013). Both, changes in water fluxes and chemical composition, are crucial for the sensitive response-systems of water-related processes within forest ecosystems and the ES derived from them.

2.1 Water balance parameters – hydrological, pedological and hydraulic basics

2.1.1 Atmosphere – plant interaction

Plants are connected to the hydraulic continuum via their stomata, roots and the xylem system, controlling the water intake and release through opening and closing mechanisms. The water flow from the soil through the plant to the atmosphere is called hydraulic soil-plant-atmosphere continuum - SPAC (Lange et al. 1982). In terms of energy, the water follows a gradient in the water potential from high to low potential energy, which determines the hydraulic conductivity of the system (Matyssek & Herppich 2019). Evapotranspiration, the total amount of water loss to the atmosphere in a plant stand, is composed of the direct physical transpiration of plants, being referred to as photosynthetically productive evaporation (Schrodter 1985, Baumgartner 1990 in Peck & Mayer 1996), evaporation from soil or free water surfaces, and interception evaporation from retained rainwater on living and dead plant surfaces.

2.1.1.1 Evapotranspiration

Evaporation (E) is driven by diffusion, i.e. due to different energetic potentials, and is therefore temperature-dependent (Baumgartner & Liebscher 1990). The saturation deficit of the air (VPD) is decisive for the absorption of water in the air: It describes the difference between the current vapor pressure of the air (e_a) at a given temperature and the saturation vapor pressure at a given temperature (e_s), i.e. the partial pressure of water vapor at full saturation. According to Dalton (1802) the evaporation process can be described as follows, when $f(v)$ is a function of wind speed:

$$E = (e_s - e_a) \cdot f(v)$$

Formula 2.1.1 (Dalton 1802)

[1] In the 1970s, attention was drawn to the phenomenon of “acid rain”, which was linked to emissions of sulfur and nitrogen compounds from fuel combustion that are oxidized in the atmosphere to form sulfuric acid (H_2SO_4) and nitric acid (HNO_3), which were associated with the reduction of biodiversity through acidification of surface waters (Levin 2000).

As a result of the metabolic processes in the plant, O_2 and CO_2 are exchanged with the ambient air through photosynthesis and respiration. While absorbing CO_2, plants release water vapor through transpiration. The amount of energy required for the process of transpiration is withdrawn from the radiant energy and the plant itself, so that at high temperatures a cooling effect sets which counteracts an overheating of the plant (Matyssek & Herppich 2019).

It is important to understand the difference between actual and potential evapo¬trans¬piration: Potential evapotranspiration is the maximum possible evaporation under the given climatic conditions. It can only be achieved in real terms if the soil can constantly supply sufficient water, and therefore it rarely occurs in real life. It can be calculated using the energy balance method that Penman developed in 1956, which was later expanded by Monteith to the Penman-Monteith model (Monteith, 1985):

$$ET_0 = \frac{0{,}408 \cdot \Delta \cdot (R_n - G) + \gamma \cdot \frac{900}{T + 273} \cdot u_2 \cdot (e_s - e_a)}{\Delta + \gamma \cdot (1 + 0{,}34 \cdot u_2)}$$

Formula 2.1.2

Et_0	=	Potential gas reference evapotranspiration [*mm/d*]
Δ	=	slope of the saturation vapor pressure curve
R_n	=	Net radiation (radiation balance) [MJ/(m2 • d)]
T	=	Air temperature [°C]
G	=	Ground heat flow [MJ/(m2 • d)]
u_2	=	Wind speed at a height of 2 m [m/s]
γ	=	Psychrometer constant [kPa/°C]
e_s - e_a	=	Saturation deficit, depending on air temperature and vapor pressure [kPa]

Actual evapotranspiration (ET) is understood as real evaporation under climatic and local conditions. If there are deficits in the soil water balance, actual evaporation can be significantly lower than potential evaporation. Furthermore, it depends on physiological properties of the leaf permeance, and is driven by photosynthetic factors such as energy balance, so that is varies with daytime and season (Monteith 1965; cf. Liebscher & Baumgartner 1990:362; Koch 1957). To determine it, current groundwater levels as well as soil and plant properties are required. It can be measured using a lysimeter and calculated using hydrological methods. In comparison to other water balance parameters, such as runoff and precipitation, measuring evaporation encounters difficulties, because it depends on so many factors. A direct metrological determination of the evapotranspiration of an entire catchment area is almost impossible and therefore usually performed using hydrological models.
Due to a high radiation balance, and the vertical stand structure promoting a high surface for evaporation and interception, forests show the highest specific evaporation rate in comparison to other forms of land use (Kirchner 1986; cf. Peck & Mayer 1996:1). Consequently, next to the climatic factors, the total amount of actual ET also depends on stand structural, as well as on soil physical factors, the latter being involved in the extent and distribution of plant available soil water (Baumgartner 1990; Wohlrab et al. 1992; Brechtel 1990). Tree species related differences in ET predominantly occur between deciduous and coniferous species, which is related to the fact that coniferous trees also transpire in winter, when deciduous trees fall dormant (Peck & Mayer 1996).

2.1.1.2 Interception

Interception is understood as the precipitation held back by the plant surfaces, some of which evaporates or sublimates directly from there, drips or flows off, and thus reaches the ground with a delay (Baumgartner & Liebscher 1990; Helvey 1964). Settling and intercepting the precipitation promotes the processes of condensation and sublimation, which in the form of dew formation and fog precipitation can lead to an increase in the water supply inside forest stands (Brechtl 1970, Baumgartner 1967 in Baumgartner & Liebscher 1990). In connection with air pollution, however, this circumstance causes a higher load on the forest for air pollutants and deposits compared to other land forms, since the additional precipitation gained through the interception increases the amount of substances carried into the forest soil (ibid.). The interception of the trees, however, outweighs that of the other plants in the forest, as the proportion of their leaf surface is much larger (Peck & Mayer 1996, Pomeroy & Schmidt 1993). In forest stands without ground vegetation and with an insulating thick soil litter, the transpiration of the trees would be the main loss in net precipitation (Baumgartner & Liebscher 1990). The morphological character of a stand also influences the level of interception evaporation. Structure, mixture and density of the stand, degree of coverage of the soil and parameters of the growth creditworthiness such as degree of canopy coverage, number and size of leaf areas, density of branching and depth of the canopy are decisive (Mitscherlich 1971; Leyton et al. 1967, Weihe 1968). An average of 30 - 40% of the outdoor precipitation is lost through interception evaporation, whereas in tree species with high stemflow, such as the beech, only 20 - 30%. Outside the vegetation period, the proportion of interception evaporation in deciduous, bare winter trees is only 10 - 20%, whereas it is constant in conifers (Balazs 1983). These values illustrate that interception evaporation is an essential part of total evaporation. Due to the larger plant surface volume, interception increases with higher stand density and, associated with this, and also with stand age. (Peck & Mayer 1996; Baumgartner & Liebscher 1990). In addition to these structural components, the interception performance also depends on the amount, duration and distribution of precipitation. When the proportion of interception is given as 20 to 21% of outdoor precipitation for deciduous trees and 28 to 42% for conifers (Peck & Mayer 1996), decreasing the amount of stand precipitation, this changes with increasing total volumes of outdoor precipitation (cf. Baumgartner & Liebscher 1990:319).

2.1.1.3 Water stress

As for water vapor in transpiration, the diffusion laws also drive photosynthesis, when CO_2 flows from the ambient air into the intercellular leaves following the concentration gradients (Brodribb 1996; Ehleringer & Cerling 1993). The net CO_2 uptake can be limited by water availability, as the gain of carbon, and therefore photosynthesis and plant growth, occurs only with the cost of water. In order to express the relationship between carbon gain and transpired water loss, the term water use efficiency (*WUE*) was found. *WUE* was originally defined as CO_2-uptake per transpiration rate or photosynthetic rate per transpiration rate (Tang et al. 2006), but it can also refer to the ratio of produced biomass to the rate of transpiration (Baumgartner et al. 2019). The ability of a plant to fix as much carbon as possible in a short period of time in order to lose as little water as possible, makes it less vulnerable to periods of poor water availability and is therefore an indication to its drought resilience. In case that the feed of water through the root-shoot system cannot match the transpiration rate due to hydraulic limitation of water transport from the roots to the leaves (Tyree & Sperry 1988; Ewers et al. 2001), the stomatal closure prevents the transpiration to exceed its maximum. In this state of dynamic stress, actual transpiration, carbon uptake and plant growth become limited (Matyssek & Herppich 2019; Brunold et al. 1996; Köstner & Clausnitzer 2011; Hesse et al. 2018). Tree species show different strategies to cope with water stress: The mechanism of stomatal regulation is either isohydric, as a reaction of stomatal closure ahead of water stress, or anisohydric, which goes along with a rather slow and more tolerant to water stress reaction of stomatal closure (Nguyen 2016). Isohydric species suffer shortage of assimilates and subsequent losses in growth rate as consequence to stomatal closure, while anisodydric species take the loss of water in order to maintain photosynthetic activity (McDowell 2011; Rukh et al. 2020). For beech trees, however, the drought response is observed to vary between isodydric and anisodydric stomatal behavior (Nguyen 2016). Drought induced reactions are related to the water storage capacity of the soil, as well as with factors of the stand structure that influence the microclimate, such as crown cover. Water stress is predicted to become more frequent with climate change. Besides hydraulic failure, carbon starvation is another critical effect of drought within plants (Tomasella et al. 2017). Both gain in importance for soil conditions with low water-holding capacity, which are therefore more prone to soil water deficits.

2.1.2 Water in the soil zone

In the complex process of soil formation, and within highly differentiated spatial patterns, the soil pedon provides three-dimensional, preferential flow paths through its matrix. This allowes solute movement, solvent movement and therefore a life below and above the ground (cf. Anderson & McDonnell 2005:33). The soil zone is to be distinguished into an upper part, the vadose zone, in which the pore spaces are only temporarily filled with seeping precipitation water, and a lower part, the phreatic zone, in which the pores are filled continuously with water and which is therefore considered to be saturated.

2.1.2.1 Water retention and movement in the vadose zone

The soil´s part in the hydrological cycle is based on its functions of regulation, storage and distribution. The distribution of soil water is tied to saturation-dependent changes in water conductivity, which is the crucial principle to water infiltration and movement within the soil (Baumgartner & Liebscher 1990). As long as the soil´s absorption capacity is not exceeded, the impinging water will infiltrate the soil zone, following the force of gravitation. Infiltration takes place as soon as the amount of water seeping in exceeds the retention capacity of the soil at field capacity (FC)[2] . The infiltration rate depends on the initial amount of water, the conductivity of the soil surface as well as on the grain and pore size of the soil particles. The disperse soil system determines the soil´s bulk density ρ, water retention, preferential water movement and aeration (ibid.; Marshall et al. 2001; Buscot & Varma 2005). The conductivity of the pore space predominantly depends on the amount of macro pores (> 50 µm), for they allow the water to flow in the first place (Glaser 2017; Frossard et al. 2006; Scheffer & Schachtschabel 1998).

The distribution of macro pores, however, is not only determined by the physical soil structure, but also by the edaphic: In case of the megafauna, earthworm burrows directly influence preferential flow paths, and therefore the solute transport. Furthermore, the burrow walls inhibit highly microbiological reactive sorption sites, which increases the biological degradation capacity (cf. Keesstra et al. 2012:510). Earthworm burrows are crucial for macro pore formation and therefore play an important role not only in diffuse infiltration into the top soil, but also in the enhancement of water movement into deeper soil layers (cf. ibid). With decreasing size of grains, the absorbing surface of soil particles increases, and so does the intermolecular bonding strength due to adhesion, which counteracts gravitation (matrix potential (Ψ_{m})), whereas gravitation (gravitational potential (Ψ_{g})) counteracts the unimpeded rise of the water column (Stahr et al. 2008). The lower the percentage water content is the higher is the suction tension. In order to adsorb water via the plant roots, the energy of the matrix potential must be expended (Pott & Hüppe 2007). The substrate-specific relationship between $-\Psi_{\mathrm{m}}$ and the soil water content in the unsaturated zone is known as the water retention curve, or pF curve (Fiedler 2001). When the soil water content drains to a value of $\mathrm{pF} > 4.2$, the remaining water adhesively bound to the medium pores with a tension of > 15 000 hPa is no longer utilizable for plants (permanent wilting point, WP). The plant available water (AW) is defined as the difference between field capacity and wilting point: $AW = FC - WP$ (Kirkham 2005:107). The linear movement of water within the soil follows the driving potential gradient in the direction of the lower potential (hydraulic potential Ψ_p). In static equilibrium the matrix potential corresponds to the distance between soil and groundwater surface, with $\Psi_p = \Psi_m + \Psi_g$ (Stahr et al. 2008). If the matrix potential is lowered, for example

[2] Field capacity is given, when the macropores in the soil are fully drained due to gravitation and the only water left is being hold adhesively by medium and fine pores (Fohrer et al. 2016).

through plant demand, the water rises from near-surface groundwater or backwater into the root zone and an upward hydraulic gradient is formed depending on the distance from the groundwater to the surface and the type of soil (Baumgartner & Liebscher 1990).
The flow rate Q that flows laminarly through the matrix of a porous medium (A), was found by Darcy to be directly proportional by the factor K_f to the hydraulic gradient i. The Darcy´s law (1856) formulates for Q/A being the flux, (or Darcy velocity) q:

$$q \quad = \quad -K_f \cdot i$$

Formula 2.1.3 (Baumgartner & Liebscher 1990)

The proportionality factor can be considered as the coefficient for permeability or hydraulic conductivity [m/d], which depends on the pore geometry, such as cracks, root or wormholes and stability of soil crumbs, as well as on density ρ and dynamic viscosity of the fluid (Kirkham 2005; Höll 2002). It differs within the main soil types: The lower the hydraulic conductivity, the lower the permeability of the soil type. As the hydraulic conductivity depends on the pore geometry, the flow rate, and thus the flow character, is controlled by the presence of large pores, which do not take capillary forces into effect (Singh 2002). The flow character in structural pores is predominantly driven by the force of gravity, and can therefore be considered kinematic in case of high rainfall intensities, though becoming diffusive at low flow intensities (ibid.).

Next to one-dimensional, vertical flow, there is also horizontal flow that occurs, when water that penetrated the soil follows the force of gravity mostly parallelly to the slope until it is accumulated at a less permeable geological layer (see **fig. 3**, d). Provided this interflow does not seep into deeper layers and is fed to groundwater formation, it may escape the ground again, with a time delay, at a penetrable point. It finally finds its way into the surface drainage system as return flow, or baseflow, either diffusing through the substrate (see **fig. 3**, c) or flowing out as source outlet (cf. Beven 2012:10; Fohrer et al. 2016:147). Though kinematic in flow character, the near-surface flow of water within the soil profile generally contributes to the hydrograph with dilatation, and thus mitigates the shock wave. Except for conditions with steep hydraulic or slope gradients and high soil hydraulic conductivities, either due to soil specific properties or to structural or biotic macropores, promoting either saturated or unsaturated subsurface stormflows with heavy storm events (Dunne 1978 in Singh 2002), subsurface response times are too long to be considered as stormflows (Beven 1982). The magnitude and timing of subsurface flow response will depend on the depth and hydraulic conditions of the unsaturated zone at the time of the storm (Beven 1981:1419).

If the amount of precipitation exceeds the infiltration capacity of the soil, the excess water flows, according to the local gradient, away as surface runoff, called Hortonian overland flow, which is defined as infiltration excess minus water that collects in terrain depressions (Horton 1933; cf. Fohrer et al. 2016:147/478; Baumgartner & Liebscher 1990). Since the infiltration capacity decreases with increasing soil moisture, the water runs off from saturation excess after Dunn, if the soil is already completely saturated and cannot absorb any further water (see **fig. 3**, a, b) (Beven 2012).
In the case of Hortonian precipitation-runoff events, however, the water flowing directly over land as effective precipitation, or storm runoff, reaches the receiving water body with a short flow time and a pronounced runoff peak. Overland runoff in most cases, especially over a slope plane and with high amounts of precipitation, is kinematic in character, and thus its motion is dominated by a kinematic wave (Singh 2002). Consequently, this leads to a sudden rise in flux and concentration with subsequent shock wave formation, showing a fast and significant contribution to the hydrograph (ibid.; Lighthill & Whitham 1955).

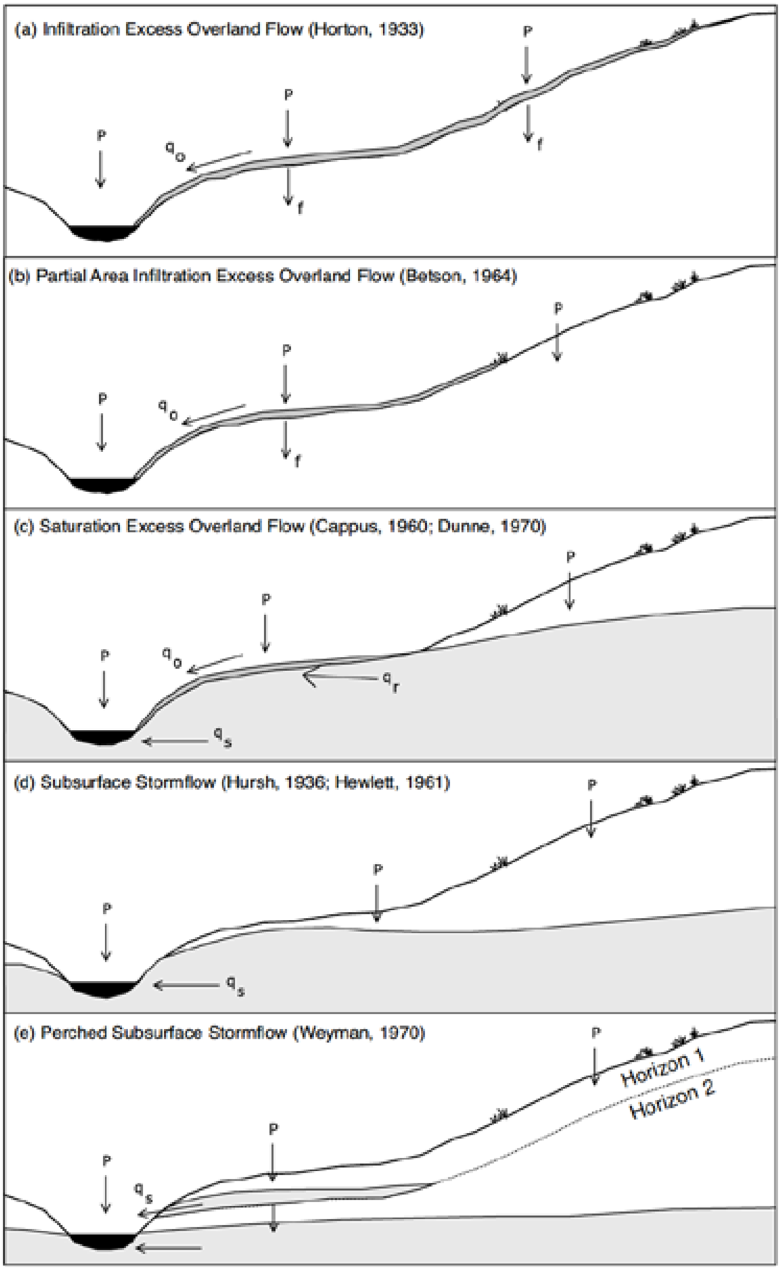

Figure 3: A classification of process mechanisms in the response of hillslopes to rainfalls (WEYMAN, 1970 in BEVEN 2012:11)

The generation of overland flow, and thus losses to infiltration in forested areas, is predominantly driven by the factors strength and duration of precipitation, vegetation cover, soil specific parameters, such as the physical conditions (inhibited infiltration capacity due to compaction or soil texture) and the hydrological conditions (water repellency due to soil desiccation). Therefore, different parts of the area are involved in feeding the surface runoff to different degrees (partial area concept after BETSON 1964 in BEVEN 2012:12; SCHÜLER 2006, BOTT 2002; BUTZEN et al. 2014). If the retention capacity is exceeded in the event of high rainfall intensity, the water from runoff generating areas will concentrate into preferred flow paths, which is accompanied by erosion processes of soil particles due to the kinetic energy of the raindrops and flowing water with subsequent superficial and rill erosion evolving (Roth 1996). The volume of runoff is directly proportional to the slope gradient and the compaction of the soil (Danacova et al. 2017). Erosion-induced nutrient export from overland flow, and thus soil and soil fertility loss (Oldemann et al. 1991), is to a significant degree provoked by only a few heavy storm events per year (Auerswald et al. 2009), which are expected to happen more frequently in the course of climate change (Butzen et al. 2014; Reiter et al. 2018). The effect on overland flow generation is expected to even aggravate, when dry periods in late spring and summer are to happen more frequently (Solomon et al. 2007), and promote soil hydrophobicity (Butzen et al. 2014). The water repellant reaction and subsequent increase in runoff coefficient is observed to be particularly severe on coniferous sites, as generally associated with the chemical composition of organic compounds released from decomposing plant litter (ibid.; Doerr et al. 2000). When undisturbed forest floors provide low erosion rates (Auerswald et al. 2009; Butzen et al. 2014), harvester tracks and forest roads show a severe increase in erosion rate due to disturbed hydraulic conductivity conditions. Therefore, they contribute profoundly to overland flow generation, sediment and nutrient delivery to the river network (Arnáez et al. 2004; Butzen et al. 2014; Eastaugh et al. 2007; Wagenbrenner et al. 2010; Croke & Hairsine 2006). This erosive potential is even enhanced on cut-slopes (Arnáez et al. 2004; Butzen et al. 2014), and also on sites with low vegetation cover such as afforestation sites or clear-cuts, as well as with decomposition regimes showing hydrophobic compounds due to plant litter species characteristics (Doerr et al. 2000; Greiffenhagen 2005).

2.1.2.2 Water in the saturated zone

From the water stored within the soil zone, the major part is eventually returned to the atmosphere through actual evapotranspiration. The part that eventually becomes groundwater recharge depends on many factors, such as the depth of the water table, the soil and aquifer properties (Todd & Mays 2004). Once the percolating water reaches the saturated zone, it fills the interconnected cavity systems. It can stay there for geological periods of time in which it is not involved in the water cycle anymore, as so-called connate water. The long residence time favors the establishment of chemical equilibria for certain processes, such as sulphate reduction (cf. Baumgartner & Liebscher 1990:406). Vadose water on the other hand is geologically young groundwater that can take long flow paths in secular periods of time, but still takes part in the general water cycle (Höll 2002). The vadose groundwater may become spring flow or discharge into streams and leave the watershed as output again after its underground or interflow travel (see **fig. 4**; Fohrer et al. 2016). A so-called capillary zone forms between the unsaturated soil zone and the freely swaying near-surface groundwater, which is, in case the groundwater level is high enough, in contact with the plant roots and the atmosphere and is therefore characterized by rapid circulation. This can lead to seasonal fluctuations in pollutants introduced to the groundwater body, such as nitrogen compounds. A shallow depth to the water table can also promote waterlogging of the ground in periods of wet weather (cf. Heath 1983:10). The capillary zone forms a transition to the saturated zone, whereas its degree of saturation decreases from bottom to top (cf. Kolymbas 2019:45). The water within the saturated zone is rather confined instead of free, and prevented from capillary ascent as a result of the separation by a low-permeability intermediate layer, the confining bed (cf. ibid.:407; cf. Heath 1983:6).

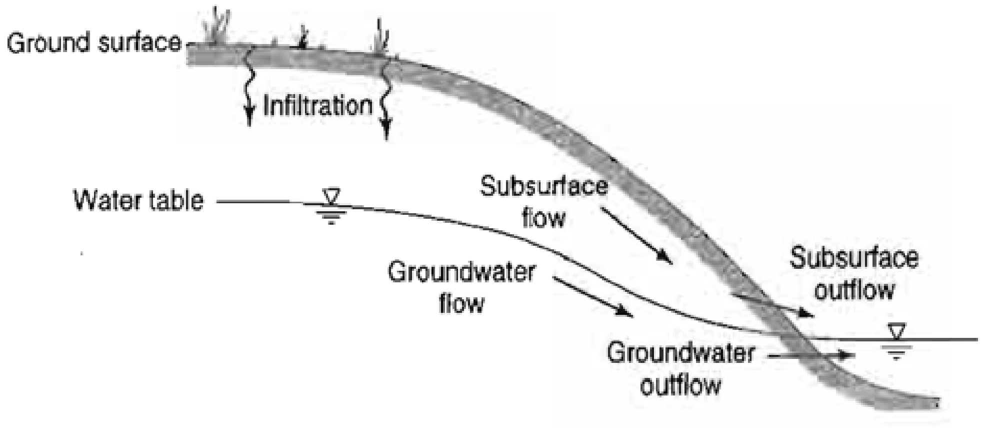

Figure 4: Subsurface outflow (Source: Todd & Mays 2004:125)

In contrast to free groundwater, the groundwater in the saturated zone has a higher hydrostatic pressure and is dominated by laminar water movement, determined by the slope of the groundwater pressure surface and the hydraulic potential field within the aquifer (Fohrer et al. 2016). It therefore depends on the conductivity properties of the rock layers (Höll 2002; Heath 1983). Depending on the hydraulic conductivity of the rock, more or less conductive aquifers, aquitardes or aquicludes form, which can occur in alternating storeys, forming the groundwater-system (see **fig. 5**; Anderson & McDonnell 2005).

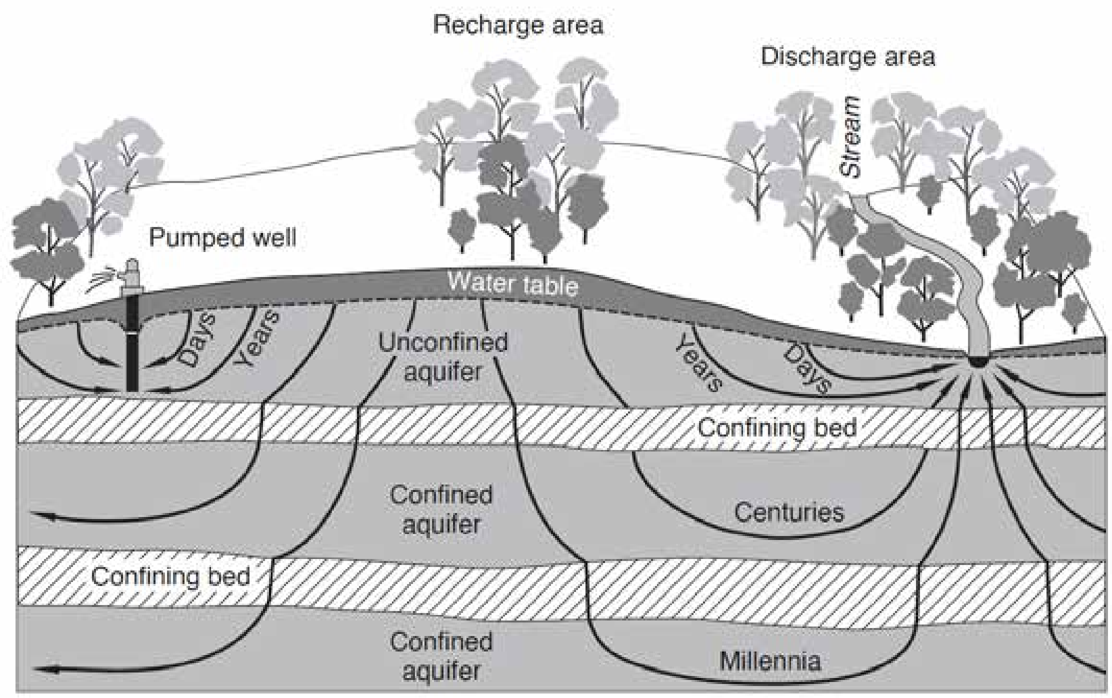

Figure 5: Groundwater system showing generalized flow paths of groundwater movement and the relative age of the water since the time of recharge (source: Anderson & McDonnell 2005:2218, modified from Heath, 1983 and Winter et al., 1998).

It stores water in the extent of its porosity and transmits water from recharge areas to discharge areas (Heath 1983:14). The volume of water supplied to the saturated zone of a certain area per unit of time is called groundwater recharge rate, or groundwater formation G (cf. Baumgartner & Liebscher 1990:411). Its water balance equation applies as follows (cf. Fohrer et al. 2016:103):

$$G = P - (I + E + T) - R_S + R_{sub}) - \Delta S = Q_B$$

Formula 2.1.4

P = Precipitation
I = Interception
E = Evaporation
T = Transpiration
R_S = Surface runoff
R_{sub} = Subsurface runoff
ΔS = Storage change
Q_B = Base flow

For the climate of temperate forests, continuous rainfalls usually occurring in the period without vegetation effectively produce groundwater formation, whereas within the vegetation period, most of the infiltrating precipitation water is evaporated or flows as interflow directly to receiving water bodies (Baumgartner & Liebscher 1990).

The concentration of solvents in the groundwater, and therefore its quality, depends on the chemical composition of precipitation, the integrity of soil filter functions, the mineral composition of the aquifer itself, and finally the solubility, toxicity and density of the respective pollutant (cf. Heath 1983:66). The distribution of pollutants is governed by the distance between the point of entry and a discharge area, the penetration depth into the groundwater body, and their residence time (cf. ibid.:67). Groundwater purification requires either extended periods of time or high expenses, both making the protection of the health-beneficial resource imperative against the background of an emerging global water crisis and the deterioration of ground water quality (Heath 1983; Höll 2002; BMU 2008).

Assuming the equation of continuity,

$$\frac{dq}{dz} = \frac{-d\theta}{dt}$$

Formula 2.1.5
Fohrer et al. 2016

q = Volume flow [m²/s]
z = Depth [cm]
θ = Water content [Vol.-%]
t = Time [d]

which says that inflow and outflow over an area A are one-dimensional, so that the flow of water results in an equivalent change in the water content in the soil (mass conversation, input = output), the following becomes apparent for the hydrological balance of the soil zone (Baumgartner & Liebscher 1990:396):

$$P = I + E + T + R_S + R_{sub} + G + \Delta S$$

Formula 2.1.6

P = Precipitation [mm]
I = Interception [mm]
E = Evaporation [mm]
T = Transpiration [mm]
R_S = Surface runoff [mm]
R_{sub} = Subsurface runoff [mm]
G = Ground Water Recharge [mm]
ΔS = Change in soil water content [mm]

2.1.2.3 Water in the stream flow

Once overland flow, emerging lateral and baseflow has collected in small channels and finally merged into streams, its flow is determined by gravity. Its volume, as well as the discharge hydrograph, follows the temporal, seasonal dynamic patterns of the flow regime (Fohrer et al. 2016; Malcherek 2019). The flow rate depends on the respective water volume of the runoff, the slope gradient, the channel dimensions and the river bed structures (Jürging & Patt 2004). Depending on the depth of the water, the flow velocity is the more unevenly distributed across the cross-section of the water, the more irregular the profile of the river bed is formed (Baumgartner & Liebscher 1990; Jürging & Patt 2004). The differences in the flow velocity promote the formation of secondary flows (Jürging & Patt 2004) and channel retention (Fohrer et al. 2016). The latter leads to the fact that discharge extremes, such as flood waves, are softened in their peaks (ibid.). In case of storm runoff generation with hillslope forces involved, however, the stream hydrograph responses with rapidly increasing stream discharge (Singh 2002). The movement of a flood wave in a river is governed by the friction of the bottom and the slope gradient, or gravity powering downstream and parallel to the free surface (Lighthill & Whitham 1955; Singh 2002). An increased runoff thus leads to higher flow velocities in the river bed (Jürging & Patt 2004), so that natural stream networks are fluctuating in their shape depending on transport and deposition of sediments within the given flow magnitudes (Fohrer et al. 2016). Both, the morphology of rivers and the sediment transported within them, are exposed to these dynamic forces, which all together determine the erosive or accumulative potential. In the event of a flood runoff, natural rivers flow out into the floodplain, so that the flow rate decreases and the aboveground and underground water and sediment retention increases. Alluvial areas therefore fulfill important functions of water and nutrient retention (cf. Jürging & Patt 2004:9). These dynamic processes promote a varied relief and increase the structural diversity and quality of living space. With high turbulences, high oxygen saturation and almost stenothermic temperatures in smaller channels, this habitat is also a vital thermal retreat for many organisms (ibid.).

Straightened and paved riverbanks show strong deep erosion, which causes the profile to deepen. In that case, the floodplain is increasingly decoupled from the flooding dynamics of the body of water, so that it can no longer fully fulfill its ecological functions (BMU & BFN 2021), with negative effects such as flood generation and eutrophication of water bodies.

2.2 The concept of ecosystem services and their operationalization

Structures, processes and functions of ecosystems that are associated with benefits for humans and therefore cover human usage requirements are understood as ecosystem services (Costanza et al 1997; MEA 2005; TEEB 2010).

The concept of ES combines socially traditional values, such as provision of services with ecological functions, in order to create a communicative vehicle that visualizes the value of services provided gratuitously by nature, and to raise social awareness for the need to maintain sustainable usability of the natural balance (TEEB 2010). The benefits that nature provides can thus be assigned to certain value categories: They can be consumed directly or indirectly, and they can be associated with utility-dependent (use-value) or utility-independent (non-use-value) use values. They therefore also cover non-material levels such as recreational, spiritual, aesthetic or psychological values (see **fig. 6**). In contrast to the goods of economy, the value of which must be measured against criteria of the market, natural resources rather correspond to a public good. They therefore are in the risk of undervaluation and overuse. The consequences of such overuse in the form of anthropogenic impairments and overexploitation of ecosystems have been discussed internationally since the beginning of the concept of sustainability in the 1970s, and recorded in numerous statements under international and national law (UN 1992; EU 2011; Article 191 of the TFEU 2012; §§ 31 ff. BnatSchG 2009; TEEB 2010). With the idea of sustainability, preservation and improvement of ES play a key role, as ES are essential to the basic, supply and regulatory services of the natural balance for nowadays and future generations. Embedded in this historical context, the term ES was coined in the 1990ies by Costanza et al. (1997), Daily (1997), Ehrlich & Mooney (1983) and others, and more recently by the Millennium Ecosystem Assessment (MEA 2005) and the TEEB-Study (The Economics of Ecosystems and Biodiversity, 2010). The approach is considered systemic, because it reflects the complex, dynamic character of multi-organismic ecological relationships, as changes or impairments of the individual members consequently lead to a change in the overall system (cf. Mainzer 1999:11). The complexity of this causal network requires that statements about future developments of the ecosystems are inevitably associated with great uncertainties, since a large number of often as yet unknown effects and factors shape the processes in a chaotically dynamic way (cf. MITCHELL 2008:123). This gives the precautionary character as well as the value categories option and existence value special importance against the background of intergenerational justice. Against this background, improving knowledge of ecosystems and the complex services that they provide for mankind are crucial for science in order to understand how to protect them and how to deal responsibly with them. Although there is broad consensus on the need to advance efforts in this field, the approaches to assessing ES are characterized by great heterogeneity, since the assignment of values is a priori normative and historically embedded. The respective selective interest, which is inevitably a purely human connotation of what is considered a reference state of ecosystem functioning, therefore determines whether the code of values is more ecologically, economically, socially or ethically justified (OTT et al. 2016). Until now, there is no systematic classification of ecosystem processes or well-being (including the contribution of nature) on global scale that allows a systemized measurement of linkages between intermediate components and ES. At the European level, the CICES project uses a Cascade Model developed by POTSCHIN & HAINES-YOUNG (2011, 2016), which does not cover interacting and overlapping ecological functions and underpinning structures and processes, as their classification would oversimplify biophysical complexity (cf. POTSCHIN & HAINES-YOUNG 2011:580). As final ES are considered to be derived from living structures and processes, the question inevitably arises how to deal with abiotic ecosystem outputs. The model is, however, in the critic to be too linear of a conceptualization, as it limits its definition of value only on elements that people perceive to have direct benefits and are willing to pay for (COSTANZA et al. 2017:5).

Based on the complex fact that several ecosystem services can arise from one ecosystem function, while at the same time several ecosystem functions can be required to create a single ecosystem service (cf. COSTANZA 1997:256 in ESER et al. 2014:70), the economic value followed in the TEEB concept (**fig. 6**) is questioned to be suitable to capture the value of nature as a whole.

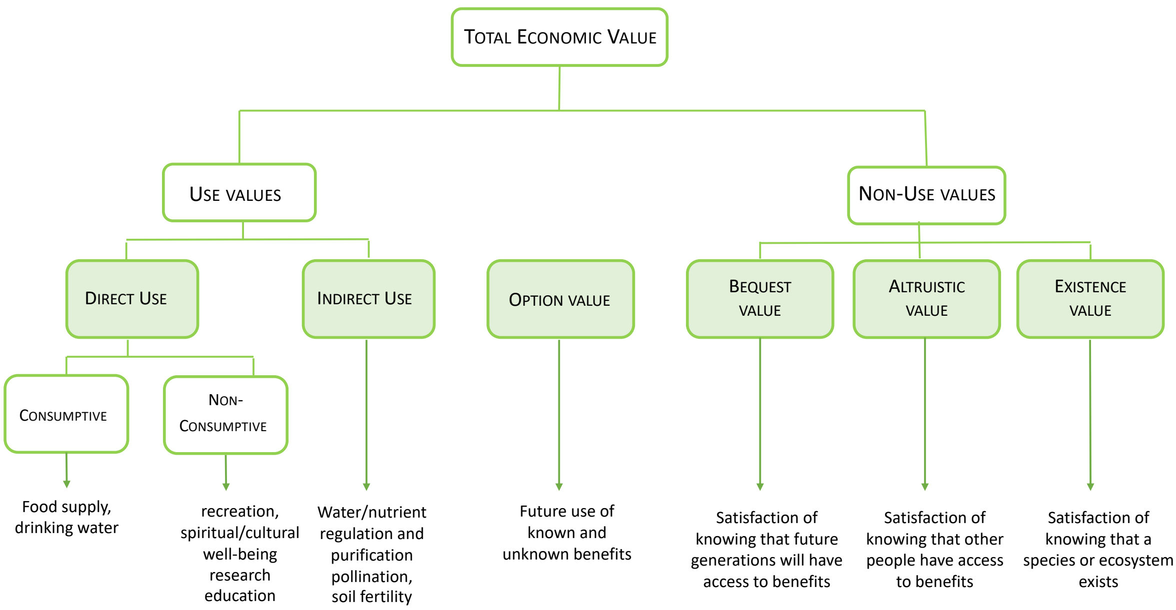

Figure 6: The Total Economic Value and ES value categories (after TEEB 2010).

It therefore rather ought to be understood as a minimum value to indicate the necessity of political action (Eser 2014, Bateman et al. 2011, Mace et al. 2011). This illustrates the difficulty in identifying and evaluating ES, and consequently the wide range of different approaches: Services of an intrinsic, altruistic or subjective nature that cannot be described as productive in themselves but can be assigned to human well-being, are difficult to quantify or generalize. In order to translate the heterogeneity of the approaches and definitions into a practically applicable general usability of the term and to make it operational, a transdisciplinary, holistic view of ES is to be aimed. This includes the development of indicators for the standardization of assessment parameters (cf. Ibisch et al. 2012:139; Albert et al. 2015, Potschin & Haines-Young 2011, Bordt & Saner 2018). Hence, to derive water-related ES of the forest, and their operationalization, this work emphasizes a holistic perspective to describe how the ecological intermediate components of the forest are linked to service outputs and how sensitive these outputs are to anthropogenic pressure, without the selective consideration of certain individual interests or an economic valuation. In the frame of the holistic view, a stepwise disaggregation of ES and linked benefits is pursued, since the complex interdependencies exclude an isolated view (cf. Bortd & Saner 2018). As the regulative processes are basal in character, they overlap in their benefit with provisioning and other levels of ES, so that some of the underlying processes could be considered to be in the risk of double counting.

Regarding this topic it must be noted that the derivation of ES is multifactorial due to the high level of interactions, and therefore double counting effects must be considered against the background of ecological complexity. In this sense, they could rather be considered as alternative proxy to measuring some direct services, not in addition to them (Costanza et al. 2017:6; **fig. 7**). In terms of a gradual valuation, processes that

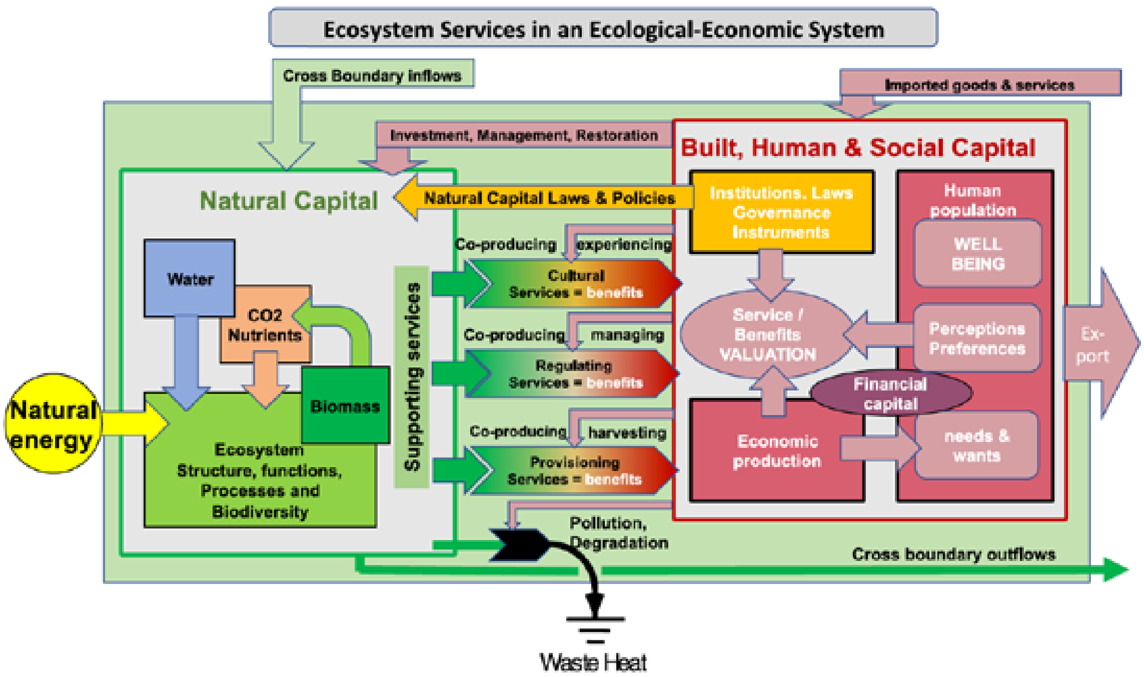

Figure 7: A dynamic system capturing the complex interactions needed to produce ecosystem services at the regional scale, driven by the flows of energy, matter, and information through the system. (source: Costanza et al. 2017)

are multiply involved and requisite in character might even be rated as a priority in the decision-making process of necessary measures of action. Furthermore, the exploration of how intermediate components are correlated with ecosystem services provides a simplification for quantitative assessments (cf. ibid). Based on the ideas stated so far, the classification approach of Schröder et al. (2012) is followed, which combines a broad applicability (ES of the forest in general) with the local case-specificity (place-based) of the study area from both a biophysical and a societal point of view (cf. Schröder et al. in Ibisch et al. 2012). Based on the primary values of intermediate components, which cannot be substituted or determined through human preferences and therefore cannot be economized (cf. Eser 204:69), indicators are defined that depict their functionality (specified for water-related ES of the forest, see **fig. 8**). The production chain implemented from Boyd & Banzhaf (2007) derives a benefit specificity, which flows into the final services that are related to well-being factors of the stakeholders connected to them. The different levels serve to clearly distinguish between ecosystem function, ecosystem service and benefit, show relevant interactions and can be expanded with qualitative values. The selection of the indicators should reflect the study area and depict the data material. It must also be suitable for assessing the integrity of the structural components in terms of healthy interactions, because this is the prerequisite for them to fulfill the human demand for natural products and processes (cf. Müller et al. in Chicharo et al. 2015:11). The parameters influencing the indicators, and possible consequences of their changes should be part of further analysis and continuous specification, and therefore should be appliable in long-term scenarios to fulfill the temporal demands (Hansjürgens et al. 2012; cf. Müller et al. in Chicharo et al. 2015:12). Furthermore, the indicators should reflect an intersubjective perspective on human action linked to environmental pressure and be transferrable to different value dimensions (qualitative, monetary, preference-based) in order to allow transparency of the decision process and mediate between different preference parties.

This study, however, primarily focuses on the services provided by forests with regard to the underlying water-balance-related intermediate components and the possible consequences of human activities on them. In line with the sustainability principle, their indicators are nature-oriented, theory-based and interdisciplinary in character (Wiggering & Müller 2003). Qualitative indicators, such as cultural significance, recreational function, the intrinsic value of nature, as well as monetary derivations in the form of willingness to pay to maintain the same, must be evaluated with a socio-economical-based approach and are only recorded schematically here. As part of a holistically based approach, the assessed intermediate components interact on all levels of derivable services. They are embedded in the multidimensional context of the totality of ES of the forest, which will be discussed in section 6 with respect to possible recommendations of actions.

2.3 Water-related Ecosystem Services of the forest

Temperate forests are determined by the climatic factor air temperature, characterized as moderately humid, with sufficient summer rain and markedly cool or cold winters (Whittaker 1975). Seasonal variations in air temperature and precipitation patterns dominate catchment hydrological conditions, such as evapotranspiration, soil wetness, groundwater level and discharge, and thus influence the biogeochemical dynamics of the ecosystem, plant physiology and soil microbe activity (cf. Delphis et al. 2011:262). Due to this complexity and the highly dynamic flow variation, temperate forests are a research object of high interest, not only for researchers but also for governments in terms of practical importance regarding flood management or the provision of drinking water in high quality and quantity. Hydrological studies of temperate forests were therefore not only conducted for biogeochemical and ecological investigation purposes, but have implemented those practical issues alongside.

Forests are based on complex networked processes, functions and structures with a vast variety of known and unknown relationships. It is important to understand the complex relationships between the components in order to be able to quantify and describe the interactions between natural processes associated with human well-being and include them in decision-making processes. As in the context of this study forest functions are analyzed that build the basis for the provision of water-balance-related ES, the focus is on regulative and provisioning ES and their intermediate components. Regulative ES unfold their benefits to human well-being through the regulation and control of biotic and abiotic factors of natural processes. The latter are defined as the complex interactions of ecosystem elements regulating the fluxes of information, energy and matter, and supporting the intactness of the ecosystem (cf. Chicharo et al. 2015:18; cf. Mace et al. 2012, Puydarieux & Beyou 2017 in Brockerhoff et al. 2017:3009). Regulative ES thus form the basic precondition for all services that can be derived from an ecosystem, but are at the same time not well pronounced in social awareness and consequently under-evaluated in public recognition. Provisioning ES are directly attributable to the antecedent regulative ES. Their focus is, however, more on human beneficial aspects arising from the natural functions and processes. They unfold their benefits on a rather socially anchored level and are consequently more pronounced in public recognition, especially due to the fact, that monetary values can be assigned to them. As the challenges that go alongside climate change intensify the public awareness about the necessity of flood control and water supply, they gain relevance within the political and public debate. An overview of the water-related ES forests provide is given in **figure 8**.

2.3.1 Water-related regulative Ecosystem Services of the forest

Water-related ES of the forest are predominantly correlated with the regulation of the water cycle, soil protection and habitat functions. In the following, water-related ES of the forest and their intermediate components are described as well as the parameters that reflect them. Furthermore, the forest-specific contribution to those ES is highlighted.

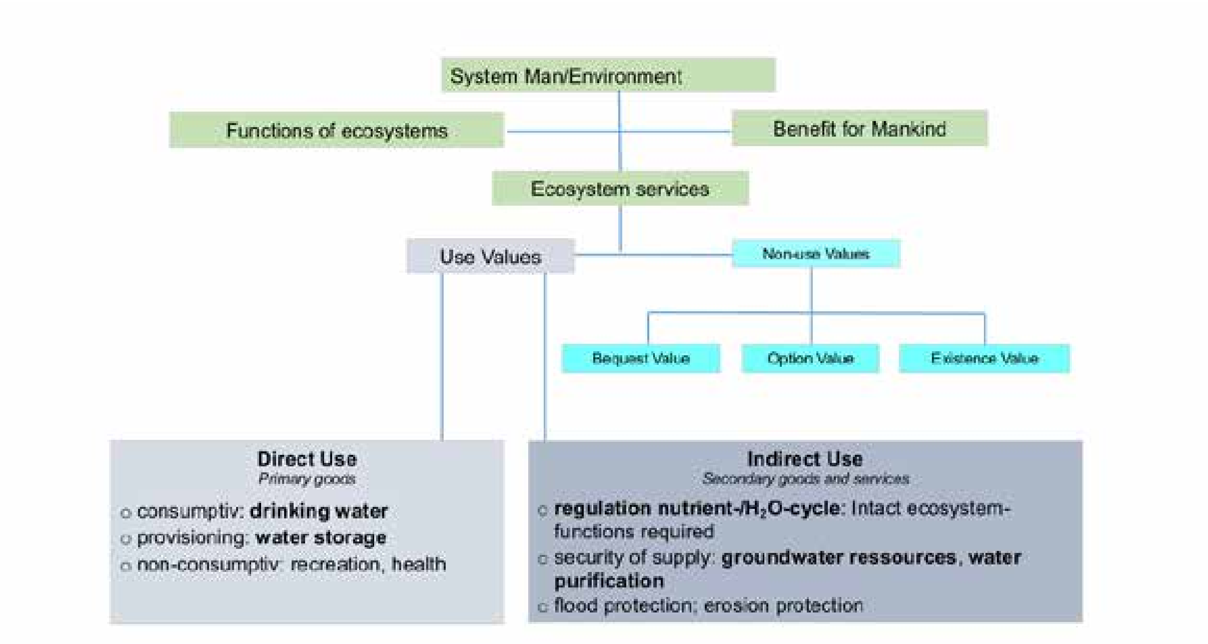

Figure 8: Water-related ES of the forest (modified after TEEB 2010)

- **Water and nutrient cycle regulation function:**
  Forests have a crucial impact on the hydrological cycle regarding the flow regime and runoff behavior, and therefore water delivery to streams and groundwater in terms of magnitude and timing. Through buffering and retarding the precipitation water, the forest counteracts runoff peaks, and promotes seepage and deep groundwater formation (Schüler 2006; Engler 1919, Günther 1979, Schwarz 1985, Hegg et al. 2004 in Nordmann 2011; EEA 2015; Bott 2002). This water retention function goes back to elementary physical-chemical, biological and structural components: A significant amount of precipitation water is retained by the forest canopy (canopy storage) through interception, and from there either drips down (canopy drip), flows down the stem, or eventually evaporates back into the atmosphere. Consequently, a large amount of water is lost to soil moisturization, subsequent groundwater formation or runoff (Peck & Mayer 1996; EEA 2015). Next to the water pressure deficit of the air, which drives evaporation processes, the species-specific phenological architecture (canopy, stem, leave roughness) and the phytomass value of the stand (determined by stand age, height, site quality class and stand density) influence the amount of water loss to leaf surface areas. Structural stand components therefore affect the quantity of groundwater formation at a given precipitation intensity significantly (Müller 2011; Klimenko et al. 2020). As a result, forests develop a negative water balance during the vegetation period, which is compensated for in the rainy winter months when the transpiration rate is lower and the canopy of deciduous trees is bare of leaves (Nordmann 2011)[3] . Through the canopy, the precipitation is distributed irregularly within the stock and the impact energy of rain droplets is softened. This causes a reduction of the erosive potential (Nordmann 2011), and results in reduced surface erosion with consequently low sediment and nutrient yields to water bodies (Neary et al. 2009). The larger and the denser the canopy of a stand is, the more water is held back and the more pronounced the retarding effect on the runoff is. Additionally, the litter layer dissipates the raindrop energy and prolongs infiltration (ibid.). Also, by forming a deep root system, trees are able to withdraw water from deeper soil layers through transpiration and make these soil layers available for water storage again (cf. Nordmann 2011:35).

  Runoff generation depends on the intensity (amount per unit time) of precipitation, on physical soil properties with respect to humus characteristics, hydraulic properties of the soil horizons (being related to soil texture, bulk density, pore system and preferential flow paths associated with root growth and biological activity), as well as on the bedrock underneath (Schüler et al. 2002; Nordmann 2011). The humus fraction contributes to water storage through its adhesive, water-binding properties, and due to the fact that decomposition and humus formation increase the pore space significantly (Hammel & Kennel 2001)[4] . A prerequisite to humus formation is given through proper living conditions for biological activity. The soil biota drive the metabolization and transformation of organic matter, shapes the pore space and thus preferential flow paths, and therefore significantly contribute to faster percolation towards the gravitational poten-

3 Delfs et al. (1958) quantify the interception storage of coniferous stands (spruce) to be around 4 mm/ha of precipitation, Benecke & v.d. Ploeg (1978) verify 2.6 mm for beech trees (cf. Nordmann 2011:36), and Gerrits et al. (2010) state 18 % of average canopy interception in leaf-on beech stands (5 % in leaf-off period) (Butzen et al. 2014). Klimenko et al. (2020) cite 5-8 mm/ha of rainfall interception in forested areas, depending on stand characteristics.

4 The organic layer can store up to 1.5 - 4.5 times more water per gram of soil substance than mineral soil (Leuschner 1998; Schäfer et al. 2002; cf. Nordmann 2011:35).

tial. The large void capacity of the organic soil layer also provides a higher gas exchange and therefore increases evaporation, which subsequently gives free water storage space in turn. The higher the infiltration capacity and hydraulic conductivity of the soil is, the higher the retention capacity of the site. Deep, permeable soils show the best peak-flow-delaying performance (cf. Schüler 2006:100). As the permeability is also correlated to the soil´s clay content, clayey soils drain slower and therefore are in the risk of generating runoff with given rainfall intensity (ibid.). Forest soils formed under humid climate conditions generally show a rather low bulk density and therefore drain sufficiently enough to mitigate runoff, as long as their water storage capacity is not exceeded and the infiltration capacity isn´t inhibited by compaction due to the use of heavy harvesting machinery (ibid). According to Bott (2002) and verified by the study of Reichardt (2002), the void capacity of a soil is directly correlated to runoff, as speed and intensity of the latter increase with lower void capacity.

Next to the soil hydraulic conditions and climatic factors the structural and phytocoenotic components of the vegetation layers (overall forest cover area, leaf area index, density of tree individuals, age, height and diameter, tree species composition) are a major influence on the retention potential, and therefore forest-management operations play a key role for retention capacity. Changes in water yield within a watershed can be observed to be immediately responsive to forest-management activities (Zhang et al. 2001; Riekerk 1989 in EEA 2015). The impact of forestry practices is, however, very site-specific, as the runoff-processes are highly site-dependent. Also, a distinction has to be made between areas where discharge develops as a contributory factor due to water saturation, and areas considered as runoff-generating, corresponding precipitation and site conditions provided (Schüler 2006). Decreasing runoff-generating areas and transforming them into contributing areas are therefore an essential task of precautionary forestry management to improve the beneficial effect of the water regulative ES of flood control and protection forests can provide (ibid.). The effect of clear-cutting on accelerated overland flow due to decreasing plant water use is reported in many studies (Moltschanov 1966, Hibbert 1967, Voronkov et al. 1976, Hoffmann 1982, Rosemann 1988, Bennecke 1992, Moeschke 1998, Mendel 2000 in Schüler 2006; Peck & Mayer 1996).

Forests also unfold essential water purifying services based on the filter function of the soil by adsorbing nutrients and pollutants, and thus lower their concentration in seepage water (Keestra et al. 2012). The underlying processes of water purification are closely linked to the carbon and nutrient cycles. They are highly dependent on biogeochemical factors that influence lithogenic and organic soil constituents (cf. Mueller et al. 2012:602). Chemical properties of the plant litter that influence the pH, mineral dissolution, cation exchange capacity, and concentrations of Al and Fe within the soil solution, affect the microbial community composition and exoenzymatic activity, and thus the retention of soil organic C and N (cf. Mueller et al. 2012:602). Tree species influence the intrinsic characteristics of soil organic matter, soil acidification and availability of hydrolyzing cations such as Al and Fe (Gruba & Mulder 2015), as well as nutrient concentrations and nutrient storage in wood and roots (Mueller et al. 2012). Their composition plays a key role in the effectivity of water purifying processes in the forests. The so formed chemical soil environment influences the biotic species diversity, which determines the decomposition rate and effectivity. Pure coniferous forest stands form an acidic litter that intensifies the processes of soil acidification (Mueller et al. 2012; Gruba & Mulder 2015; Bredemeier et al. 2011). The chemical soil environment, however, is also sensitively affected by the entry of potential acid formers, and so are chemical exchange processes, cation exchange capacity and nutrient supply of the stocks. Due to persistent N accumulation in the soil, many forest areas in Europe have already reached nitrogen saturation, which subsequently leads to a progressive increase in nitrate leaching into the groundwater and spring water (Bredemeier et al. 2011:103). The retention of precipitation in the canopy must be considered to significantly increase the concentration of dissolved nitrogen compounds in the stand precipitation (Eugster & Haeni 2013; Bredemeier et al. 2011). Also, many sites are "contaminated" in the form of stored sulphate from the high sulfur inputs of the last century, so that in connection with the base removal from wood harvest and the leaching of basic cations as a result of soil acidifying effects, no adequate buffering of the acid load can be expected.

- **Soil protection function:**
  Functioning as well as productivity of forest ecosystems is strongly interrelated to soil properties, form of humus and carbon cycling manifestation (Dixon et al. 1994). Under natural, undeteriorated conditions forest floors provide the fundamental functions of soil formation by decomposition of accumulated organic material and the subsequent release of nutrients into the soil environment (Fabiánek et al. 2009). They contribute to erosion prevention predominantly through control of overland flow generation (vegetation and litter cover, soil specific parameters such as soil moisture and compaction due to heavy machinery) (cf. Butzen et al. 2014:202).

  In the process of decomposition, mineralization and humification different levels of decomposition regime bring about a structural heterogenous pore system with an accordingly high variety of macro- and medium-pores (Neary et al. 2009). Especially against the background that forest floors usually tend to be low in clay content and pH level, the soil organic matter (SOM) becomes important for maintaining the cation exchange capacity (CEC), by retaining essential cations, and thus supporting forest productivity (Grigal & Vance 2000). The dynamics of decomposition are driven by the quantity and the fractional composition of annual falling debris (AFD), and therefore by the phytocoenosic composition, the pedo-ecological conditions influencing the decomposition rate (biological activity of the edaphon, C:N ratios, base saturation stage), soil chemistry as well as climatic and microclimatic conditions (Kõlli 2017). Quantity and fractional composition of AFD depend on the tree species composition on the stand: The litter of deciduous trees is rich in basic cations and promotes decomposition and alkaline rich humus formation. Deciduous tree stands open up the canopy to direct throughfall in winter by shedding their leaves and thus enhance AFD quantity and quality. Coniferous trees on the other hand produce a rather acidic litter (Nilgård 1971; Gruba & Mulder 2014; Lelong et al. 1990 in Bredemeier et al. 2011) due to slow decomposition rates of their needles (Kõlli 2017). Monocultural spruce stands show lower pH values and base-exchange compared to beech stands, as well as a lower C:N ratio, which is associated with enhanced nitrogen wash-out from the ecosystem (Emmer 1998, Emmer et al. 2000, Emmett et al. 1998 in Fabiánek et al. 2009; Ulrich 1983). Both, chemical soil properties, implying the composition of the organo-mineral horizon, stand trophy and biodiversity, as well as physical soil conditions, implying the permeability for air and water, are a prerequisite to the soil habitat function for biological diversity and thus activity. At the same time the soil pore system formation is reciprocally being shaped by edaphic biota, so that the vitality of the latter is an essential part of the soil function integrity and water-conducting properties. The soil biota therefore must be included in the conceptualization of indicators linked to regulative intermediate components of water-related ES. Being incorporated into the chemical flows of the saturated soil zone, and as a major driver of soil acidification enhancement, nutrient inputs from air deposition are involved in the control, metabolization, recycling and storage. They therefore indicate nutrient regulation and water purification services.

- **Habitat function:**
  Soil organisms, and therefore the prerequisite to their living conditions, play a vital role in the decomposition process, release of plant-available nutrients (mineralization), and enhancement of soil structural characteristics linked to the soil water and air continuum (Grigal & Vance 2000). They must therefore be considered a major driver in the fluxes of water and nutrients (Canessa et al. 2020). As soil biota are involved in the process of aggregate formation (Jastrow & Miller 1990)[5], they stabilize the soil against rainfall droplet energy. This prevents soil crusting and detachment, and contributes to a higher infiltration rate (Neary et al. 2009). The ecological distribution patterns in plant and animal communities are sensitive to microclimatic conditions (temperature, moisture, wind, and light), and thus determined by structural features in the course of silviculture (stocking density, overstorey coverage, and species composition). They are therefore highly site-specific (Chen et al. 1999; Canessa et al. 2020). Dry conditions, especially with soil water contents below field capacity, inhibit decomposition rates (Canessa et al. 2020), which might become crucial for forest site nutrition supply throughout drought periods within the vegetation period. Next to abiotic factors, the litter composition and its chemical traits determine litter decomposability, chemical-enzymatic splitting and thus nutrient accessibility for decomposers (Canessa et al. 2020). Therefore, silvicultural factors such as tree species composition, and stand structural aspects affecting soil moisture also influence decent living conditions for and productivity of soil organisms. Linked to the flowing regime quantitatively through aggregate formation, and qualitatively through plant nutrition and nutrient cycling, adequately intact habitat functions are indispensable for water-related ES such as water retention, soil formation, erosion protection and eutrophication prevention.

2.3.2 Water-related provisioning ecosystem services of the forest

As a direct consequence of water regulating processes related to forest ecosystem functions, forests provide the benefit of water storage and the primary good of clean drinking water. The latter has gained attention in the drought summer periods of 2018, 2019 and 2020, when public recommendations restricted water consumption beyond essential needs (NLWKN 2020). In summer 2021, drought was washed away by heavy storm events, and the disastrous flooding in western Germany. When researching the causes of this catastrophe of the century, the decentralized flood protection forests can provide gained attention. In both cases, provisioning ES are involved, that do unfold monetary dimensions. In the following, those services and their benefits are described.

- **Drinking water supply**
  Delayed discharge processes, enhanced infiltration, and chemically intact exchange processes based on vital soil functions, including the diversity of pedocenoses, enable forest soils to convert the water they take in and pass on to the best drinking water quality.
  In Germany, around 70 % of the water supply is covered by groundwater (BMU 2008; StatLa RLP 2016; UBA 2022[6]). The water resource is used as drinking water, industrial process and cooling water or for agricultural irrigation.
  The situation is similar throughout European

[5] Through metabolizing nutrients in the soil, saprobic fungi interlink and glue soil particles due to their excretion products and growth habit (Lehmann & Rilling 2015).

[6] https://www.umweltbundesamt.de/daten/wasser/wasserwirtschaft/oeffentliche-wasserversorgung#grundwasser-ist-wichtigste-trinkwasserressource (21.4.2022)

countries – one third of the total water supply is sourced from groundwater (OECD 2018 in Riedel & Weber 2020). With respect to the density of population, decreasing groundwater tables have a large socio-economic impact on European societies.

According to the technical implementation of Article 5 of the Water Framework Directive (WFD) and Directive 2006/118 / EC (protection of groundwater against pollution and deterioration) by the Groundwater Ordinance (GrwV) (Federal Law Gazette I p.1044), a nationwide uniform assessment of the quantitative and qualitative status of groundwater bodies is checked regularly (every 6 years) (LAWA 2019). Current measurements (from 2016) show that only 4.2 % of the groundwater bodies in Germany fail the "good quantitative State " (LAWA 2016). The groundwater resources regarding the yield are, however, irregularly distributed throughout Germany (see **fig. 84**, app). There are areas with a lower resource yield, which are therefore more prone to supply shortfall: In the dry years of 2018 and 2019, for example, the pressure of use and climate change led to a lowering of the groundwater measurement levels in the state of Lower Saxony (NLWKN 2020). The trend with below-average climatic water balance and falling groundwater levels, which has been ongoing since the early 2000s, is a result of increasing annual mean air temperatures and increasing evaporation values due to climate change (MU/DWD 2018 in NLWKN 2020). Extreme events such as droughts and floods are to be expected more frequently, so that the changes observed so far in the trend are likely to continue (MU/DWD 2018, Scheihing 2019 in NLWKN 2020). But, also in areas with more efficient yield of groundwater, falling groundwater levels are observed since the past decades (KLIWA 2017). The groundwater recharge in Rhineland-Palatinate has decreased by 21 % in 2010-2015 compared to the period 1951- 2010 (KLIWA 2021)[7]. Numerous measuring points in Rhineland-Palatinate show falling groundwater levels (see **fig. 83** app.).

According to the UBA (2017b), the detected pressure of use, however, does not exceed the groundwater reserve capacities. Enhanced plant demand due to the extension of the vegetation period (Reiter et al. 2018; see **fig. 81**), and the associated increased losses via evapotranspiration are discussed as causes (Kampf 2021; KLIWA 2017). Additionally, in the drought years 2018, 2019 and 2020, the soil water content dropped persistently (see **fig. 85** app.). As a result, the replenishment of the soil water supply to field capacity, which is the prerequisites for deep seepage, was postponed later in the year (Hermann et al. 2014). This shortened the period of groundwater formation and promoted increasing deficits for groundwater recharge due to the negative trend in the climatic water balance (MUVF 2007; Kopp et al. 2018). Though records of the past decades show a significant increase in winter rainfall (Reiter et al. 2018; Anders et al. 2014 in Riedel & Weber 2020), regional divergences that report a decrease in winter rainfall support discussions of an additional recharge loss factor (KLIWA 2017). A couple of drought years in a row may not endanger the good quantitative status of groundwater bodies, but with predictions of changed patterns of frequency and intensity of climate extremes, supply shortfall and disappearance of ecosystems may become more likely – and so does the loss of ecosystem services connected to them (Aquilina et al. 2012, McMahon et al. 2006, Jasechko et al. 2016, Havril et al. 2018, Devitt et al. 2019, Qui et al. 2019, Tran et al. 2019 in Riedel & Weber 2020). This affects not only the public supply situation with drinking water, but also groundwater-dependent terrestrial ecosystems such as beech forests,

[7] For the period 2010 - 2020 an even higher decrease of - 25 % in Rhineland-Palatinate compared to 1952 - 2010 is discussed (Kampf 2021).

wet meadows and moors. A lowering of the groundwater level leads to a reduction in the capillary rise of the groundwater and thus, depending on the depth to the groundwater table, to supply shortfall in the water demand of the vegetation.
Against this background, provisioning services from forested catchment areas for drinking water supply are of high importance due to favorable conditions for groundwater formation. Furthermore, by reducing surface runoff, and thus erosion and transport of substances into surface waters (Neary et al. 2009; Wagenbrenner et al. 2010), the financial expenditure for drinking water treatment can be reduced (Munich Re 2000), as well as for nature conservation measures (UBA 2017a). Intact ecosystem functions are, however, a prerequisite for maintaining a sustainable supply. For this purpose, not only must the establishment and maintenance of intact soil functions in the forest be achieved, but efforts to reduce nitrogen inputs from agriculture must also be intensified. Maintaining soil functionality and the associated water-related processes through forest management includes all factors that have a profound effect on the chemical and physical conditions of the soil: tree species composition, stand structure and age, harvesting methods, harvest intensity and rotation (Mueller et al. 2012; Gruba & Mulder 2015; Bredemeier et al. 2011; Keesstra et al. 2012; Schüler et al. 2002; Nordmann 2011; Leuschner 1998, Schäfer et al. 2002).

- **Decentralized flood control**
  Regarding past and current flood disasters, the high financial expense that arises from insufficient use of natural retention potentials is evident. According to the "Study on Economic and Social Benefits of Environ¬mental Protection and Ressource Efficiency Related to the European Semester", which deals with questions of the social and monetary effects of flood events in the EU since 2002, the European Commission estimates the cost of flood damage within the European Union in the years 2002 to 2013 at 72 billion €, of which 19 billion € account for Germany (EU 2014). According to the Federal Government of Germany, the cost of the flood disaster in 2013 was 2 billion € and the Elbe flood in 2002 was 1.7 billion €, with damage reports from the individual federal states totaling 6.7 billion € (BMI 2013).
  In the generation of flood disasters along major rivers, the contribution from smaller tributaries to their water volume is considerably significant (Schüler 2006). With this respect, forested areas play an important role in the spatial distribution, types and intensities of surface runoff, as they inhibit runoff generation (Moltschanov 1966, Hibbert 1967, Voronkov et al. 1976, Rosemann 1988, Moeschke 1998, Mendel 2000 in Schüler 2006). The mitigation and retarding of runoff peaks in these areas can be achieved by effective water-retention and runoff-delaying measures according to the given geological and soil factors, which need to be differentiated hydraulically (Schüler 2006). Therefore, flood-generating forest areas, or critical source areas (CSA) must be identified. Since the runoff behavior in forest ecosystems correlates with the near-surface intermediate runoff and deep seepage (Ernstberger 2000), runoff quantity and rate are largely dependent on the properties of the respective forest location (Bennecke 1992; Hoffmann 1980; Hoffmann 1982; Peck & Mayer 1996; Müller & Schüler 2021). In forests on soils with geogenically or pedogenically dense subsoil, or anthropogenically compacted topsoil, a significantly higher proportion of water flows off near the surface (Schenk et al. 2001), the smaller the pore capacity, the less thick the water-absorbing topsoil and the greater its water storage capacity is exhausted, the faster and more intensely (Müller & Schüler 2021). Since, in addition to the basic hydraulic equipment and climatic factors, the structural and phytocoenotic components of the vegetation layers also have a major influence on the retention potential, forest management (silviculture, felling, har-

vesting methods) plays a location-specific key role for establishing water-retention efficiency (Zhang et al. 2001; Riekerk 1989 in EEA 2015).

Even if retention measures in the forest only have a limited impact on large flood events on the mesoscale level (Grant 2005), every additional flood prevention measure in the microscale area leads to a reduction of harmful flood peaks, because the limited effect of a large number of individual measures adds up to a clearly noticeable reduction of the retention volume. The threshold of the latter depends on the size of the climatic event as well as on the location, soil, geology, land use and landscape features. The aim of spatial flood protection planning should be to predict the respective risk threshold depending on the damage potential in catchment areas. Flood prevention cannot be limited to forestry concepts alone. It requires the intersectoral cooperation of and integration of eco-hydrological concepts in water management, agriculture, viticulture, spatial planning and domestic politics (Müller & Schüler 2021).

Figure 9 highlights water-related ES of the forest after the holistic approach described in section 2.2.

2.3.3 Current and future challenges

Forest ecosystems are under anthropogenic pressure with wide-spread influences: Climate change induced drought periods lead to an extensive tree mortality, known as New Forest Die-off (Huang et al. 2019; Goulden & Bales 2019; Margalef-Marrase et al. 2020). Air pollution brings about altered soil conditions, severely disturbed nutrient cycles and plant nutrition, tissue damage and growth inhibition. Sinking groundwater levels and habitat fragmentation intensify the negative effects (BfN 2020b). The so promoted deficits in vitality make forest stands more vulnerable to

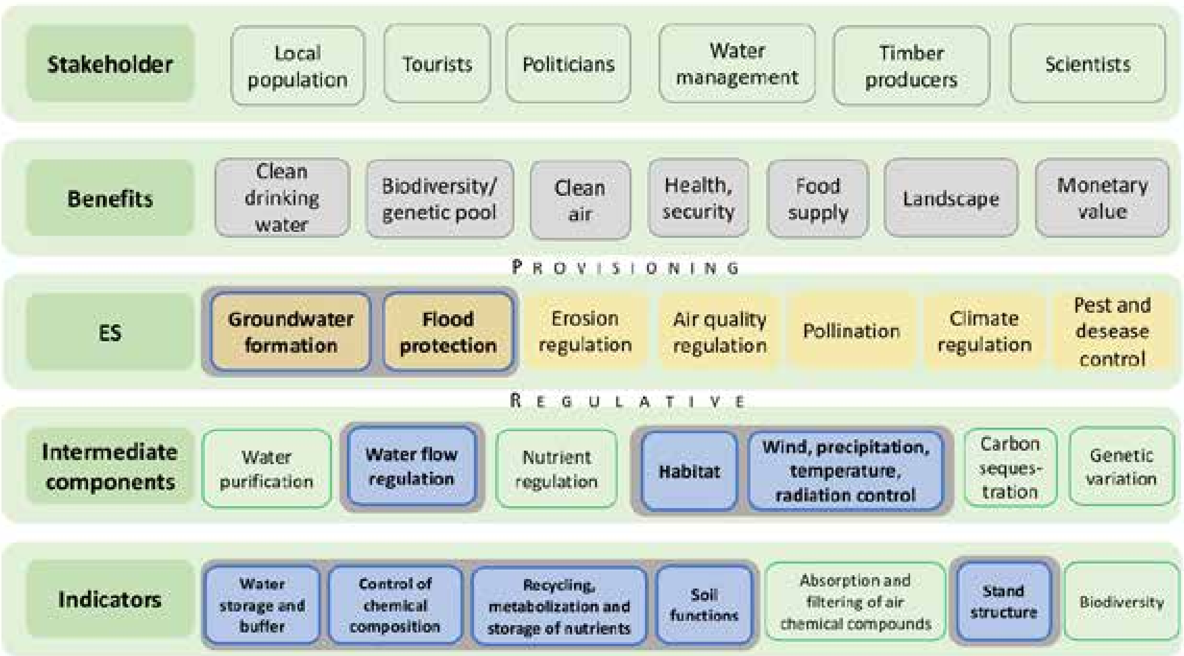

Figure 9: Highlighted water-related regulative and provisioning ES of the forest developed after the holistic approach from Schröder et al. (2012).

pathogens and pests. Exclusively growth-oriented management pratiques that alter the microclimatic conditions of the forest climate, the hydrological stand characteristics or the conditions of nutrient availability in a negative way, have a large impact on all interlocking forest functions. In the following, the challenges that go along these pressures are highlighted.

2.3.3.1 Climate change

The rapidly advancing, anthropogenically caused change in the global climate is accompanied by ecological, social and economic cuts, as well as the degradation of forest ecosystems effective worldwide. In connection with water-related ES of the forest, this can be traced back to the basic functions in the complex structure of the forest that are involved in the harmonization of the water cycle. Changes in the water balance, as forecasted by climate projections, affect both ecological and material-physical processes. Impairments to the water retention capacity (retention potential) and changes in the soil water balance are of particular interest in connection with water-related ES of the forest. With drought periods and heavy storm events in late spring and summer to happen more frequently (**fig. 10**; Reiter et al. 2020; Solomon et al. 2007), water repellency of the soil, losses to tree vitality, enhanced tree mortality. Consequently, the occurrence of bare fallen sites as consequence of calamities and windthrow are likely to increase surface runoff. Contributions to flood generation, nutrient export from the ecosystem and eutrophication risks in adjacent water bodies are possible consequences. Plant-physiological drought stress (Schröck 2020) and forest fires are also expected to happen more frequently (Bolte & Ibisch 2014).
Due to the longevity (production periods of 100 to 200 years) and the local ligation of forest ecosystems, they are tied to the environmental conditions and location factors of the respective forest stand. With a polar shift in temperature limits of 40 km/decade (Hansen et al. 2006), a

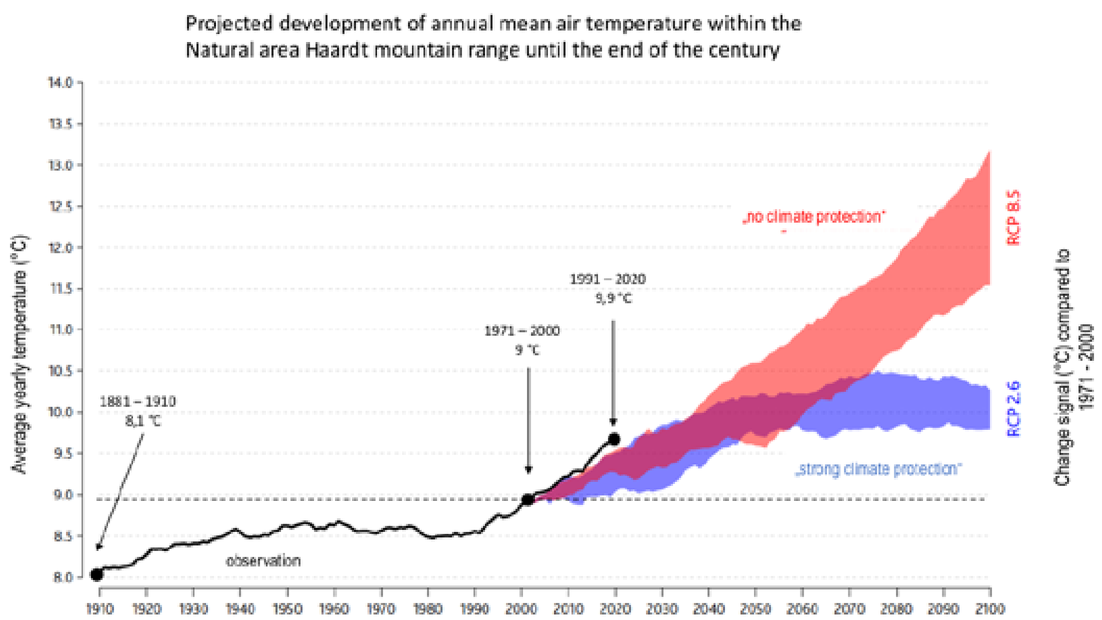

Figure 10: Projection of the future development of mean average temperature (Reiter et al. 2020). Blue area: RCP2.6 corridor ("strong climate protection"), red area = RCP8.5 corridor ("no climate protection"), pink area: overlap of both corridors.

global area shift of the habitats of certain species of 6.1 km per decade establishes alongside (Parmesan et al. 2003). The rapidly changing living conditions force long-lived species such as trees to perform evolutionary processes of adaptation beyond their abilities (Bolte & Ibisch 2014). The main drivers of the hydrological cycle in a forest ecosystem, precipitation, temperature and evaporation, are recorded to have changed and are predicted to continue so in the future. When precipitation has not changed so much in total amounts (up to 2.8 mm per decade in the period from 1946 to 1999, Klein Trank et al. 2002; Scherrer et al. 2016 in Riedel & Weber 2020), changed patterns alter the distribution and water budgets on regional scale.
With rising temperatures, the vapor pressure deficit of the air increases, and so does evaporation as well as interception, as reported from many sites throughout Europe (Duethmann & Blöschl 2018, Stanhill & Möller 2008, Trnka et al. 2015, Zhang et al. 2016, Ukkola & Prentice 2013, Teuling et al. 2019, Vince-Serrano et al. 2019 in Riedel & Weber 2020). Over-heating of the sun leaves has been reported at an increase of 3K in deciduous forests (cf. Hohnwald et al. 2020:12). Extreme heat waves in summer are observed to increase the susceptibility to tissue damage on old trees and the mortality of young plants. At temperature levels near 40 °C, the photosynthetic electron transport and CO_2 assimilation of beech are found to be inhibited (Hohnwald et al. 2020).

This indicates alterations in the localization of xeric limits of beech distribution in Central and western Europe (Hohnwald et al. 2020; Garamszegi & Kern 2014; Stojanovic et al. 2013). With higher temperatures within the stands, higher evapotranspiration and shrinking soil water content, trees also struggle increased interspecific competition for water (del Rio et al. 2014). The consequences of drought stress caused by climate change, such as a decline in vitality, are recorded not only for drought-sensitive species such as spruce, but also for beech, which is dominant in the Palatinate Forest (MUEEF 2019)[8] . But not only the tree species are endangered in their resilience. Higher annual mean air temperatures bring about biotic effects such as a higher occurrence of insect pests. But also the extinction of species of important individual members in the biotic species network (pollinators, symbionts) weakens the stand health (Bolte & Ibisch 2014). Warm winters, on the other hand, promote the mobilization of reserve materials and, in combination with late frosts in spring, lead to insufficient frost hardness and consequently to frost damage (Müller & Schüler 2021). All factors weakening stand stability bring about a higher susceptibility for windthrow and calamities, and, as a consequence to it, stands are falling bare, as recorded for many forest sites in Germany in 2019 (BT-Drucks. 19/11093 in BfN 2020b).
Regarding Climate Change, phenological effects are observed that show the beginning of the vegetation period about two weeks ahead of time in early spring[9]. Increasing deterioration of crown conditions is observed as an indicator for drought stress in all main tree species, particularly in the past 3 years (2018-2020), accompanied by an increased occurrence of harmful insects with weakening effects on the populations (MUEEF 2020).

All those conditions are inextricably connected to forest management in terms of tree species composition, harvest operations affecting soil function, stand structure and stock hydrological continuity, which are thus to be considered against this background.

2.3.3.2 Forest management

Anthropogenic pollution and the significant influence of human activities on water-related forest functions make the examination and review of silvicultural treatment indispensable for forestry practice with regard to the protection

[8] The proportion of trees without visible damage in 2019 was 18 % (MUEEF 2019).

[9] https://www.kwis-rlp.de/daten-und-fakten/phaenologie/ (8.4.2021)

and maintenance water-related ES of the forest. The modification of hydrological conditions through forest management do, however, remain with uncertainty regarding predictions about the influence they have in an insufficiently predictable future (cf. Riedel & Weber 2020). Forestry is characterized by long production times, which make it difficult to predict the production conditions over the entire production period and the risks that arise during this period. Errors in management usually show negative effects only after a considerable delay and can then often no longer be effectively corrected (Müller & Schüler 2021). It is, though, evident that alterations of land use have a large impact on watershed hydrology, and thus groundwater resources (Riedel & Weber 2020). Forest management therefore is facing the challenge to fundamentally reorientate, accounting for the aspects of unpredictability and the diversity of today´s and future ecosystem services by leaving as broad as possible options for action and development (Jenssen 2007, Lawler et al. 2010, Ogden & Innes 2009, Puettmann et al. 2008 in BfN 2020b).
As with climate change, droughts and heavy storm events are prognosed to become more frequent, future forest management faces a severe challenge in promoted tree mortality and growth reduction (Ryan 2011; Stovall et al. 2019; Rukh et al. 2020), as well as water losses due to increased runoff generation in the course of heavy storm events (Schüler 2006). Managing the water cycle, and therefore maintaining the range of functions and ES in terms of preserving and improving the hydrological continuity within a stand, must therefore focus on both, increasing the retention potential and stabilize stand growth conditions. Against the background of prediction uncertainty and gap of knowledge, measures must be based on the precautionary principle. In accordance to this model, targeting conditions for maintaining a positive climatic water balance seem to be of major interest. In this manner, forest management must emphasize

- ➢ climate and species-appropriate selection of tree species complying with the xeric distribution and chemism (humus form),
- ➢ harvesting methods to maintain soil protection, high infiltration rates and protection against erosion and nutrient deprivation (type of cut, traffic, harvest intensity),
- ➢ preservation of stand and crown structures to improve thermal conditions and to control crown transmissivity (forest interior climate),
- ➢ control of runoff by identifying and reducing forest areas that contribute to runoff generation (increase of retention potential) and restoration,
- ➢ maintenance and protection of balanced nutrient balances (nutrient-sustainable extraction, liming).

The following components of forest management are inextricably linked to this:

- Silvicultural and stand structural components

As the composition of tree species shapes the climate resilience of a stand, the effects of climate change on tree species that are vulnerable to drought and heat, such as spruce, is observed nationwide in the past drought years (2018 - 2020): the bark beetle pests in stands dominated by spruce resulted in large bare areas (MUEEF (eds.) 2020; BfN 2020b). The hydrothermal and biocoenotic consequences of such deforestation processes are serious. The tree species composition also influences the chemical soil properties as well as the biological activity with consequences for litter degradation, mineralization rate, and the development of the secondary pore system, which is also crucial regarding the vulnerability to compaction. The role of forest management in maintaining the soil's functionality and the associated water-purifying processes is extensive: next to tree species composition, stand structure and age, harvesting methods, intensity and rotation also have a profound effect on the chemical and physical conditions of the soil (Mueller et al. 2012; Gruba & Mulder 2015; Bredemeier et al. 2011; Keesstra et al. 2012).

Since the thermal and hydrological stand conditions correlate strongly with the stand structure, leaf area and canopy transmissivity, forestry practice influences the severity and speed of the effects of hydrothermal changes caused by climate change, and therefore also the stand resilience against anthropogenic and pathogenic stressors (Hohnwald et al. 2020; Scheffer & Schachtschabel 1998:329, Ulrich 1983). Sukachev & Dylis (1964) discusses tipping points at low levels of forest cover in the transpiration of beech stands. The shade tree species beech naturally grows closed canopies with higher leaf area indices, reduced air turbulences and low radiation transmissivity to the ground, and thus a relatively cool and humid site-specific microclimate (Leuschner & Ellenberg 2017; Tüxen 1986; Korpel 1995; Brunet et al. 2010). Changes in the canopy structure related to an enhanced heat flux therefore show negative impacts on the beech stand´s water balance. Schabel (2020) confirmed area losses of beech in southwest Germany´s planar and colline locations, which most likely is connected to the occurrence of drought-induced cavitation in the xylem carrying vessels (Tomasella et al. 2017; Bréda et al. 2006; Ryan et al. 2006; Choat et al. 2012; Strasburger 1967; Czihak et al. 1996). Stand structural factors are discussed in this context: Due to thinning in beech stands, exposed beech trees receive more radiation and are therefore more stressed by heat due to their anisohydric strategy (Leuschner 2009, Roetzer et al. 2017). The drought sensitivity, however, is species specific and correlates with stand properties and mixing effects (Rukh et al. 2020).

Under drought conditions, the altered overall forest stand dynamics and energy balance (Stovall et al. 2019) lead to inhibited growth and carbon fixation (Rukh et al. 2020; Huang et al. 2019). Both factors put the forests´ contribution to the ES carbon storage and climate change mitigation at risk. Also, mixing effects with other species that promote interspecific facilitation under drought stress are discussed to potentially mitigate growth loss and mortality increase (Rukh et al. 2020).

There is, though, more research needed in the field of site acclimation and tree species morphological plasticity to comprehend adaption capabilities to climate change (Rukh et al. 2020).

- Retention potential

Runoff-inhibiting effects of the forest are site-specific and must therefore be assessed in a differentiated manner depending on the respective local hydraulic properties (Schüler 2003). Forest management influences the site-specific retention potential, and the associated water-related ES, through all actions that effect the physical and chemical properties of the soil: silviculture, felling and harvesting methods (Zhang et al. 2001; Riekerk 1989 in EEA 2015; Mueller et al. 2012; Gruba & Mulder 2015; Bredemeier et al. 2011; Keesstra et al. 2012). The hydro-ecological effectiveness of the forests can be improved through near-natural multidimensional structures, when small-scale vertical and temporal horizontal structures with serving and regrowing trees in the lower and middle storeys, are established (Müller 1996; BfN 2020b).

Another important contributor to runoff generation in a forest is the path system, as practically 100 % of the precipitation runs off due to high compaction (Grunert & König 2000). Path density and type of path drainage can, however, control the runoff behavior (Bott 2002). The runoff water must be diverted away from the paths in order to infiltrated into the adjacent forest area. Runoff generating and flood contributing areas need to be identified and measures for re-draining the water back into the stock need to be emphasized (Peichl 1998; Gaumitz 1991).

With storm events to happen more frequently, all measures that help inhibit runoff generation need to be accounted for in order to improve decentralized flood control and stabilize the hydrological continuity of forest stands. This also includes near-natural retention areas, into which excess surface water can be discharged wherever the surface profile of the landscape allows (Assmann & Gündra 1999). Floodplains have a very important hydroecological and socio-economic (Oppermann et al. 2009; BUMB 2015) function, as they allow the stream to expand in the event of rising water levels, and therefore prevent flood generation (Müller & Schüler 2021; BfN 2020a). By establishing morphologically natural conditions along floodplains, an increase in the flow velocity is counteracted and the retention capacity is increased (Koehler 1998; Schaich 2009). The retention potential (water and nutrient) of floodplains is highest when the dynamics of the water levels in the floodplain can adapt to the respective water supply, and their ecologically important habitat function can develop (Penka et al. 1985; Müller & Schüler 2021). With the linear straightening of river beds, a decreased width/depth and the associated increase in flow velocity, bank, sediment and nutrient erosion, scouring and sandbanks arise (Wagenschein 2006). The climatic function of floodplain forests is also very important, as they affect the microclimatic cooling effect (Penka et al. 1985).

All in all, a large number of individual measures in smaller catchment areas increase the effective retention volume for larger catchment areas. If this retention volume is exceeded, engineering measures for flood protection are indicated (Schüler 2006).

- Operating methods

Next to stand structure and tree species composition, the type of operating methods used in forest management influences the hydrological continuity. Clear cutting has, in particular, negative pedological and hydrological effects: On clear cutting areas of 1 ha and more, both the continuous supply of litter fall and the interception performance of the stand are interrupted (Keenan & Kimmis 1993; Vestin et al. 2020). This increases the amount and intensity of precipitation on the ground, while simultaneously the vegetation demand for water is lowered drastically. Since the soil is exposed to solar radiation, it heats up, which causes the mineralization rate to increase sharply (Vestin et al. 2020; Hedwall et al. 2013). This goes along with the consumption of humus and changes in the material and energy cycles. Nutrients bound in humus are released, and since the nutrient element storage decreases considerably due to the lack of vegetation, they will wash out or gas out into the atmosphere (Hedwall et al. 2013). Nutrient and carbon losses are the result. In the adjacent surface waters, the nutrient loads lead to eutrophication (Lee & Samuel 1976 in Keenan & Kimmis 1993). Forms of permanent forest, on the other hand, support the steady state of biomass, the distribution of tree species and numbers of stems, and therefore have a stabilizing effect on internal factors to the ecosystem (Burschel & Huss 1997; Hildebrand 1996; Rehfuess 1990). Since the majority of European forests shows an incipient or advanced nitrogen saturation, measures that bring about exposed soil or high concentration of felling residues increase the humus turnover and thus the release of nitrate and other nutrients (above all Potassium, Calcium and Magnesium) with subsequent release to the seepage water (Block et al. 2016).

On clear cut or bare fallen areas, rejuvenation establishes, either in the form of natural succession, or as an operational measure. Rejuvenation generally is a natural phenomenon of the forest development phases, which allows the phase cycle to start again after the age and decay phase and thus initiates the generational change (Wilhelm & Rieger 2013). In natural primeval forests, the alternation between the decay and the rejuvenation phase can be found in rather small-scale mosaic structures, with the ‘climax forest’ on small parts of the area showing different development phases within the climax forest community, and different stages of forest succession at the same time (Leibundgut 1984). Besides this natural cycle, rejuvenation can occur through various factors, such as extreme weather events caused by climate change, wild fires, and the massive occurrence of calamities. It can also be part of silvicultural measures, either to convert the forest in a targeted manner towards climatic plasticity (Landesforsten RLP 2020) or due to economically oriented cut forms. Each of these cases are considered to be a direct consequence of human activities, and are forecasted to occur more frequently as climate change advances, as do their effects on the water balance alongside.

Juvenile stocks differ from mature ones in terms of canopy cover, rooting depth, LAI, and therefore show poorer nutrient and water consumption, and thus smaller transpiration rates until they reach full development (cf. Pretzsch 2019:294). Also, the unclosed canopy cover enhances soil evaporation, and does not allow for microclimatic cooling, so that next to precipitation also the heat fluxes correspond rather to an open field but to the forest (cf. Hiege 1985:128; Mitscherlich & Moll 1970; Peck & Mayer 1996). Due to the poor cover, the droplet energy of rainfall unfolds higher forces on the soil particles (Neary et al. 2009), which makes juvenile stocks favorable to enhanced surface runoff and erosion processes. Under natural conditions, ground vegetation develops quite rapidly to form a shrub or herb layer, which contributes significantly to total transpiration rates of the stand (Gobin et al. 2015; Schmaltz 1969; Hager 1988).

Another serious factor in forest management is nutrient loss due to export with timber harvest. Through nutrient export, that is not site-adapted, soil fertility is endangered and nutrient-storing clay minerals are destroyed in the long term (Block et al. 2016). With respect to nutrient sustainability, nutrient balances must be accounted for (ibid.). If the comparison with the respective soil reserves show intolerable deficits due to excessive harvest extraction, the extent of extracted biomass is recommended to be reduced by suitable measures (ibid.).

- Compaction

Ecological impairments associated with the use of heavy forest machines in the long term must be weighed against the economic advantages in the short term, as they endanger the sustainable usability (Schönauer et al. 2021). Negative changes in ecological soil functions, losses in growth performance (Schönauer et al. 2021; Zenner et al. 2007) and water-related ecosystem functions of regulatory and supplying nature are unsustainable on an ecological, economic and social level.

The mechanical stress caused by the contact surface pressure of heavy forest machines introduces changes in the soil structure. Thereby soil physical parameters such as bulk density, pore volume, water and air conductivity, infiltration rate and penetration resistance are impaired and have negative consequences for the edaphic biological activity and the water and the nutrient balance of the forest stands (Bottinelli et al. 2014; Schönauer et al. 2021; Zenner et al. 2007; Schjønning et al. 2016). If the soil is loaded beyond its inherent stability, the soil particles and soil aggregates are pushed together and consequently the proportion of solids increases until an equilibrium with the pressure establishes (Terzaghi 1943; Osipov 2015). Soil water even promotes this process, since it acts as a lubricating film for particle movement, which is why wet soils are more sensitive to compaction (Zenner et al. 2007; Terzaghi et al. 1996; McNabb et al. 2001; Reichardt 2002). In the course of increase in bulk density the inter-aggregate pores are destroyed, which consequently leads to a reduction of soil hydraulic conductivity and air permeability (Horn et al. 1995; Dehner et al. 2015), and inhibits exchange processes in the soil (Fründ & Averdiek 2016). Macro pores, especially > 50 µm, are affected significantly more by soil compaction than micropores due to the decrease in pore volume (Page-Dumroese et al. 2006; Bottinelli et al. 2014; Dehner et al. 2015). As a result, the transfer of water and nutrients is limited, which leads to water stagnation and hypoxic conditions, promotes denitrification, and reduces living conditions for soil macro- and microorganisms. Consequently, the processes of bioturbation, mineralization, mycorrhizal activity, and also water purification are restricted. Especially the deficiency in aeration has a severe impact on soil ecology, which depends on gas diffusivity through the pore system of the soil matrix.

CO_2 levels in soils disturbed by vehicle driving is observed to increase, resulting from impaired diffusivity (Fründ & Averdiek 2016). Alterations in soil water content affect temperature flux, and therefore subsequently change the microclimatic conditions being decisive for root growth and causing the site being more susceptible to losses in stand productivity (Page-Dumroese et al. 2006; Grigal & Vance 2000). For bulk density, deteriorating effects are more severe with fine-textured soils. The increase in initial bulk density in coarse-textured soils is observed to be less pronounced (Page-Dumroese et al. 2006; Reichardt 2002; Schneider 2015). In the case of sands, pore redistributions appear to be primarily at the expense of air capacity, so that more densely stored sands have even higher field capacities (Dehner et al. 2015:4).) Increase in bulk density to a depth of 30 cm, with at the same time poor recovery exhibited in subsoils is confirmed by many studies (Labelle & Jaeger 2011; Cambi et al. 2015 in Fründ & Averdiek 2016; Schneider 2015; Page-Dumroese et al. 2006). But overall, the spatial distribution of increase in bulk density shows a large variability and must be regarded as multifactorial.

Figure 11 shows the interaction of the wheel load and the contact surface pressure, and their combined effect on ground pressure. The severity of damage depends on the area which is impacted by driving, the depth of impact and the duration in exposure or irreversibility of structural damages (cf. Fründ & Averdiek 2016:225). The impairment of soil properties increases non-linearly with the number of passes, but is observed to be the most detrimental to soil quality during the first pass (Reichardt 2002; Zenner et al. 2007).

Regarding natural recovery, macro-porosity is observed to evolve in coarse-textured soil within several years at 0-7 cm depth, associated with higher exposure to variations in temperature and water content and rooting of understory vegetation (cf. ibid.:15), whereas the recovery is less in the subsoil (Page-Dumroese et al. 2006; Reichardt 2002). Climatic conditions that promote drying shrinkage and freeze-thaw cycles, as well as macrofauna activities, depending on the occurrence of earthworms and enchytraeidae, support macropore regeneration. Residual effects regarding physical soil properties, however, endure in the long term: For forest sites, the regeneration

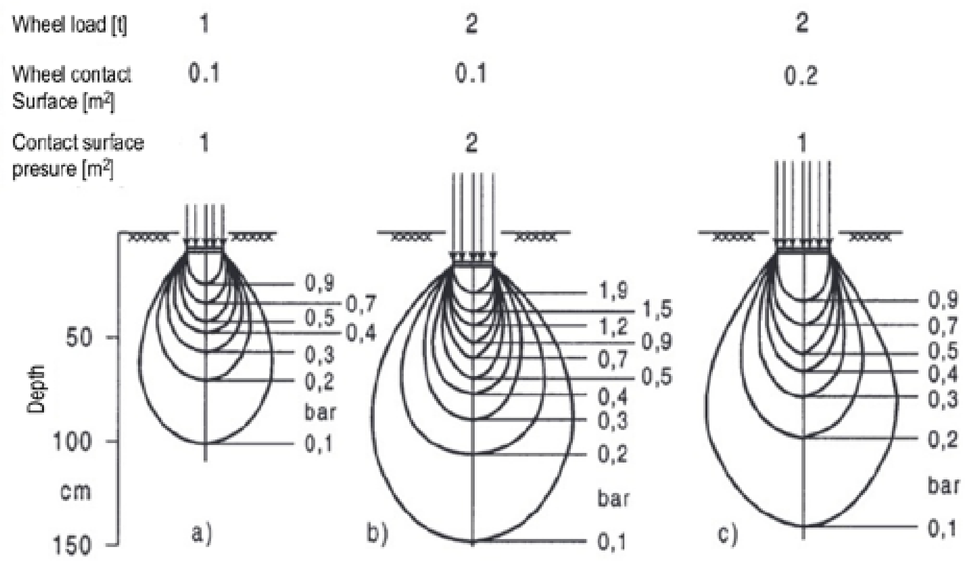

Figure 11: Pressure bulb depending on wheel load and soil depth (source: Reichardt 2002; BMVL 2001).

of bulk density is shown to take several years to decades, depending on soil characteristics, severity of the impairment, climatic conditions and biological activity (Brais 2001, Croke et al. 2001, Goutal et al. 2012, Greacen & Sands 1980, Labelle & Jaeger 2011, Page-Dumroese et al. 2006, Rab 2004 in Bottinelli et al. 2014; Reichardt 2002; Zenner et al. 2007), as well as on site specific differences in water regime and clay content (Fründ & Averdiek 2016; Terzaghi et al. 1996).

The soil pore system is directly linked to the performance of soil functions and hence to the ecosystem services derived from them. The key functions impaired by compaction can be categorized as follows:

- Inhibition of biomass production: With an increase in packing density and soil strength, root growth becomes restricted (Shierlaw & Alston 1984; Page-Dumroese et al. 2006). This results in inhibited nutrient and water uptake (cf. Shierlaw & Alston 1984:25), reduces the respiratory activity of the roots (Zenner et al. 2007; Fründ & Averdiek 2016), and promotes inhibition of biomass production (Schjønning et al. 2016). Root distribution is therefore critical to understanding the susceptibility of a stand to losses in productivity due to compaction (cf. ibid.:562). The reduction in tree growth due to physiological stress or interspecific competition can persist for several decades (cf. McNabb et al. 2001:1238). Also, low aeration and high bulk density promote late germination and low germination rates, as well as a higher mortality (Nawaz et al. 2012), and thus deteriorates the seed bed function (Hartge 1976, Ehlers 1982, Hildebrand 1983 in Reichardt 2002).
- Storage, filtering, buffering and transformation: Since infiltration is inhibited, surface runoff is promoted, and therefore the discharge of nutrients being transported overland, which increases the potential of erosion induced eutrophication of waterbodies (McNabb et al. 2001; Page-Dumroese et al. 2006). For the portion of water that does infiltrate the soil zone, altered hydraulic conductivity conditions inhibit diffusive, and alongside filtering processes. They also increase the risk of preferential flow, which supports leaching of nutrients, pesticides, pathogens, and soil colloids to deeper zones (cf. Schjønning et al. 2016:76; Iversen et al. 2011). Linear structures free from tillering, as they occur with machine paths, skid trails and rope routes, contribute to higher surface runoff, particularly on slopes with higher incline.
- Losses to biodiversity: Soil compaction decreases soil biodiversity by deteriorating the living-conditions of soil biota, which goes along with decreased microbial biomass, enzymatic and mycorrhizal activity (cf. Nawaz et al. 2012:291).
- Emissions of greenhouse gases: Changes in physicochemical soil properties have an impact on nitrogen and carbon cycles (Nawaz et al. 2012). The compaction-induced reduction of aeration of the soil matrix promotes anaerobic conditions, and therefore denitrification with subsequent release of greenhouse gases (N_2O, CH_4) to the atmosphere is promoted (Schjønning et al. 2016). This ultimately turns forest soils from a sink to a source of climate-relevant gases (Ruser et al. 1998, Teepe et al. 2004 in Schjønning et al. 2016).

The impairing consequences of compaction on the sustainable usability and productivity of forests and losses with regard to their ES have led to the enforcement of permanent skidding trails by certification agencies (FSC: Forest Stewardship Council, PEFC: Program for the Endorsement of Forest Certification Schemes) and forest managers (in Germany e.g. Landesforsten Rheinland-Pfalz 2018). These regulations provide threshold values as damage indicators to cease harvesting activities in case of unacceptable soil damage, and spatial skid trail restrictions as a compromise between economic demands and ecological conservation of soil functions (Landesforsten Rheinland-Pfalz 2018; Fründ & Averdiek 2016). Nevertheless, further investigation on multidisciplinary levels addressing diverse effects in different soil compartments, long-term measurements of relevant parameters with improved data treatment, progress in sensors in soil physics and soil chemistry, and developments in the field of modelling soil compaction regarding heterogenous types of soils and different types of climates, as well as more dynamic approaches relating stress rate and strain rate are required (Nawaz et al. 2012).

2.3.3.3 Air pollution

Due to persistently high inputs, many areas in Europe have reached nitrogen saturation (Bredemeier et al. 2011; Block et al. 2016). The multitude of damage symptoms, which are summarized as "new types of forest damage", have complex causes, are not spatially related to pollutant sources, and are still not fully understood (Ulrich 1991 in Mohr et al. 2005). Ecological changes and losses to biodiversity induced by N deposition especially occur in naturally low-N systems, such as forests, with species adapted to N deficiency. Nitrogen eutrophication of such systems leads to proliferation of rather N-affine species who subsequently out-compete species with lower demand (Krupa 2002). Cumulative effects between changes in hydrothermal conditions, induced by climate change, and anthropogenic nitrate saturation in forest ecosystems have already been demonstrated in experimental studies: In dry periods, the increased biomass production (due to enhanced N supply in the leaves) can lead to elevated water consumption, which changes the area's water balance and even reduces the groundwater recharge rate (Van der Eerden et al. 1990a, Van der Eerden & Pérez-Soba 1992 in Krupa 2002)[10]. Although oversaturation is associated with increased growth rates in the short term, the buffer system of the forest soil becomes severely impaired and consequently the ecosystem balance does, too, due to altered habitat conditions (Eugster & Haeni 2013; Krupa 2002; Ulrich 1983). Acidic soil conditions inhibit the development of mycorrhiza with all the negative consequences for symbiosis partners. The initial increase in growth opposes harmful effects in the event of long-term exposure, which is inevitable to forest stands due to their longevity and a semi-closed substance balance, which collects, converts and releases pollutants and nutrients in the long term (Ellenberg 1996). The original function of the forest as a substance sink and pollutant filter can even be reversed by an exhausted absorption capacity due to N-saturation, and lead to the release of dissolved (NO_3-) and gaseous (NO, N_2O) N-compounds. The impairment of forests increases with weakly buffered soils and N-sensitive tree species (conifers), high fragmentation with the associated edge effects and the spatial proximity to emitters (Mohr et al. 2005). The N-excess induced nutrition imbalance makes trees less drought- and frost-resistant and more susceptible to insects and pests (ibid.; Meeseburg et al. in Brumme & Khanna 2009). Anthropogenic soil acidification leads to serious changes in the material cycle, the vitality and the composition of the entire forest community (Veerhoff et al. 1996 in FAWF 2012).

[10] Evaporation rates are even enhanced by an increase in shoot growth induced by shoot uptake of NHx, while root growth is rather inhibited, leading to higher shoot: root ratios. Consequently, the water supply for the larger canopy can hardly be covered by the roots during periods of drought (cf. Krupa 2002:202).

3 STUDY AREA

The *Palatinate Forest* (Pfälzerwald) is a diverse, rocky red sandstone landscape with a high proportion of forest (76 %, with close to 90 % in the central area) of predominantly acidic beech and pine stands in an area of 178,497 ha in the south of the German state of Rhineland-Palatinate (StatLa RLP 2016; Weiss 1993; Geiger 1987). The Nature Park ***Palatinate Forest*** originally was founded in 1958, and transferred to the Palatinate Forest Northern Vosges Biosphere Reserve with recognition by UNESCO in 1992. In 2020, the nature park ordinance was replaced by the state ordinance on the Palatinate Forest Biosphere Reserve as the German part of the cross-border Biosphere Reserve between Germany and France (Biosphärenreservat Pfälzerwald-Nordvogesen 2021; JM 2021). It extends from north to south for around 60 km, from west to east 30 - 40 km. In the South it continues in the Northern Vosges on the French side (Weiss 1993). The nature park essentially comprises the Palatinate Forest itself, which borders in the north on the North Palatinate Uplands with the ***Kaiserslauter Senke***. To the east the low mountain range ***Haardtrand*** adjoins, with the highest elevation being the ***Kalmit*** (673 mamsl.), which drops off to the Upper Rhine lowlands (***Deutsche Weinstrasse***) to the east, with prevailing viticulture. To the west, a sparsely populated low mountain area (***Zweibrücker Westrich***) adjoins, with around 430 mamsl., and to the south, the so-called ***Wasgau***, which is separated from the rest of the Palatinate Forest by the ***Queichtal*** with 576 mamsl. at the top (***Rehberg***), with more pronounced agricultural use (ibid.). On the whole, the elevation ranges from approx. 100 mamsl. on the eastern edge to over 600 mamsl. in the center or in the northeast of the area. It is characterized by the ***Variskan mountain formation***, and represents the eastern branch of the Southwest German Cuesta (Erdmann 1995; Koehler et al. 2010). The ***Palatinate Forest*** area is Germany's largest contiguous forest area with 134,000 ha, which is characterized by a relatively low population density and small settlement sizes (Weiss 1993).

3.1 Climate

The Palatinate Forest Biosphere Reserve is located in the temperate climate zone between the Atlantic and Continental climate types, and is characterized by the topographical north-south barrier of the mountains on the left bank of the Rhine, primarily by front systems approaching from the west with Atlantic influence and relatively high wind speeds (Fass 1995; DWD 2021; MWKEL-RLP 2021; Geiger 1987). As it is assigned to the colline, and in large parts also the submontane altitude level, the area can be considered as a transition area between land and sea climate with oceanic influence dominating in higher altitudes (Weiss 1993). As a result, luff effects come into play in the western part of the Palatinate Forest, which cause the Atlantic air masses to rise and rain to a greater extent on the edge of the ***Haardtrand*** (DWD 1957; Geiger 1987). In this area, precipitation of 800-1000 mm/a is recorded, whereas on the eastern side of the mountains under leeward influence only 500 to 600 mm/a are effective (ibid.). To the ***Deutsche Weinstrasse*** the climatic conditions change into the basin climate of the Palatinate Rhine Plain, which is considered a naturally caused bioclimatic stress zone with foehn-like uplift, local slope updrafts (Hahn-Herse et al. 1980 in Weiss 1993). For the south-western part of the Palatinate Forest, precipitation values average 850 mm/a. The effect of the mountains also effects the frequency and intensity with heavy precipitation (> 20 mm/m^2) being more frequent in the most elevated areas to less frequent in the ***Deutsche Weinstrasse*** (ibid.).
The low mountain range is in the moderately cool temperature range with relatively low annual fluctuations in air temperature due to the oceanic character (Reiter et al. 2018), following an altitude gradient of mean annual 6 °C at the highest altitudes up 10 °C in the valleys and the ***Haardtrand*** and ***Deutsche Weinstrasse*** region (MWKEL-RLP 2021; Geiger 1987). The snow cover only reaches small amounts and short durations (40 - 60 days/a) (Weiss 1993). The vegetation period covers 200-220 days (verbal information

from M. Greve, May 2019; www.kwis-rlp.de ; Geiger 1987). Due to high precipitation in connection with a high geohydrological storage capacity, low thermal loads and a comparatively high level of air purity, the forested catchment shows favorable conditions for high quantitative and qualitative new groundwater formation in principle (Geiger 1987).

The degree of pollution is reflected in the values of the critical loads for air pollutant deposition (Nagel & Gregor 1999): The inputs of potential acids in the study area are above the values considered harmless for the maintenance of the self-regulation of forest ecosystems and their nutrient cycles (FAWF 2012). According to the UBA (2004), an average of 6.6 kg/(ha*a) is deposited at the Deuselbach measuring station close by the catchment area (UBA 2004). Adding up the load of the dry deposition results in a base load of 13.5 kg/(ha*a) total deposition of nitrate (ibid.).

Climate Change shows already clear effects: The mean annual temperature in the state of Rhineland-Palatinate has risen by 1.5 °C since the end of the 19th century, in winter even by 1.6 °C, which is also reflected in the increase in the long-term average temperature from 1988 to 2017 to 9.6 °C (*Reiter* et al. 2018). The number of frost days has declined, especially at high altitudes, with a simultaneous increase in the number of summer days in the average mean by 20 days per year since 1951, which is accompanied by an increasing number of heat waves and heavy storm events in the summer (ibid.).

3.2 Geology, Hydrogeology and Pedology

The Palatinate Forest consists predominantly of sandstones stocking on the *Variscan* basement, which is covered by layers and conglomerates of the *Rotliegend* and the *Zechstein* (Spuhler 1957). At the beginning of the *Mesozoic* the *Saar-Nahe Basin* sank, and formed a depression between the *North Palatinate Uplands* and the *Vosges*, in which up to the Lower Permian (Lower *Rotliegend*, 270 million years) around 400 m thick, various sedimentary of red to yellowish-white sands of the sandstone were deposited, which practically included the entire area of the Palatinate Forest and created the Palatinate Saddle in the northwest and the Palatinate *Mulde* in the south-east (Haneke & Weidenfeller 2010). As a result of rise and fall processes in the Lower and Upper Permian and desertification in the Lower and Middle Triassic, a geological sequence of layers with higher and lower rock strength was formed through deposits of different characteristics (ibid.). Its lithostratigraphy, differentiated beginning with the Zechstein of the Upper Carboniferous, is shown in **table 1**.

The massive Red Sandstone block is topographically characterized by a moving relief, with the towering *Haardtrand* forming the highest elevations. It is divided geologically into the lower, middle and upper red sandstone, with the middle red sandstone forming the thickest layer of up to 400 m (main red sandstone). To the north, the Palatinate Forest is bordered by the permocarboniferous North Palatinate Uplands, to the east by the *Rheingraben*, to the west by the layered limestone of the *Westricher Hochfläche*, reaching into the *Paris Basin*, and to the South it merges into the northern *Vosges* without geomorphological delimitation (Geiger 1987; Spuhler 1957).

The North and East of the area is characterized by distinct strata and fracture stages: To the north, the *Staufer*, *Rehberg* and *Karlstal* layers form 40 to 200 m thick strata, to the east the mountain edge forms a 300 to 400 meter high fracture step made of rocks from the lower and *Middle Red Sandstone* with narrow notched valleys (Geiger 1987; Beeger et al. 1989). The prevailing rock sequences in each case produce a variety of different mountain shapes, depending on weatherability and erosion. In the central Palatinate Forest, the rock of the Lower and *Middle Red Sandstone* is characterized by deep and narrow notched valleys with narrow valley bottoms and steep side slopes. In the south and north, on the other hand, box valleys with a wider valley floor dominate (Geiger 1987; Meynen & Schmithüsen 1960).

The stratigraphic structure is closely based on the petrographic differentiation of the *Red*

Sandstone: Layers of the *Lower* and *Upper Red Sandstone* have clay-bound sandstones to claystones, whereas the *Trifels, Rehberg* and *Karlstal* layers, due to their widespread distribution in the Palatinate Forest are also referred to as *Main Red Sandstone*, are rather poor in clay (Spuhler 1957). Although both form sequences of aquifers with varying hydrological conductivity, the fluvially formed *Zechstein*, made of clay-rich layers, rather form damming spring horizons, whereas the triassic *Middle* and *Upper Red Sandstone* show a higher permeability due to higher proportions of coarse-grained conglomerates (Haneke & Weidenfeller 2010). The *Rotliegend* is characterized by low-conductive rocks. In the north-western part of the area, fractured aquifers of the *Upper Carbon* dominate, in the south and south-western part the Red Sandstone is covered by low-permeability dolomite and Sandstone banks of the *Shell Limestone*. The *Annweiler* strata in the southern Palatinate Forest consist of an alternating sequence of silty-clayey fine Sandstones with layers of siltstones to clay stones, the so-called *Leberschiefern*. In the northern *Palatinate Forest*, the Lower Red Sandstone is represented by the *Stauf* layers. These are characterized by an alternation of coarse to medium-grained, but also fine-grained, partly scree-bearing and weakly consolidated sandstones (Heitele 1993). The *Trifels* strata in the *Lower Red Sandstone*, which lie above the *Annweiler* and *Stauf* strata, consist predominantly of coarse-grained sandstones and, due to their thickness and good water permeability, form the most important aquifers in the area (Heitele et al. 1987 in Geiger 1987). The *Stauf* layers often form a retention horizon for the groundwater flowing in from hanging *Trifels* layers. They cannot be clearly demarcated from one another hydrologically and form an almost homogeneous groundwater body with mostly a free groundwater table. The *Rehberg* strata belonging to the *Middle Red Sandstone* represent an alternation of strong rock banks of the *Karlstal* type that come to light at the base of these strata, provided they are not below valley level (LGB & LfW 2004). On top of this, the *Karlstal Rockzone* form an abundant aquifer, which is covered by a lower conductive aquifer of the *Upper Karlstal* layers, and thus by the overlying *Upper Rockzone*, the *Hauptkonglomerat* and the rocks of the Upper Red Sandstone and Shell Sandstone, which show alternating conductivities. The permeability values result in a wide spread between 5 x 10^{-4} to 1 x 10^{-6} m/s, with the sequence of the Rehberg and Trifels layers showing the highest permeability values with maxima at 5 x 10-3 m/s (ibid.).

From the fine-grained to medium- and coarse-grained pebbly sandstone layers of the Middle Red Sandstone, rock poor in base and clay form, which bring about acidic, nutrient-poor, sandy Ranker and Brown Soils with a weak to medium layer of humus, form, tending to podsolate (Mainberger 1987 in Geiger 1987). Low pH values, relatively high moisture penetration, unfavorable forms of cultivation in the past such as forest pasture, litter use and the cultivation of coniferous wood on deciduous-suitable locations, as well as persistent inputs of acid formers from the air deposition promote acid bleaching of the soil and raw humus formation (Weiss 1993; Geiger 1987). Although petrographically homogenous, the soils vary regarding depth and water supply tremendously (Geiger 1987). Especially on south-facing slopes and on mountain ridges shallow soils with a low water supply dominate, that significantly limit tree growth (ibid.). In some places under the influence of dust and loess loam deposits, Brown Soils are formed from loamy sands and sandy loams of low to medium saturation (Geiger 1987; Weiss 1993). More clayey raw material from the sandy shale clays of the *Lower Red Sandstone* and the *Oberrotligend* produce medium to heavy soils of the Ranker, Brown Soils and Pelosols in the Wasgau (Weiss 1993). Due to the sandy soils that emerged from the weathering of the red sandstone, the sites of the Palatinate Forest pedologically have good aeration and rootability, which means that the nutrient supply, although sparse, is evenly distributed (Mainberger 1987 in Geiger 1987).

Table 1:

Lithostratigraphic layering and aquifer properties in the Palatinate Forest, differentiated for the Triassic (modified after LGB & LFW 2004; AG Geologie 2021; Spuhler 1957; Geiger 1987)

<table>
<tr><th colspan="5">Sequence of layers</th><th>Hydraulic conductivity of the aquifer</th></tr>
<tr><td rowspan="14">Triassic</td><td colspan="2">Shell Limestone</td><td colspan="2">Shell Sandstone</td><td rowspan="6">alternating lower an high conductive</td></tr>
<tr><td rowspan="13">Red Sandstone</td><td rowspan="2">Upper Red Sandstone</td><td colspan="2">Voltziensandstein</td></tr>
<tr><td colspan="2">Zwischenschichten</td></tr>
<tr><td rowspan="5">Middel Red Sandstone</td><td colspan="2">Violette Grenzzone</td></tr>
<tr><td colspan="2">Hauptkonkonglomerat</td></tr>
<tr><td colspan="2">Upper Rockzone</td></tr>
<tr><td colspan="2">Upper Karlstal</td><td>Low conductive</td></tr>
<tr><td colspan="2">Karlstal Rockzone</td><td>alternating lower and high conductive</td></tr>
<tr><td rowspan="6">Lower Red Sandstone</td><td colspan="2">Schlossberg</td><td>Low conductive</td></tr>
<tr><td colspan="2">Rehberg</td><td rowspan="7">alternating lower and high conductive</td></tr>
<tr><td colspan="2">Trifels</td></tr>
<tr><td rowspan="3">North Palatinate</td><td>South Palatinate</td></tr>
<tr><td>Speyerbach</td></tr>
<tr><td>Annweiler</td></tr>
<tr><td rowspan="3">Permocarbon</td><td colspan="2" rowspan="2">Zechstein</td><td rowspan="2">Stauf</td><td>Rothenberg</td></tr>
<tr><td>Queich</td></tr>
<tr><td colspan="4">Rotliegend</td><td>Low conductive</td></tr>
</table>

In the valley floors of streams and rivers with fine, medium-grain sands and adjacent groundwater, predominantly alluvial Gley Soils form. At the source horizons of steep slopes, slope gleyes merge into podsolized forms of the steep slopes (ibid.).

3.3 Surface waters and water regime

Streams have shaped the deep valleys of the Palatinate Forest (Hahn et al. 2000). They drain in a radial network of water towards the Rhine and Moselle. The headwaters of numerous spring streams cut through steep notch valleys, their central reaches flow through box valleys, carry fine granular debris and mix with large amounts of taut, oxygen-rich groundwater (ibid.; Geiger 1987).

[11] Wieslauter, Queich, Speyerbach, Isenach, Eckbach, Eiswoog, Moosalbe, Schwarzbach and Rodalbe.

A watershed of the 1st order crosses the Palatinate Forest from north to south and separates the rivers in an easterly direction with a tributary to the Rhine from those in a western direction with a tributary to the Saar catchment area. The larger rivers[11] have a relatively balanced water flow. The water quality of the Red Sandstone streams lies in the range between "moderately polluted" and "unpolluted to slightly polluted" and can be summarized as good (Weiss 1993:21).
The water runoff is very low due to high evaporation values in the predominantly wooded area and the favorable infiltration, storage and retention properties of the Red Sandstone (Heitele et al. 1987 in Geiger 1987), so that both high water peaks and low water levels in dry periods are mitigated. The high infiltration rates (1/4 of the mean annual precipitation) also feed the continuous groundwater inflows from numerous springs, which counteract water shortages in summer dry periods. Floods generally occur as a result of snowmelt in March, but also in connection with heavy summer rain in June/July (Weiss 1993). Nevertheless, most of the streams were used for water management at the beginning of the 19th century and canalized for the wood drift, so that until today they do not have natural brooks, which enhances the risk of flooding in local urban areas (Hahn et al. 2000; Weiss 1993).
A large number (approx. 80%) of the region-specific springs is anthropogenically influenced today (Fiedler-Weidmann & Hahn 1996 in Hahn et al. 2000). Spring tapping, acidification as a result of spruce plantings and high pressure of use have impaired both the quality and the quantity of the springs. The level of pollution at the Haardtrand is particularly high due to nutrient and pollutant inputs from viticulture (cf. ibid.:13).
The pore and fissured aquifers of the Red Sandstone have a large storage capacity and high groundwater recharge rates (Heitele et al. 1987 in Geiger 1987). A distinction is made between loose rock aquifers in the box valleys and clearly stratified aquifers in the rock zone, the former being characterized by very good groundwater quality (Hahn et al. 2000). The shallow aquifers of the rock zone, on the other hand, are often affected by acidification (Trilling 1996, Hahn, Preuss & Friedrich 1998 in Hahn et al. 2000:11). The main direction of groundwater run-off runs along the layers of the Red Sandstone slab, which are inclined to the west. Leachate flows along the fault zones of the geological structure towards the western edge of the mountain, so that the west benefits more from the water supply than the east (cf. Weiss 1993:22). Parts of the groundwater of the loose rock aquifers feed the groundwater resources of the ***Haardtrand*** and supply the ***Upper Rhine Plain*** (Heitele et al. 1987 in Geiger 1987). The eastern communities along the ***Haardtrand*** cover their drinking water supply completely with groundwater of the forest valleys, so that the groundwater reserves are under high usage pressure (Müller & Theobald 1996 in Hahn et al. 2000; Weiss 1993). 10 to 12% of the groundwater formed annually in the Palatinate Forest is used as drinking water (Hahn et al. 2000: 11).

3.4 Vegetation

The potential natural plant community in the Palatinate Forest corresponds to the plant-geographical natural characteristics of rather species-poor oak-beech forests (*Luzulo-Fagetum*) (Hailer 1971, Mainberger 1987 in Geiger 1987; Ellenberg & Leuschner 2010:85), with a close to natural tree species composition of dense beech sites with oak, mountain ash and birch in moderately steep areas to the southeast (Weiss 1993).
The actual tree species composition in the area varies depending on the topographical characteristics of the terrain, and the associated growth conditions: Spruce (*picea abies*) dominates on fresh, shady lower slopes, pine (*pinus sylvestris*) on south to south-west exposed locations, beech (*fagus sylvatica*) on more humid and nutrient-richer areas, whereas moderately moist and nutrient-supplied plateau areas and eastern slopes predominate Sessile oak (*quercus petraea*). Beech, oak and pine are considered to be autochthonous in the area (Hailer 1971, Mainberger 1987 in Geiger 1987). The European larch (*larix decidua*) can also be found mixed in with beech stands, as well

as Sweet chestnut (*castanea sativa*) and Douglas fir (*pseudotsuga menziesii*), mostly in the pure stand (Weiss 1993; Mainberger 1987 in Geiger 1987). In the *Wasgau* there are also fir forests as the northern branches of the closed natural fir occurrence in the Vosges (Hailer 1981 in Geiger 1987). In shallow, less precipitation and more acidic locations of the *Haardtrand*, more warmth-adapted species displace the beech. Today the pine is predominantly settled there, with poor sessile oak and birch forests (*Quercetum medioeuropaeum*) forming the real natural form of vegetation (Hailer 1981, Mainberger 1987 in Geiger 1987). The cultivation of the pine was promoted at the beginning of the 19^{th} century as part of replanting activities by the Bavarian forest administration. As a result of large-scale deforestation in order to meet the wood requirements of industrialization, the original mixed stands of beech and oak were replaced by fast-growing tree species such as spruce and pine in the course of these reforestation activities (Leonhardt 2003). Even after the two world wars, renewed reforestation efforts were required (ibid.), so that between 1970 and 1995 mostly deciduous tree areas were driven over with heavy machinery in the course of planting (LWF aktuell 2003).

Based on the concept of near-natural silviculture in accordance with natural and anthropogenic factors, which is at the center of the basic instruction on forest regeneration 2020 for Rhineland-Palatinate, today's tree species composition in Rhineland-Palatinate is dominated by mixed deciduous forests (Landesforsten Rheinland-Pfalz 2020), with a tree species composition of pine 47 %, beech 27 %, spruce 6 %, oak 9.8 %, douglas fir 6 %, and mixed forest of other tree species about 4 % (Forest Inventory data 2021). In older stands (> 160 - 120 years) there is a balanced relationship between deciduous and coniferous trees, whereas in younger stands (120 - 40 years) the conifers predominate due to historical cultivation preferences. These imbalances have recently been compensated for in silvicultural terms by an increasing focus on mixed forests with an expanded range of tree species (Mainberger 1987 in Geiger 1987). The ownership shares of the forest areas are distributed differently in Rhineland-Palatinate: the state forest owns 25.6 %, federal forest 1.6 %, corporate forest 46.1 % and private forest accounts for 26.7 %. In the Palatinate Forest, the distribution is 55 % state forest, 25 % federal forest, and up to 20 % private and corporate ownership (Forest Inventory data 2021).

4 MODELLING METHODOLOGY

Based on the water input (precipitation, snowmelt), water balance models mathematically determine the water output (discharge) in the catchment area using evaporation components (interception, evapotranspiration), storage components (leaf, soil, groundwater) and runoff components (interflow, runoff). The objective of this thesis includes the assessment of soil water balance and evapotranspiration, the recording of runoff formation and concentration as well as calculations of current and future groundwater, channels and watercourses in a meso- to macroscale catchment. Basic requirements for modeling to meet the objective can be formulated as follows:

- Hydrologically relevant sub-processes of the water cycle such as precipitation, interception, evapotranspiration, soil water storage, runoff concentration, seepage and retention must be specifically recorded and calculated using the most precise methods possible.
- Determination of the soil water flows in the rooted and non-rooted soil to determine the infiltration and mass transfer rates, soil water balance and deep seepage to groundwater.
- Determination of the water supply for vegetation. In this context, the procedural recording of forest growth dynamics is necessary.
- Determination of conditions of excess water supply as well as water scarcity.
- Mapping of management impacts on the water balance, such as compaction in the course of heavy harvest machinery usage and rejuvenation.
- The temporal dynamics and spatial variability of water cycle components in the forest require an adequate resolution of temporal processes based on daily values, as well as the simulation over long periods of time and into the future.
- The model should be well documented and tested in use.

The monolithic, semi-distributed, physically based continuous eco-hydrological SWAT+ model was found to meet with these requirements. In addition to the spatially differentiated simulation of hydrology, it also processes water quality (nutrients and pesticides), erosion and agricultural management practices of different plants and crops (Arnold et al. 1998; Lam et al. 2010 in Hörmann et al. 2014), and is also suitable for examining the effects of global change (Hörmann et al. 2014; Beven 2012). It is also found and modified to successfully represent the hydrological and ecological processes within forested watersheds (Watson et al. 2005, 2008; Wattenbach et al. 2005; Kirby & Durrans 2007; McKeown et al. 2005). SWAT+ provides preset parameterization sets for various agricultural systems, including commercial forests. Forest ecosystems in a protected area differ from commercial forest plantations in terms of plant growth and biomass as well as in terms of management intensity and techniques. The parameter set of SWAT+ allows the adjustment of variables related to those issues. Growth-specific (e.g. leaf area index LAI, radiation use efficiency) as well as management related (e.g. harvest intensities) variables were adaptable, the data of which was provided by a very extensive data set from the Research Institute for Forest Ecology and Forestry (FAWF). The data is based in-situ measured data from permanent observation areas in addition to forest specific literature. Although SWAT is widely used and tested in the agricultural field, studies examining its performance in forest ecosystems are rarely conducted. This makes the contribution of forest-related model examinations to future directions for model improvement an important issue to the scientific community, especially against the background of the important role of forests in carbon, water, and nutrient cycling and their complex interactions on regional and global scale (Yang & Zhang 2016). By estimating specific output values related to ES, SWAT+ allows for the comparison of relative differences between different scenarios (Norman et al. 2012 in Francesconi et al. 2016), and provides the option to analyze degradation impacts, so that it is a capable tool of examining water-related ES, even in the sense of continuous monitoring (Francesconi et al. 2016).

4.1 The hydrologic model SWAT+

SWAT+ is a physically based, continuous-time, dynamic catchment model that operates on a daily time step and is capable of long time period simulations of weather, hydrology, soil temperature and properties, plant growth, nutrients, pesticides, bacteria, pathogens and land management (Gassman et al. 2007). Its predecessor SWAT was originally developed by the Agricultural Research Service of the U.S. Department of Agriculture (USDA) to map and forecast sediment and chemical loads as well as effects on the water balance in longer time series in the meso and macroscale range (Gassman et al. 2007; Arnold et al. 1998). It is also widely used around the world, published in many papers and journals, and well documented in different languages[12] . Its relevant application categories are summarized as streamflow calibration and related hydrologic analyses (e.g. Leta et al. 2015; Faramarzi et al. 2015), climate change impacts on hydrology, pollutant and nutrient load assessments (e.g. El-Khoury et al., 2015; Baffaut et al., 2015; Holvoet et al., 2008), as well as intrinsic modelling aspects, such as sensitivity analysis and calibration techniques (Gassman et al. 2007). Its open source code provides the adaption to specific environments and application needs, and is continuously improved and developed further by the developer team since it was created in the 1990ies (Arnold et al. 2012; Gassman et al. 2007). Multiple modifications finally resulted in the development of SWAT+, a completely revised version of the model, developed to enhance the spatial discretization of elements and processes within a watershed, and to foster configuration related processes, but based on the same algorithms of process calculation (Bieger et al. 2016). It incorporates several interface tools and other software supporting the pre- and postprocessing of data and model construction, such as the QGIS interface for setting up the watershed, the in-process database engine SQLite[13], as well as the R environment for statistical computing and graphics[14]. Since its official release by the SWAT group in 2018, the number of publications is increasing steadily, but only a fraction compared to its predecessor SWAT. For both, SWAT and SWAT+, only a few studies have so far examined the performance in forest ecosystems (e.g. Yang & Zhang 2016; Bieger et al. 2016; Müller & Schüler 2021, Schüler et al. 2016).

SWAT+ directly simulates evapotranspiration (optionally by the equations of Penman-Monteith, Monteith 1965, Priestley-Taylor, Priestley & Taylor 1972 or Hargreaves, Hargreaves et al. 1985), surface runoff, percolation, lateral flow and base flow based on the water balance equation (see **fig. 12**). Actual evapotranspiration is calculated equivalent to Ritchie (1972), interception is computed by a canopy storage model, surface runoff is either simulated using the SCS curve number method (USDA-SCS 1972) or the Green & Amp (1911) infiltration equation, and lateral flow is computed using the kinematic storage model of Sloan & Moore (1984). For percolation, a storage routing technique allows the water to flow from one soil layer of the parametrized soil profile to the subjacent at field capacity, provided the subjacent layer is not saturated (cf. Watson et al. 2008:147). Water that flows from the vadose zone to the shallow aquifer as baseflow may contribute to streamflow, whereas water that enters the deep aquifer is considered lost to the water cycle of the watershed (ibid.). The channel network routing is computed either by the method of Williams (1969), or the Muskingum method (Chow 1959).

[12] https://www.card.iastate.edu/swat_articles/ (30.11.2021).

[13] https://www.sqlite.org/about.html (11.10.2021).

[14] https://www.r-project.org/about.html (11.10.2021).

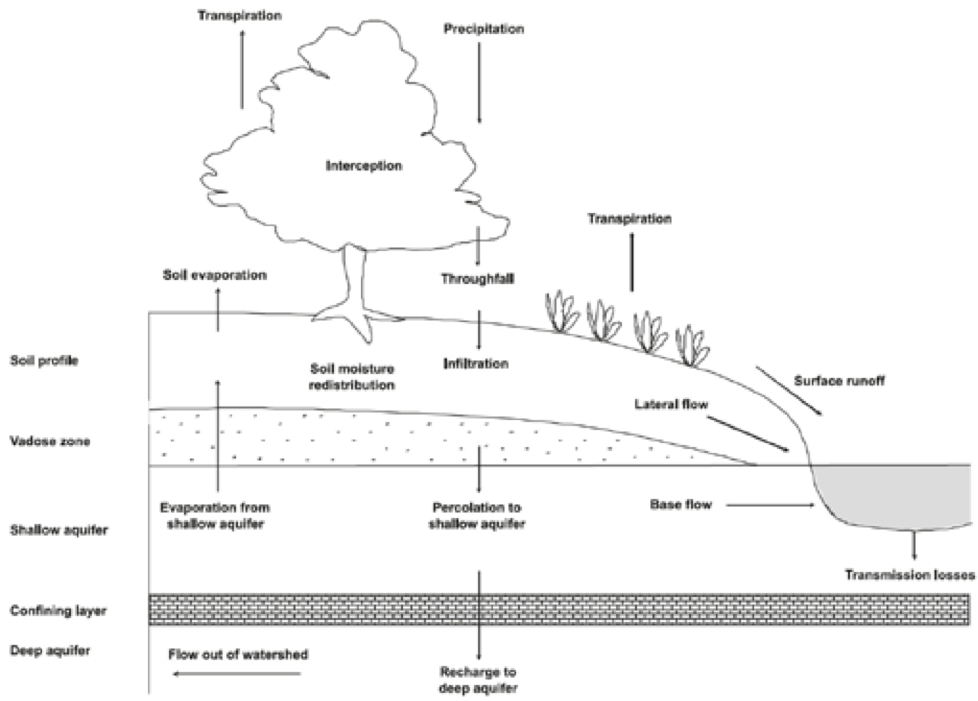

Figure 12: Hydrological processes simulated by SWAT+ (source: Watson et al. 2008:148, adapted from Neitsch et al. 2005).

SWAT+ divides a watershed into multiple subbasins, which are subdivided into areas of homogenous land use, management, soil and slope characteristics, so-called hydrological response units (HRUs) (Neitsch et al. 2011). Though showing a high efficiency in computation, the HRU approach hinders the identification of so-called critical source areas (CSAs): Lumping areas of similar characteristics leads to the summation of water and pollutant yields at subbasin level, adding them directly to the stream, which does not allow a differentiation of transport and deposition processes in the landscape (Arnold & Fohrer 2005; Gassman et al. 2007). **Figure 13** shows a conceptualization of flow paths of water between the most important spatial objects in SWAT+.

A clear advantage of the modified HRU approach in SWAT+ is, however, that aquifers, channels, reservoirs, ponds, and point sources are operated as separate spatial objects, whose hydrologic interaction can be defined by the user to meet the physical environment of a watershed (Bieger et al. 2016). Although still divided into subbasins, the subdivision now follows into water areas and one or more landscape units (LSUs) of topographic characteristics necessary to calculate the time of concentrations. This approach allows a differentiation between uplands and floodplains, and furthermore allows the floodplain as a separate LSU to saturate in the event of a flooding, which accounts for saturation excess overland flow. The actual HRU in SWAT+ is thus applied as a contiguous, user-defined field, aggregated on LSU level (ibid.).

To meet the specific requirements of simulating a forested area with SWAT+, a research funding was assigned to, and carried out by Dr. T. Tigabu and Dr. P. Wagner under the direction of Prof. Dr. N. Fohrer, department of hydrology, University of Kiel, aiming the assessment of relevant hydrological processes in the forest, supporting the research objective and developing SWAT+ further with regard to an appropriate application in forested areas. In the following, the most relevant hydrological processes with respect to the research objective are highlighted with regard to their model application.

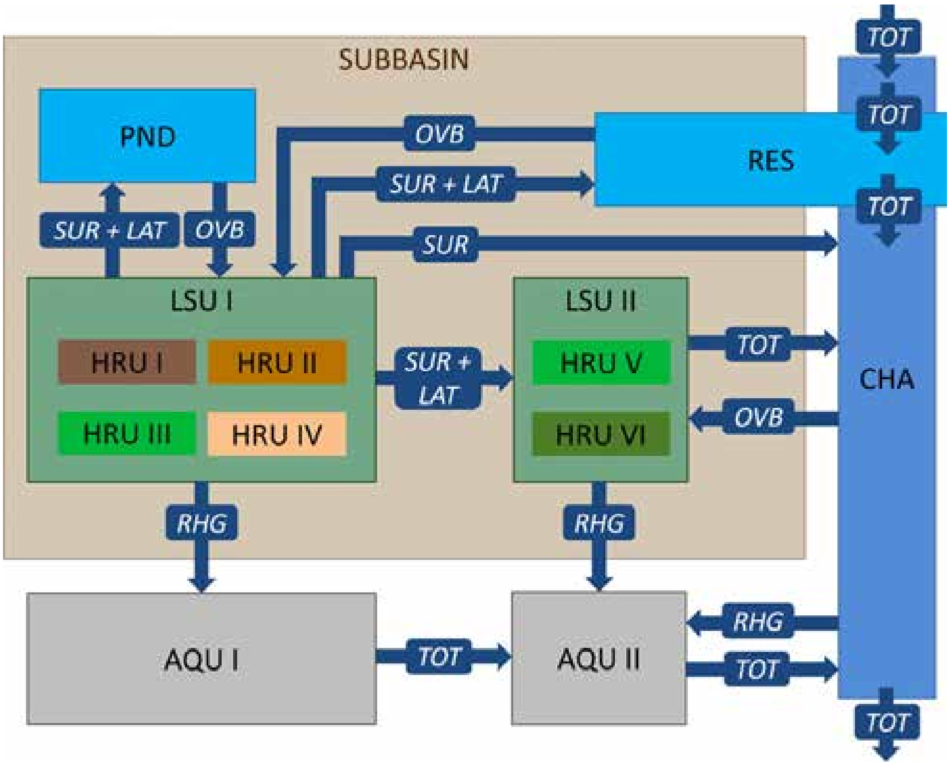

Figure 13: Conceptual flow paths of water between the most important spatial objects in SWAT+. AQU, aquifer; CHA, channel; HRU, hydrologic response unit; LSU, landscape unit; PND, pond; RES, reservoir; LAT, lateral flow; OVB, overbank flow; RHG, recharge; SUR, surface runoff; TOT, total flow (source: BIEGER et al. 2016:3).

4.1.1 Surface Runoff

SWAT+ defines runoff generation to be part of the hydrological processes of the land phase, based on the water balance equation (see Neitsch et al. 2011:9):

$$SW_t = SW_0 + \sum_{i=1}^{t} (R_{day} - Q_{surf} - E_a - w_{seep} - Q_{gw})$$

Formula 4.1.1

SW_t = Final soil water content *
SW_0 = Initial soil water content on day *i*
t = Time (days)]
R_{day} = precipitation on day *i* *
Q_{surf} = surface runoff on day *i*
E_a = evapotranspiration on day *i* *
w_{seep} = Water entering the vadose zone on day *i* *
Q_{gw} = Return to flow on day *i* *

*= [mm H_2O]

The algorithm used in SWAT+ lets surface runoff emerge, once all topographic depressions have filled due to persistent excess in water application surpassing the infiltration capacity, known as Hortonian overland flow generation. This supports the assumption that runoff is more pronounced on steeper slopes with higher surface gradient due to less storage capacity in surface depressions (Bieger et al. 2015). Following the U.S Natural Resource Conservation Service (NRCS), SWAT+ incorporates four classes of soils varying in infiltration characteristics and thus runoff potential (A = high infiltration rate and transmissivity, B = moderate infiltration rate and transmissivity, C = slow and transmissivity rate, D = very slow infiltration and transmissivity rate), with higher runoff potential being exhibited on areas with less transmissivity (respectively hydraulic conductivity).
Based on the concept of HRUs, SWAT+ calculates different runoff volumes according to different land uses, soil and slope classes, being lumped on HUR level and transmitted to the main channel on subbasin level (Bieger et al. 2015). In this study, the SWAT+ modification of the SCS curve

number method by USDA (1972) was used for computing surface runoff, which accounts for the runoff producing key characteristics in a watershed such as soil type, land use and treatment, surface condition, and antecedent moisture condition, multiply revised and extended to different environments including forests (Mishra et al. 2018). With CN being a function of the soil´s permeability, the highest possible value of CN is equivalent to an impermeable watershed with no retention potential at all, whereas the lowest CN value represents the opposite respectively: An infinitely withdrawing watershed (Mishra et al. 2018; Neitsch et al. 2011). As Broughton (1989) remarks, the SCS-CN method resembles the spatially varied saturation overland flow model, with CN indicating the variation in surface storage capacity (Boughton 1987 in Boughton 1989). The CN calculation furthermore accounts for initial abstractions to the runoff volume from interception of the canopy storage, depending on the actual LAI (referred to as CANMX in the SWAT input variables). Following the SCS-CN approach, that defines the antecedent moisture conditions based on the rainfall of the preceding five days (Boughton 1989), SWAT+ categorizes three antecedent moisture condition: dry (wilting point), moderately wetted and wet (field capacity) (Neitsch et al. 2011).

SWAT+ also uses a modified rational method to calculate the peak runoff rate for a given storm event, depending on the time of concentration, and therefore on rainfall intensity and size of the watershed. The time of concentration is composed by the overland flow time and the channel flow time, both contributing to the flow at the outlet of the watershed (Neitsch et al. 2011), accounting for the Manning´s roughness coefficient (Engman 1983) for the surface, is an indicator for the erosive potential of a storm event to predict sediment losses. The equivalent goes with the channel flow time of concentration, being related to the average channel flow rate, the average channel velocity, the channel slope and the Manning´s roughness coefficient for the channel (Chow 1959). For large watersheds, whose time of concentration exceeds one day, SWAT+ calculates a lag for a portion of surface runoff to discharge to the main channel (SURLAG). The amount of water stored from the previous day is higher, the smaller the SURLAG value is, which consequently mitigates the flood wave, and therefore the discharge hydrograph (Neitsch et al. 2011). Erosion is computed as a function of rainfall energy allocating a runoff factor based on the Modified Universal Soil Loss Equation (MUSLE) (Williams 1975 in Neitsch et al. 2011). For ephemeral channels, that can occur either in semiarid/arid regions, or in small channels of temperate forests, which run dry periodically in warm summers, SWAT+ accounts for transmission losses that lead to a reduction in runoff volume, as the water is assumed to contribute to the shallow aquifer (ibid.).

In order to assess the effect of management practices on surface runoff generation, such as soil compaction due to heavy harvesting machinery, an evaluation on watershed level with one or more gauges for streamflow may not be expedient regarding spatial variation in geomorphologically heterogenous environments, such as mountainous forest areas (Bieger et al. 2015). An analysis on HUR level may capture more adequately areas more sensitive to driving with heavy machinery, and environmental variables related to it (e.g. slope inclination, soil type, soil moisture content). As shown by Bieger et al. (2015), SWAT sufficiently depicts the dependency of surface runoff on the moisture content of the soil, being related to the depth of the soil layer, the soil texture and soil parameters, such as bulk density, saturated hydraulic conductivity and available water capacity. Runoff simulation on HRU level therefore is expected to detect spatial variations related to soil type.

4.1.2 Water movement in the soil zone

Water that enters the soil zone by infiltration fills the soil´s pores shaped by the three-phase system (solid, liquid and gaseous) of the respective soil type either completely or partially. The pore space is calculated based on the soil´s bulk density, being the relation of the mass of solids and the total volume of air, water and solids together (Neitsch et al. 2011). The soil porosity, expressed as a fraction of the total soil volume, depends on the particle density and therefore on the mineral composition of the soil matrix. Clay soils contain more meso and micro pores, whereas sand soils predominantly contain macropores, so that consequently the latter have a higher magnitude of hydraulic conductivity. Regarding soil water content, two conditions are differentiated: Field capacity (FC) as the water content of a wetted soil after two days drainage (defined as a tension of 0.033 MPa), and permanent wilting point (WP) as the stage when there is no further soil water available for plant uptake (defined as a tension of 1.5 MPa). The margin between those tensions is considered the plant available water content ($AWC = FC - WP$), defined for each soil type based on the texture[15]. Due to their lower particle density, sandy soils drain more easily and consequently do not remain at field capacity for long, whereas clayey soils have a more pronounced water holding capacity due to their net negative charge, and therefore show a higher water retention.

SWAT+ simulates saturated flow only, following the force of gravity downwards, whenever field capacity is surpassed in a given soil layer, and given that the soil´s temperature is > 0 °C (Neitsch et al. 2011). SWAT+ records the water content of each soil layer, considering it to be evenly distributed within the respective layer. Horizontal flow is indirectly simulated by the amount of water taken up by plants via evapotranspiration. Percolation therefore occurs from one soil layer to the subjacent, if the overlaying soil layer is saturated and the subjacent is unsaturated, given the soil is not frozen (ibid.). The amount of percolating water is defined by the drainable amount of water in the soil layer on a given day within an hourly time step with the texture-related travel time of the soil layer, using storage routing methodology (ibid.). Reaching the undermost soil layer, water surpassing the layer specific field capacity directly flows into the vadose zone between the bottom of the soil layer and the top of the aquifer (ibid.). Percolation is inhibited in case the subjacent layer is saturated, or in the case of seasonally highly drained HRUs with constant water contents close to saturation. Saturation is reached once the water content of the layer surpasses field capacity (ibid.). In this case, the water will be stored in ponds in the upper layer, causing waterlogging. Waterlogging also occurs on subjacent impermeable layers, when the storage capacity of the bottom layer is exceeded and the water subsequently fills the overlying layer, forming a saturated zone that drains into lateral flow as soon as the storage capacity is surpassed (ibid.). Lateral flow is calculated based on the mass continuity equation, using the kinematic storage model for subsurface flow proposed by Sloan & Moore (1984), which predicts macropore flow responsible for stormflow response of steeply sloping forested watersheds, as well as soil matrix flow contributing to the delayed response of base flow (Sloan & Moore 1984). Subsurface flow is most likely on soils with high hydraulic conductivity in addition to an impermeable or semipermeable layer, that supports waterlogging, which preferably occurs in humid forested watersheds, showing high percolation rates in the uppermost layers promoted by organic litter in addition to a pronounced rooting system (Sloan & Moore 1984). Beven (1981, 1982) has shown that both, saturated Darcian flow on hillslopes, and unsaturated flow can sufficiently be depicted using the simplified model of kinematic theory as approximation to the theoretically more correct extended Dupuit-Forchheimer equation, assuming that the hydraulic gradient is equal to the slope of the water table throughout the depth of the saturated zone

[15] Giving the volumetric water content, the AWC of sand = 0.04, of loam = 0.24, of clay = 0.21.

(Beven 1981). As before with overland flow, a lag in contribution to the main channel is assumed for subsurface flow in large watersheds, so that the amount stored from the previous day is accounted for within the calculation of lateral flow discharge on a given day. The travel time for lateral flow can be defined by the user, so that the mitigation of streamflow contribution for lateral flow is modifiable.

Regarding groundwater, SWAT+ simulates an unconfined shallow aquifer for each subbasin, integrated in the catchment-internal water cycle, and a confined deeper aquifer, contributing to water bodies outside the catchment (Arnold et al. 1993 in Neitsch et al. 2011), with the innovation compared to the precursor version SWAT, that the spatial connectivity is HRU-independently user-definable (Bieger et al. 2016), and thus groundwater can be passed from one aquifer to another within the same subbasin, transmitted by simple passing of flow rates rather than driven by hydraulic gradients (cf. Bailey et al. 2020:3). The aquifer of a given HRU is, however, considered homogenous in hydraulic conductivity and specific yield.
For calculating the water storage in the shallow aquifer on a given day, SWAT+ accounts for the additive recharge entering that day to the amount of water storage of the preceding day, with the determination of losses due to groundwater/base flow into the main channel, water movement into water-deficiencies in the soil due to plant demands (termed REVAP) and water withdrawal. The abstraction of water from the aquifer via plant demand is the only realization of water motion in an upward direction against gravity in SWAT+, accounting for environments where deep rooting occurs, and implying a user-defined threshold value for the water level in the aquifer for REVAP to occur at all (Neitsch et al. 2011). The time delay for the recharge water to enter the shallow aquifer from the soil profile is estimated using an exponential decay weighting function (Venetis 1969; Sangrey et al. 1984), embedded in a precipitation/ groundwater response model. Only a fraction of the daily recharge is partitioned from the shallow aquifer to contribute to the deeper one, calculated with an aquifer percolation coefficient. The equations for groundwater flow imply a linear relation between the flow and the rate of change in water table height, which does not account for nonlinear flow within unconfined aquifers (Bailey et al. 2020).
For the connectivity between the shallow aquifer and the main channel, SWAT+ assumes the amount of baseflow discharging to the reach to depend on the hydraulic conductivity of the aquifer, its specific yield as well as distance from the aquifer ridge to the main channel, the water table height and the amount of recharge to the shallow aquifer on a given day, considering a baseflow recession constant as a direct index of groundwater flow response to recharge (after Hooghoudt 1940 and Smedema & Rycroft 1983 in Neitsch et al. 2011). SWAT+ implies the assumption of the general establishment of steady-state responses of groundwater flow to recharge with fluctuations in water table occurring periodically (Neitsch et al. 2011; Bailey et al. 2020). It also assumes a storage threshold to be exceeded as prerequisite for groundwater flow to streams instead of an elevation-driven, reciprocal flow gradient between the aquifer water table and the stream (Bailey et al. 2020).

4.1.3 Plant growth

Plant growth is simulated in SWAT+ using a simplified version of the EPIC plant growth model (Erosion-Productivity Impact Calculator) (Neitsch et al. 2011), which was originally developed to determine the effects of soil erosion on soil productivity by the USDA (Williams et al. 1989).
It contains physically based components to simulate daily erosion, plant growth, and related processes, based on unique parameter values for each crop, with the exclusion of detailed root growth, micronutrient cycling and toxicity response in the case of SWAT+ (Neitsch et al. 2011). Growth is simulated based on the heat unit concept (Boswell 1926; Magoon & Culpepper 1932; Barnard 1948), which assumes linear plant-growth-temperature relationships, with

plant growth only to occur, if the daily average temperature exceeds a species-specific threshold (base temperature), indicating the thermal distribution limits (Brown 2013). Within the growing period, plants accumulate heat units, one unit per rising degree in temperature, until their species-specific total in heat units is reached, representing the plants maturity (Neitsch et al. 2011). As the EPIC plant growth model computes the allocation of assimilated carbon to vegetation biomass as a linear function of heat units throughout the growing season (Neitsch et al. 2009; Yang & Zhang 2016; Williams et al. 1989), the Net Primary Production (NPP), considered as a direct indicator for plant growth, is calculated as a function of solar radiation, and the capability of a plant to convert it into biomass (Neitsch et al. 2011). In SWAT, carbon uptake through photosynthesis is limited by multiple factors, including radiation use efficiency (RUE), N, P, water, and temperature (Yang & Zhang 2016:3). Next to RUE, the key parameters related to carbon fixation are: maximum LAI (BLAI), optimum and base temperature as well as the leaf to biomass fraction, all modifiable in the plant database.

SWAT+ accounts for plant specific optimum growing conditions, which include a state of stress related to daily average temperatures above the growing optimum envelope. In the context of heat-induced shifting of distribution boundaries in the course of climate change, limitation to growth is furthermore captured in the model in terms of plant response to water deficiency. Water stress is calculated based on the relationship between actual and potential plant transpiration. The actual plant transpiration equals the actual water uptake of a plant on a given day, so that growth-limiting water stress occurs once the potential plant transpiration exceeds the actual water uptake due to soil water deficiency (Neitsch et al. 2011). Together with potential nitrogen/phosphorous stress, SWAT+ accounts for water, temperature and nutrient dependent constraints for actual plant growth influencing the plant growth factor for a species on a given day.

Tree growth is partitioned between leaves/needles and wood, and varies with age relative to the years of the tree species to reach full development (years to maturity, $yr_{fulldev}$). Until the trees on a stand (considered to be of the same age) have reached full development ($bio_{fulldev}$), the yearly accumulated biomass (bio_{annual}) is restricted by the current age (yr_{cur}):

$$bio_{annual} = 1000 \cdot \left(\frac{yr_{cur}}{yr_{fulldev}} \right) \cdot bio_{fulldev}$$

Formula 4.1.2
(Neitsch et al 2011:320)

A similar assumption is made for daily height growth of forest trees, being related to the maximum canopy height for the tree species, the current age and the years to maturity. Both assumptions result in linear yearly growing curves for height and diameter growth of trees.
For tree rooting, SWAT+ assumes the maximum rooting depth to meet the plant and soil specification. The EPIC plant growth model considers soil strength determined by bulk density, texture, and water content, as influencing factors for root growth (cf. Williams et al. 1989:503), and therefore potentially depicts root growth deterioration as consequence of soil compaction.

For the application to old, protected forest communities, modifiable parameters of the plant´s database can be used in order to approximate the model setup closer to the given forest conditions, within the given limitations of the EPIC plant growth model. Plant growth related parameters, as well as water consumption related structural components of the forest cover, such as ET, are considered to affect hydrological as well as biogeochemical dynamics (Yang & Zhang 2016; Bosch & Hewlett 1982). Therefore, adapting the plant growth model performance closer to the addressed field conditions appears to be necessary for an adequate investigation of water fluxes, including the key performance indicator quantitative groundwater recharge. Consequently, variables representing age, stand and canopy structure as well as plant growth should be analyzed and tested, depending on data availability and reliability.

4.2 Watershed configuration

In the following, the work steps implementation, parameterization, sensitivity analysis, calibration and validation are described in detail. All relevant input data was covered by hard data collected in the area. Soft data on evapotranspiration and results for groundwater recharge simulated by other studies were used as a formal check on reasonableness and consistency of the model performance (Arnold et al. 2015). The working steps watershed delineation, calibration and validation were supported and executed by the Department of Hydrology and Water Resources Management of the Kiel University, namely Dr. T. Tigabu, Dr. P. Wagner and Prof. Dr. N. Fohrer from October 2019 to January 2022.
As a whole, four different SWAT+ models were built based on digital elevation model data (DEM), and 7 river gauging stations (Hardenburg, Neustadt, Siebeldingen, Hirschtal, Thaleischweiler, Steinalben, and Moosalbtal) along the Biosphere Reserve area border as outlet points with long-term streamflow records provided by the State Office for the Environment Rhineland-Palatinate (LFU RLP) from 1955-2019: Bobenthal, Thaleischweiler, Neustadt, and Hardenburg. They were constructed with the QSWAT+ version 2.1.6, and the long-term release of QGIS version **3.18.2** to delineate the watersheds, and processed for implementation using the SWAT+ editor version **2.0.4** (Tigabu et al. 2022). The catchments were first calibrated separately, and then treated as sub-catchments for regionalization of the entire Palatinate Biosphere Reserve catchment (shown in **fig. 14**). In each case, no thresholds for land use/soil/slope were used in HRU definition, in order to account for all possible combinations (Her et al. 2015 in Tigabu et al. 2022). The subbasins were subdivided into upland and floodplain areas. In order to achieve the best possible model performance with regard to hydrograph and flow duration curves, as well as statistical indices, the Hargreaves method was preferred to the Penman-Monteith method for calculating evapotranspiration (see section **5.1.1**). Furthermore, the variable storage method was used for channel routing, and the soil moisture function for calculating the average daily curve number (CN) values (Tigabu et al. 2022).
Regarding the representation of groundwater-processes, SWAT is in the critique to perform poorly in groundwater-driven watersheds due to simplified flow equations (Bailey et al. 2020). In order to improve the representation of fast and slow groundwater responses and the connectivity between surface and sub-surface hydrological processes, a second aquifer layer was created with an equivalent number of spatial objects and extent as the first groundwater layer, and the respective groundwater files (´aquifer.aqu´, ´aquifer.con´, ´aqu_catunit.ele´, and ´object.cnt´) were modified accordingly (Bailey et al. 2020; Tigabu et al. 2021, 2022). The final catchment construction resulted in 99 subbasins, 405 channels, 795 routing units, 49705 HRUs, and 197 aquifers.

The constructed Palatinate Forest catchment was 128,537.75 ha of size, with 89 % upslope, and 11 % floodplain area, and an elevation range from 92 to 662 meters. For slope band classification, a terrain analysis was executed with QGIS, based on which 5 slope categories were built, representing the local conditions for inclination and reflecting an applicability for the evaluation of slope effects with soil compaction in the course of harvest operations with heavy machinery: 0-2 %, 2-10 %, 10-15 %, 15-20 % and >20 %. The majority of the area (62.6 %) was identified as above 20 % slope, followed by 14.5 % with 2-10 %, 11.2 % with 10-15 %, 10.5 % with 15-20 %, and 1.2 % with 0-2 % incline. The land use types (**fig. 3**) included all main tree species (oak, beech, spruce, douglas fir, pine, and mixed forest stands), the soil types were classified into 5 different soil groups, representing pure sands (SS), loamy sands (LS), silty sands (SU), sandy loam (L), and silt (U).

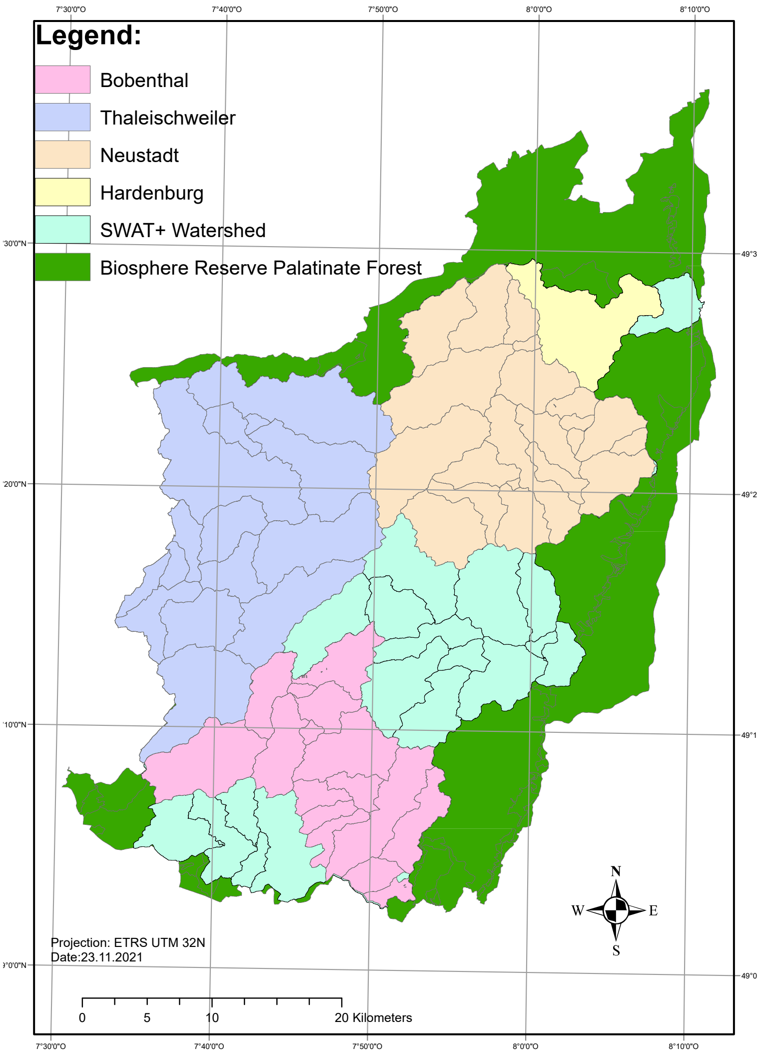

Figure 14: Delineated entire SWAT+ watershed, its sub-catchments Bobenthal, Neustadt, Thaleischweiler, Hardenburg with their sub-basins, and the Biosphere Reserve it is embedded in.

Bobenthal2 catchment

For investigating the effects of disrupted areas with rejuvenation, the Bobenthal2 catchment was chosen for an experimental model setup of two general plant parametrizations: mature and juvenile stocks, described in section **4.2.5**. The model was built, calibrated and validated independently ahead of the regionalization process. The inputs data, as well as the model implementation and delineation procedures were analoguous to the Palatinate Biosphere Reserve catchement. The Bobenthal2 catchment was 22,336.9 ha of size, included 16 subbasins, 52 channels, 101 routing units, 5332 HRUs, and 32 aquifer objects for the first groundwater layer, and the exact same number of aquifers and spatial extents for a second aquifer layer (cf. Tigabu et al. 2021:4). The main tree species oak, beech, pine, spruce, and mixed forest are represented, also 4 of 5 soil types (SS, LS, SU and L). From the stated slope bands, 70 % are in the range of 20 % incline and above, almost 20 % are in the range of 10 to 15 % incline, and another 10 % are assigned to floodplains.

4.2.1 Model implementation

The model feeding requires gridded spatial data including a digital elevation model (DEM), land use/land cover and soil maps. The DEM was provided by the dataset of the State Office for Surveying and Geospatial Information (LVermGeo RLP) in a 10 m x 10 m resolution. For calibration and validation, long-term streamflow records are necessary, which were available from the State Office for the Environment Rhineland Palatinate (LFU) for different timelines for each gauge station, ranging from 1955 to 2019. **Table 2** shows an overview of available input data and the respective data source.

Table 2:

Spatial data and data sources used in the SWAT+ model

Dataset	Spatial resolution	Time resolution	Source
Topography	10 x 10 m	1 dataset	LVermGeo RLP
Climate	1000 x 1000 m	1951-2020	Climate Competence Centre, DWD
Land use	10 x 10 m	1 dataset	University of Trier; ATKIS
Soil	1: 50,000	1 dataset	LGB 2020
Streamflow	Five gauge-stations	1955-2019	LfU 2020

4.2.1.1 Climate and climate projection data

As input data for climate, SWAT+ requires a consistent timeseries of daily values for precipitation, maximum and minimum temperature, relative humidity, sunshine duration (solar radiation) and wind speed. The data was provided and interpolated by the Climate Competence Centre of Rhineland-Palatinate, based on data by the DWD (German Meteorolocal Service), in a 1000 m by 1000 m resolution for the timeline from 1952 to 2020. The data sets were based on the InterMet program package (interpolation of meteorological parameters), which includes error correction and interpolation techniques (Dobler et al. 2004).

For simulating climate change, high-resolution statistical and dynamic regional models were used based on the BIAS-adjusted REKLIES and EURO-CORDEX simulations RCP2.6 and RCP8.5 over the HYRAS area using downscaling methods[16]. The global climate model (GCM) projections from the EURO-CORDEX project have already been brought to the local level in advance by means of regional climate models (RCMs) and then bias-adjusted once again by the DWD as part of the BMVI-ExpN project and interpolated over 5 km (the HYRAS grid). The processed 6 climate projections for each RCP2.6 and RCP8.5 were then combined with the water balance model SWAT+.

[16] CCLM4.8.17, RACMO22E, RCA4, CLM, WRF361H

4.2.1.2 Land use data

The required gridded spatial data on land use for forested areas was taken from remote sensing based on LiDAR technology by the university of Trier. Integrated into the forest management system for the federal state of Rhineland-Palatinate, and based on operational forest survey methods, satellite-derived forest information layers were built in order to generate accurate and up-to-date information on the spatial distribution of forest type, forest cover, and tree species composition within the optimum phenological time-windows (Stoffels et al. 2015). The sentinel-2-dataset provides a differentiation between the dominant tree species, as well as for mixed stocks. The data on forested areas was intersected with data from the official topographic-cartographic information system (ATKIS) dataset of the State Office for Surveying and Geospatial Information RLP in ArcGIS to cover all other land use types. The derived types of land use for the Palatinate Biosphere Reserve catchment are shown in **table 3**, and **table 4** for the Bobenthal2 catchment respectively.

The current SWAT+ model provides a plant parametrization for four key forest types (deciduous, mixed, evergreen forests and temperate evergreen forests) based on their phenology. Sierra et al. (2009) and Yang & Zhang (2016) suggest, however, that this aggregation may lead to an oversimplification in terms of controlling factors for plant growth (e.g. carbon fixation). In order to meet structural differences among different forest types, the plant parametrization was adjusted according to data from the monitoring program of the FAWF and related literature, that covers area-specific characteristics of the classified forest types. Parameter modification, default settings and applicated changes of selected plant parameters used for the model setup are described in section **4.3.2. Figure 15** shows a map of used land use types and their distribution in the Palatinate Biosphere Reserve watershed.

Table 3:

Land use types generated for SWAT+ and their distribution in the Palatinate Forest watershed.

Land use type	SWAT code	Description	Distribution	
			Area [ha]	% of watershed
oak	oak	Oak forest	14913.5	11.6
beech	frsd	Beech forest	36049	28
spruce	frse_tems	Spruce forest	16691.8	13
douglas	frse	Douglas forest	8270.6	6.4
pine	pine	Pine forest	27372.2	21.3
mixed	frst	Mixed forest	6811.3	5.3
agrc	agrc	Agricultural land	11030.3	8.6
watr	watr	Water	128.5	0.1
urbn	urbn	Urban area	5112.8	4
urbn_ind	uidu	Urban industrial area	484.2	0.4
urbn_inst	uins	Urban institutional area	154.5	0.1
urbn_transp	utrn	Urban area for transport	525.2	0.4
grass	migs	Grassland	993.9	0.7

Table 4:

Land use types generated for SWAT+ and their distribution in the Bobenthal2 watershed.

Land use type	SWAT code	Description	Distribution	
			Area [ha]	% of watershed
oak	oak	Oak forest	1704	7.6
beech	frsd	Beech forest	4961	22.2
spruce	frse_tems	Spruce forest	3462	15.5
pine	pine	Pine forest	5259	23.7
mixed	frst	Mixed forest	1944	8.7
agrc	agrc	Agricultural land	2042	9.1
watr	watr	Water	2644	0.1
urbn	urbn	Urban area	714	3.2
urbn_ind	uidu	Urban industrial area	107	0.5
urbn_inst	uins	Urban institutional area	21	0.1
urbn_transp	utrn	Urban area for transport	62	0.3
grass	migs	Grassland	173	0.7

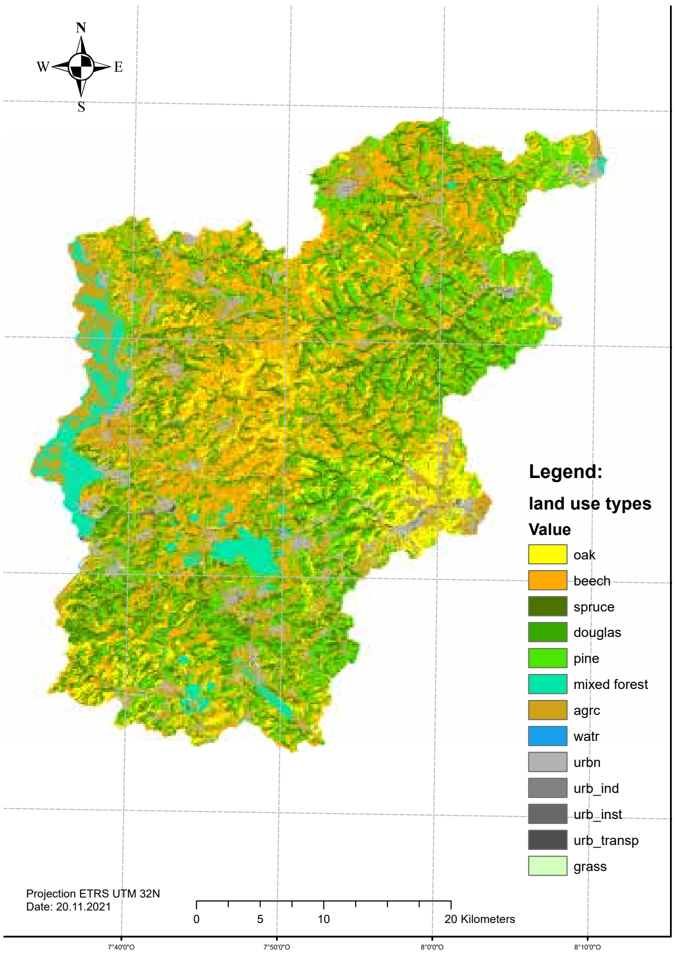

Figure 15: Land use types generated for the SWAT+ model and their distribution in the Palatinate Biosphere Reserve watershed.

4.2.1.3 Soil data

The soil data was provided by the State Office for Geology and Mining (LGB) of Rhineland Palatinate in a scale of 1:50000 (BFD 50) in vector data format with detailed information on the required soil parameters based on pedological mapping instructions. All soil profiles have been analysed for layer depth, texture, bulk density, available water capacity, saturated hydraulic conductivity, organic carbon content as well as clay-, silt-, sand- and rock fragment content. The layering of the original dataset was classified, which goes along with a simplification, in order to generate 5 soil types (soil classes), aggregated according to pore size and their respective hydrological properties, based on the Forest Site Survey (2016, p. 91). Since SWAT+ requires values for moist bulk density, and the available data only provided dry bulk density, an excel template was used, which calculates SWAT soil parameters using the Pedo Transfer Function (PTF) developed by Saxton & Rawls (2006). The template was also used to derive SWAT-conform values for available water capacity (AWC). The derived soil classification data was transferred into a vector data set, and converted into grid with ArcGIS. **Tab. 5** shows all generated soil classes used in the SWAT+ model, and their hydrological properties used as basis for classification. **Fig. 16** shows a map of all soil classes represented in the Palatinate Biosphere Reserve watershed.

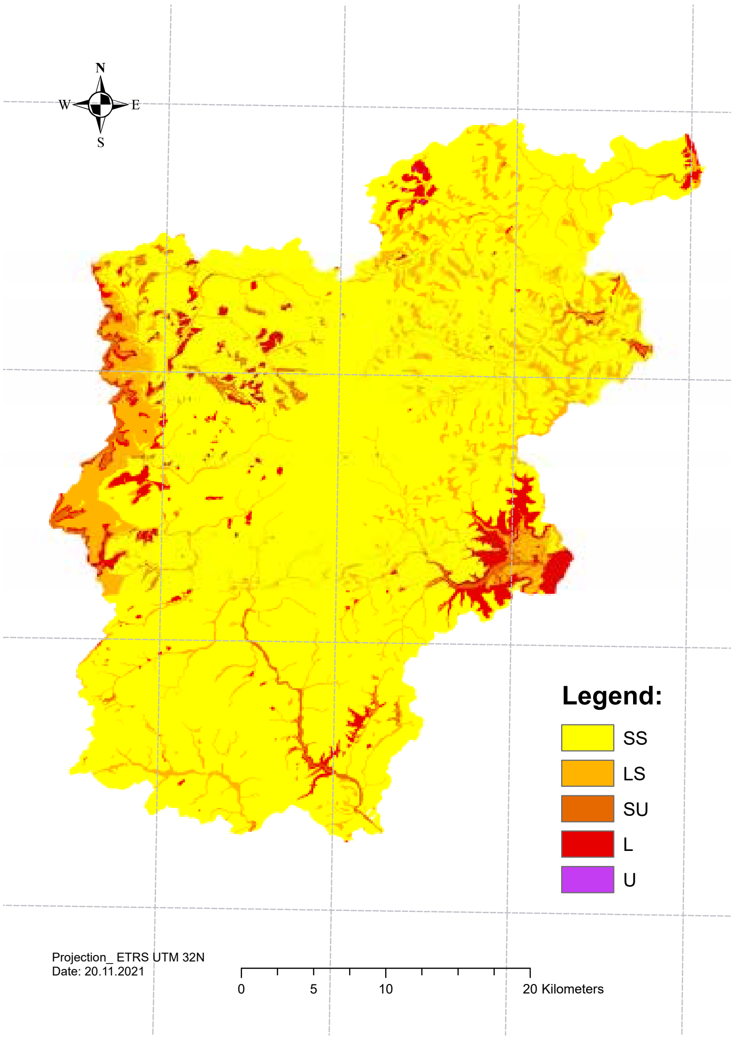

Figure 16: Soil classes generated for the SWAT+ model and their distribution in the Palatinate Biosphere Reserve watershed.

Table 5:

Soil classes aggregated for SWAT+, their physico-hydrological properties, mass percentages, hydrological groups assigned by SWAT+, and distribution in the watershed (kf = hydraulic conductivity, AWC = available water capacity). The soil class serves only for name-asignment in SWAT+.

Soil class	Definition			Hydrological properties			Distribution			
		Hydrol. Group	layer	Moist bulk density [g/cm^3]	kf [mm/hr]	AWC [mm H_2O/mm soil]	Clay [%]	Silt [%]	Sand [%]	% of watershed
SS	Pure sands		1	1.54	169	0.04	2.5	5	92	
			2	1.59	101	0.06	4	14.8	81	
		A	3	1.61	98	0.06	4	13.6	79.8	82.4
			4	1.57	151	0.04	2.7	5.5	89.3	
			5	1.56	133	0.04	3.4	6.7	89.8	
LS	Loamy sands		1	1.62	58	0.08	6.9	22	71	
			2	1.62	57	0.08	7	21.5	71	
		B	3	1.62	60	0.07	7	20	73	11
			4	1.61	63	0.07	7	18	75	
			5	1.61	52	0.05	11	5	84	
SU	Silty sands		1	1.65	23	0.13	9	45	46	
			2	1.65	29	0.12	8	42	50	
		B	3	1.65	29	0.12	8	42	50	2
			4	1.64	16	0.13	13	41.4	45.6	
			5	1.61	70	0.05	8	5	84.8	
L	Sandy loam		1	1.65	7	0.13	19.2	37.5	37	
			2	1.60	6	0.14	20	45	35	
		C	3	1.60	7	0.13	20	41.6	38.4	4.6
			4	1.61	9	0.13	19	38	41.8	
			5	1.63	15	0.11	15.8	32.5	50.5	
U	Silt		1	1.68	8	0.16	12	55	26.5	
			2	1.64	9	0.18	10.6	64	25.4	
		C	3	1.65	38	0.12	6	41	53	0.02
			4	1.54	171	0.04	2.5	5	92.5	
			5	1.61	86	0.05	5.6	8.6	82.6	

4.2.2 Sensitivity analysis

4.2.2.1 Plant parametrization

The extent of forest cover, and thus plant growth and canopy expression, are reported to influence the hydrological and nutrient dynamics of forest ecosystems (Yang & Zhang 2016; Bosch & Hewlett 1982; Hewlett et al. 1969; Hibbert 1967). Since the interlink between plant growth, and water consumption through evapotranspiration is essential to understanding ecosystems dynamics and responses to environmental changes (cf. Yang & Zhang 2016:2), accuracy in the representation of the catchment conditions is vital to hydrologic modelling, that aims practical management recommendations. It is therefore recommended to approximate the model as close to reality as possible to ensure model robustness (Francesconi et al. 2016). In order to evaluate SWAT+ simulations of water fluxes, and analyze possible improvements for a locally-adapted model parametrization, plant specific parameters have been applied based on long-term in-situ measurements at site scale, and literature, tested on watershed level, addressing plant growth and water consumption performance. The collected field data included phenology (LAI), biomass, and harvest operational information. **Table 24** in the appendix shows an overview of all modified parameter values, their default configuration, and references for adaption.

Plant parameters such as stomatal conductance, maximum plant height and rooting depth, and *LAI* were found to be sensitive to water balance parameters (Lenhart et al. 2002). For adapting the SWAT+ model to the conditions of local permanent, protected forest communities, a simple manual sensitivity analysis was carried out, varying one plant parameter at a time, and evaluating the effect on growth performance and *ET*. To define the parameter variation, the parameter values derived from measured field observation data and literature reviews based on comparable forest conditions was used. The effect of change was analyzed based on the default settings, using the Penman-Monteith method for *ET* calculation in order to analyze all parameters presumed to be potentially sensitive. In the following, the identified sensitive plant growth and ET related plant parameters and their modification are highlighted:

- Radiation use efficiency (*RUE*): SWAT calculates the plant growth as product of the amount of dry biomass produced per unit intercepted solar radiation, expressed in *RUE* [kg/ha*(MJ/m^2)$^{-1}$], and the amount of intercepted photosynthetically active radiation on a given day [MJ m^{-2}]. It also accounts for climate change induced changes of CO_2 concentration sin the atmosphere (cf. Neitsch et al. 2011:318). Being a decisive factor for plant growth, and found to perform unsatisfactory in terms of forest dynamics in the default SWAT setting (Yang & Zhang 2016), reviewed studies were analyzed to determine plausible values for the given forest conditions. Based on the findings of Gower et al. (1999), Garbulsky et al. (2010), and Bartelink et al. (1997), the absolute value for *RUE* was set to 18 instead of 15 [kg/ha*(MJ/m^2)$^{-1}$] for all classified tree species.

- Harvest index (*HI*): The *HI* is defined as the fraction of the above-ground plant dry biomass removed as dry economic yield (Neitsch et al. 2001:338). Since the *HI* consequently expresses the performance-related growth rate of the stands, which varies among tree species and is also flattened by the age degression that occurs in older stands. The values were adapted based on Matyssek et al. (2010) according to tree species.

- Potential *LAI* and minimum *LAI*: In accordance with the Global Terrestrial Observing System (GTOS 2009), the leaf area index is defined as the vertically projected horizontal leaf area per unit horizontal ground area [m^2/m^2]. It thus influences the transpiration rate, the canopy water storage, canopy resistance as well as biomass production (Neitsch et al. 2011). In the SWAT plant database there is no differentiation between tree species. Tree species do, however, differ in *LAI*. The values used in the model setup were derived from measurements of the FAWF monitoring program using direct harvesting methods. Standardization and cross-validation between methodologies with other studies has been carried out (oral information Dr. Greve, FAWF). SWAT+ calculates the LAI for a given day according to the potential heat unit concept, and in relation to the current age and the years to reach full maturity:

$$LAI = \left(\frac{yr_{cur}}{yr_{fulldev}}\right) \cdot LAI_{mx} \cdot \frac{(1 - fr_{PHU})}{(1 - fr_{PHU,sen})} \qquad fr_{PHU} > fr_{PHU,sen}$$

Formula 4.2.1 (Neitsch et al. 2011)

LAI	=	Leaf area index [dimensionless]
yr_{cur}	=	Current age [years]
LAI_{max}	=	Maximum LAI [dimensionless]
$yr_{fulldev}$	=	Years to maturity [years]
fr_{PHU}	=	Fraction of potential heat units on a given day [dimensionless]
$fr_{PHU,sen}$	=	Fraction of potential heat units at which senescence becomes dominant [dimensionless]

Consequently, at the beginning of a default simulation, SWAT+ assumes the trees to be juvenile and homogenous in age, and therefore not to have reached the maximum potential LAI yet, until they reach the age (years) of maturity. Regarding the LAI, however, the majority of stocks in the study area show a heterogenous age pattern with fully developed LAI performance (as estimated based on field data), which is why the initial age needs to be adjusted according to the study area conditions at full development. The modification of the LAI contained both, absolute values on minimum and maximum LAI for each tree species, as well as the adaption of the LAI development curve (`lai_max1´, `lai_max2´, `hu_lai_decl´, `dlai_rate´), which requires detailed phenological information provided by the FAWF monitoring program for the study area.

- Canopy height: The canopy height [m] is used in SWAT+ to calculate wind speed as part of the estimation of ET after Penman-Monteith (Monteith 1985). The development of canopy cover height for trees is controlled by the maximum possible canopy height for the tree species, the current age of the tree, and the years to reach full maturity. The parameter was found to be sensitive regarding biomass production, and also governs the droplet energy of rainfall in connection with erosive forces (Neitsch et al. 2011).

$$h_c = h_{c,mx} \cdot \left(\frac{yr_{cur}}{yr_{fulldev}}\right)$$

Formula 4.2.2 (Neitsch et al. 2011)

h_c	=	Current canopy height [m]
yr_{cur}	=	Current age [years]
$h_{c,max}$	=	Maximum canopy height [m]
$yr_{fulldev}$	=	Years to maturity [years]

The values were adapted based on Eder & Dong (2003), accounting for the conditions of fully developed, permanent tree communities.

- Stomatal conductance: In the calculation of ET after Penman-Monteith, the canopy resistance is considered as a function of stomatal conductance and LAI. For actual ET, stomatal conductance is considered connected to the vapor pressure deficit (Neitsch et al. 2011): SWAT+ assigns a threshold for the vapor pressure deficit, triggering stomatal conductance to drop, which can be considered as a representation of stomatal closure, preventing the plant from desiccation at low soil water availability.

  The default value for leaf conductance is set to 0.002 [m•s^{-1}]. The modification was derived from Hayes & Bangor (2017, p. 35), used with a conversion equation by Matyssek & Herrpich (2019). The calculations resulted in values for oak to be 0.01 [m•s^{-1}], for beech 0.009 [m•s^{-1}], for spruce 0.005 [m•s^{-1}], and for douglas fir and for pine to be 0.01 [m•s^{-1}]. The mixed stands were calculated as average values of the other species, resulting in 0.008.

- Vapor pressure deficit (VPD): In the calculation of actual ET with the Penman-Monteith method, SWAT assumes the *VPD* to affect leaf conductance (Stockle et al. 1992 in Neitsch et al. 2011). Therefore, a plant-specific threshold for VPD is defined that induces a drop of leaf conductance per increase in *VPD* (ibid.). Furthermore, according to literature (stated in Neitsch et al. 2011), SWAT assumes a linear relationship between *RUE* and *VPD*, with *RUE* decreasing with increasing *VPD*. To match both, higher *RUE* values, as described above, and the values on *VPD* for forest communities found in related literature (Mills et al. 2017:35), the *VPD* value was modified to be 3.1 [kPa] for deciduous, and 3.0 [kPa] for coniferous tree species, instead of the default 4 [kPa].

- Root:shoot ratio: This unitless ratio describes the relation between aboveground (shoot) and belowground (root) biomass, and is crucial in the allocation and storage of carbon (Cairn et al. 1997 in Mokany et al. 2006), and thus important for plant growth. The default values range from 0 for deciduous trees to 0.4 for conifers, and have been modified based on Mokany et al. (2006), who state 0.29 for oak, 0.24 for beech, and 0.2 for the coniferous species.

Both simulations, the default and the modified plant configurations, were ran with the same basic model setup. Since within the calibration process, the Hargreaves method for calculating *ET* was found to result in the most sufficient model performance (see section **5.1.1**), using the Penman-Monteith method was dismissed accounting for the objective targets groundwater recharge and runoff behavior. Therefore, the identified sensitive plant parameters stomatal conductance, *VPD* with respect to *ET* calculation, and canopy height were disabled in the simulations. In both scenarios, however, the simulation was started with fully developed mature stocks. Therefore, the years to maturity, as well as the initial age were set to 30 (Peck & Mayer 1996; Hiege 1985). The maximum biomass on a stand for both cases was set to values derived from Bartsch & Röhrig (2016, p. 264) based on similar field conditions. The initial biomass was derived from yield tables provided by Block et al. (2016) equivalent to the given initial age, in order to generate a corridor for plant growth as basis for comparison of growth performance (**Tab. 6**). The simulations were executed within the same time period from 2000 to 2010.

Table 6:

Basic biomass and age settings for both simulations, default and modified plant parameters, as basis for comparison of growth performances, used for sensitivity analysis.

Parameter	**Tree species**					
	oak	beech	spruce	douglas fir	pine	mixed
Years to maturity [years]	10	10	10	10	10	10
Maximum biomass on a stand [t/ha] *	185	289	215	215	113	150
Initial biomass [t/ha]	65	85	56	78	85	70
Initial age [years]	50	35	30	25	30	30

* = derived from Bartsch & Röhrig (2016)

To evaluate the differences in growth performance, a growth rate was calculated for each tree species, based on formula 4.2.3. The formula used for calculation was tested with and confirmed valid by data of reference tables for Forestry of the FAWF (Block et al. 2016). It applies as follows, with R_{growth} being the growth rate, $Bioms_y$ being the biomass of the second simulation year, and $Bioms_x$ being the biomass of the first simulation year,

$$R_{growth} = \frac{(Bioms_y - Bioms_x)}{Bioms_x}$$

Formula 4.2.3

So that the yearly increase in biomass (G_{yr}) for a given year is calculated as follows, with $Bioms_{1styr}$ being the initial biomass in the first year, and Bioms prev yr being the biomass of the years ahead:

$$G_{yr} = Bioms_{prev\,yr} + (Bioms_{1styr} \cdot R_{growth})$$

Formula 4.2.4

The calculation was used to determine growth rates simulated by SWAT+, as basis for comparison with the growth rates found valid for the data provided by Block et al. (2016), which is based on in-situ field data from the study area. For evaluating differences in tree specific growth performance, the HRUs were intersected with forest inventory data on site specific yield classes, in order to match with site-dependent growth conditions, and to generate propriate growth rates for the selected HRUs overlapping with the respective site. The chosen HRUs for each tree species (land use class) were allocated to yield class III, which was calculated to have a yearly growth rate of 0.015 kg/ha in case of oak, 0.009 kg/ha for beech, 0.05 kg/ha for spruce and for douglas fir, 0.006 kg/ha for pine. As the calculations of the field data were generated with the forest growth model SILVA, which uses algorithms different to SWAT+ and which assumes an unimodal growth curve (Pretzsch 2019), the attempt is not suitable for a direct comparison of absolute values, but considered as an orientation whether the modifications point to an indication of model improvement regarding plant growth in local forests, or not.

Regarding evapotranspiration, a hard-data based comparison could not be followed due to lacking field measurement data. In this case, a comparison of change in values was pursued, in order to detect the model sensitivity to the applied parameter changes, and compare the ET performances with stated literature information, provided by Peck & Meier (1996) on tree specific annual average ET values.

4.2.2.2 Model parameters

As preparation of the calibration process general model parameters, as well as specified aquifer-related parameters were tested manually by checking the effect of value decrease/increase on hydrological processes, such as streamflow hydrographs and basin water balance components. The analysis was based on discharge data, as streamflow was the only continuous hard data available covering the required time-resolution for proper calibration. The daily measured streamflow data covered the period 1991 to 2020.

In case of aquifer-related parameters, the effects of groundwater discharge to the streamflow were thoroughly checked, and subsequently reasonable values, providing minimal changes in the hydrologic process, were identified ahead of calibration (Tigabu et al. 2022).

Analyzing the effect of decrease/increase of other model parameters on streamflow and basin water balance components, resulted in 16 parameters identified to be sensitive, for which reasonable value ranges could be determined.

4.2.3 Calibration and validation

4.2.3.1 The Palatinate Forest catchment

With the results of manual calibration as a basis, automatic calibration was conducted, again following the multiple flow segment calibration approach based on performance metrics and signature metrics after Pfannerstill et al. (2014a, 2014b) and Haas et al. (2016). Based on discharge data of all gauged streams, five years warm-up (from 1985 to 1990) were considered for the model performance to level at equilibrium and define proper initial conditions (Tigabu et al. 2022). In order to evaluate the model performance, the R packages FME (Soetaert & Petzoldt 2010) and hydroGOF (Zambrano-Bigiarini 2014) were used, the latter for parameter calculation based on the Latin hypercube algorithm.
In a first step, the sub-catchments Bobenthal, Neustadt, and Thaleischweiler were evaluated with regard to model efficiency and parameter settings based on 250 runs each. The best results on parameter ranges of these runs were then transferred to another 3000 model runs. Following Moriasi et al. (2007), the best parameter combination depicting the discharge hydrograph was then chosen with respect to quantitative statistics, Nash-Sutcliffe efficiency (NSE), percent bias (PBIAS), Kling-Gupta efficiency (KGE) and ratio of the root mean square error to the standard deviation of measured data (RSR). Due to data-gaps in the discharge timelines of the catchments Thaleischweiler and Hardenburg, the best parameter combinations found within the calibration process for Bobenthal and Neustadt were transferred to the whole catchment and then used for validation (Tigabu et al. 2022).

4.2.3.2 The Bobenthal2 catchment

Model parameters influencing the hydrologic processes were identified, and calibrated to improve the performance of the default model based on streamflow data. The calibration period was 2009 to 2019, the validation period 1994 to 2003, with three years warm-up ahead of simulation to maintain equilibrium conditions of the model. The multiple flow segment calibration approach (Pfannerstill et al. 2014a, Pfannerstill et al. 2014b, Haas et al. 2016) and the SWATplusR package (Schürz 2019) were used for calibration processing and performance metrics and signature metrics evaluation. Sensitive parameters were identified by applying change methods on parameter values manually, one parameter at a time, and then included into 2000 iterations for narrowing down the parameter ranges, and another 5000 iterations for calibration. Following Guse et al. (2020), parameters which showed clear trends in improving the model performance were continued with for another 1500 iterations (Tigabu et al. 2021). The selection of the final calibration parameters was based on optimizing Kling Gupa Effieciency Coefficient (KGE) for streamflow (ibid.).

4.2.4 Simulation of soil compaction

In order to simulate the effect of soil compaction on the water balance in the area, georeferenced data, provided by the department for strategic planning and service of the Landesforsten RLP on road network, pathway system, machine routes, and skid trails, the latter generated with tracking technology (as part of the geographic information system WaldIS of the Forest Inventory), was used to create compaction layers in ArcGIS. According to the spatial exploitation guideline from "Landesforsten Rheinland-Pfalz", roads are specified to be of 5 meters width, skid trails of 4 meters (Landesforsten Rheinland-Pfalz 2018:15, 45). The respective line features for paths/machine roads and skid trails were buffered accordingly, and intersected with the SWAT+ soil map, using a raster overlay function in ArcGIS in order to define the spatial coverage of compacted areas, and the respective soil properties. The soil parameters were adjusted according to data from driving tests carried out on areas in the Palatinate forest in 1989, 2002 and 2015 (Reichardt 2002; Schneider 2015). **Figure 17** shows the spatial distribution of the pathway system, within the catchment area, covering the Palatinate Forest

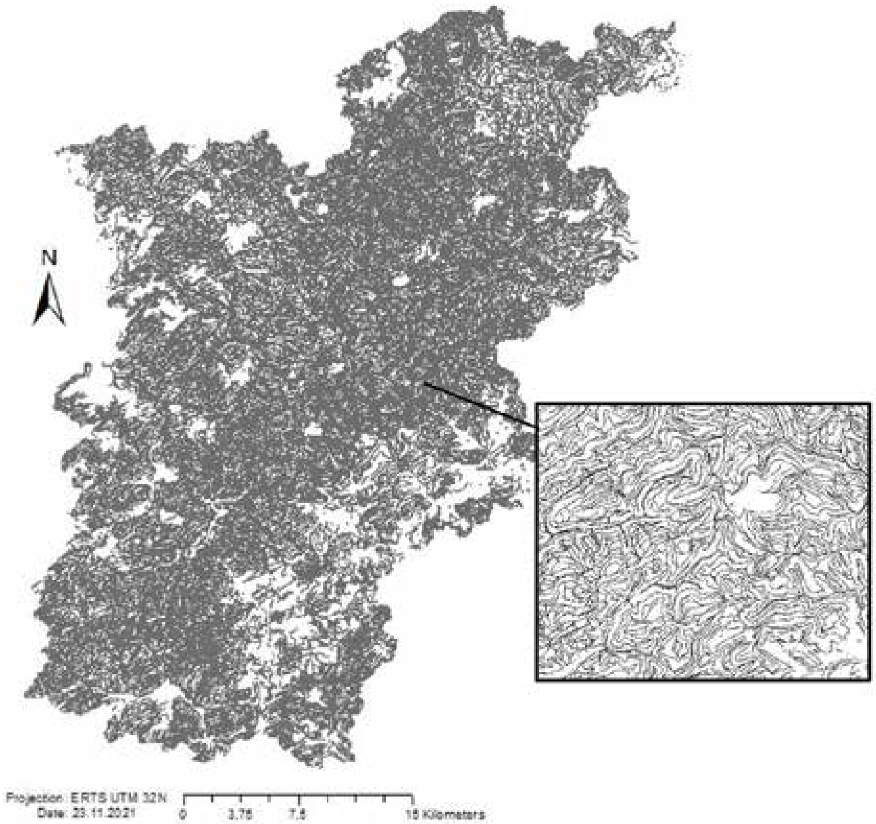

Figure 17: Spatial distribution of the pathway system within the catchment area, covering 11 % area extent of the Palatinate Forest Biosphere Reserve catchment

Biosphere Reserve, plus a cutout with a higher resolution of the buffered line structures, covering approximately 11 % in total of the watershed area.

According to the guidelines of Landesforsten Rheinland-Pfalz (2018) on skid trail specification, the upper limit for the area used on skid trails is supposed to be 13.5 % of the cultivated forest area. Formerly used skid trails, going back to regulations of past times, must, though, be considered to be still effective with regard to soil compaction, when accounting for the poor regeneration capacity of deteriorated soils, so that 13.5 % of the area can be concluded as the undermost limit, or minimum dimension of skid trail compaction in the study area. Additionally, areas of 30 to 50 years old oak trees, which were driven on extensively in the course of afforestation activities from 1970 to 1990 (LWF AKTUELL 2003), must be assumed to also show soil deterioration from driving with heavy machinery. The preloaded area sums up to 2678 ha, the cultivated forest area of the SWAT+ Palatinate Biosphere Reserve watershed, from which the core protected zone (5,400 ha)[17] was subtracted, results in 104,708.6 ha. From this cultivated forest area in the watershed, 13.5 % account 14,135.6 ha, which adds up with the preloaded stocks to 16,813.8, equivalent to 13 % of the SWAT+ Palatinate Biosphere Reserve watershed considered to be affected by harvest compaction. Therefore,

[17] https://www.pfaelzerwald.de/blog/kernzonen-im-biosphaerenreservat-pfaelzerwald/

the simulation results on (C2), which are based on the spatial extent of the current progress on skid trail tracking carried out by Landesforsten RLP in 2021, accounting for 4.1 % of the watershed in total, are multiplied by the factor 3.1 in order to calculate reasonable estimates for 13 % compacted area of the entire watershed due to harvest operations.
The following compaction scenarios were assessed separately, each with a newly constructed SWAT+ model:

(C0) Uncompacted model

(C1) Existing forest road and path network, including machine routes.

(C2) Skid trail network plus additional areas of 30 to 50 years old oak trees, which were driven on extensively in the course of afforestation activities from 1970 to 1990 (LWF AKTUELL 2003).

In case of (C1) the number of HRUs increased to be 80773 based on the new soil information, (C2) resulted in 58494 HRUs accordingly.
For the path and road network, extreme compression was assumed based on studies on ecological damaging compaction: Following Ampoorter (2012), Zemke et al. (2019) and LUNG MV (n.d.), bulk density was increased by 0.2 g/m^3 in the uppermost 50-60 cm. Since AWC and kf were included in the calibration parameter set, there were not considered for alterations of soil properties in the compaction models in order to prevent interferences. Consequently, also for skid trails and preloaded areas, only bulk density was adjusted according to the studies of Reichardt (2002) and Schneider (2015): Within the affected layer depth (0-50 cm), the change signal for bulk density before and after compaction was calculated for each compaction scenario, and applied to the SWAT+ soil dataset. **Table 7** shows an overview of the applied changes on bulk density for the respective compaction scenarios. For both scenarios, new ´usersoil´ input files were created for the SWAT+ model.

Based on the concept of HRUs, SWAT+ calculates different runoff volumes according to different land uses, soil and slope classes, being lumped on HUR level and transmitted to the main channel on sub-basin level (Bieger et al. 2015). For computing surface runoff, the SCS curve number method by USDA (1972) was used. In order to simulate the effect of compaction with respect to overland runoff generation, SCS curve number (CN) values were modified. As the CN governs the infiltration process, the measured field data regarding the influences of compaction on the infiltration rate by Reichardt (2002) was used as a basis for value adaptation in case of skid trails and preloaded areas. According to Reichardt (2002), the infiltration rate decreased by -26 % after the first crossing with heavy machinery, and by -58 % after five passes. Since for skrid trails and preloaded areas more than five crosses must be assumed, 58 % decrease was applied to the CN values. This resulted in a change in case of soil class SS (pure sands) from 45 to 71, in case of soil class LS (loamy sands) and SU (silty sands) from 66 to 104, and in case of L (loam) and U (silt) from 77 to 121. The threshold limit for CN in wooded areas is 95, which therefore defines the maximum limit for CN values for each soil class. L and U were therefore set to 95. Since sand soils in general show a coarse texture, and are therefore not as susceptible to compression as fine textured soils (Reichardt 2002; Schneider 2015), they still allow for infiltration, even though to a lesser extent under compacted conditions. In order to account for this, the infiltration capacity reflected in CN values for sand soils (LS, SU) was not assumed to reach the maximum level of inhibition. LS and SU were set to 83 instead, which is equivalent to a decrease in infiltration rate of -26 %, which matches with hydrologic Group D, but still allows for infiltration. **Table 23** in the appendix gives an overview of the applied changes to CN values for the respective land use classes.
In case of the pathway system, which consists of a different material than the forest soils, the gravel and road metal it is constructed with is not equivalent to urban sealing, but inhibits infiltration almost completely. The maximum value for

Table 7:

Soil parameter modification for compaction scenarios in layer depth 0-40 cm for bulk density (BD [g/cm³]), calculated based on REICHARDT (2002) and SCHNEIDER (2015).

Soil class	Uncompacted	Compaction scenarios	
	(C0)	(C1) Pathway systems	(C2) Skid trails, preloaded stocks
	BD	BD	BD
0-20 cm			
SS	1.54	1.74	1.69
LS	1.61	1.82	1.78
SL	1.64	1.85	1.82
L	1.64	1.85	1.82
U	1.67	1.88	1.85
20-50 cm			
SS	1.58	1.79	1.75
LS	1.62	1.82	1.69
SL	1.64	1.85	1.82
L	1.59	1.80	1.67
U	1.64	1.84	1.71

CN (95) is therefore assumed for all soil classes. The respective files (´cntable.lum´, ´lu_mgt´, `hru-data.hru´, ´CN2´ column of ´landuse.lum´) were modified accordingly (TIGABU et al. 2022).

The calibration setup based on the HARGREAVES method for ET was used for all scenario models. As baseline the uncompacted scenario (C0) was used for the evaluation of impact of the respective compaction scenarios (C1-C2) on water balance components.

4.2.5 Simulation of rejuvenation effects on water balance

In order to depict the impact of human activities in case of disrupted areas with rejuvenation, two different artificial extreme scenarios were assumed: scenario MAT representing a near-natural development towards a permanent forest society without further human intervention (mature stocks), and scenario JUV representing high level of human intervention with rejuvenation on the entire catchment area (juvenile stocks), be it through intensification of felling measures, climate change-related windthrow, pests or the death of tree communities due to drought stress. The artificial scenarios were carried out in the catchment area Bobenthal2, that was generated ahead of regionalization, which can be considered representative for the Palatinate Forest, and in which the main tree species (oak, beech, spruce, pine, mixed stands) occur. A time series from 2010-2020 was used to assess the performance differences between juvenile and mature stocks regarding water balance parameters.
To simulate the scenarios JUV and MAT, two plant parametrization setups were created, that account for age-related modifications. This primarily refers to the parameters maximum canopy height, maximum rooting depth, initial age and biomass at the beginning of the simulation, as well as years to reach maturity. Regarding the latter, the juvenile setup is supposed to represent

the growing up phase analogous to the yearly increase in LAI before reaching full development. According to Peck & Mayer (1996), the greatest water consumption occurs in the phase of strongest growth, or in case of pine, the strongest formation of needle mass. For oak and spruce, the years to maturity were therefore set to 70 years, for beech, which shows a high plasticity and sustained crown development even into old age (cf. Hiege 1985:128), the value was set to 80, whereas for pine, based on Peck & Mayer (1996) and Hiege (1985), 30 years were assumed. Since forest stands reach the transition between open-field and closed stand conditions between the ages of 5 and 13 (cf. Hiege 1985:128), the development span from 3-10 years age was simulated in case of juvenile stocks in order to depict the greatest differences in water balance compared to mature stocks. The initial biomass and age are set to 0, with 3 years model warm-up ahead of the simulation for the water balance to level. Furthermore, in case of juvenile stocks, which have not reached full root development, the rooting depth was limited to 1 m in case of oak (Collet et al. 2005), which shoes a rapid taproot development (Lyr & Hoffmann 1967), and 0.5 m in case of all other species (cf. Gilman 1990:217).
For simulating mature stocks on the other hand, years to maturity was set to 3 for all tree species in order to start the simulation after 3 years warm-up period with fully developed LAI and growth performances. **Table 8** shows an overview of plant database modifications for juvenile and mature stocks. The simulation was executed based on the time period 2010 to 2020.
In order to evaluate the plausibility of juvenile and mature model simulation, literature values stated by Peck & Mayer (1996, p.8) regarding age-related differences in yearly actual ET were used as an orientation. Though smaller leaf areas have a limiting effect on evaporation, the reduction in canopy expression does not automatically lead to a proportional decrease in total stand evapotranspiration, since soil evaporation can increase significantly (Schmaltz 1969; Hager 1988; Peck & Mayer 1996), in case the soil has no plant cover. The level of coverage of a soil is decisive for the process of soil evaporation.

Table 8:

Plant database modifications for juvenile (scenario JUV) and mature (scenario MAT) tree species.

File	Parameter	Plant configuration									
		mature					juvenile				
		oa	be	sp	pn	mx	oa	be	sp	n	mx
plant.ini	initial LAI [m²/m²]	0.01	0.01	5	2.9	2.5	0.01	0.01	4	2	2
	initial biomass on the stand [t/ha] *	185	289	215	113	150	0	0	0	0	0
	initial age [years]	70	80	70	40	50	0	0	0	0	0
plants.plt	maximum canopy height [m]	34	33	40	32	35	5	5	5	5	5
	maximum rooting depth [m]	2	2	2	2	2	1	0.5	0.5	0.5	0.5
	years to maturity [years]	5	5	5	5	5	70	80	70	30	50

Bartsch & Röhrig p. 264

As SWAT+ does not assume the development of ground vegetation on forested stocks, the amount of total *ET* fed by soil evaporation rises in case of bare, uncovered soils on stocks that have not yet developed a closed canopy. Thus, higher amount of soil evaporation is expected on juvenile stocks, with at the same lower total *aET* values, reflecting undeveloped canopy cover with lower *LAI* values. When comparing the calibrated model setup for juvenile and mature stocks, both aspects meet the expectation, as shown in **table 9**.

Table 9:

Averaged actual *ET* (*aET*) and soil evaporation (Esoil) for juvenile and mature stocks before plant database configuration for the period 2010 to 2020 based on the calibrated SWAT+ model for Bobenthal2

Parameter	Juvenile plant setup	Mature plant setup
aET [mm]	472	545
Esoil [mm]	97	80

SWAT+ provides the option to compile multi-layered vegetation types on one stock, which potentially allows for simulating a shrub layer, but as in the context of this study the effect of herbal vegetation on the water balance is not the subject, multi-layered vegetation stands are dispensed for this setup.
Applying the modifications to the plant database resulted in *LAI* performances for both age scenarios that depict the growing up period before full *LAI* development in case of juvenile, as well as fully developed *LAI* performance in case of mature stocks, as shown in **fig. 18**, exemplified for oak (for other trees species see **fig. 22**).

The growth performance was also analyzed based on biomass development. As shown in **figure 19**, the growth performance for juvenile stocks develops linearly, as given by the model internal equation for plant growth (formula 4.1.2), while mature stocks show a growth stagnation (exemplified by oak).

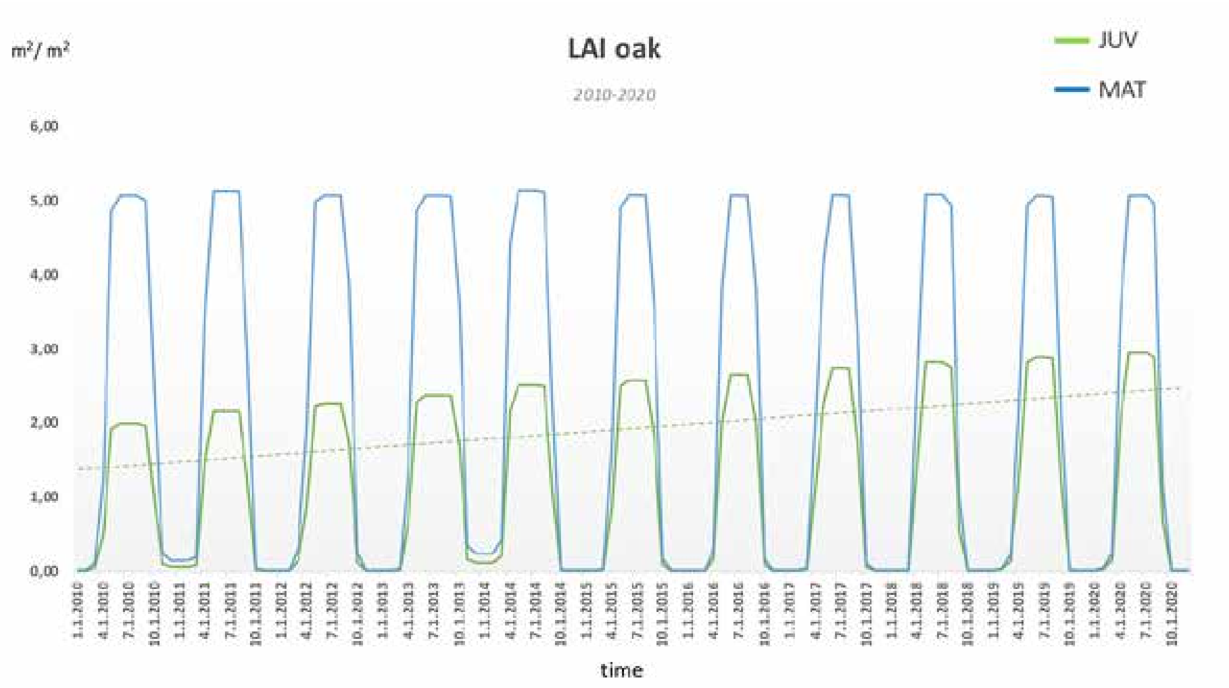

Figure 18: *LAI* curves for mature and juvenile oak stands for the baseline period 2009 to 2020 after applying age-related plant database adaptions.

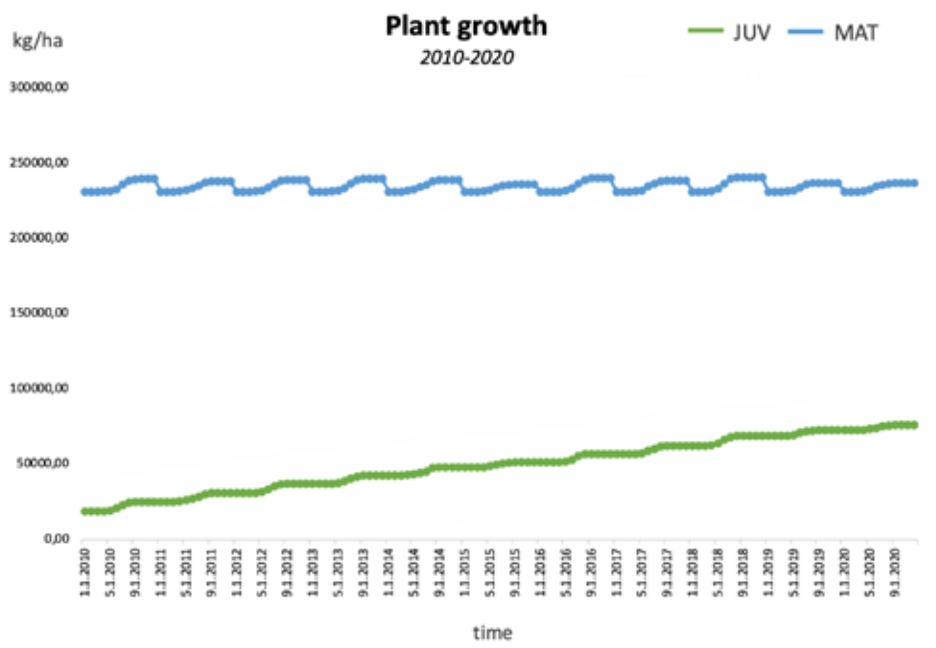

Figure 19: Growth performance for juvenile and mature stocks simulated with SWAT+, for the period 2010 to 2020.

In order to identify basal hydrological controlling factors, a comparison with contrasting climatic conditions was evaluated, which were found between 1971 and 1981. Compared to the last decade (2010-2020) the farer past showed higher precipitation inputs, lower air temperatures and a consequently less pronounced atmospherical evaporative demand.

5 RESULTS

5.1 Parameter sensitivity analysis

5.1.1 Plant parameters

In order to evaluate differences between the default plant settings and the applied modifications of the plant parametrization with regard to plant growth and ET, both setups were executed with the same basic settings, except for the plant parameters in **table 24**, app. (described in section 4.2.3.1). The simulation was executed for the time period 2000 to 2010. In both cases, mature stocks were assumed at the beginning of the simulation, with equal maximum biomass on a stand, specified for each tree species, and with equal initial biomass and age. Both model simulations where then evaluated based on actual ET and biomass performance.
Regarding actual ET, the plant parameter modification resulted in a small decrease of -4.6 % based on average annual values on watershed level (see **fig. 20**).

The situation became more distinct, when evaluating on HRU level for each tree species. The comparison showed a decrease by -15.7 % in case of oak, and -13 % for beech, whereas coniferous trees showed a negligible change of 0.5 % increase in case of spruce, 1.4 % increase in case of douglas fir and 3 % for pine. For mixed stands, which lacked measured data, and were therefore predominantly derived by averaging the other tree species, an increase by 3.6 % was shown for aET. Due to the lack in accurate data, they are considered to be less conclusive, and must be parametrized more carefully for future setups, which urges for specified data survey. **Figure 21** shows the differences in aET for selected tree species in the given time period.

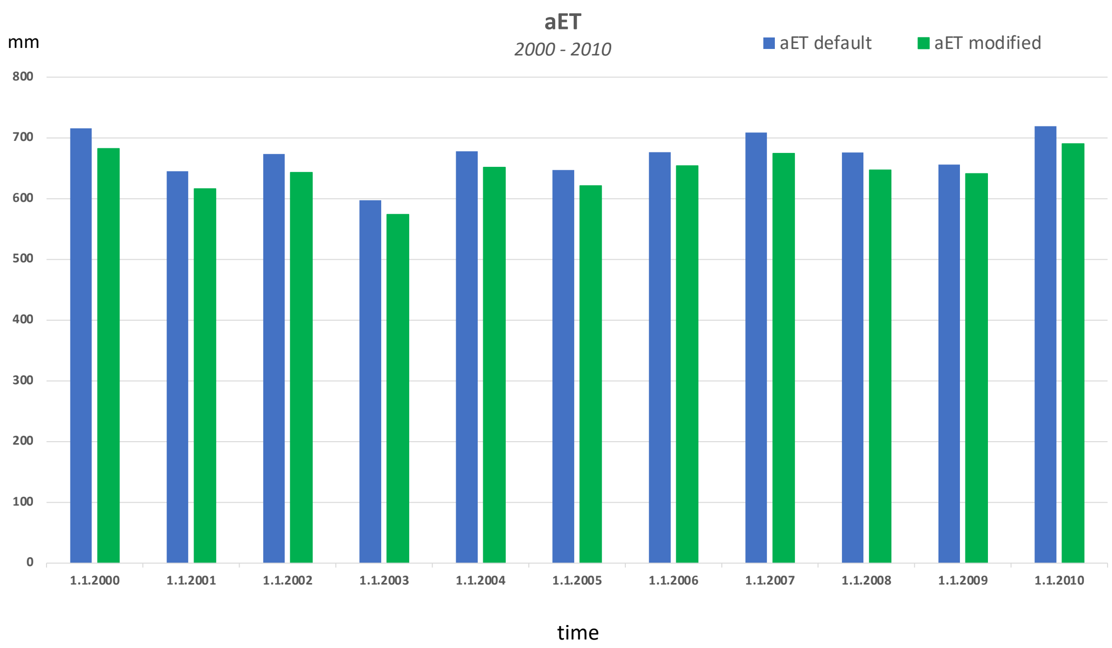

Figure 20: Simulated differences in actual ET (aET) performance for default and modified plant setups for the time period 2000 to 2010, based on yearly values.

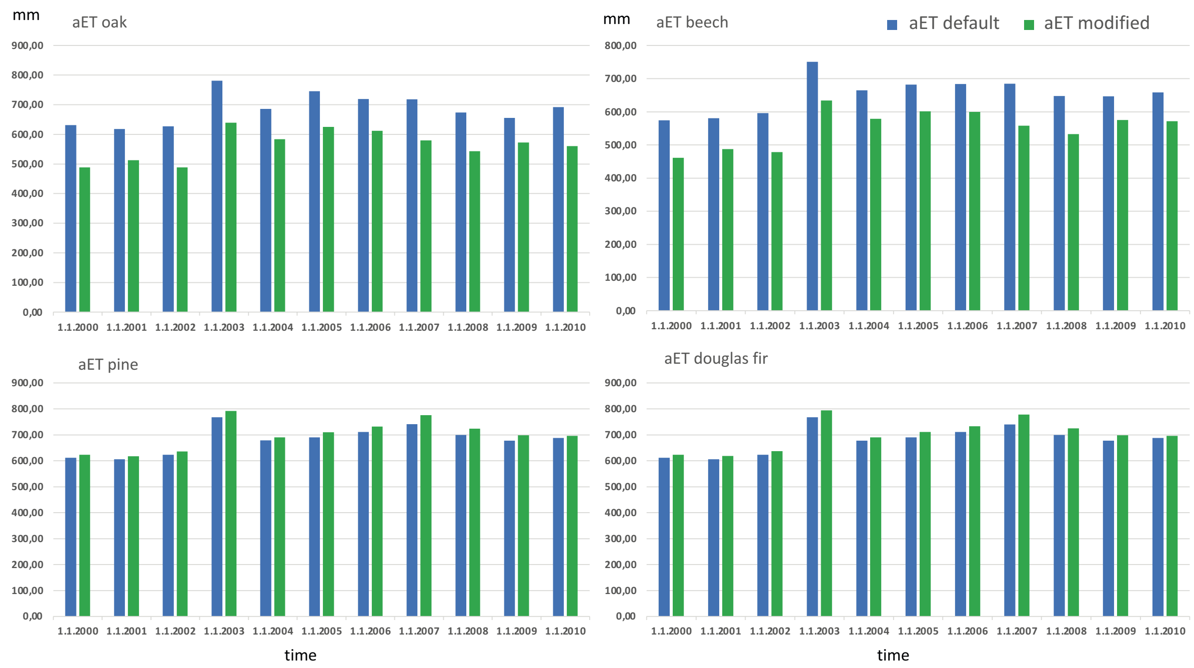

Figure 21: Simulated differences in aET for the tree species oak, beech, pine, and douglas fir for default (def) and modified (mod) plant setups for the time period 2000 to 2010, based on yearly values.

Based on average annual values, the default plant setup accounted 722 mm/aa aET in case of oak, whereas the modifications calculated 609 mm/aa. In case of beech, 659 mm/aa was the default value, and 573 mm/aa the modified. For spruce, the default simulations showed 782 mm/aa, and a very small increase to 782 mm/aa, douglas fir was 730 mm/aa with the default setup, and 740 mm/aa after modification. Pine resulted in 624 mm/aa for default, and 643 mm/aa after modification. Mixed stands showed 722 mm/aa in the default case, and 748 mm/aa with the modified plant parametrization.
The decrease in aET for deciduous tree species suggests an improvement for the model plant parametrization compared to referenced literature values, stating 561 mm/aa for beech, and 450 mm/aa for oak (Peck & Mayer 1996). Values for spruce, stated with 609 mm/aa, and pine (576 mm/aa) exceeded the expectation in the default setup, and even more so after the modification, as the values rose. For douglas fir, the average annual aET is stated with 752 mm, which was almost matched by the modification, so that the increase here appeared conclusive. The increase in aET performance for coniferous species after modification most probably was caused by higher LAI values, especially within the dormant period. **Tab. 10** gives an overview of default and modified LAI settings for each tree species, the LAI performance curves for the tree species in both simulations are shown in **Fig. 22**.

The modification undercut default minimum LAI values in the dormant period for deciduous species, and exceeded default maximum LAI values for all species except for oak and pine. Pine showed lower LAI within the vegetation period, and a significantly higher one within the dormant period. Especially the differences in minimum LAI are presumed to cause the increase in aET, since except for spruce, all coniferous species were set to 0.75 in the default setting, allowing less transpiration within the dormant period compared to the modified setting. The minimum LAI was therefore identified to be the major influence in modified aET performances.

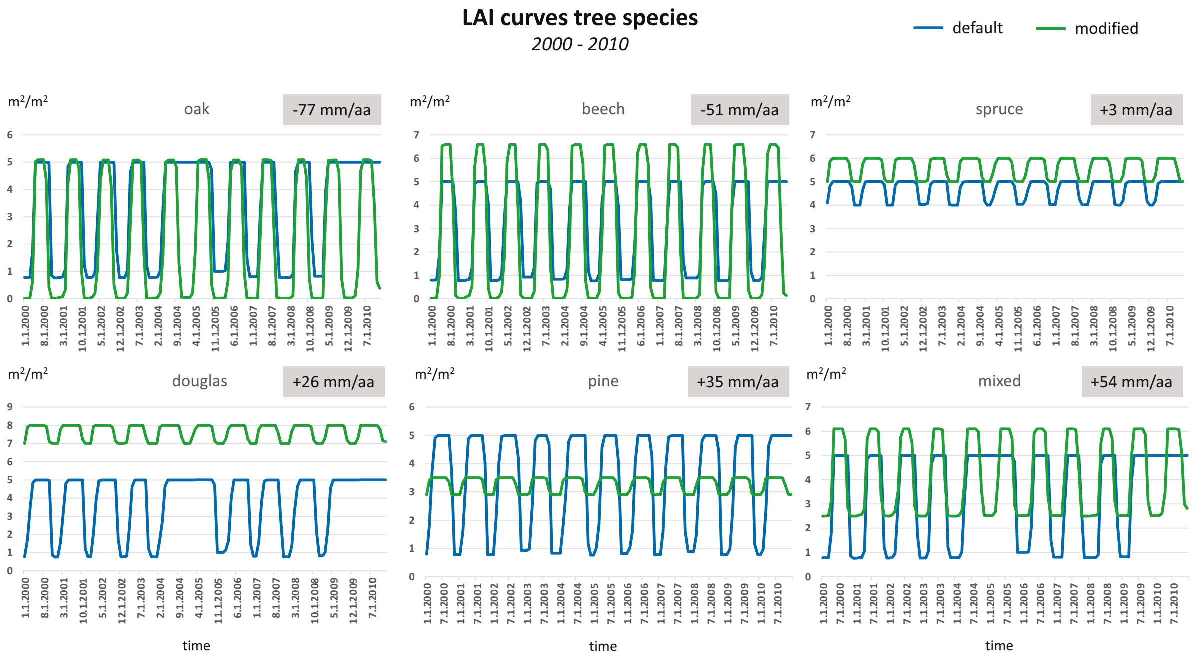

Figure 22: *LAI* curves for the dominant tree species in the study area, default and modified model setup, for the time period 2000 to 2010.

Table 10:

LAI settings for default (def) and modified (mod) model performances.

Parameter	Tree species											
	oak		beech		spruce		douglas fir		pine		mixed	
	def	mod	def	mod	def	mod	def	mod	def	mod	def	mod
Minimum *LAI* [m²/m²]	0.75	0.01	0.75	0.01	4	5	0.75	7	0.75	2.9	0.75	2.5
Maximum *LAI* [m²/m²]	5	5.2	5	6.7	5	6	5	8	5	3.5	5	6.1

In order to determine the plausibility of dormant aET performances of coniferous and deciduous trees, the data was analyzed on monthly basis, considering potential ET as indicator for evaporative demand. Since in winter, the atmosphere lacks the impetus for evaporation, aET and pET are expected to be close together in case of coniferous trees, as they still transpire. As can be seen from **figure 23**, the modification showed an expectedly small interval between aET and pET, whereas in the case of the default setting it was implausibly large.

Furthermore, for deciduous tree species, which stop transpiration within the dormant period, very small aET values are expected, which was valid only in case of the plant database modification, but not so in the default setup. The plots show, that with increase in pET, and thus evaporative demand, deciduous aET rose ahead of bud burst due to triggered interception. The modified aET curves were thus found to be very plausible for both, coniferous and deciduous tree species throughout the dormant state.

For evaluating the plausibility of aET performances within the vegetation period, a dry year (2003) was chosen, in order to depict evaporative demand in addition to water stress, reflected through the soil water storage, and to conclude an indication of transpiration controlling factors in tree specific aET.

Regarding deciduous trees, a clear response to pronounced soil water depletion showed off in the aET development curve of the selected HRU for beech, expressed by a decline in aET, as shown in **figure 24**. As SWAT+ equals actual transpiration and actual water uptake, the driving factor in the restriction of aET is the soil water content falling below the range to meet the evaporative demand. SWAT+ considers plant available soil water (AWC) to range between field capacity (FC = 0.0033 MPa) and the soil water content at

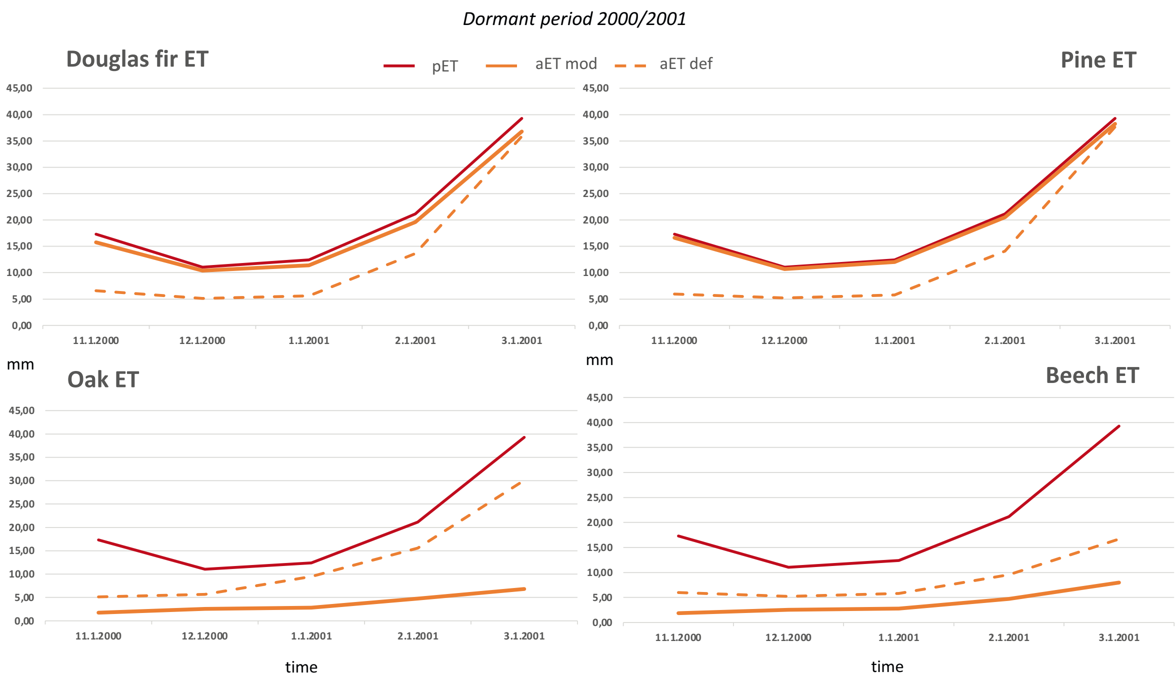

Figure 23: ET performance for coniferous and deciduous tree species within the dormant period 2000 to 2001, default (def) and modified (mod) simulations, compared to potential ET, indicating the evaporative demand.

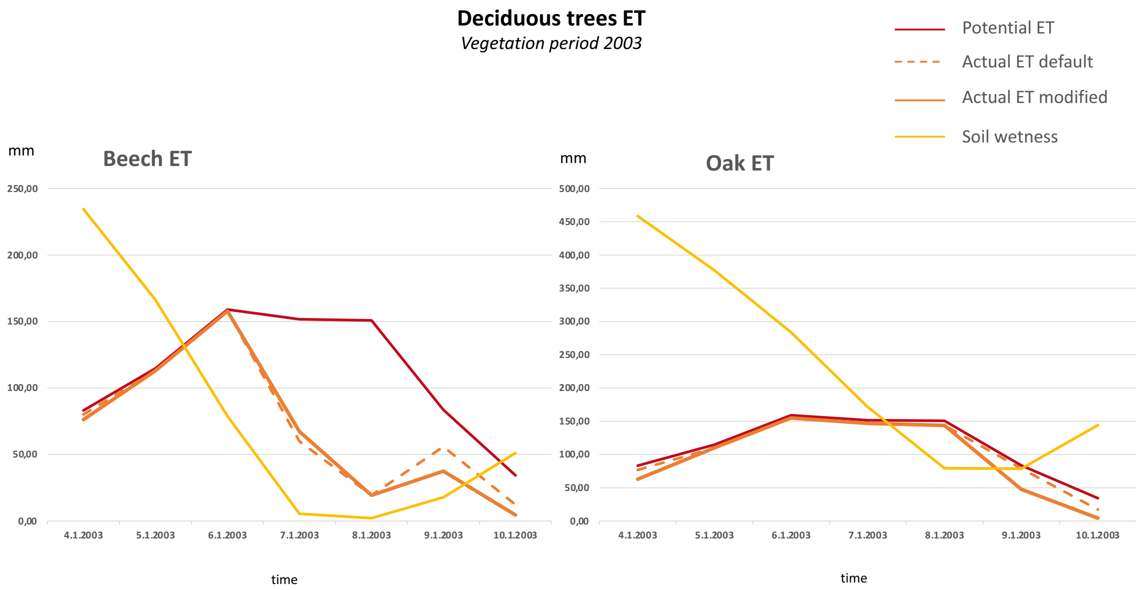

Figure 24: ET performance for deciduous tree species within the vegetation period 2003 for default (def) and modified (mod) model setups, compared to potential ET and soil wetness as indicators for plant water stress, based on monthly values.

permanent wilting point (WP = 1.5 MPa) (Neitsch et al. 2011). Within this range, plants are allowed to extract water from deeper soil layers in case a layer does not meet the given demand, to the extent defined by the plant uptake compensation factor epco (0 – 1, in case of this model setup 0.67). The potential water uptake for a layer is limited in case the soil water content undercuts a threshold in AWC:

$$w''_{up,ly} = w'_{up,ly} \cdot exp \left[5 \cdot \left(\frac{SW_{ly}}{(25 \cdot AWC_{ly})} - 1 \right) \right]$$

Formula 5.1.1 (Neitsch et al. 2011:328)

when SW_{ly} < (25 • AWC_{ly})

$w''_{up,ly}$	=	Potential water uptake for the layer adjusted for initial soil water content [mm H_2O]
$w'_{up,ly}$	=	Adjusted potential water uptake for the layer, taking epco into account [mm H_2O]
SW_{ly}	=	Soil water content of the layer at the given day [mm H_2O]
AWC_{ly}	=	Available water capacity for the layer [mm H_2O]

The actual water uptake for a day ($wactualup$) is the sum of potential water uptake of all plant accessible layers, taking *epco* and the minimum of available plant water into account. The respective constraints in soil water content inducing a decline in transpiration evoke water stress (0 – 1) to occur, which is considered as the ratio between actual plant transpiration (= $wactualup$) and the maximum plant transpiration. The beech site was very much affected by a rapid decrease in soil water in 2003, which entailed an equivalent drop in aET, for both, default and modified settings. SWAT+ equals the maximum transpiration (E_t) and E'_o, the latter being the potential evapotranspiration minus evaporated water from the interception storage ($E'_o = pET - E_{can}$), when LAI > 3:

$$E_t = E'_o \qquad LAI > 3.0$$

Formula 5.1.2 (Neitsch et al. 2011:135)

Consequently, in case of sufficient soil water content, but no free water in the canopy due to lacking precipitation (E_{can} = 0), with at the same time high evaporative demand, as valid in the drought period in summer 2003, pET and aET correspond at fully developed LAI, as can be seen in **figure 24** for oak, when the HRU-specific soil water dropped moderately. **Table 11** summarizes simu-

lated evapotranspiration throughout the vegetation period for the dominant tree species.
The drop in aET at the end of the vegetation period is rather induced by falling LAI values, adapted from phenology data, and thus improved with regard to phenological accuracy compared to the default setting. As for oak, the modified LAI curve in case of beech also matched an adequate development towards the end of the growing season, whereas the default setting simulated an implausible rebound. In case of coniferous tree species, **figure 25** (as well as **table 11**) suggest that SWAT+ did not detect any water stress, and therefore simulated no constraints in transpiration, resulting in corresponding aET and pET, given that $LAI > 3$, $E_{can} = 0$, and soil evaporation = 0. The drop of default aET for pine and douglas fir at the end of the growing season resulted from lower LAI values considered for default minimum LAI of these species.
It must be emphazised, that the model simulations were executed using the Hargreaves method for calculating evapotranspiration, as it showed the best model performance with respect to the target objective (see **tab. 25**, and **fig. 86**, app.). The Hargreaves method is purely empirical and temperature based, accounting only for minimum, maximum temperature and solar radiation (Hargreaves et al. 1985, Amatya et al. 1995). Nevertheless, numerous studies also achieved the best model performance in the forest using this method (e.g. Amatya et al. 2016).

Table 11:

Simulated evapotranspiration in 2003 for summer months with fully developed canopy at maximum LAI.

Month	Tree species	Parameter				
		pET [mm]	aET [mm]	Soil evaporation [mm]	average Soil wetness [mm]	water stress factor [0-1]
06/2003	oak	154.9	154.9	0	299.4	0
	beech	157.8	157.8	0	82.8	0
	spruce	156.6	156.6	0	281.7	0
	douglas fir	157.8	157.8	0	241.9	0
	pine	157.8	157.8	0	244.1	0
07/2003	oak	146.7	146.7	0	184.6	0
	beech	150.4	71.2	0	6.43	0.5
	spruce	150	150	0	171	0
	douglas fir	150.4	150.4	0	149.3	0
	pine	150.4	150.4	0	149.7	0
08/2003	oak	143.6	143.6	0	89.8	0
	beech	146.2	19.3	0	2.2	0.8
	spruce	145.4	145.4	0	82.7	0
	douglas fir	146.2	146.2	0	47.36	0
	pine	146.2	146.2	0	68.4	0

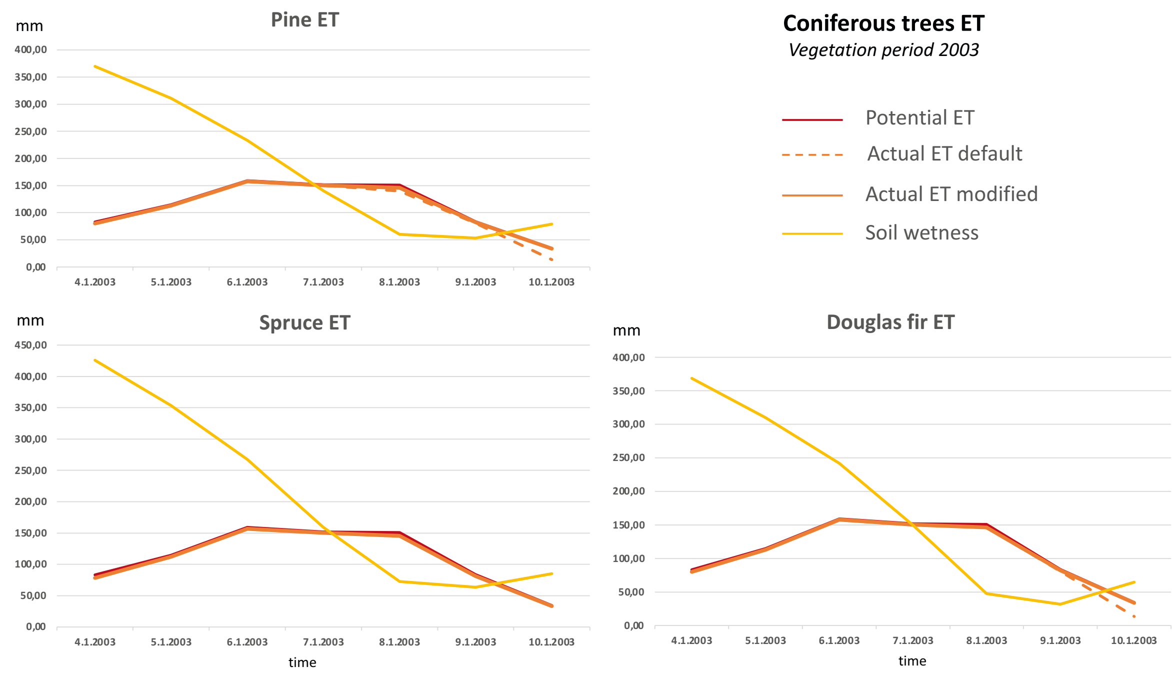

Figure 25: ET performance of coniferous tree species within the vegetation period 2003 for default (def) and modified (mod) model setups, compared to potential ET and soil wetness as indicators for plant water stress, based on monthly values.

The results on HRU level support the conclusion, that the LAI is the major factor in aET development for both, dormant and growing season, sufficient plant water supply given.
When evaluating the ET performance on watershed level, however, a plausible deviation between pET and aET became evident for the simulation period 2000 to 2020: The reaction of aET to soil water depletion indicated, that besides the influence of interception storage, an adequate number of HRUs showed drought induced decline in transpiration on the whole, which proofed the model to be effective on the larger scale (**fig. 26**).

Regarding plant growth, the data was compared to growth rates for each tree species, derived from Block et al. (2016), as described in section **4.2.3.1**, all based on yield class III.

The SWAT+ simulations showed a growth rate of 0.00073 kg/ha/a for the default setup, and an increase by 1.25 % for the modified setup in case of oak, resulting in a growth rate of 0.00074 kg/ha/a. Beech showed a growth rate of 0.00061 kg/ha/a in the default, and 0.00062 kg/ha/a in case of the modified setup, increased by 3.8 %. In case of spruce, the default setup resulted in a growth rate of 0.00134 kg/ha/a, whereas the modified was increased by 1.7 % (0.00135 kg/ha/a). Douglas fir increase by 0.17 % from 0.00131 kg/ha/a to 0.00134 kg/ha/a after modification. Pine increased by 0.82 % from 0.00129 kg/ha/a in the default to 0.00133 kg/ha/a in the modified simulation. Only in case of mixed stands, which are poorly depicted due to lacking data, a total decrease by -0.76 % was shown after modification.

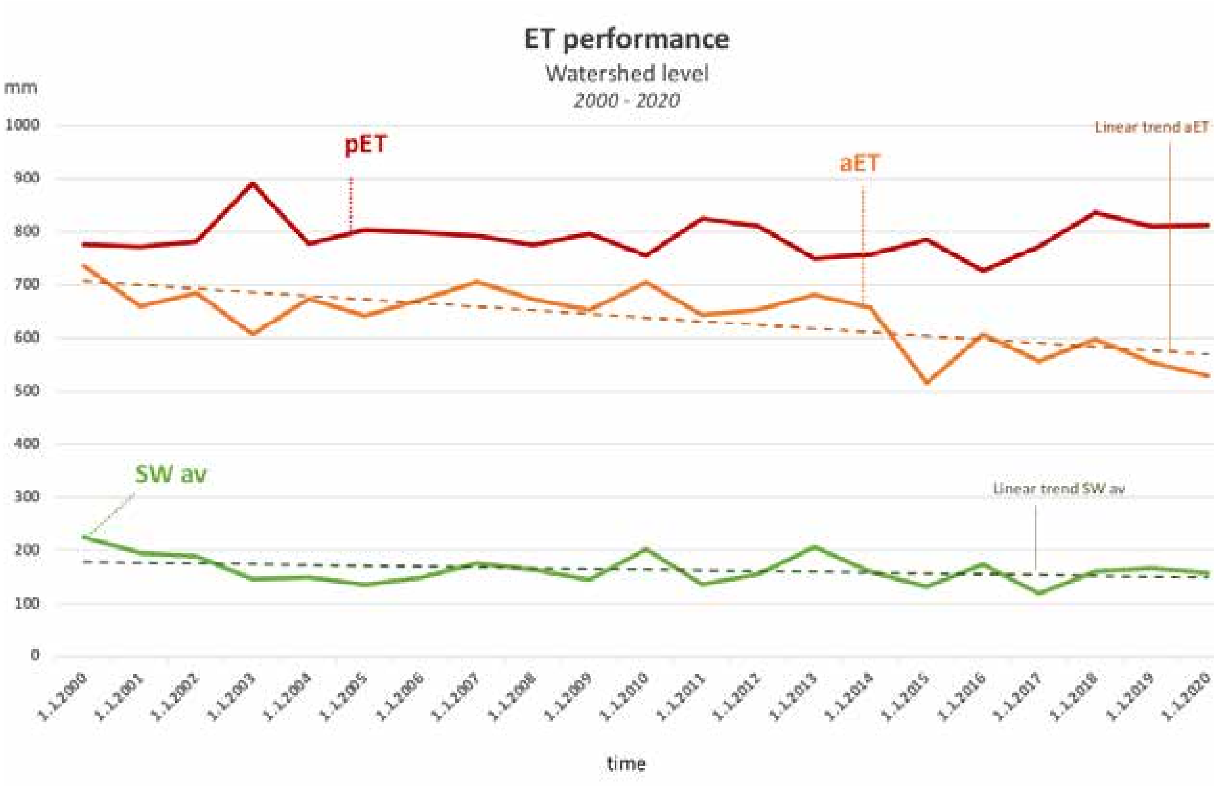

Figure 26: Performance of potential ET (pET), and actual ET (aET) for both, modified and default settings, as well as average soil wetness (SW_av) on watershed level, depicting an accurate reaction of aET decline according to soil water content, as well as an overall plausible deviation between aET and pET.

The absolute changes in plant growth were very small, but point into the right direction compared to the yield table data, suggesting an increasing trend. The large deviation between the stated yield table growth rates, and the simulated is most probably related to differences in growth performance, and growth influencing factors between the plant growth models EPIC used in SWAT+, and SILVA used for the generation of the yield table data. For instance, the model SILVA, does account for neighboring effects such as growth compensation in case of timber extraction (Pretzsch 2019).

5.1.2 Sensitive model parameters and manual calibration

5.1.2.1 The Palatinate Biosphere Reserve catchment

The manual sensitivity analysis resulted in the conclusion that aquifer parameters were the dominant governing factor of low flows of the hydrograph (Tigabu et al. 2022). Parameters identified to be effective with regard to significant influence on simulated streamflow performance were baseflow alpha factor (alpha_bf), deep aquifer percolation fraction (rchg_dp), revap (reavp_co), minimum aquifer storage to allow return flow (flo_min), threshold depth of water in the shallow aquifer (revap_min), depth-mid-slope surface to water table (dep_wt), and flow distance (dep_bot). The parameter values fitted for the first and second aquifer layers were different. Identified best fitted values for aquifer parameters are listed in **table 12**.

Table 12:

Aquifer model parameter identified sensitive through manual calibration procedures, fitted for the first and second aquifer layer.

Aquifer parameter	**Type of change**	**Fitted value**	
		First layer	Second layer
alpha_bf	absolute value	0.8884	0.44585
rchg_dp	absolute value	0.3	0.01
revap_co	absolute value	0.2	0.08528
flo_min	absolute value	0.35378	9.41929
revap_min	absolute value	2.13279	7.96882
dep_wt	absolute value	1.23045	10.61029
dep_bot	absolute value	4	10

Parameters identified to be sensitive throughout the automatic calibration process are shown in **figure 27** (for the Bobenthal catchment) and **figure 28** (for the Neustadt catchment).

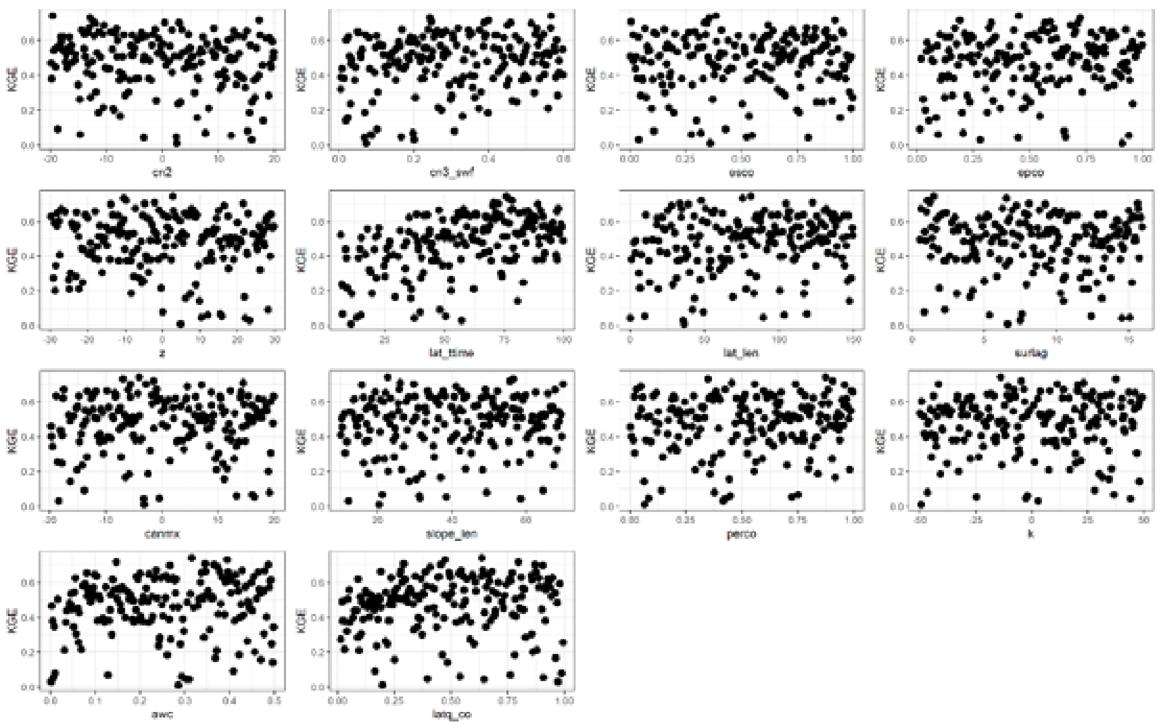

Figure 27: Effective model parameters that influence the efficiency of the model performance under increasing/decreasing values for the Bobenthal catchment. Horizontal and vertical axes represent parameter and model efficiency, respectively (Tigabu et al. 2022:9)

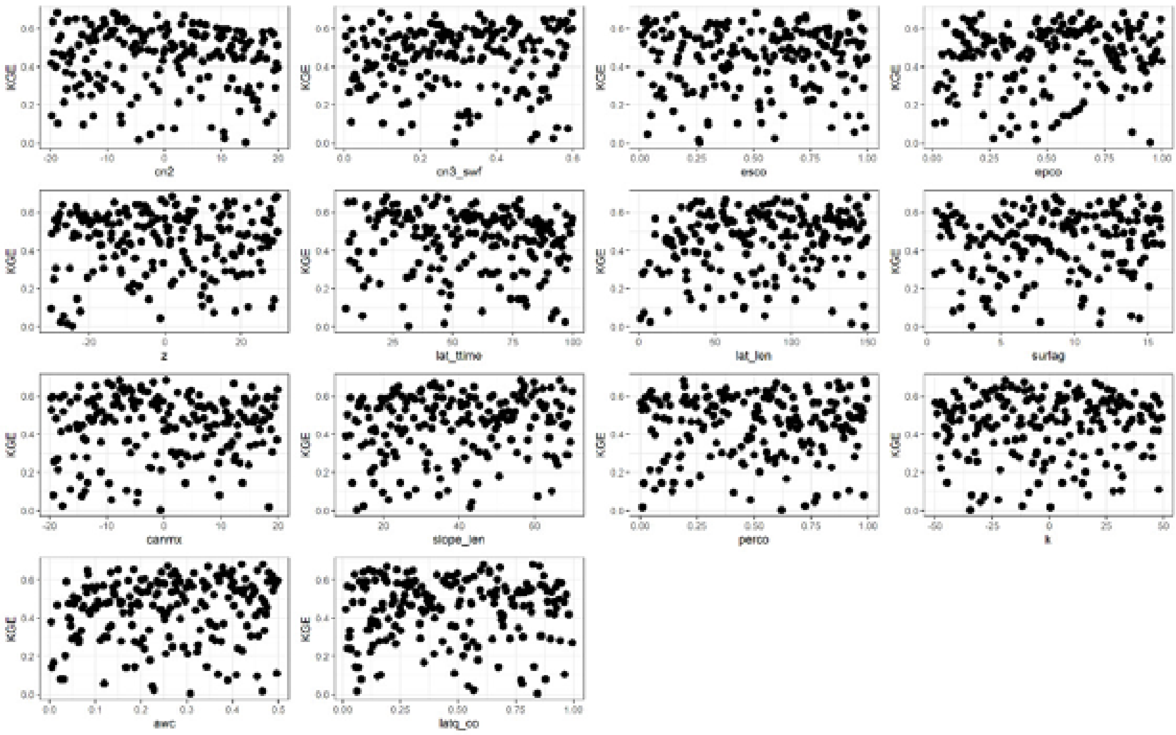

Figure 28: Effective model parameters that influence the efficiency of the model performance under increasing/decreasing values for the Neustadt catchment. Horizontal and vertical axes represent parameter and model efficiency, respectively (Tigabu et al. 2022:10).

5.1.2.2 The Bobenthal2 catchment

Sensitive model parameters were identified manually following appropriate change methods on the parameter values, by testing one parameter at a time (cf. Tigabu et al. 2021:4). Regarding the aquifer section, the parameters listed in **table 13** were found sensitive

After their identification, the sensitive parameters were included in the automatic calibration procedure, described in section **5.2.2**. **Figure 29** shows the influence of parameters on the model efficiency under increasing/decreasing parameter values.

Table 13:

List of sensitive aquifer parameters for the Bobenthal2 catchment, and their minimum and maximum ranges and manually calibrated values (Tigabu et al. 2021).

Parameter	Change type	Min	Max	Fitted value	Parameter description
alpha_bf	absolute value	0	1	0.47000	Baseflow alpha factor [1/days]
rchg_dp	absolute value	0	1	0.20000	Deep aquifer percolation fraction

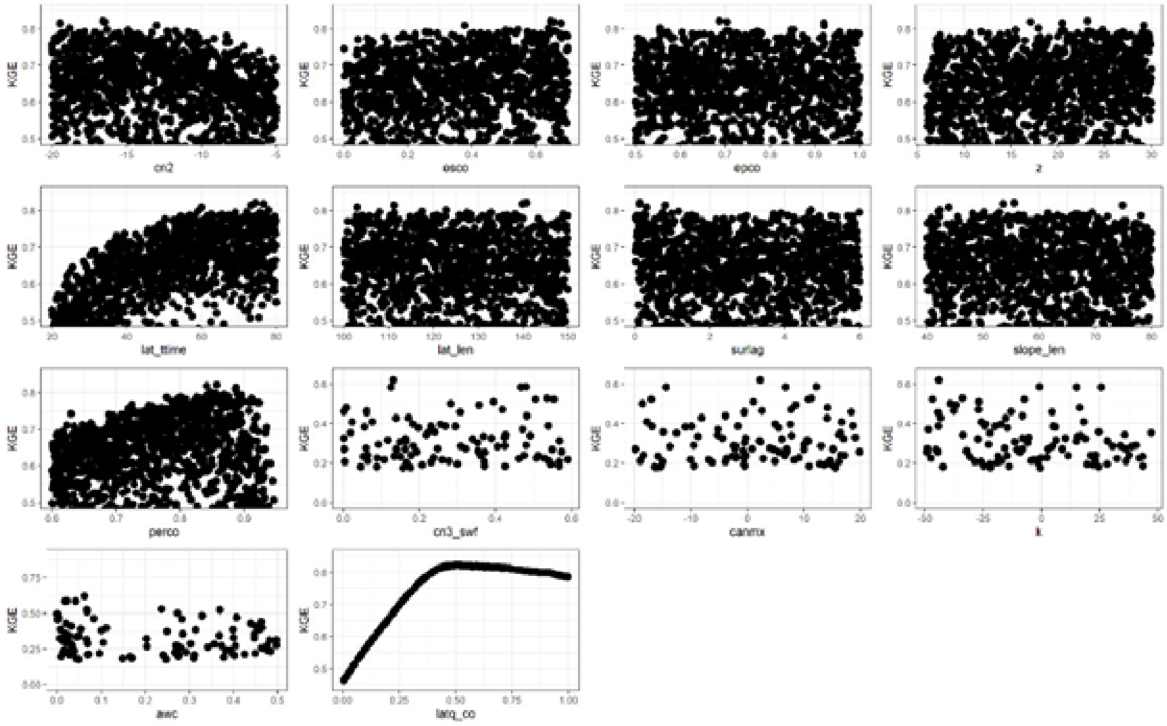

Figure 29: Dotty plots showing the influence of parameters on the efficiency of the model under increasing/decreasing parameter values for the Bobenthal2 catchment. Horizontal and vertical axes represent parameter and model efficiency, respectively (Tigabu et al. 2021:5).

5.2 Calibration and validation

5.2.1 The Palatinate Forest Biosphere Reserve catchment

The automatic calibration procedure for the regionalized model included the parameters listed in **table 14**. The catchments Bobenthal and Neustadt were calibrated independently. In order to further improve persisting disparities in the observed and simulated hydrographs, the manually identified best fitting aquifer parameters were included in the calibration process (Tigabu et al. 2022). **Figure 30** shows the improved hydrograph after aquifer parameter adaption for the sub-catchment Bobenthal, and **figure 31** the equivalent for the sub-catchment Neustadt. Furthermore, the applied plant parameter modification described in section **4.3.2** resulted in an improvement of model performance with respect to statistical indices KGE, NSE, PBIAS and RSR. For instance, the default plant parameter settings showed a best model fit with the KGE value being 0.70, whereas the modified plant parametrization resulted in KGE being 0.74 for the Bobenthal catchment (ibid.). The final best fitting parameters for both, Neustadt and Bobenthal catchment, were transferred to the other sub-catchments in the Palatinate Biosphere Reserve catchment (ibid). **Table 15** shows the model performances with respect to statistical indices values based on simulated and measured streamflow time series data for (1) the best calibration outputs for Bobenthal and Neustadt transferred to the other sub-catchments, and (2) best model parameters combination for each catchment independently. As can be inferred from it, the best fitted calibrated model parameter setup for Bobenthal was more sufficient in depicting the hydrological processes than the individually calibrated catchments. With 3000 simulation runs, the best KGE value for the Bobenthal catchment corresponded to the second best of Neustadt, so that the calibrated Bobenthal parameter set was chosen to be used for regionalization to the entire Palatinate Biosphere Reserve catchment (ibid). When this attempt worked sufficiently good for the gauges of Neustadt and Siebeldingen, the rather poor performance regarding NSE of Thaleischweiler, Haderburg, and Moosalbtal indicated that a local calibration would have been recommended to represent local dynamics in these subcatchments. Anyway, the PBIAS ranging within the threshold limit of -25 % to 25 % confirmed that the long-term mean water balance was reasonably approximated (except for the validation period at Moosalbtal). But since the data availability was limited with regard to these subcatchments, using the derived parameter set from the Bobenthal sub-catchment for regionalization was considered a good first model approximation for the entire study area (ibid.).

Table 14:

List of sensitive parameters and their minimum and maximum ranges and calibrated values. absval = absolute value, abschg = absolute change, pctchg = change in % (Tigabu et al. 2021)

Parameter	Change type	Min	Max	Fitted value	Parameter description
CN2	abschg	-20	20	-5.55181	Condition II Curve Number
CN3_SWF	absval	0	1	0.56684	Soil water factor for condition III CN
esco	absval	0	1	0.1	Soil evaporation compensation factor
epco	absval	0.01	1	0.85191	Plant uptake compensation factor
z	pctchg	-30	30	2.82143	Depth of soil-zone layer from surface [mm]
lat_ttime	absval	0	120	90	Lateral flow travel time [d]
snomelt_tmp	absval	-5	5	4.89693	Temperature of snowmelt [°C]
snowfall_tmp	absval	-5	5	1.17065	Temperature of falling snow [°C]
lat_len	absval	0	150	80	Slope length for lateral subsurface flow [m]
surlag	absval	0	15	7.41828	Surface runoff lag coefficient
slope_len	absval	10	70	22.68735	Average slope length for erosion [m]
perco	absval	0	1	0.87406	Percolation coefficient
canmx	pctchg	-20	20	-4.04053	Maximum canopy storage [mmH_2O]
latq_co	absval	0	1	0.63586	plant ET curve number coefficient
k	pctchg	-50	50	-13.85028	Saturated hydraulic conductivity [mm/hr]
awc	abschg	0	0.5	0.07107	Available water capacity [mmH_2O/mm soil]

Table 15:

Calibrated (cal) and validated (val) model performances with respect to statistical indices values based on simulated and measured streamflow time series data for (1) the best calibration outputs for Bobenthal and Neustadt transferred to the other sub-catchments, and (2) best model parameters combination for each catchment independently (source: Tigabu 2022).

Objective Function	**Sub-catchments**											
	Bobenthal		**Neustadt**		**Thaleischweiler**		**Moosalbtal**		**Hardenburg**		**Siebeldingen**	
(1)	*cal*	*val*	*cal*	*val*	*cal*	*val*	*cal*	*val*	*cal*	*val*	*cal*	*val*
KGE	0.86	0.74	0.74	0.57	0.64	0.57	0.21	-0.65	0.33	0.19	0.72	0.6
NSE	0.73	.049	0.49	0.1	0.25	0.1	-0.51	-3.07	0.03	0.001	0.61	0.38
PBIAS	-0.3	-3.6	16.8	15.4	4.5	-0.9	17.1	-55.9	0.3	13	9.5	2
RSR	0.51	0.71	0.71	0.95	0.86	0.95	1.22	2.02	0.98	0.99	0.62	0.79
(2)												
KGE	0.86		0.74		0.48				0.19		0.25	
NSE	0.73		0.47		-0.09				0.03		-0.37	
PBIAS	-0.3		6.7		-5.4				-12.6		-16.6	
RSR	0.51		0.72		1.05				0.99		1.17	

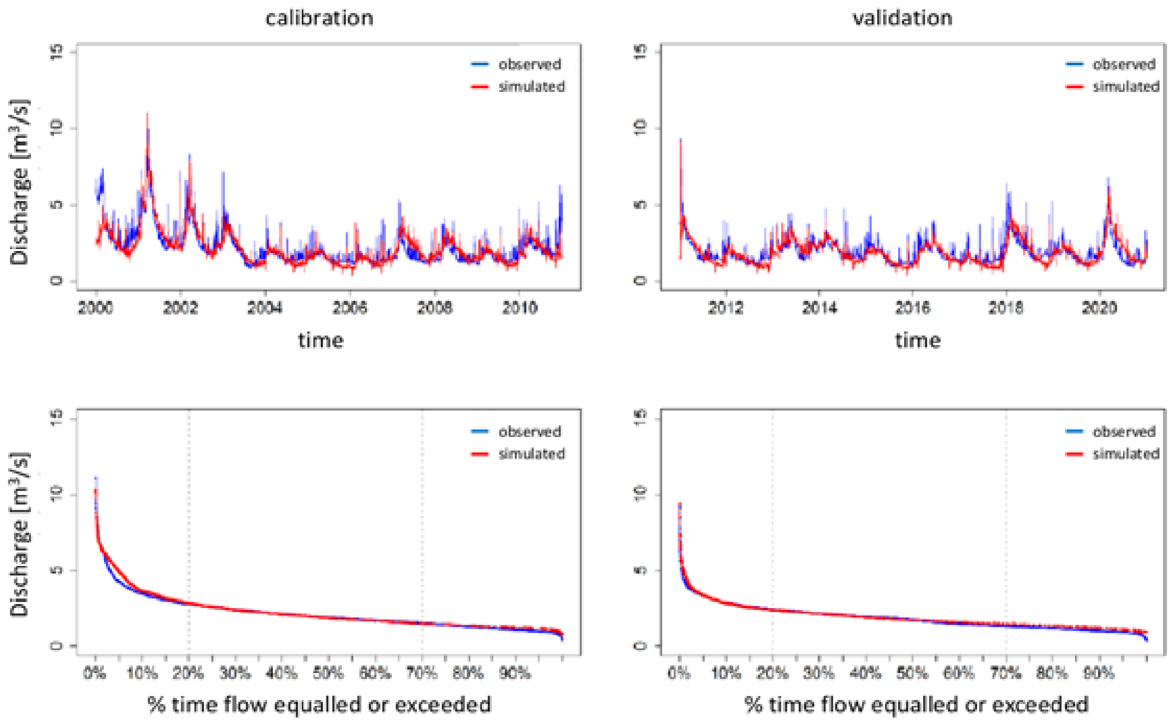

Figure 30: Daily time series hydrographs of simulated and observed streamflow of the sub-catchment Bobenthal for calibration and validation period (source: Tigabu et al. 2022).

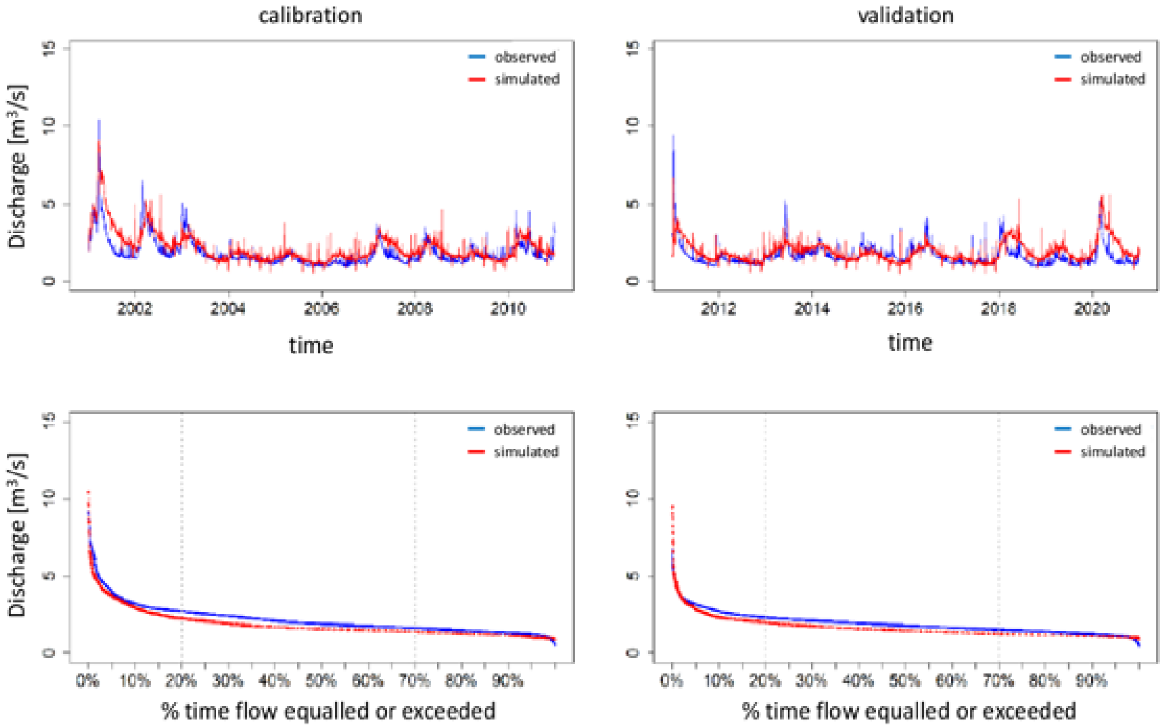

Figure 31: Daily time series hydrographs of simulated and observed streamflow of the sub-catchment Neustadt for calibration and validation period (source: TIGABU et al. 2022).

5.2.2 The Bobenthal2 catchment

For calibration analysis, simulation outputs of relevant water balance components such as lateral flow, surface runoff, actual ET and groundwater recharge were considered (TIGABU et al. 2021). Sufficient model performances with respect to satisfactory model performance indices were only found with the HARGREAVE´s method for calculating aET. The so found optimal calibration parameters are listed in **table 16**.

Applying those parameter changes to the model resulted in the hydrographs and flow duration curves shown in **figure 32**, which was found reasonable also with regard to model performance indices (shown in **table 17**). The SWAT+ model reproduced the measured daily streamflow sufficiently and was found capable of depicting the hydrological processes and flow dynamics in the catchment in all seasons. Following MORIASI et al. (2007) the model performance indices are above satisfactory for both, calibration and validation period, although less satisfactory for the entire simulation. There was a data gap for precipitation between 2004 and 2008, which was compensated with the SWAT+ internal weather generator based on monthly statistics, which does not allow for a precise depiction of precipitation and streamflow on daily resolution, and thus resulted in a less satisfactory model performance.

Remaining deviations between observed and simulated streamflow might be related to the small catchment size, since the gridded precipitation input data was downscaled for the catchment from the input data generated for the entire Palatinate Forest Biosphere Reserve area (TIGABU et al. 2021).

Table 16:

List of sensitive parameters and their minimum and maximum ranges and calibrated values. absval = absolute value, abschg = absolute change, pctchg = change in % (Tigabu et al. 2021).

Parameter	Change type	Min	Max	Fitted value	Parameter description
CN2	abschg	-20	20	-16.58715	Condition II Curve Number
CN3_SWF	absval	0	1	0.13143	Soil water factor for condition III CN
esco	absval	0	1	0.64612	Soil evaporation compensation factor
epco	absval	0.01	1	0.6876	Plant uptake compensation factor
z	pctchg	-30	30	23.16295	Depth of soil-zone layer from surface [mm]
lat_ttime	absval	0	120	74.49358	Lateral flow travel time [d]
lat_len	absval	0	150	140.75675	Slope length for lateral subsurface flow [m]
surlag	absval	0	15	0.11945	Surface runoff lag coefficient
slope_len	absval	10	70	55.56029	Average slope length for erosion [m]
perco	absval	0	1	0.85713	Percolation coefficient
canmx	pctchg	-20	20	2.23619	Maximum canopy storage [mmH_2O]
latq_co	absval	0	1	0.51856	plant ET curve number coefficient
k	pctchg	-50	50	-44.03878	Saturated hydraulic conductivity [mm/hr]
AWC	abschg	0	0.5	0.06213	Available water capacity [mmH_2O/mm soil]

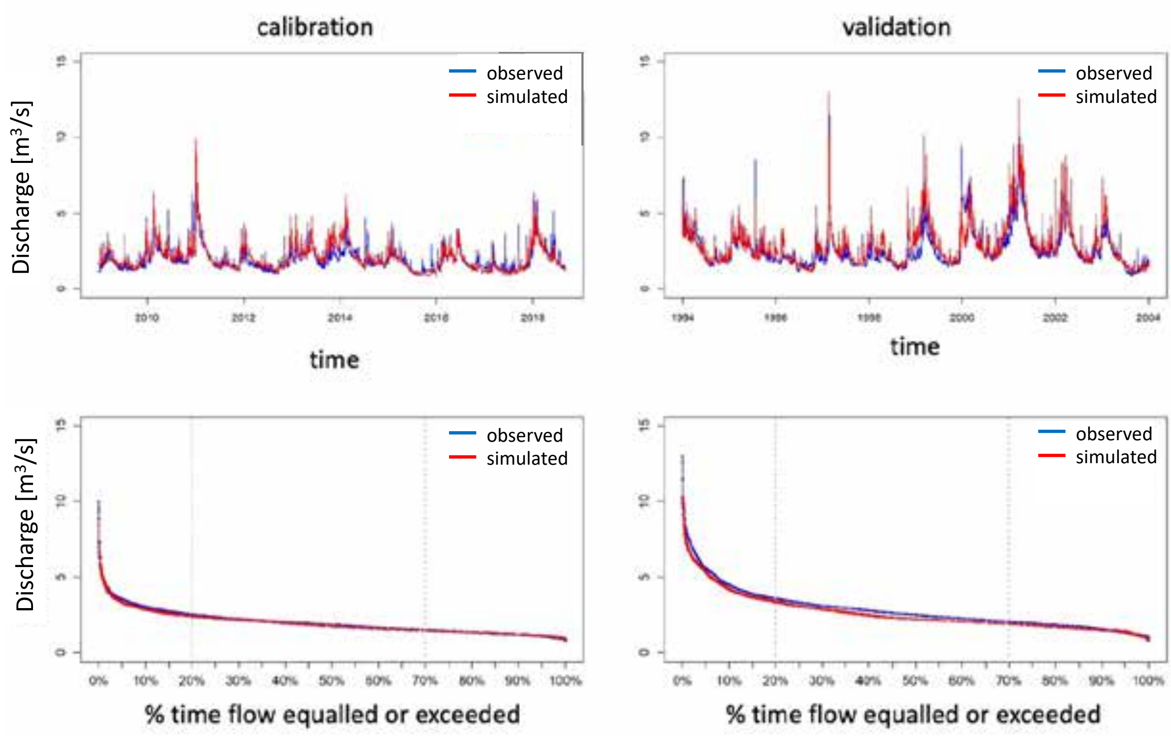

Figure 32: Hydrographs and flow duration curves for Bodenthal2 catchment for calibration and validation periods (source: Tigabu et al. 2021).

Table 17:

Efficiency of the SWAT+ model as evaluated for calibration, validation and entire simulation periods. The quantitative statistics are computed based on a daily observed and simulated streamflow data (Tigabu et al. 2021).

Objective function	**Warm up period (1991-1993)**		
	Calibration (2009-2019)	**Validation (1994-2003)**	**Full simulation (1994-2019)**
KGE	0.82	0.83	0.76
NSE	0.64	0.65	0.53
PBIAS	-1.0	-8.1	9.4
RSR	0.60	0.60	0.68

5.3 Water balance

5.3.1 The Palatinate Forest Biosphere Reserve catchment

After regionalization, the entire catchment of the Palatinate Biosphere Reserve was analyzed regarding water balance components and flow dynamics in order to calculate the available water budgets and their distribution in the watershed. The time period used for analysis was 2000 to 2020. Within this period, the long-term annual average water inputs through precipitation was 821 mm. A major part of precipitation (77 %) was shown to be evaporated back into the atmosphere as actual ET, amounting 635 mm/aa. SWAT+ captured the seasonal variability in ET throughout the years properly, as exemplified for the period 2004 to 2008 on monthly basis in **figure 33**.

Regarding surface runoff, only a small part of 1.5 % was transported as overland flow on average annual level (12.5 mm/aa). For the depiction of the temporal-quantitative distribution of overland flow, the finest possible resolution is required, which in case of SWAT+ is a daily resolution. There was a quick drain reaction detected in surface runoff responding to elevated precipitation values as response to higher amounts of precipitation, which lead to a distinct peak in surface runoff, as can be concluded from **figure 34**.

A similar short circuit drain reaction was observed regarding the contribution to streamflow, as shown in **figure 35** based on monthly values.

A dominant factor in water yield (93 %), and therefore contribution to the stream, was lateral flow, accounting for 169 mm/aa, which was 20 % of the long-term average annual precipitation. Consequently, surface runoff and lateral flow added up to 181.7 mm/aa water yield, feeding the discharge at the outlet point.

The second dominant factor in water distribution dynamics was found to be groundwater recharge (**fig. 36**).

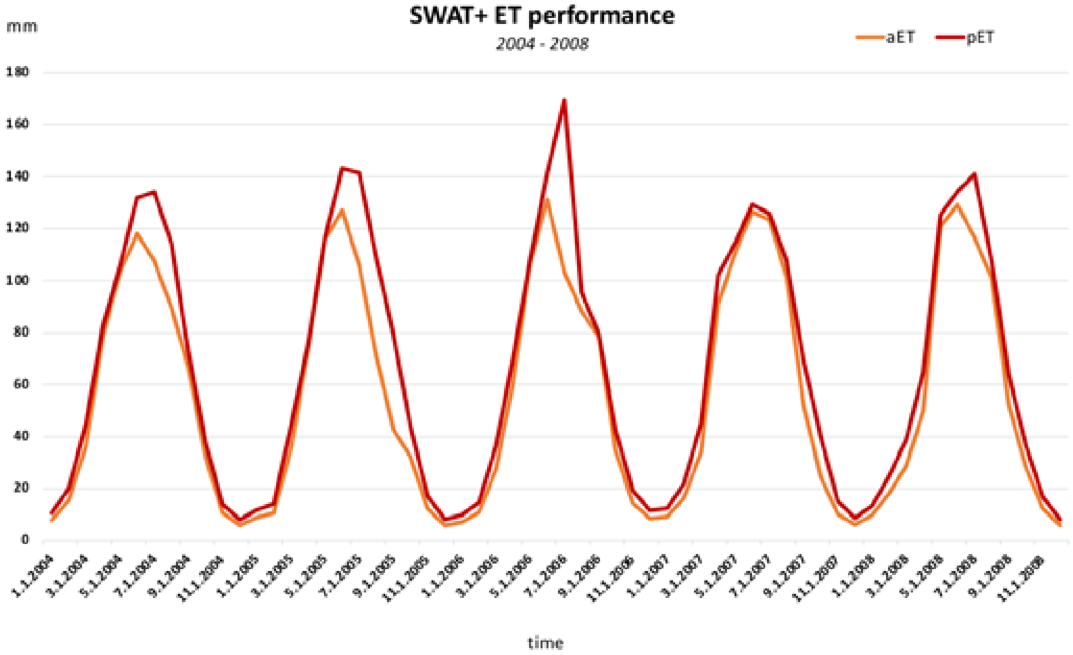

Figure 33: SWAT+ performance of seasonal variability in potential ET (pET) and actual ET (aET), exemplified for the timeline 2004 to 2008, based on monthly values.

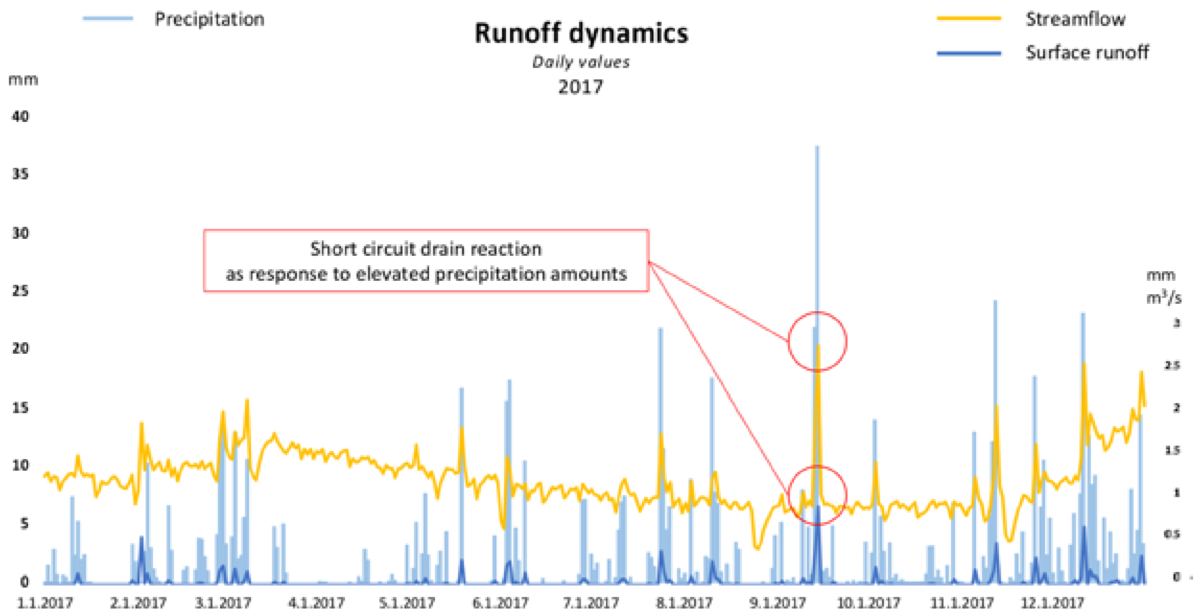

Figure 34: Response in surface runoff [right ordinate mm] and streamflow [m³] to elevated precipitation [left ordinate mm] amounts in the Palatinate Biosphere Reserve catchment in January 2017, based on daily values.

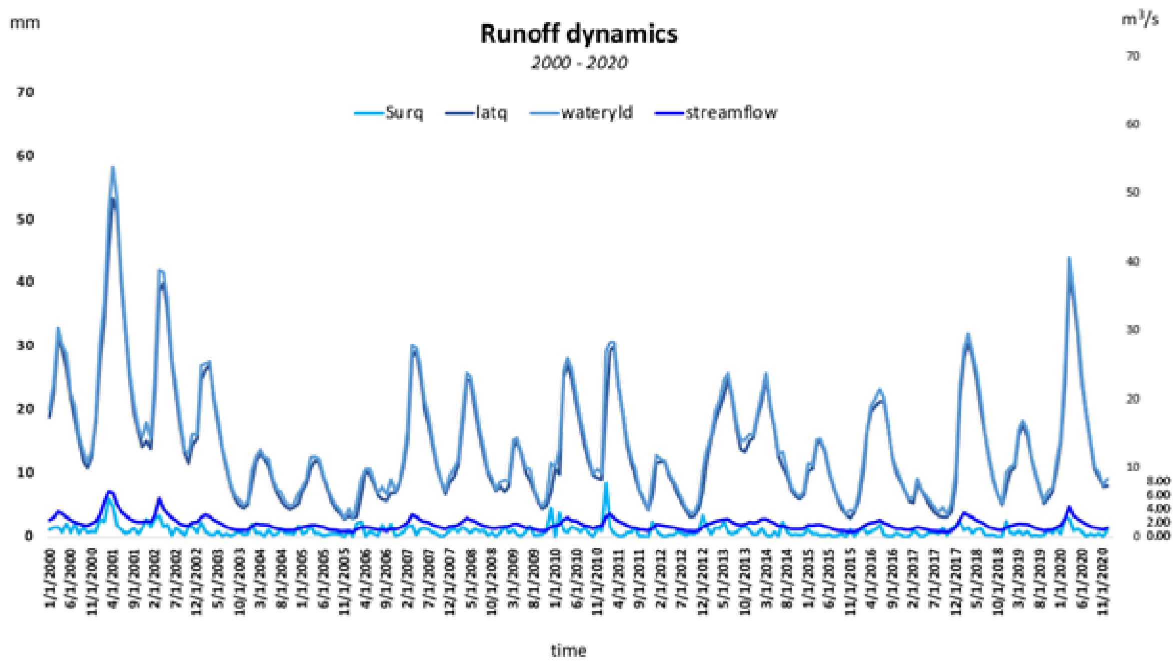

Figure 35: Runoff drain reaction in the Palatinate Biosphere Reserve catchment from 2000 to 2020, based on monthly values for streamflow [m³/s], Water yield (wateryld) [mm], surface runoff (Surq) [mm], and lateral flow (latq) [mm].

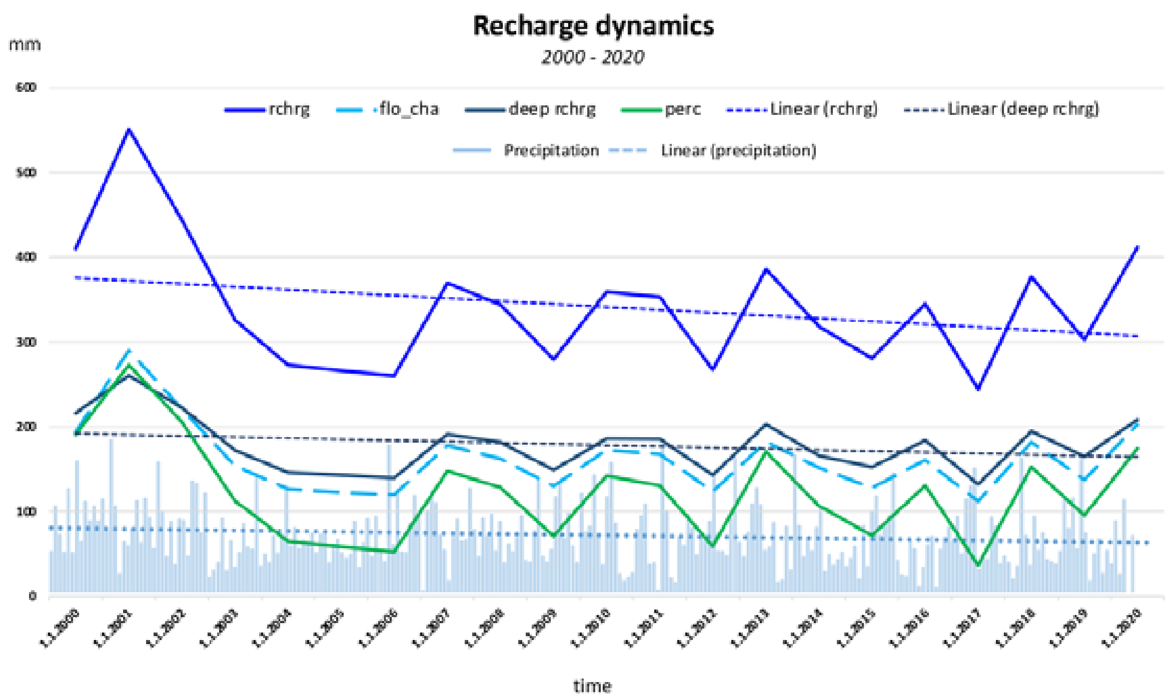

Figure 36: Flow dynamics of groundwater and precipitation, including percolation (perc), shallow aquifer recharge (rchrg), baseflow (flo_cha), and deep groundwater recharge (deep rchrg) based on annual values in the Palatinate Biosphere Reserve from 2000 to 2020, with trend lines indicating decreasing values.

With high amounts of the precipitation inputs percolating to the vadose zone (122 mm/aa), the shallow aquifer was fed by 340 mm/aa, from which 162 mm/aa discharged back to streams as baseflow. The deep aquifer recharge therefore accounted for 21.6 % in total of the average annual precipitation, which was 177 mm/aa. The model results roughly corresponded to the model results of LGB & LfW RLP (2004) after Wundt, Kille and the MNQ method, according to which 11 – 30 % of the annual precipitation (244 mm/a) were determined for the deeper, large-scale groundwater aquifer. The groundwater recharge rate in the entire area can therefore be classified as high, which reflects the seepage and flow properties described in section **3.2**. The groundwater recharge of the shallow and deep aquifer took place with one to two months delay after autumn and winter months precipitation, with a minimum in September till November (**fig. 37**). Corresponding to a decreasing trend in precipitation for the period from 2000 to 2020, the groundwater recharge also showed falling trends since the beginning of the century.

Figure 38 shows selected water balance components for the time period. The falling trends in precipitation and recharge were opposed by an increase in potential ET, which is considered a direct consequence of elevated mean air temperature in the course of climate change. The decreasing trend in actual ET, however, can be explained by progressive scarcity in soil water, which was found evident for the simulation (**fig. 39**).

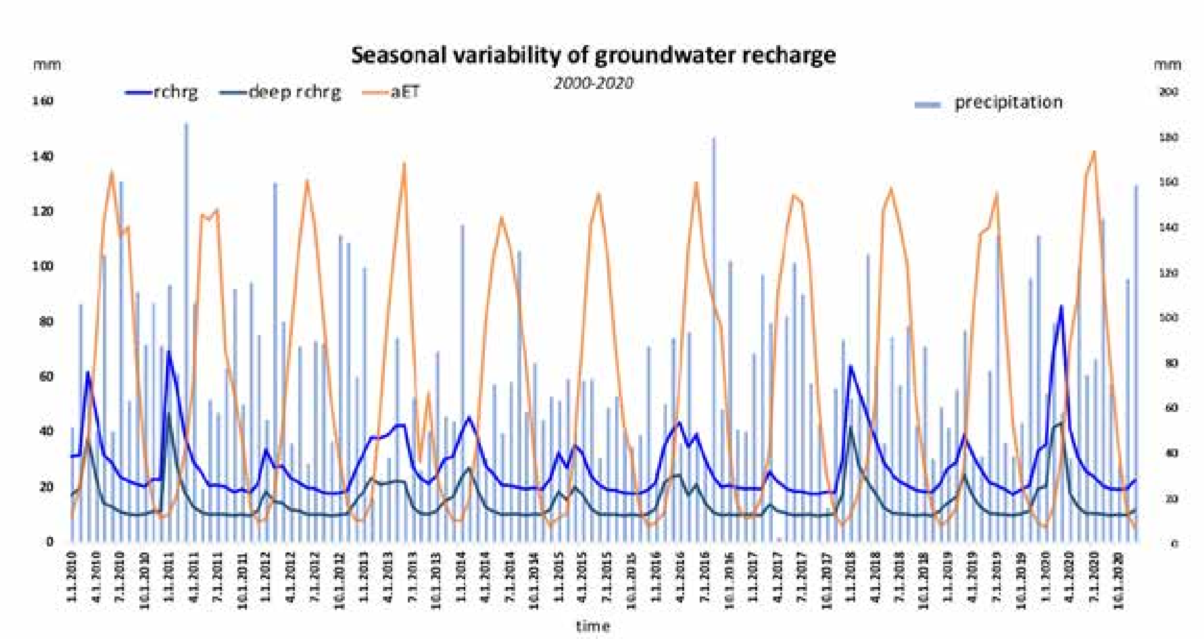

Figure 37: Seasonal variability of groundwater recharge in the catchment area based on monthly values from 2000 to 2020, depicting minima and maxima of shallow aquifer recharge (rchrg) and deep groundwater recharge (deep rchrg) correlating with precipitation inputs, plant extraction outputs (aET).

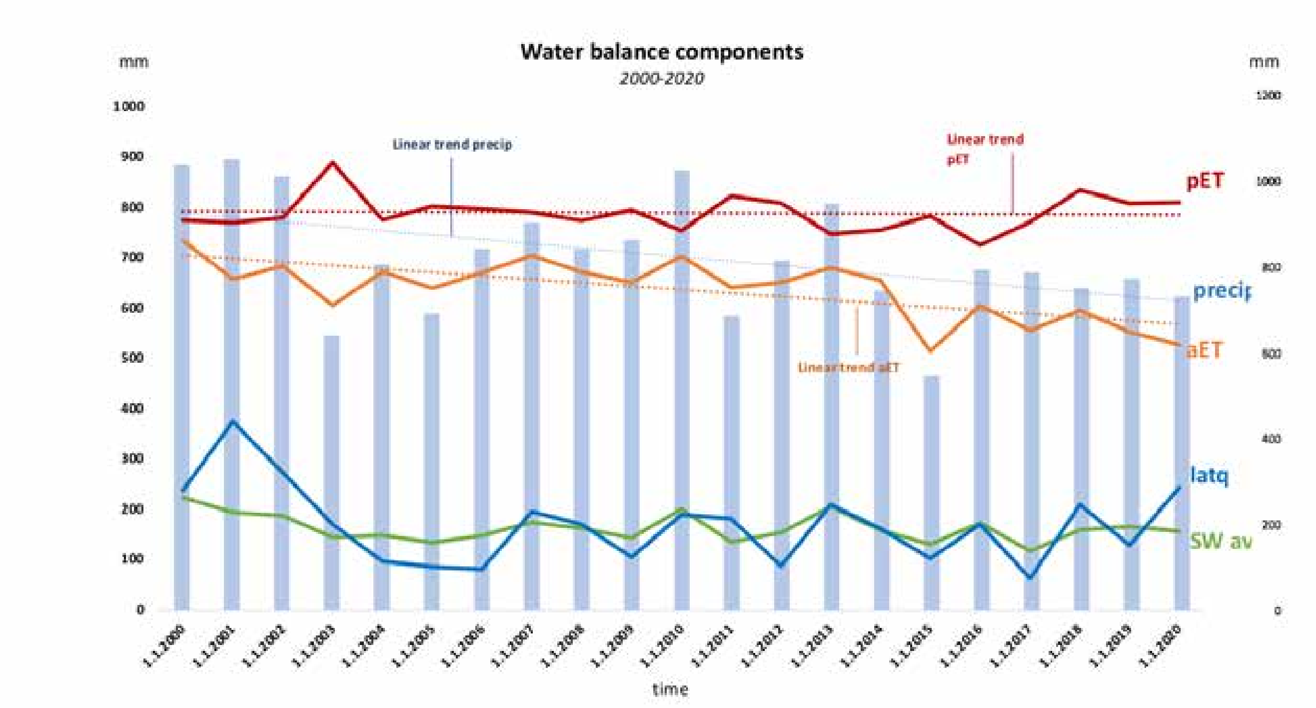

Figure 38: Selected water balance components simulated with SWAT+ in the Palatinate Biosphere Reserve from 2000 to 2020 based on yearly values, showing decreasing trends in precipitation (precip, right ordinate), and actual ET (aET, left ordinate), and an increasing trend in potential ET (pET, left ordinate). Also, average soil wetness (SW av, left ordinate) and lateral flow (latq, left ordinate) depict the patterns in precipitation.

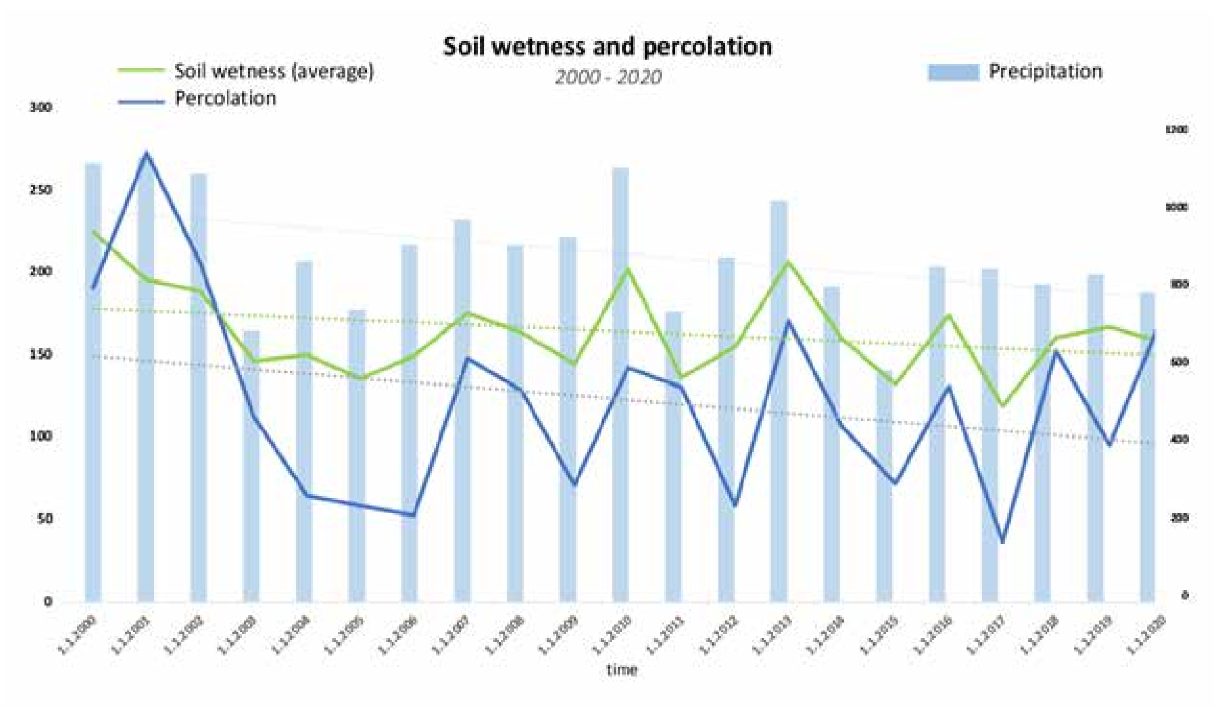

Figure 39: Development of soil wetness and percolation within the time period 2000 to 2020, simulated with SWAT+, showing decreasing trends due to a decrease in water input.

Soil water showed a general dynamic of replenishment in the dormant period, and depletion throughout the vegetation period, so that SWAT+ can be considered to capture the seasonal variability of plant water consumption and canopy cover expression sufficiently. The soil water dynamics were found to correlate strongly with water availability through precipitation inputs and plant extraction, the latter being governed by the atmospheric evaporative demand (potential ET). When in years with sufficient water inputs throughout the vegetation period, represented by 2014 in **figure 40**, the deviation between actual and potential ET, as well as soil water depletion from plant water consumption, were not distinctively pronounced, drought periods, as recorded in 2018 (represented in **fig. 41**), 2019 and 2020 (see **fig. 42**), showed a large deviation between pET and aET.

As can be interfered from **figure 41** and **42**, soil water depletion with at the same time rising evaporative demand, resulted in a higher deviation between aET and pET, indicating a simulated decline in transpiration due to scarce water availability.

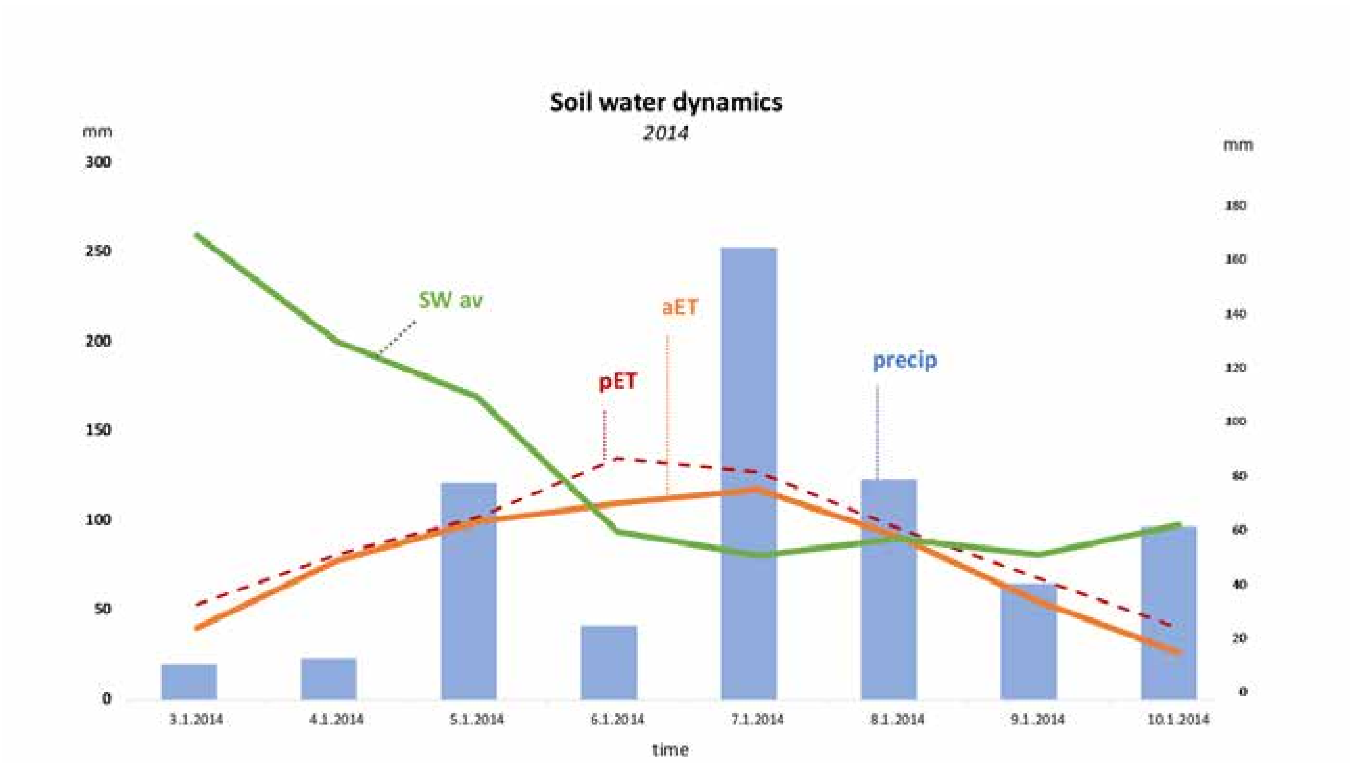

Figure 40: Interplay of water inputs, soil water content, potential ET, and actual ET in soil water dynamics in 2014 with sufficient plant water availability throughout the vegetation period, simulated with SWAT+. SW_av = average soil water content (left ordinate), precip = precipitation (right ordinate), pET = potential ET (left ordinate), aET = actual ET (left ordinate).

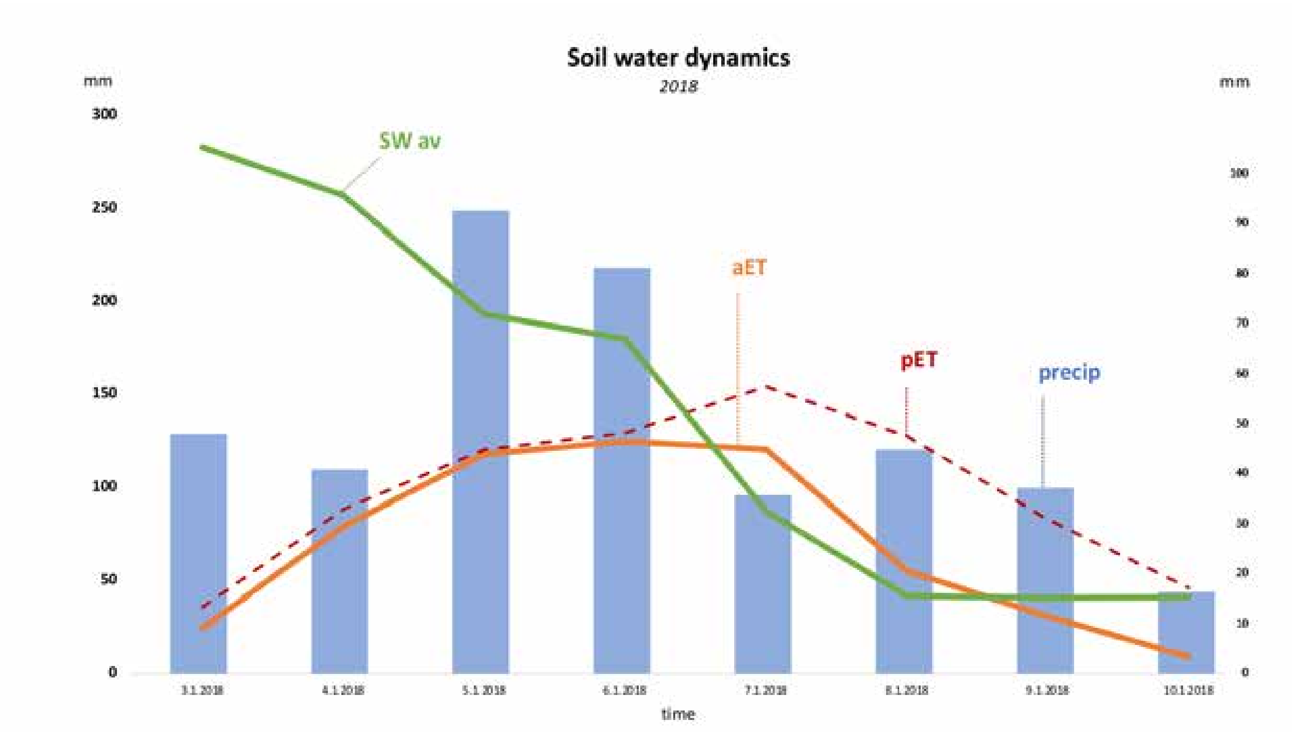

Figure 41: Interplay of water inputs, soil water content (SW av, left ordinate), potential ET (pET, left ordinate), and actual ET (aET, left ordinate) in soil water dynamics in 2018, with scarce precipitation (precip, right ordinate) throughout the vegetation period simulated with SWAT+.

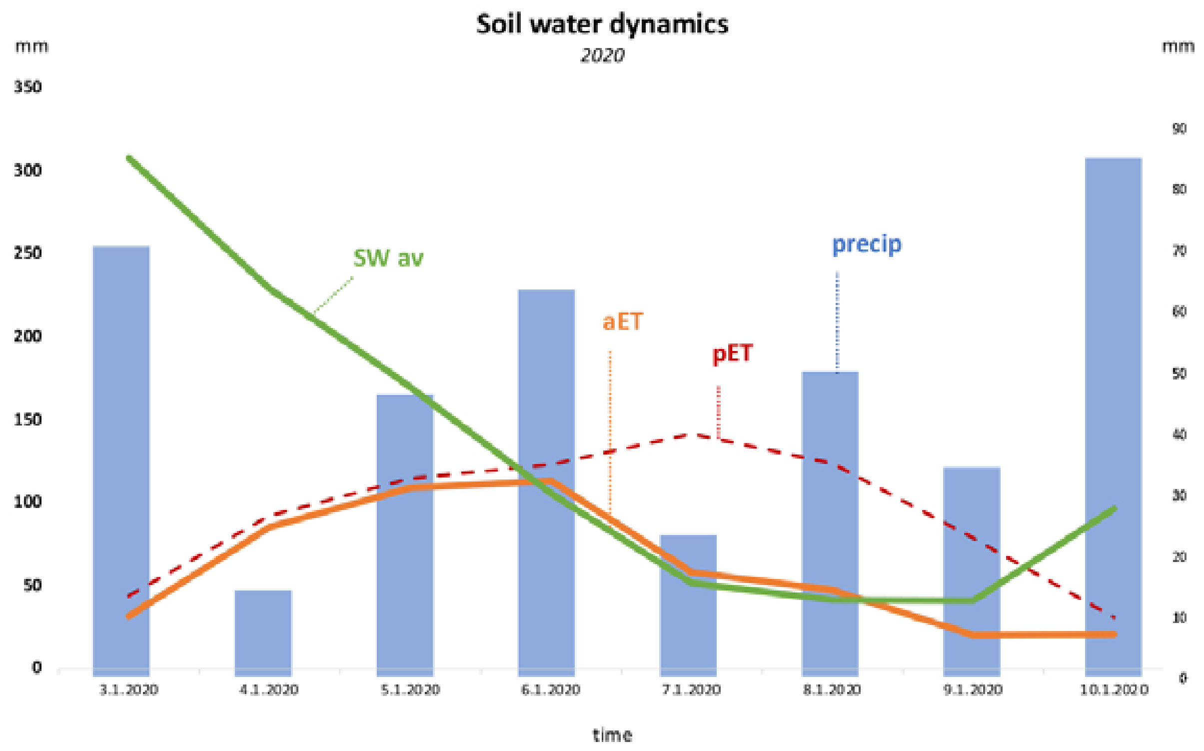

Figure 42: Interplay of water inputs, soil water content (SW av, left ordinate), potential ET (pET, left ordinate), and actual ET (aET, left ordinate) in soil water dynamics in 2020, with even less precipitation (precip, right ordinate) throughout the vegetation period compared to 2018.

5.3.2 The Bobenthal2 catchment

Based on the calibrated model, the water balance components of the Bobenthal2 catchment were analyzed regarding hydrological dynamics relevant for the objective of the study within the time period from 1999 to 2019. The Bobenthal2 catchment area was used as an artificial attempt to carry out the simulation of age-related stocking patterns, differentiated in juvenile and mature stocking types, the results of which are presented in section **5.5**. In this section, however, the general model results regarding the water balance of the calibrated base model are presented, in order to confirm its plausibility.

As expected for forested areas, the results for the Bobenthal2 catchment also confirmed the high proportion of water loss to actual evapotranspiration. With an annual average share of 51 % of precipitation (880 mm/aa), aET was shown the dominant loss factor in water balance (450 mm/a), influencing soil water contents, as well as heat fluxes between land surface and atmosphere. A second dominant factor was identified to be water yield, contributing to the streamflow at the outlet point, accounting for 31 % of the mean annual precipitation, which is equivalent to 274 mm/aa. The main contributor (96 %) to water yield was lateral flow with 264 mm/aa, whereas surface runoff showed a negligible share of 4 % of water yield, and 1.2 % of the annual average precipitation (10.8 mm/aa). This emphasizes the mitigating effect of forested watersheds on runoff volumes, which was also reflected in very low annual average flow volumes of the main channel of 2.94 m^3/s. The model results indicated that the majority of the seepage water volume contributes to the recharge of the deeper, large-scale coherent aquifer, accounting for 26 % of annual average precipitation (231 mm/aa), again coinciding with the results of LGB & LFW (2004), accounting 11 – 30 % of the annual precipitation (244 mm/a). The shallow aquifer accounted for 603 mm/aa, from which 372 mm/aa discharged back into the channels as baseflow. The temporarily stored shallow aquifer was shown to be primarily effective in flow delay. The groundwater formation rate in the Bobenthal2 area can therefore also be classified as high, which, again, can be attributed to the ideal seepage and flow properties of the geological subsurface. The groundwater recharge in the shallow aquifer occured with a delay of one to two months after the precipitation events of the autumn and winter months, with a minimum in September and October.

Figure 43 shows the hydrographs with temporal dynamics of simulated and observed discharge and precipitation from 2009 to 2018.

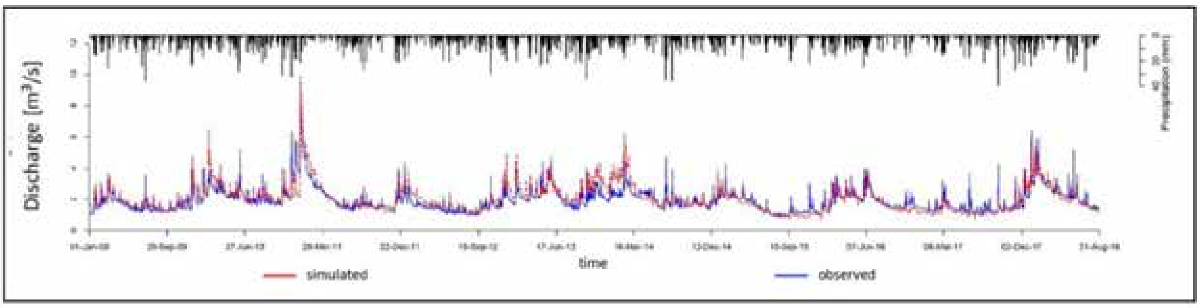

Figure 43: Temporal dynamics of major hydrologic processes in the Bodenthal2 catchment (source: Tigabu et al. 2021).

Figure 44 shows long-term trends of major hydrologic processes in the Bodenthal2 catchment from 1999 to 2019, and **figure 45** depicts the groundwater flow dynamics. As **figure 44** reveals based on yearly values, there was a slide decreasing trend for water yield and actual *ET* from 1999 to 2019, resulting from a decrease in precipitation and a slight increase in evaporative demand (potential *ET*) during that period. Also, for groundwater recharge, there was a clear falling trend for the shallow aquifer, which interacted dynamically with baseflow discharge, whereas the deep aquifer, reacting less dynamic, only showed a slight decreasing trend throughout the time period. Regarding runoff dynamics, **figure 46** shows the interplay of precipitation, streamflow and surface runoff, and depicts the immediate drain dynamics, reacting with higher peaks to elevated precipitation volumes. Although the total runoff volume must be considered low due to the strongly mitigating effect of forest vegetation cover, elevated peaks might contribute to the generation of flash floods in receiving water bodies in the event of a heavy storm.

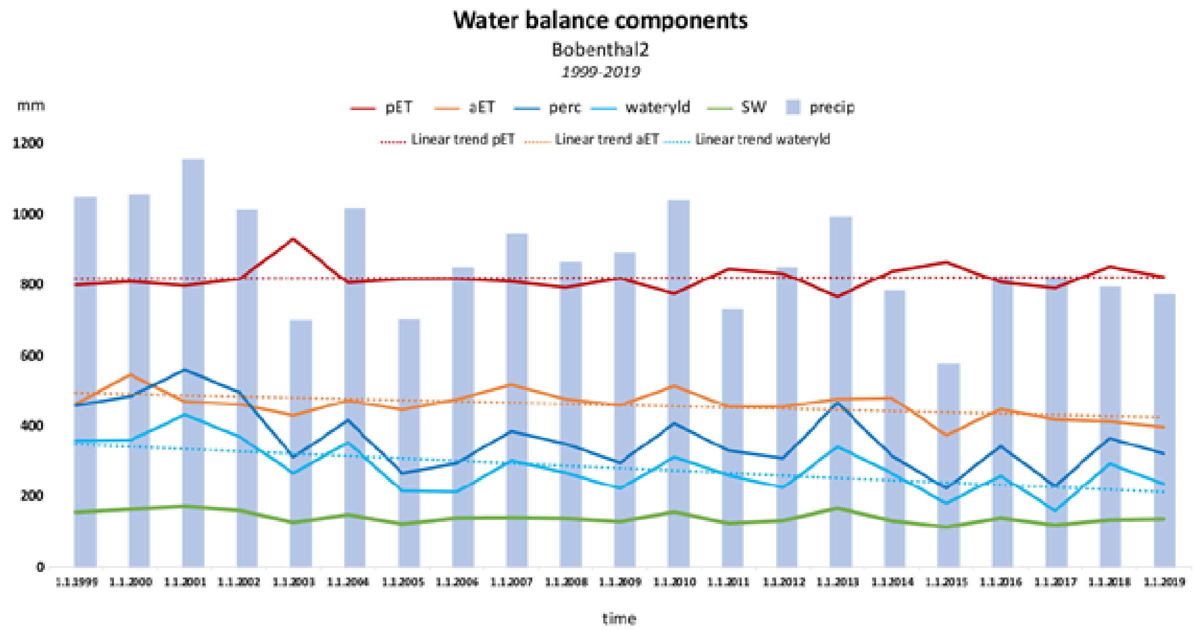

Figure 44: Long-term trends of selected water balance components in the Bodenthal2 catchment from 1999 to 2019, based on annual values: pET = potential ET, aET = actual ET, perc = percolation, wateryld = water yield, SW = average soil wetness, Precip = precipitation.

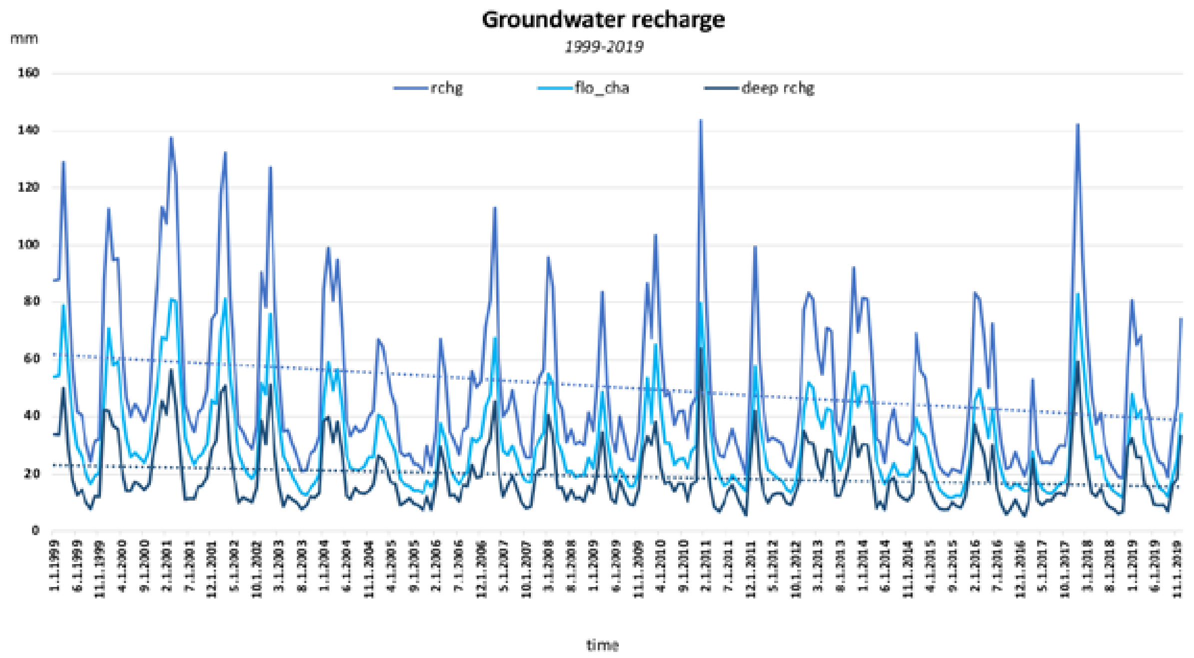

Figure 45: Groundwater recharge of the shallow aquifer (rchg), and the deep aquifer (deep_rchg) from 1999 to 2019 in the Bobenthal2 catchment, showing decreasing trends especially for the shallow aquifer, which shows a higher dynamic corresponding to baseflow interactions (flo_cha), based on monthly values.

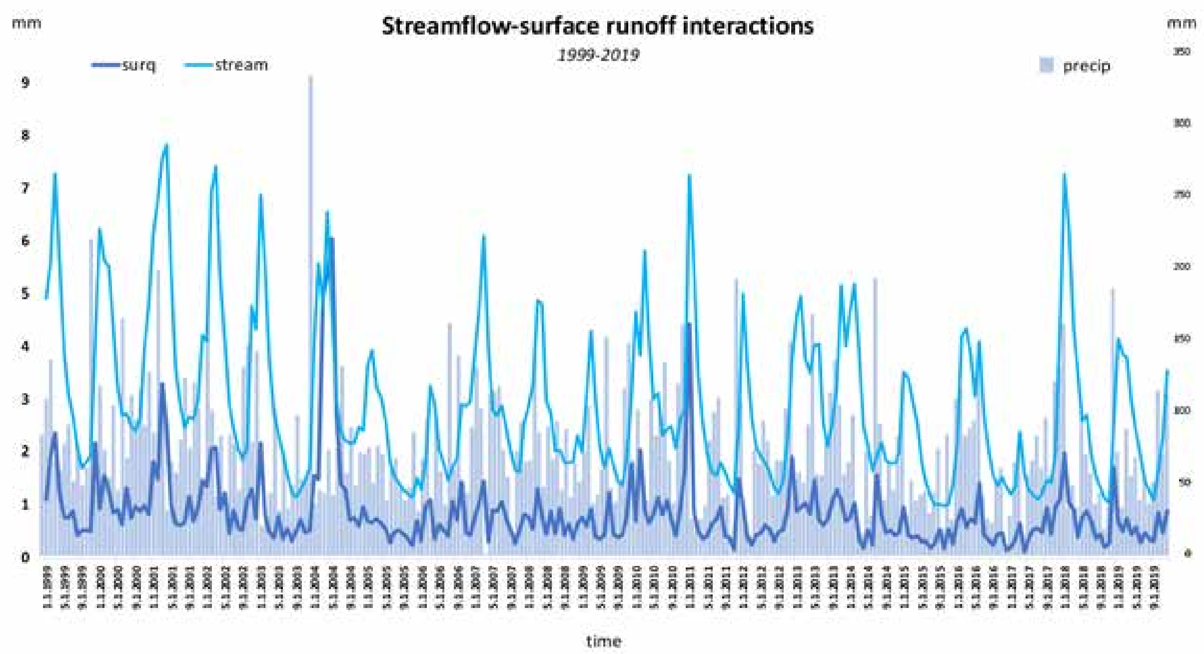

Figure 46: Interaction between streamflow (stream), surface runoff (surq) and precipitation (precip) in the Bobenthal2 catchment from 1999-2019, based on monthly values.

5.4 Future climate projections

The analysis of the climate scenarios was based on the reference period 1961 to 1990 and evaluated with main focus on possible future developments of water balance parameters reflecting the objective: Surface runoff and groundwater recharge. Other variables, that served as an indication for hydrologically functional processes of forest ecosystems, were also investigated. The baseline period was compared to an ensemble of 6 different climate scenarios, each for RCP2.6 (strong climate protection) and RCP8.5 (no climate protection), within the projection periods 2031 to 2050 and 2071 to 2099. For all climate projections, minimum, and maximum values were calculated in order depict a corridor of possible developments. The change signals of relevant water balance components were then calculated for the projections, and compared to the baseline period. **Table 18** provides an overview of the change signals of all analyzed water balance components for both future timelines, the long-term mean annual values of the baseline as basis of calculation, and the change in % of the period 2071 to 2099 compared to the period 2031 to 2050. It also includes the period from 2000 to 2020 as an overview of nowadays impact of climate change compared to the baseline. Both periods differ strongly regarding water balance dynamics: When the baseline period was characterized by quite stable conditions, the period 2000 to 2020 showed a more dynamic development with a pronounced heterogeneity of climatic conditions, as depicted in **figure 47**.

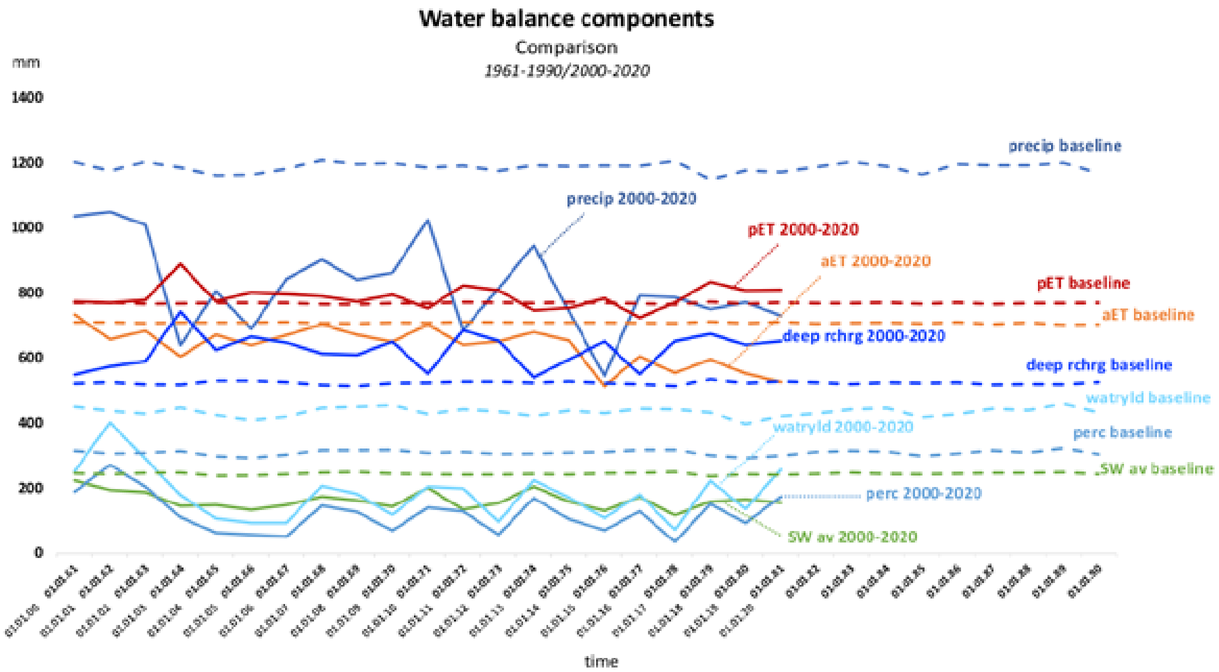

Figure 47: Comparison of water balance dynamics of the timelines 1961-1990 (baseline period), and the near past (2000 to 2020) simulated with SWAT+, showing significant differences in dynamic character of climatic conditions. With precip = precipitation, pET = potential *ET*, aET = actual *ET*, deep rchrg = deep groundwater recharge, watryld = water yield, perc = percolation, SW av = average soil wetness.

Table 18:

Change signals in water balance components of climate scenario RCP2.6 and RCP8.5 for the timelines 2000-2020, 2031-2050 and 2071-2099 compared to the baseline period 1961-1990, as well as change in % between the future projection timelines, based on annual average values.

	Change % of baseline							Change between future periods
	RCP2.6							
timeline	1961-1990	2000-2020		2031-2050 (a)		2071-2099 (b)		
	baseline	*Absolute values*	*% of baseline*	MIN	MAX	MIN	MAX	*% (b) of (a)*
Precipitation [mm]	1184.56	821.38	-30.66	-32.34	-3.77	-36.01	-7.08	-3.46
Potential ET [mm]	768.29	787.32	2.48	1.66	17.18	0.53	19.68	0.71
Actual ET [mm]	707.13	635.7	-10.10	-14.91	3.48	-17.43	4.11	-1.20
Soil Evaporation [mm]	115.40	110.26	-4.45	-17.91	-0.89	-22.71	9.67	0.83
Lateral flow [mm]	404.90	169.26	-58.2	-56.95	-4.26	-67.77	-16.63	-14.67
Soil wetness [mm]	246.08	164.17	-33.29	-32.48	-8.55	-38.50	-9.10	-2.55
Percolation [mm]	309.28	122.24	-60.48	-60.86	-12.69	-70.82	-19.67	-7.4
GW recharge [mm]	285.7	177.6	-37.8	-39.45	-9.23	-41.18	-7.92	0.07
Surface runoff [mm]	30	12.47	-58.43	-62.18	-13.30	-63.13	-6.07	-0.18
Water yield [mm]	434.9	181.73	-58.21	-58.47	-9.98	-67.50	-17.03	-9.92
Streamflow [m^3/s]	3.65	2.3	-36.99	-55.41	-13.69	-59.64	-12.79	-2.36
	RCP8.5							
Year	1961-1990	2000-2020		2031-2050 (a)		2071-2099 (b)		
	baseline	*Absolute values*	*% of baseline*	MIN	MAX	MIN	MAX	*% (b) of (a)*
Precipitation [mm]	1184.56	821.38	-30.66	-36.37	-4.12	-30.22	2.02	5.40
Potential ET [mm]	768.29	787.32	2.48	0.24	16.76	2.34	23.74	3.76
Actual ET [mm]	707.13	635.7	-10.10	-15.07	3.76	-14.47	4.28	-0.48
Soil Evaporation [mm]	115.40	110.26	-4.45	-18.84	6.75	-16.33	7.53	1.64
Lateral flow [mm]	404.90	169.26	-58.2	-59.47	-14.67	-55.67	2.68	7.90
Soil wetness [mm]	246.08	164.17	-33.29	-34.52	-7.52	-31.70	-6.90	0.60
Percolation [mm]	309.28	122.24	-60.48	-61.23	-16.14	-38.52	-34.27	2.62
GW recharge [mm]	285.7	177.6	-37.8	-37.96	-9.47	-35.89	2.07	5.5
Surface runoff [mm]	30	12.47	-58.43	-59.00	-13.79	-59.80	28.90	17.49
Water yield [mm]	434.9	181.73	-58.21	-59.04	-15.17	-55.66	4.06	8.23
Streamflow [m^3/s]	3.65	2.3	-36.99	-53.84	-16.36	-41.38	0.12	6.64

For the middle of the century, both RCP scenarios predicted a decrease in precipitation compared to the baseline period. RCP2.6 ranged from -32 % to -3.7 %, while the decrease for RCP8.5 was even slightly higher, with a minimum of -36 % to a maximum of -4 %. Under RCP2.6, the decrease even aggravated by -3.5 % until the end of the century, with a minimum of -36 % to a maximum of -7 %. Only in case of RCP8.5, an increase by 2 % in precipitation was projected in maximum values for the end of the century compared to the baseline period, though the minimum still showed a decrease by -30 %. **Figures 48** and **49** provide a more detailed insight in the development of precipitation throughout the future timelines for both scenarios, based on yearly values. The trendlines indicated a decline in precipitation for RCP2.6 in 2031 to 2050, but a very slight increase for 2071 to 2099, as well as an increasing trend for RCP8.5 within both future periods, which matched the precipitation projections of the Competence Centre of Climate Change Impacts RLP in general[18]. Despite the increasing trend within the far future timeline, an overall mean decreasing trend for RCP2.6 for the timeline 2071 to 2099 compared to the middle of the century can also be inferred by **fig. 49**. Except for a few peaks in maximum values, the climate projections undercut, however, the precipitation amounts of the baseline period, although an approximation can be inferred for the end of the century, as well as a slight convergence of the scenarios RCP2.6 and RCP8.5. With a change of -30 % compared to the baseline, the past two decades (2000-2020) already approximated projected minimum values for the future.

The lower water inputs to the system were projected to be counteracted by clear increasing trends in evaporative demand, resulting from higher air temperatures, as in line with predictions of the Competence Centre of Climate Change Impacts RLP until the end of the century (see **fig. 10** in section **2.3.3.1**). RCP2.6 indicated an increase in potential ET ranging from 1.6 % (minimum) to 17 % (maximum) for the middle of the century, 0.24 % to 16.7 % for RCP8.5 respectively, and at least 0.5 % to maximal 19 % until the end of the century, 2.3 % to 23.7 % for RCP8.5 respectively.

The approximately 2.5 % gain in potential ET observed throughout the past two decades (2000 -2020), however, already matched the minimum value projected for the worst case scenario (RCP8.5) by the end of the century. The current development thus indicated an accelerated progression of climate change, exceeding the expectations suggested by the climate projections. At the same time, actual ET was projected to decrease in minima through all future timelines and scenarios, whereas maximum values indicated a slight increase: RCP2.6 ranged from -14 % by the middle of the century, and -17 % to 4 % by the end of the century compared to the baseline. RCP8.5 showed a range for actual ET from -15 % decrease to 3.7 % increase by the middle, and approximately analogous values (-14 % to 4 %) until the end of the century. The smaller decrease in minima for RCP8.5 by the end of the century can be explained by increasing precipitation, which mitigated soil water deficiencies in plant water availability. In 2000 to 2020 on the other hand, decline in plant transpiration due to scarce soil water availability was found reflected in a decrease in aET by -10 %.

This was also found reflected in values for soil wetness, when the soil water content depleted by -33 % in mean values in 2000 to 2020. For the near future minima were found to match the current development with -32 %, but aggravated for the farer future with -38 % soil wetness compared to the baseline, whereas the maxima ranged from -8 % to -9 % respectively.

RCP8.5 showed a slight recovery of soil water in minimum values from -34 % in the middle, to -31 % by the end of the century, when more precipitation inputs replenished the storage. Maxima remained quite constant in that case, with -7.5 % to -7 %.

[18] See www.kwis-rlp.de

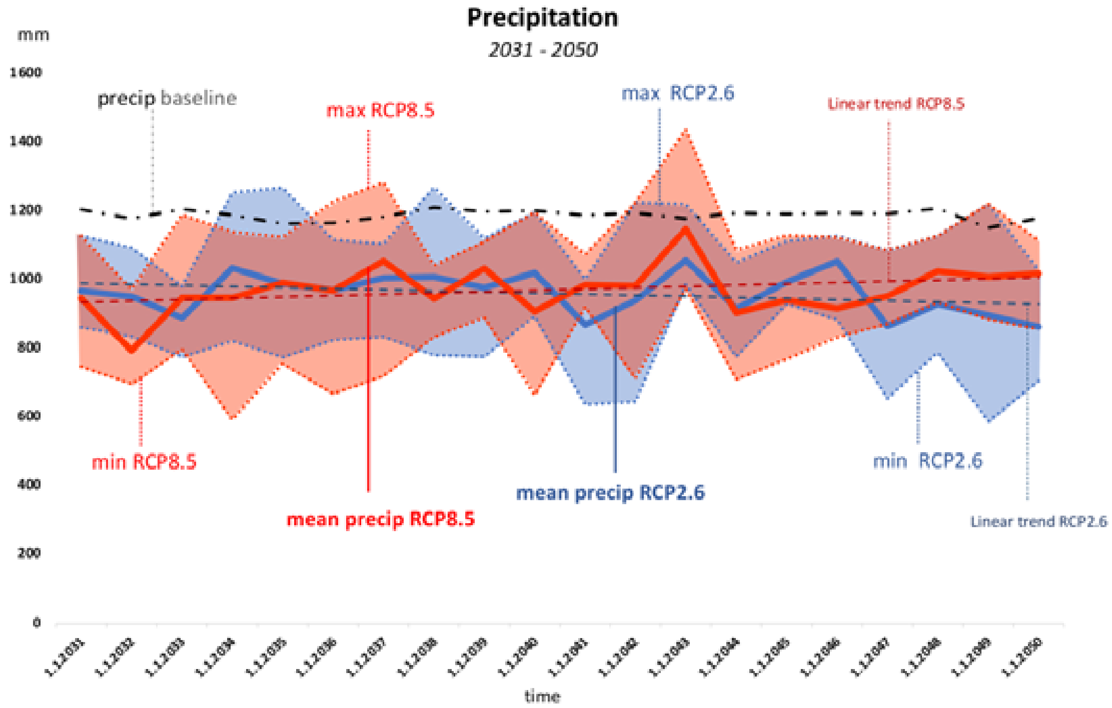

Figure 48: Projected development of precipitation (precip) for both scenarios, RCP2.6 and RCP8.5, within the timeline 2031 to 2050, based on yearly values, with minimum and maximum corridors for both scenarios, and compared to the baseline period 1961 to 1990.

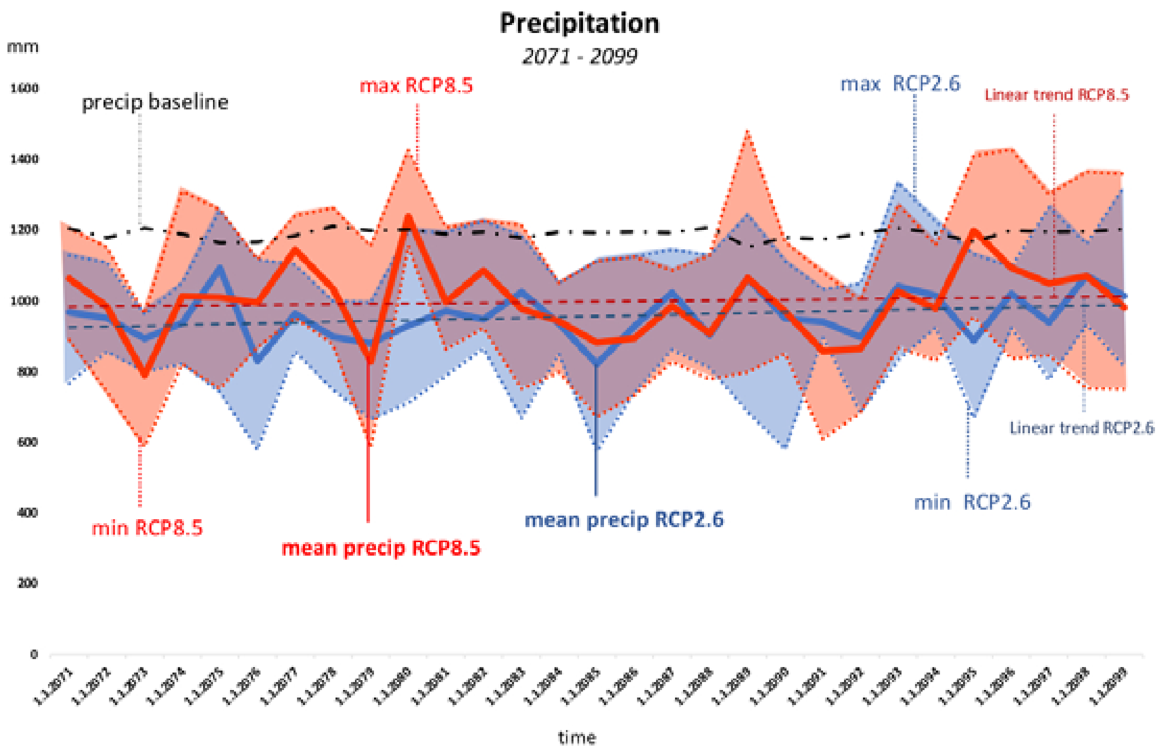

Figure 49: Projected development of precipitation (precip) for both scenarios, RCP2.6 and RCP8.5, within the timeline 2071 to 2099, based on yearly values, with minimum and maximum corridors for both scenarios, and compared to the baseline period 1961 to 1990.

The overall lower water inputs reflected in future projections compared to the baseline period also caused a clear trend of loss in groundwater recharge, due to significantly pronounced decreases in percolation, ranging from -60 % in minima by the middle, to -70 % by the end of the century for RCP2.6, and from -61 % to -38 % for RCP8.5 respectively. Maxima still showed a decrease by -12 % in the near future, to -19 % by the end of the century for RCP2.6, and -38 % to -2 % for RCP8.5 respectively. Again, the projected gain in precipitation in the farer future was found effective in mitigating losses in percolation. As groundwater recharge is fed by percolation water entering the vadose zone, previously stored percolation water at the bottom layer, and bypass flows (cf. Neitsch et al. 2011:172), all entering the aquifer in a given timestep, the recharge is directly affected by lower inputs of percolation, which resulted in a decline in minima of -39 % (2031-2050) to -41 % (2071-2099) for RCP2.6, with maxima ranging from -9 % to -7 % respectively, and -38 % (2031-2050) to -36 % (2071-2099) for RCP8.5, with maxima for the middle of the century of -9 % of the baseline. Only in case of RCP8.5 by the end of the century, maximum values were predicted to match, and even slightly exceed past times (2 % gain compared to the baseline), so that groundwater storage depletion was assumed to recover again due to elevated precipitation inputs. With approximately -38 % decrease in groundwater recharge compared to the baseline, the current development (2000 to 2020) already resembled future projection minima. **Figure 50** shows the predicted development of deep groundwater recharge for both scenarios until the middle of the century in average annual values, plus minimum and maximum corridors. For both scenarios, maximum values reached the baseline recharge volumes in peaks, but cannot be considered sustainable in replenishment.

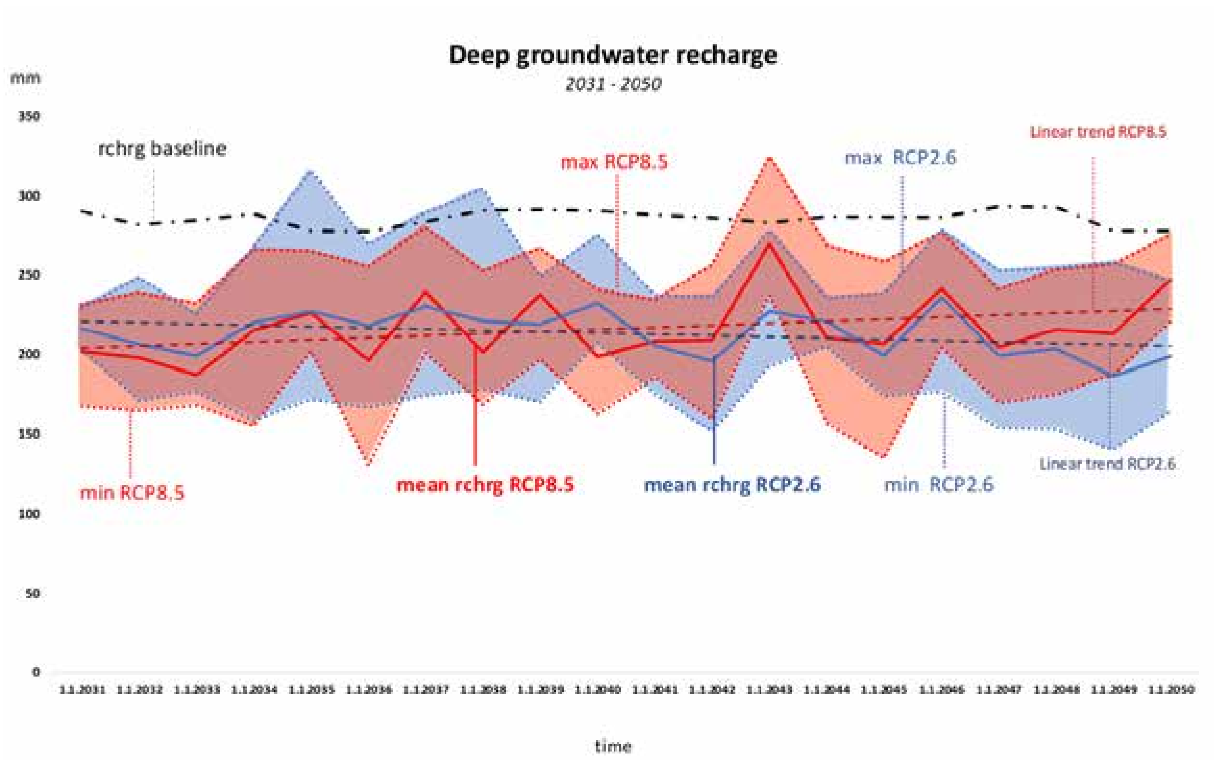

Figure 50: Projected development of deep groundwater recharge (rchrg) for RCP2.6 and RCP8.5 within the timeline 2031 to 2050, based on annual values, and compared to the baseline period 1961 to 1990, showing a decreasing trend for RCP2.6, and an increasing trend for RCP8.5.

Figure 51 gives the projection of deep groundwater recharge for RCP2.6 and RCP8.5 within the timeline 2071 to 2099. The yearly resolution allows for further conclusions: Throughout the period 2071 to 2099, RCP2.6 showed a slight increasing trendline, which also matched the precipitation patterns adequately, although decreasing in overall mean values (-25 % in mean values compared to the baseline). The time resolution also allowed for a more detailed perspective on possible developments with respect to maximum values: RCP8.5 exceeded the baseline period in more frequent peaks, and even constantly close to the end of the century, when even for RCP2.6 a conjunction with the baseline period can be inferred regarding maximum peaks. When in the middle of the century, the maximum for RCP8.5 was around -9 % compared to the baseline, the steep rise within only half a century indicated a very accelerated change in climatic conditions for this worstcase scenario, potentially bringing about a chaotic progression. This incidence can be considered a potential tipping point regarding the recovery of groundwater formation. But, as soil water depletion was still effective within the vegetation period, as can be inferred from **figure 52** for RCP8.5 at the end of the century, this cannot be considered an easing signal for future living conditions of tree communities: Forest ecosystems are tightly bound in their vitality to functional hydrological continuity, and are therefore vulnerable to extreme weather conditions, such as progressive drought periods throughout the vegetation period. **Figure 52** also supports the assumption that the low peak of soil water content was reached far earlier in the year: when in the baseline period, the lowest values in soil wetness were reached by the middle of September, the farer future development suggested soil water to be depleted in August already.

The overall lower water inputs to the system for future scenarios also resulted in lower amounts of runoff water, may it be lateral flow, overland flow, or streamflow. The overall water yield decreased by -58 % in minimum values by the

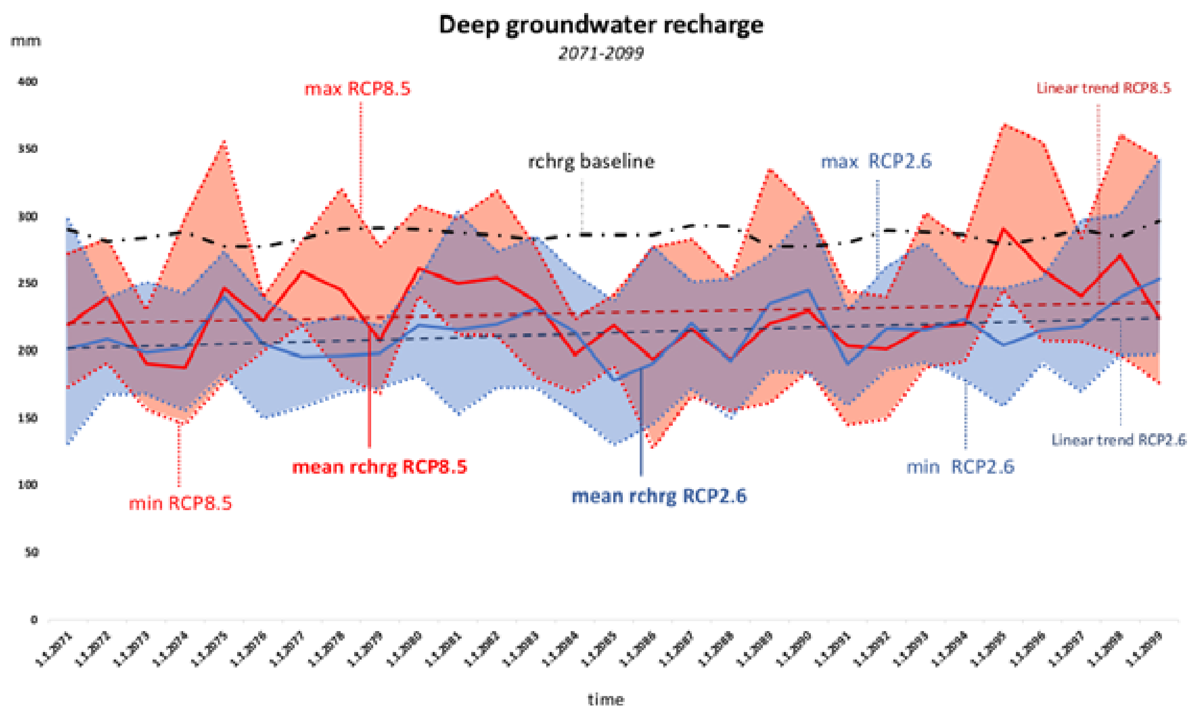

Figure 51: Projected development of groundwater recharge (rchrg) for RCP2.6 and RCP8.5 within the timeline 2071 to 2099, based on annual values, and compared to the baseline period 1961 to 1990, showing an increasing trend for both scenarios, though undercutting the baseline recharge amounts.

middle of the century in case of RCP2.6, -67 % for RCP8.5 respectively, and almost -59 % until the end of the century, -55 % in case of RCP8.5 compared to the baseline. Maximum values ranged from approximately -10 % decline for RCP2.6 by the middle of the century (-15 % in case of RCP8.5), to -17 % in the farer future. Only in case of maximum values, RCP8.5 indicated a gain in water yield by 4 % at the end of the century compared to the baseline. The relative rise in water yield for RCP8.5 at the end of the century, again, correlated with the rise in precipitation, and was found to be also reflected in streamflow, with a small gain of 0.1 % of the baseline in maximum values (-41 % decrease in minima). The most significant decrease was found for RCP2.6 in minima by the end of the century, with approximately -60 % in streamflow with corresponding decline in precipitation (-36 % in that case). With also scarce precipitation inputs for both scenarios by the middle of the century, minima remained quite constant around -55 %, whereas maxima reached -13 % (RCP2.6) to -16 % (RCP8.5). With about -37 % streamflow compared to the baseline, the current situation (2000 to 2020) already reflects the effect of decrease in precipitation inputs on streamflow volumes.

The strong correlation with precipitation inputs was also found valid for surface runoff, ranging from a decrease by around -63 % in minimum values for both future timelines in case of RCP2.6, to -59 % in case of RCP8.5. For the latter, however, maximum values reached an increase by almost 29 % compared to the baseline with elevated precipitation by the end of the century. In this case, the contribution to the streamflow was projected to be negligible (4 % increase in water yield compared to the baseline), but the spatial and temporal distribution patterns play a major role in potential flash flood generation, thus not well depicted in climate projections. **Figure 53** and **54** give an impression of the development of surface runoff based on yearly values for both

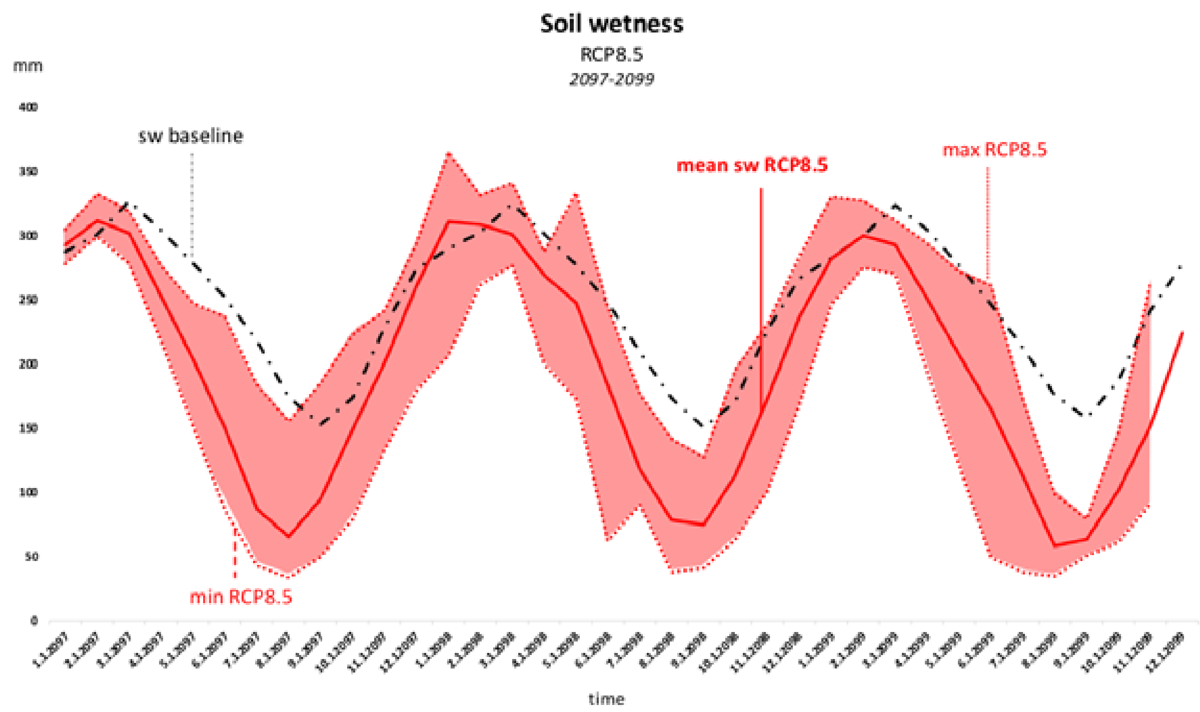

Figure 52: Projected development of average soil wetness (sw) for RCP8.5 within the timeline 2097-2099, based on monthly values, and compared to the baseline period 1961-1963, with minima and maxima building the corridor for mean values.

climate scenarios, suggesting an increasing trend for RCP8.5 in both timelines, and also in case of RCP2.6 for the period 2071 to 2099, again in line with predicted precipitation amounts, considering mean values. With increasing trends in precipitation, as projected for RCP8.5 within the timeline 2071 to 2099, the maximum runoff peaks became, however, much more pronounced.

In order to depict a higher time resolution, **figure 55** and **56** zoom in to monthly values for a timeline of 3 years for each period, with 2031 to 2033 representing the middle of the century, and 2097 to 2099 the end.

The patterns depict the correlation between the peaks in rainfall and surface runoff, and give a clear impression of the hydrological response system to higher amounts of precipitation: With high peaks in precipitation, also the surface runoff rose significantly with a slight lag, especially with respect to maximum projection values. Furthermore, for the years 2032 and 2034, RCP8.5 showed very scarce rainfall inputs compared to RCP2.6 throughout the growing season, indicating possible drought.
The strong drain reaction to high amounts of input water became even more pronounced in 2097 to 2099. Compared to the middle of the century, a stronger dynamic in precipitation patterns was found to intensify the amplitudes in surface runoff, again especially with respect to possible values of the maximum range. The peaks in rainfall were, however, projected to be predominantly concentrated in the winter and early spring months, so that with the soil water storage being refilled and with longer duration of rainfall, more runoff appeared to be generated until early summer as response to hydraulic saturation.

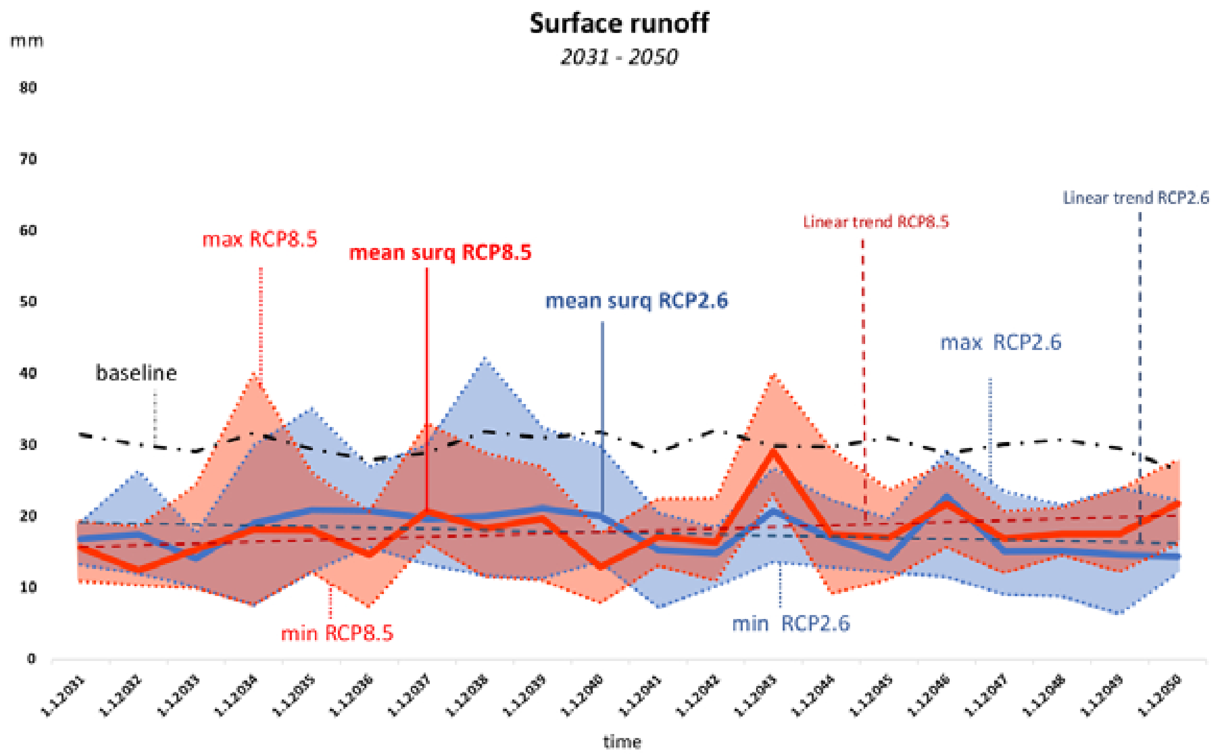

Figure 53: Projected development of surface runoff (surq) for RCP2.6 and RCP8.5 within the timeline 2031 to 2050, based on annual values, and compared to the baseline period 1961 to 1990, showing a decreasing trend for RCP2.6, and an increasing trend for RCP8.5, aligned with the development for precipitation.

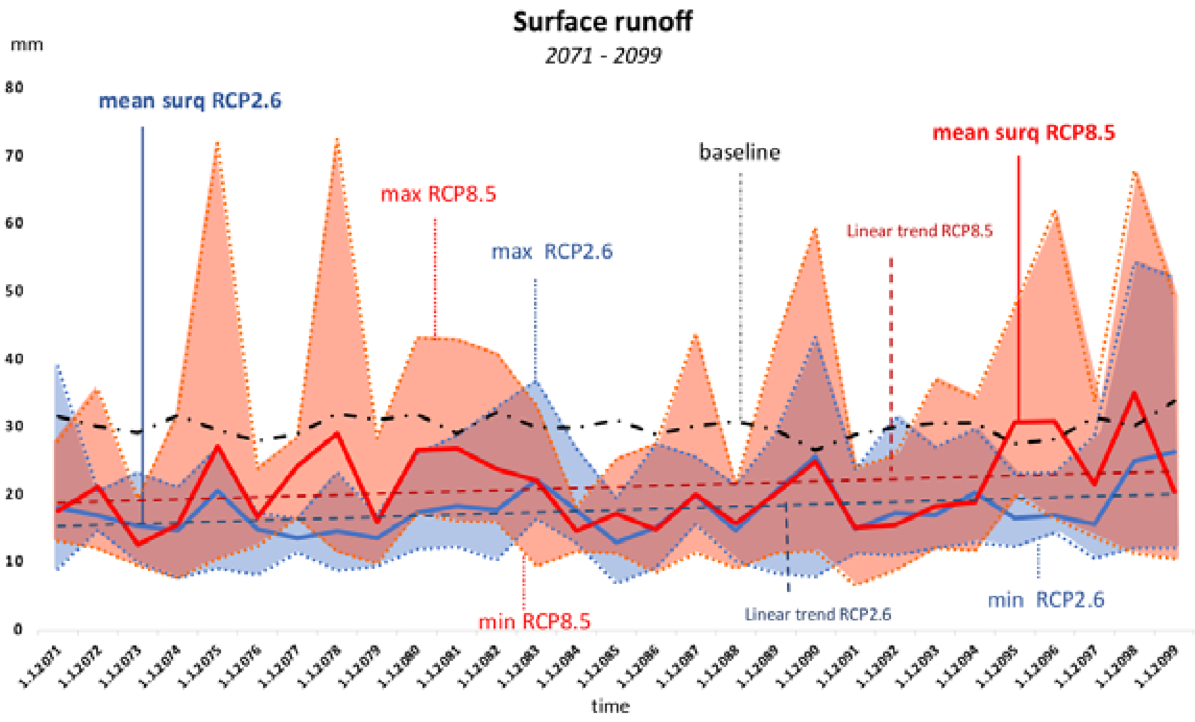

Figure 54: Projected development of surface runoff (surq) for RCP2.6 and RCP8.5 within the timeline 2071 to 2099, based on annual values, and compared to the baseline period 1961 to 1990, showing an increasing trend for both scenarios, aligned with the development for precipitation.

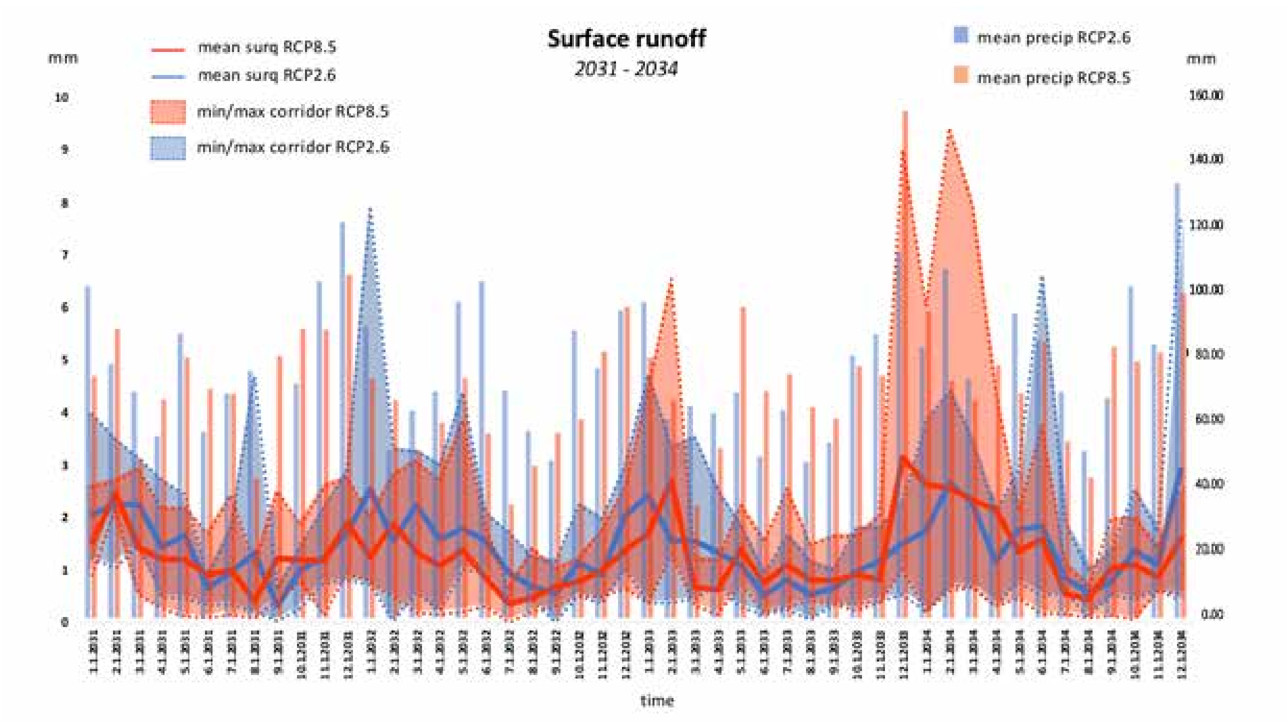

Figure 55: Projected development of surface runoff (surq) combined with precipitation (precip) for RCP2.6 and RCP8.5 within the timeline 2031 to 2034, based on monthly values.

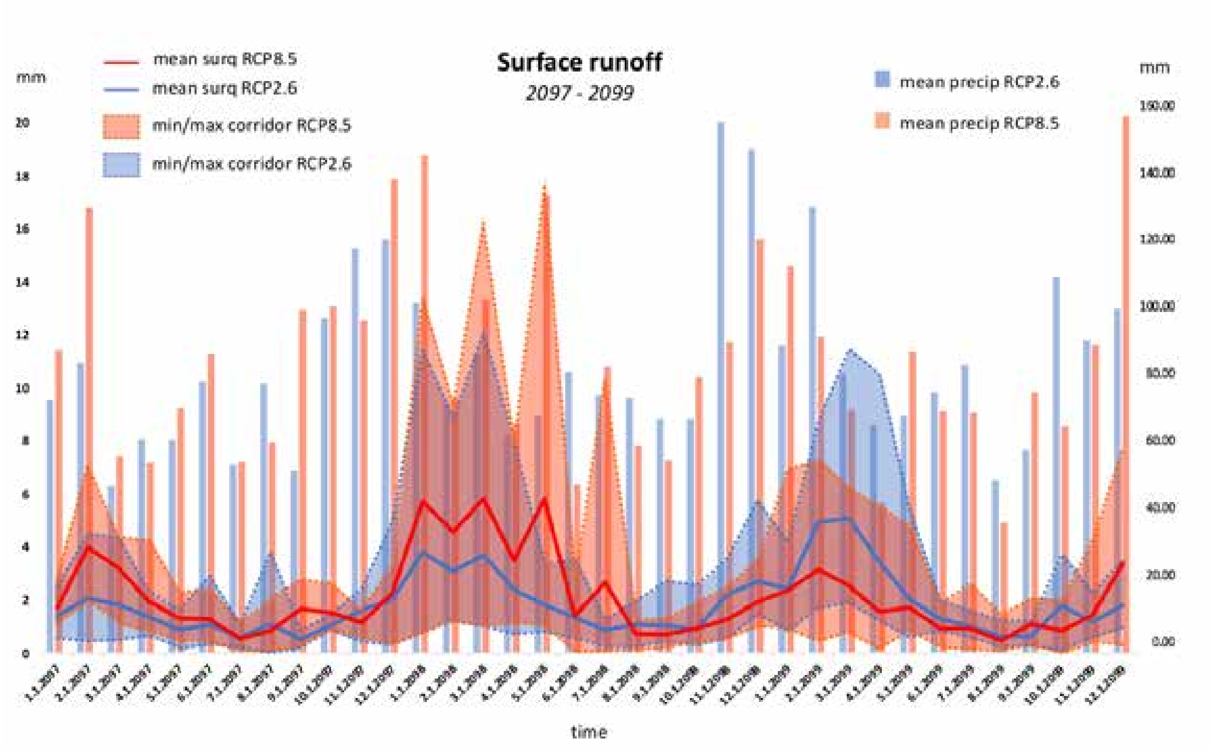

Figure 56: Projected development of surface runoff (surq) combined with precipitation (precip) for RCP2.6 and RCP8.5 within the timeline 2097 to 2099, based on monthly values.

5.5 Soil compaction

For both compaction model setups, a timeline from 1990 to 2000 was chosen as basis for evaluation. The respective uncompacted model was used as reference for the analysis of changes on water balance components affected by soil compaction.

Regarding the pathway system, the compaction resulted in an increase in surface runoff on watershed level by 36.2 %. Since infiltration was inhibited, lateral flow and percolation decreased by -2 %, and -2.6 % respectively, resulting in an overall increase in water yield by 12.3 % contributing to the receiving waters in the catchment. The groundwater recharge decreased by 2 % on watershed level due to the limited spatial extent the line structured compacted pathway system covered. **Table 19** gives an overview of changes in water balance components due to both compaction scenarios.

As **figure 57** shows in a daily resolution, the increase in surface runoff is mostly effective in higher peaks as response to elevated precipitation inputs. This emphasizes that the informative value of averaged values as basis for evaluation is limited with regard to significant single events. The change signal of surface runoff due to soil compaction along the pathway system accounted 242 % change in peaks compared to uncompacted conditions on 30th of December 2001, with a single event of 28 mm daily precipitation prior to it, 197 % on 9th of March 2006, with 15 mm precipitation, and 133 % on February 2nd 2010 with 13 mm daily precipitation prior to it. The equivalent pattern was also found reflected in the response of streamflow to elevated precipitation in daily resolution.

Table 19:

Impact of soil compaction due to the pathway system (C1) and skid trails and preloaded areas in the course of harvest operations (C2) on water balance parameters in % of uncompacted conditions (C0) on watershed level, based on average annual values within the simulation period 2001 to 2010.

Parameter	**(C1) Pathway system**	**(C2) harvest compaction**
	Change in %	Change in %
Surface runoff	36.2	0.8
Lateral flow	-2	0.4
Water yield	12.3	0.5
Percolation	-2.6	-0.18
Soil evaporation	-0.04	-0.02
Shallow groundwater recharge	-2	-0.1
Deep groundwater recharge	-1.7	-0.2

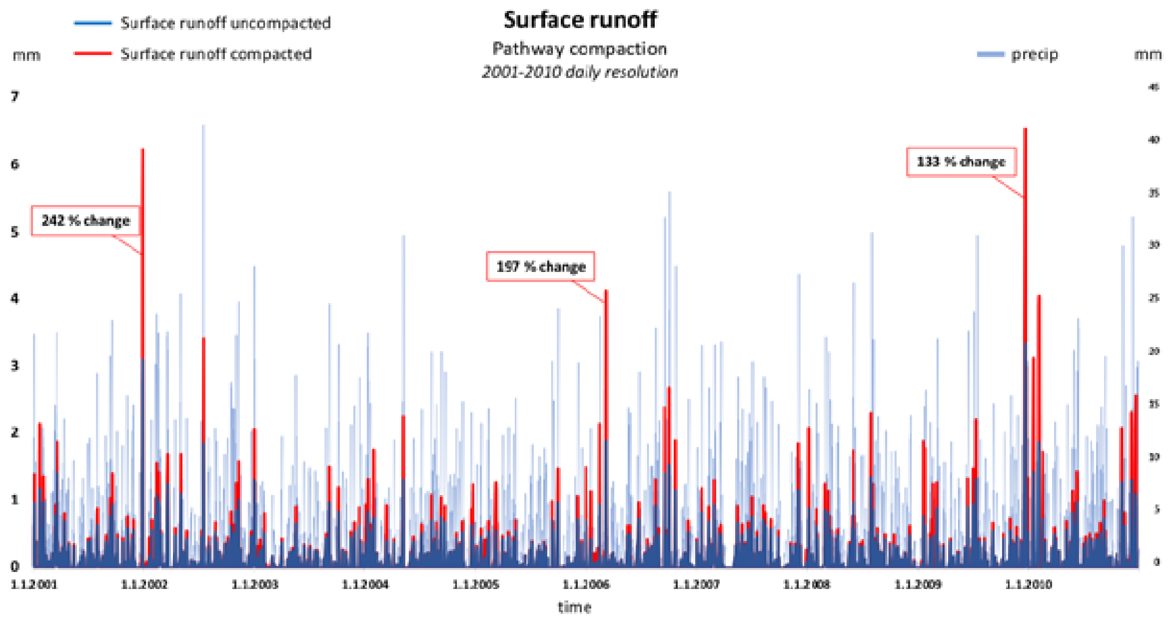

Figure 57: Surface runoff (surq) for uncompacted (uncomp) and compacted (comp) conditions due to the pathway system in daily resolution from 2001 to 2010, combined with precipitation (precip) patterns, highlighting high peaks as response to elevated precipitation inputs.

Figure 58 gives the impression of steep rises in streamflow peaks under the scenario (C1). Analogous to surface runoff, which contributes to streamflow in the already identified short circuit drain reaction, streamflow showed a 110 % higher peak at the end of December 2001 for (C1) compared to (C0), 95 % higher discharge on 9th of March 2006, and 80 % at the beginning of February 2010.

For skid trails and preloaded areas, the overall increase in surface runoff due to compaction was found to be approximately 1 % on watershed level. Within the timeline 1990 to 2000, lateral flow showed a small increase of 0.4 % compared to uncompacted conditions, which consequently increased water yield by 0.5 %. The increase in lateral flow can be explained by the fact that sandy soils, which dominate the area, still allow for infiltration, though to a smaller extent, so that water still enters the soil. There it was found to be inhibited to percolate by -0.2 % in averaged annual values on watershed level. Consequently, groundwater recharge decreased negligibly by -0.2 %.

The situation became more distinct, when evaluating the water balance components for different soil classes on a daily time resolution. The (C2) model setup was evaluated in this regard, based on the area of the soil classes given through the available tracking data on skid trails and preloaded areas on HRU level, to which the results shown in **table 20** need to be put in relation. The soil class U (silt) did not occur in the affected area, because of its small percentage of 0.02 % in total of the watershed. Since the CN values, as well as the gravel construction material, was considered unitary for all soil classes in case of (C1), the evaluation with regard to differences in soil types was not considered conclusive for this scenario.

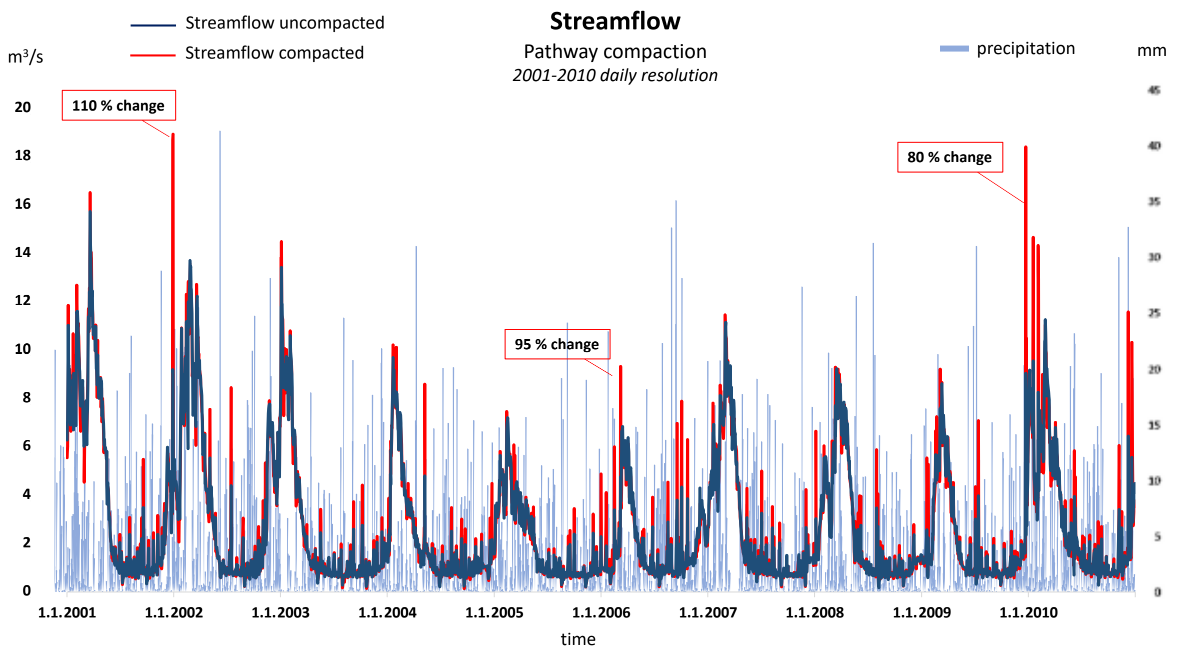

Figure 58: Streamflow for the scenarios (C0) (uncomp) and (C1) (comp) depicting the impact of compaction due to the pathway system on discharge, and the interrelation with precipitation (precip) patterns in daily resolution from 2001 to 2010, highlighting high peaks as response to elevated precipitation inputs.

Table 20:

Impact of soil compaction due to harvest operations (C2), differentiated for soil classes of the SWAT+ setup in change in % of uncompacted conditions (C0) for selected water balance components.

	Change in % for water balance components					Area [km^2]*
Soil class	Surface runoff	Lateral flow	Water yield	Percolation	Soil evaporation	
SS	9.00	0.88	1.40	-0.98	-0.05	4,896.49
LS	11.18	0.37	1.68	-1.00	-0.07	293.49
SU	126.10	-17.74	-9.04	-1.43	2.71	71.39
L	46.03	-2.21	8.86	-5.48	-0.07	68.79

The results shown in **table 20** suggest, that the higher the proportion of larger pore sizes, as for sand dominated soils, the less susceptible to compaction the soil matrix was. This was found reflected in only small changes on water balance components for the soil classes SS (pure sands) and LS (loamy sands): 9 % increase in surface runoff for SS, 11 % for LS respectively, an increase of 0.8 % in lateral flow for pure sands, 0.3 % for loamy sands, 1.4 % gain in water yield for SS, 1.7 % in case of LS, small losses to percolation of -1 % for both, and also for soil evaporation, with -0.05 % for SS, and -0.07 % for LS. With a high proportion of fine and medium sands with coarse pores (Ø > 50 µm) and therefore low clay content, the air and water conductivity of the sandy soil was simulated to be still given, so that the flow of macropores in the sandy soil could be considered maintained. Since the soils in the study area are dominated by sandy substrates (82 % SS, 11 % LS, 2 % SU, 4 % L, and 0.02 % U), the small impact of soil compaction due to harvest operations on watershed level seemed reasonable.

With a higher proportion of loam (L), on the other hand, which is characterized by a high percentage of micro pores, the reduction in percolation was most pronounced (-5.5 %). The lacking seepage water was partitioned into increasing surface runoff (46 % gain), and lateral flow, which decreased only to a small extent of -2 %, so that both together added up in an increase by almost 9 % in water yield contributing to the channels. Also, soil evaporation became limited by approximately -0.1 %, indicating small losses to soil aeration. With a higher proportion of silt (SU), the infiltration decreased most significantly in mean values, so that surface runoff was increased by 126 %, whereas lateral flow, and consequently water yield, decreased by -18 %, and -9 % respectively. Percolation became inhibited by -1.4 %, whereas soil evaporation increased by 2.7 %. This gives incidence that due to the decrease in pore size, secondary water logging became promoted due to losses in hydraulically conductive macro and meso pores, resulting in enhanced evaporation.
In order to evaluate on single HRU, or forest site level, a representative HRU for each soil class was selected, that contained both, skid trails and a preloaded area of sessile oak, to a high percentage of cover. **Figure 59** shows the location of the sub-basins, and HRUs embedded in, overlayed by the harvest compaction layer, and also provides a cutout for a closer impression of the compacted area on HRU level.

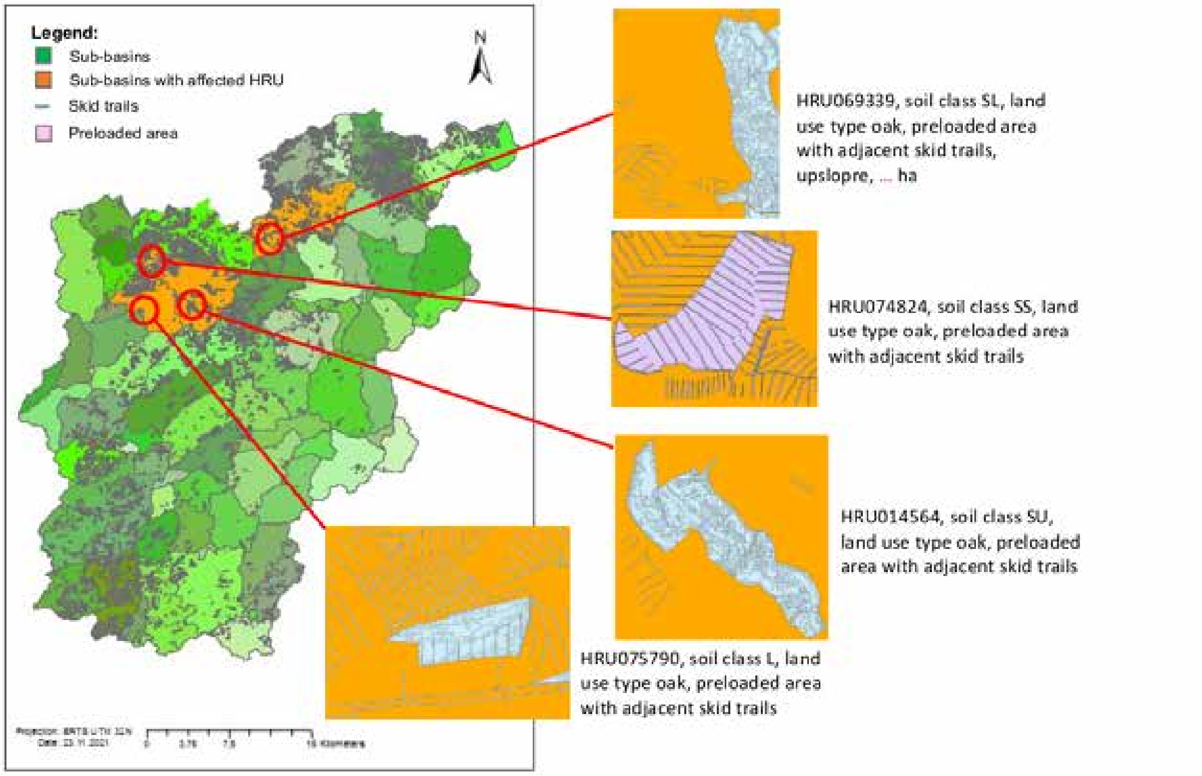

Figure 59: Location of selected sub-basins in the Palatinate Biosphere Reserve watershed, and cutout of highly compaction affected HRU, with high spatial coverage of skid trails and preloaded areas for the soil classes SS, LS, SU, and L.

For the HRU with soil class SS, the following changes in water balance components were simulated based on average annual values: Surface runoff was zero under (C0) and (C2), lateral flow and water yield were increased by 3 %, which appeared conclusive on pure sand soils with infiltration still occurring under compacted conditions. Soil evaporation, considered as indicator for air capacity, was reduced by -0.03 %, soil wetness by -1.3 %, and percolation by -10 %.
The simulated changes on water balance components on the selected HRU for soil class LS indicated small increases in surface runoff under compacted conditions due to a slightly higher percentage of silt and clay components compared to SS, but confirmed less pronounced susceptibility for soil compaction, as percolation, soil wetness, and aeration (soil evaporation) remained unchanged. A negligible rise in water yield by 0.2 % due to higher surface runoff and 0.2 % higher lateral flow in case of (C2) was calculated. **Figure 60** gives the daily resolution of changes in surface runoff between scenario (C0), and (C2) within the given time period, which confirms the small impact of compaction on sand dominated soils.

The resulting increase in water yield on daily basis for (C2) was up to 1.5 % compared to (C0), which is equivalent to 0.04 mm, with 28 mm precipitation on 21st March 2002, which demonstrated again (see **fig. 61**) the very high, and even under compacted conditions still maintained hydrological conductivity of sand dominated soils, absorbing precipitation amounts to a large extent.

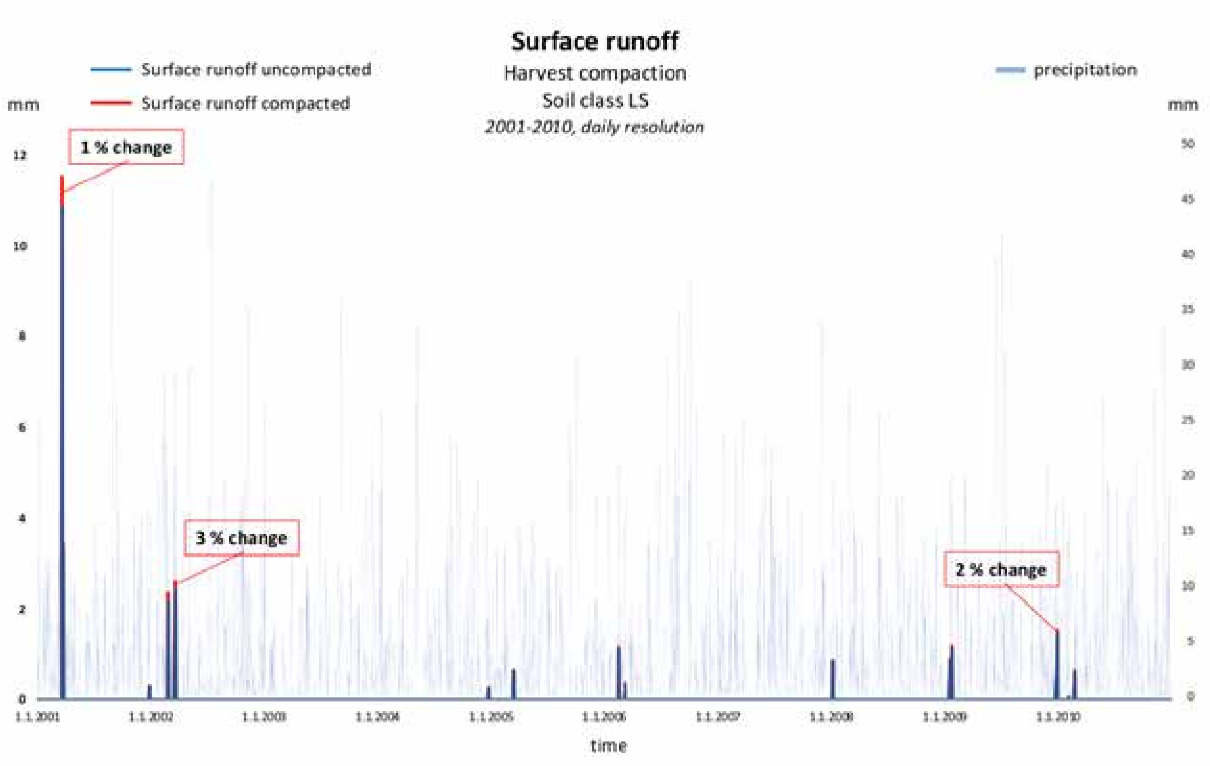

Figure 60: Comparison of uncompacted surface runoff (surq_uncomp), and compacted surface runoff (surq_comp) according to the compaction scenarios (C0 uncompacted) and (C2 harvest compaction) for soil class LS on single HRU level from 2001-2010.

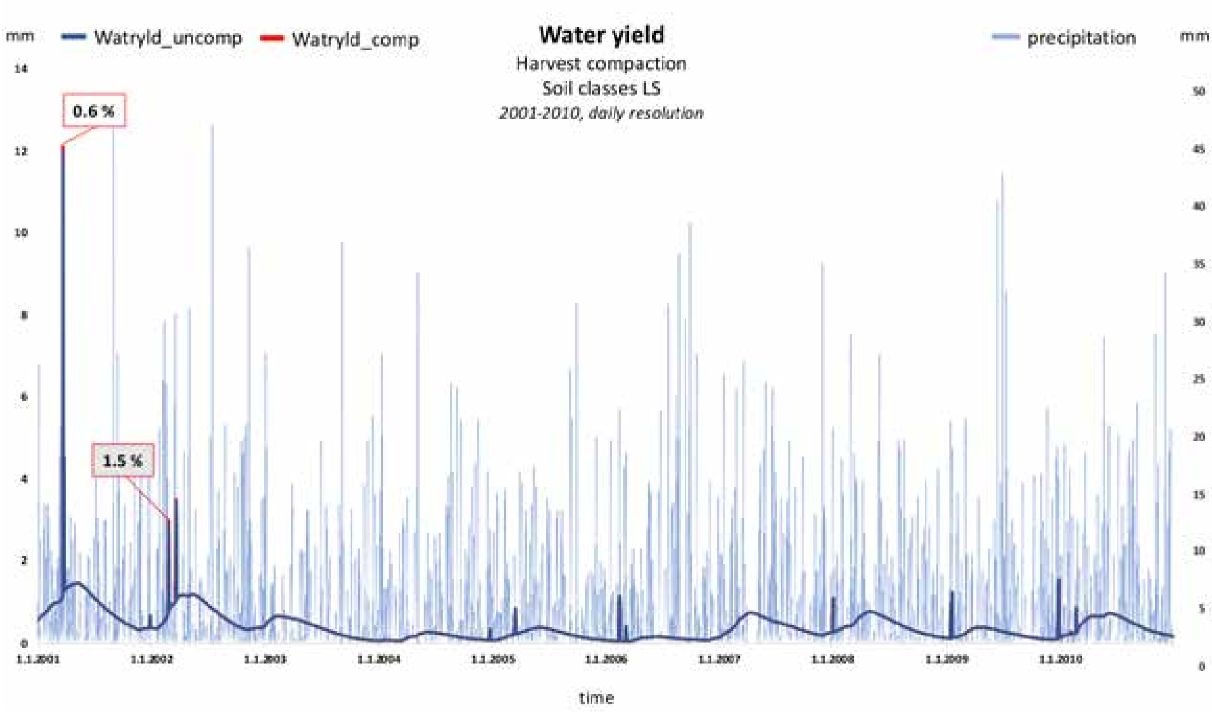

Figure 61: Comparison of uncompacted water yield (Watryld_uncomp), and compacted water yield (Watryld_comp) according to the compaction scenarios (C0 - uncompacted) and (C2 – harvest compaction) for soil classes LS on single HRU level in daily resolution from 2001-2010.

Soil class SU resulted in an increase from 1.3 mm/aa under undisturbed conditions to 27 mm/aa under (C2) on the selected HRU (2618 %), which contributed to a rise in water yield by 116 %, whereas lateral flow, soil wetness, soil evaporation, and percolation decreased by -6 %, -5.4 %, -0.06 %, and -36 % respectively. **Figure 62** gives the daily resolution of surface runoff on this HRU in the given time period for the scenarios (C0) and (C2). This specific HRU showed very small surface runoff volumes under undisturbed soil conditions with an initial CN value of 66, but increased significantly under compacted conditions, with CN 83. Consequently, elevated precipitation amounts that induced no surface runoff under (C0), as on 16th of July 2002 with 45 mm precipitation inputs, lead to overland flow generation of 8.4 mm in that case. As result, also for water yield significantly higher peaks were simulated to contribute to channels from the specific HRU: In the given example, water yield rose from 0.3 mm to 8.7 mm, as can be inferred from **figure 63**.

Soil class L was simulated on HRU level with an increase of 32 mm/aa from 5.7 mm/aa for (C0) to 32.6 mm/aa under compacted conditions, an equivalent increase in water yield of 40 mm/aa, with at the same time reduced lateral flow (-11 %), percolation (-15 %), soil wetness (-1.7 %), and soil evaporation (-0.03 %). **Figure 64** shows the surface runoff for both scenarios in the given time period based on daily values. This specific HRU already showed a higher surface runoff volume under uncompacted conditions than the HRU examined for the other soil classes. This is plausible considering the lower hydraulic conductivity and thus limited infiltration capacity of

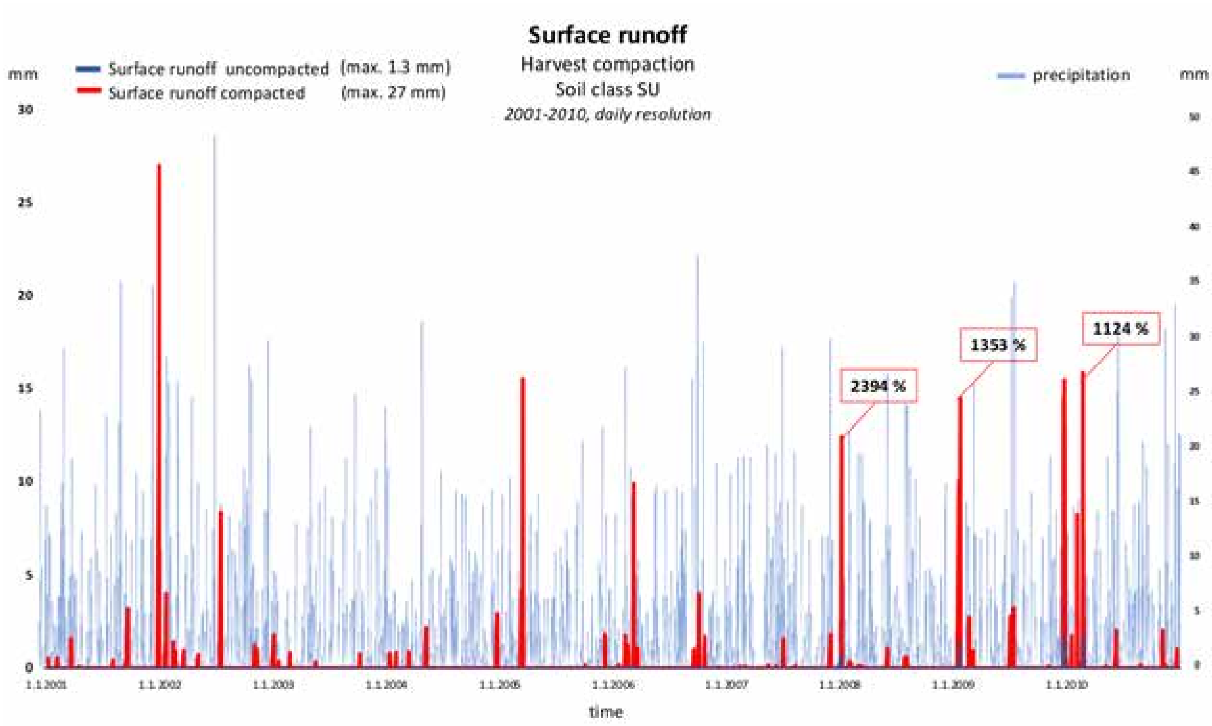

Figure 62: Comparison of uncompacted surface runoff (surq_uncomp), and compacted surface runoff (surq_comp) according to the compaction scenarios (C0 - uncompacted) and (C2 – harvest compaction) for soil class SU on single HRU level from 2001-2010.

more clayey soils, also reflected in default and adapted CN values: Under default, uncompacted conditions, soil class L was classified to have a CN value of 77 for the selected HRU. The applied CN value after compaction was 95. The high initial CN of 77 explained the already higher amounts of simulated overland flow even under undisturbed conditions. The altered flow dynamics resulted in equivalent peaks in water yield (**fig. 65**) contributing to streamflow from this HRU, as found on 29th of December 2001, when 28 mm precipitation inputs evoked a rise in water yield from 2.9 mm to 19.3 mm, with an equivalent rise in surface runoff prior to it. Soil class L showed the smallest share of lateral flow on water yield (64 % of water yield under uncompacted conditions, compared to 96 % in case of SU, 97 % in case of LS, and 100 % in case of SS), and thus a more pronounced share of surface runoff than the other soil classes. With the most pronounced surface runoff even under scenario (C0), also the water yield contributions to the channel for soil class L were already fed by inflows kinematic in character to a larger degree than for the other soil classes.

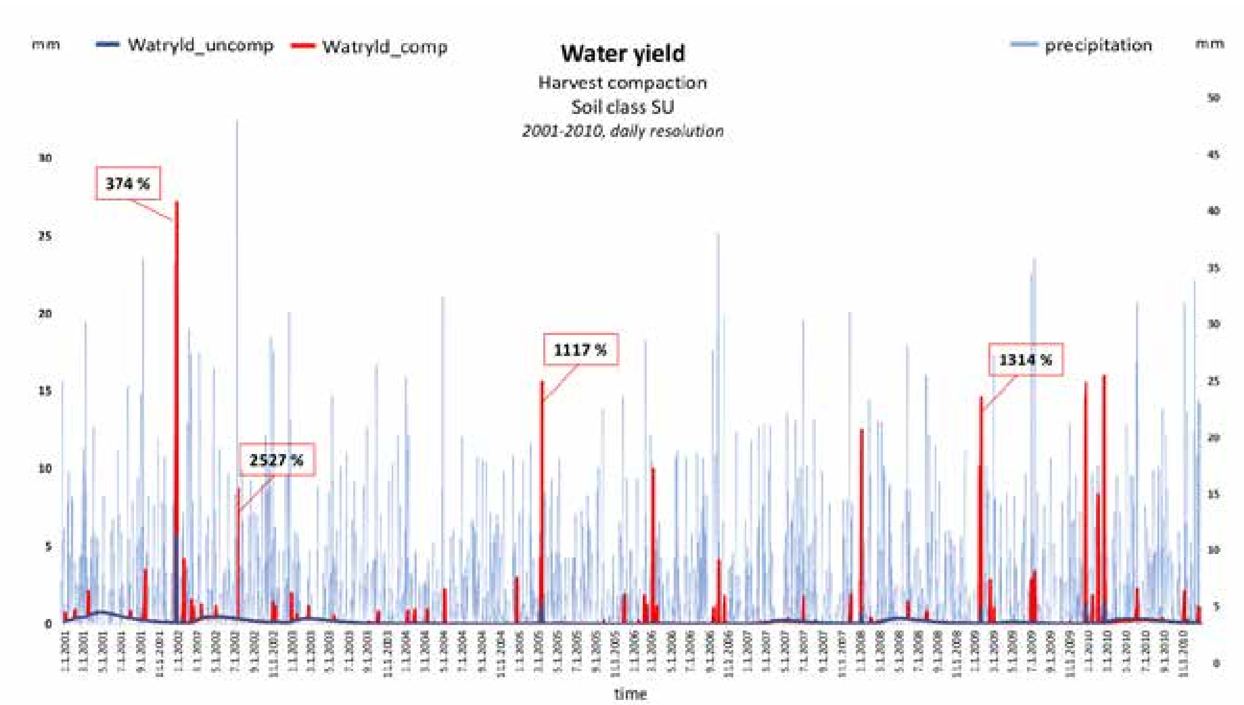

Figure 63: Comparison of uncompacted water yield (Watryld_uncomp), and compacted water yield (Watryld_comp) according to the compaction scenarios (C0 - uncompacted) and (C2 – harvest compaction) for soil classes SU on single HRU level in daily resolution from 2001-2010.

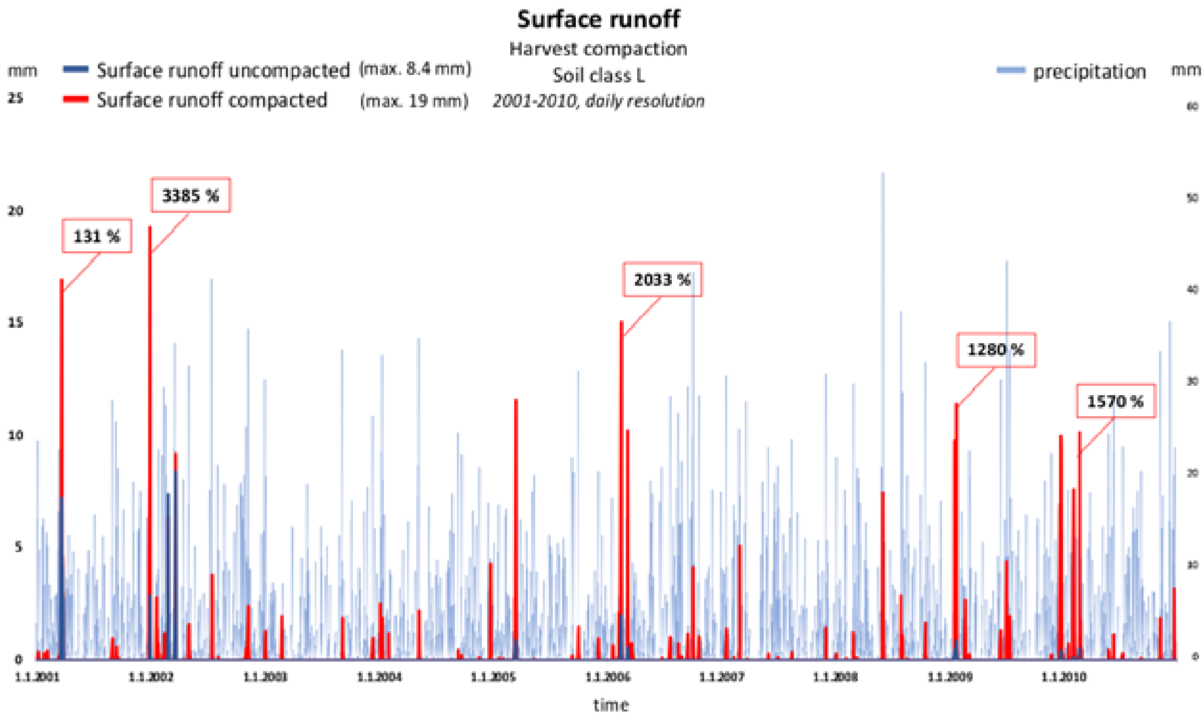

Figure 64: Comparison of uncompacted surface runoff (surq_uncomp), and compacted surface runoff (surq_comp) according to the compaction scenarios (C0 - uncompacted) and (C2 – harvest compaction) for soil class L on single HRU level in daily resolution from 2001-2010.

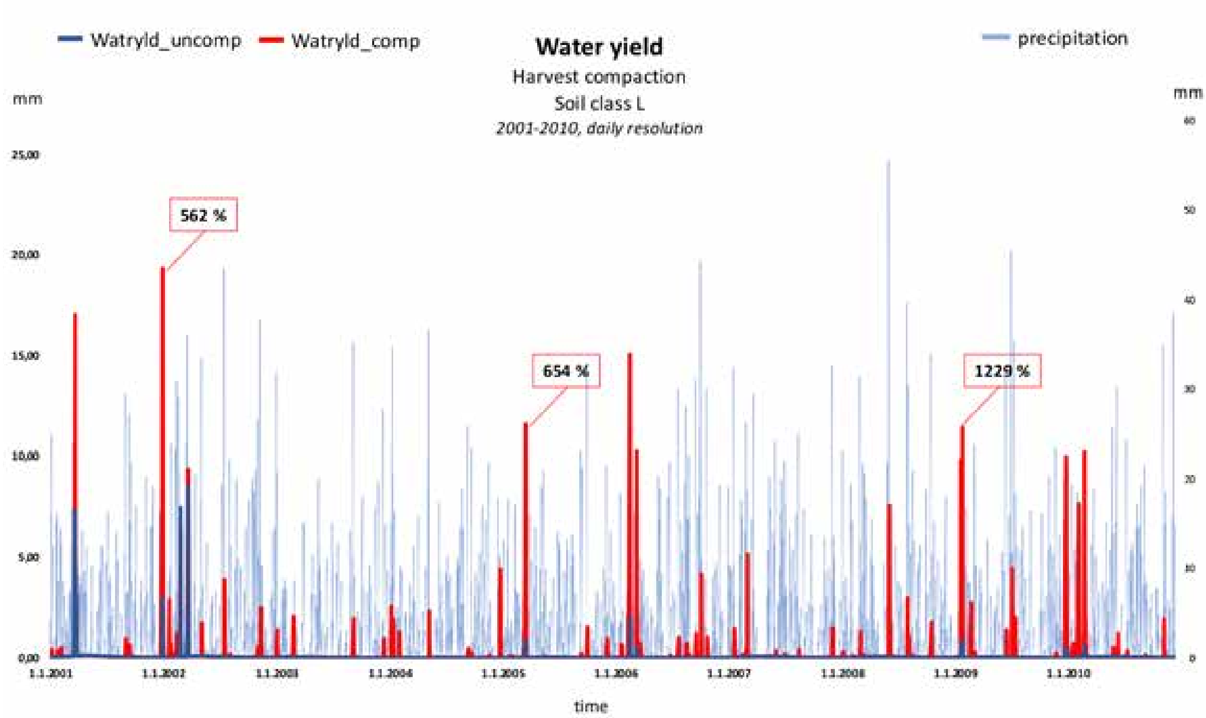

Figure 65: Comparison of uncompacted water yield (Watryld_uncomp), and compacted water yield (Watryld_comp) according to the compaction scenarios (C0 - uncompacted) and (C2 – harvest compaction) for soil classes L on single HRU level in daily resolution from 2001-2010.

5.6 Disrupted areas with rejuvenation

The tested performances for juvenile tree species on HRU level resulted in simulated lower overall *ET* performance on watershed level compared to the mature scenario (**fig. 66**). The annual mean *aET* for the time period 2010 to 2020 showed 474 mm/aa for scenario JUV, compared to 548 mm/a for scenario MAT, which is equivalent to 13.4 % deviation in average between the age-scenarios. The overall decreasing trend in actual *ET* for both scenarios can be explained with rising temperatures, and thus rising values for potential *ET*, promoting exhausted soil water contents due to increased water consumption in the course of climate change, and thus inducing a decline in transpiration throughout the vegetation period. With 42 % higher soil evaporation on juvenile stocks compared to mature, soil evaporation was simulated to be the dominant factor in *ET* differences between the scenarios, primarily concentrated on the vegetation period, with atmospheric evaporative demand given. As evaporation from the soil is calculated in SWAT+ as a function of soil cover (see Neitsch et al. 2011, p.135), the lower above ground biomass and canopy storage promote elevated evaporation from the soil is case of juvenile stocks.

Figure 67 shows the dynamics in soil evaporation for both age scenarios based on monthly values, depicting higher soil evaporation at younger age stages with less canopy cover, as well as a progressing decline in soil evaporation on juvenile stocks, as the saplings grew up, converging with mature conditions at the end of the simulation period, when canopy closure is approximated. Furthermore, **figure 68** shows the dependency of soil evaporation patterns on precipitation, when sufficient soil water availability with at the same time high atmospheric evaporative demand throughout the growing season enhance soil

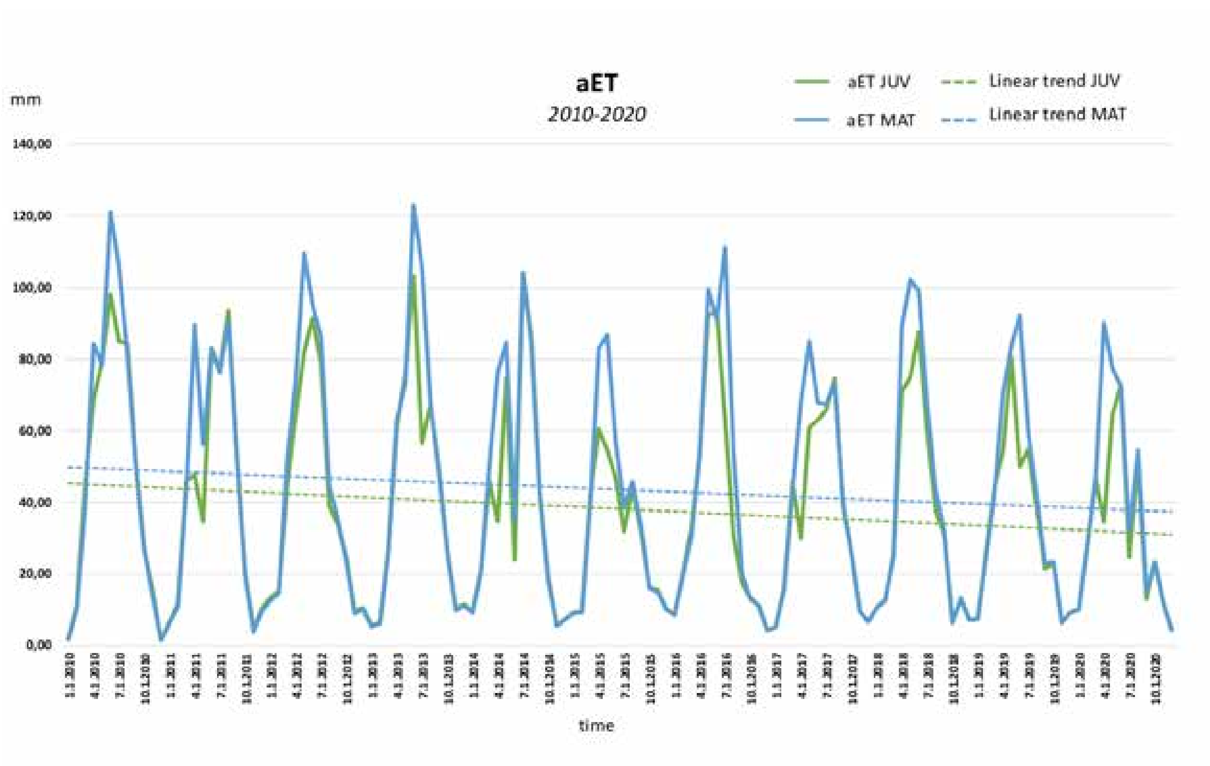

Figure 66: Actual ET performance on watershed level after age-related plant modification for scenario MAT (mature) and JUV (juvenile) for the baseline period from 2010 to 2020 based on monthly values.

evaporation on juvenile stocks, whereas mature stocks exhibit more balanced conditions due to the closed crown cover. With low evaporative impetus in winter months, the deviation between JUV and MAT leveled out.

The lower water consumption on juvenile stocks compared to mature ones lead to changes in water dynamics on watershed level such as a mean of 27.5 % higher percolation in case of scenario JUV, which is equivalent to 62 mm/aa (287 mm/aa compared to 225 mm/aa in case of scenario MAT). In combination with precipitation inputs based on monthly values, **figure 69** reveals that although mean values suggested a significant difference, the deviation between the scenarios predominantly appeared only in peaks, being mostly concentrated on winter months, except for the case of higher water inputs throughout the vegetation period, as in 2014.

Also, 32.7 % increase in average soil wetness was shown for juvenile stocks (140 mm/aa for scenario JUV, compared to 105 mm/aa for scenario MAT, see **fig. 70**). There was a very constant trend of significantly higher soil water content in case of JUV throughout the vegetation period, whereas the situation leveled out in the winter months as the soil water content replenished.

The overall decreasing trend in soil wetness due to rising evaporative demand caused by higher air temperatures was also reflected here, being more pronounced in case of mature stocks due to higher water consumption into deeper soil layers. In the upper soil layer (up to 300 mm depth) on the other hand, juvenile stocks showed a small decrease by -1.2 % compared to mature within the first 5 years, which leveled off as the trees grew up by the end of the simulation.

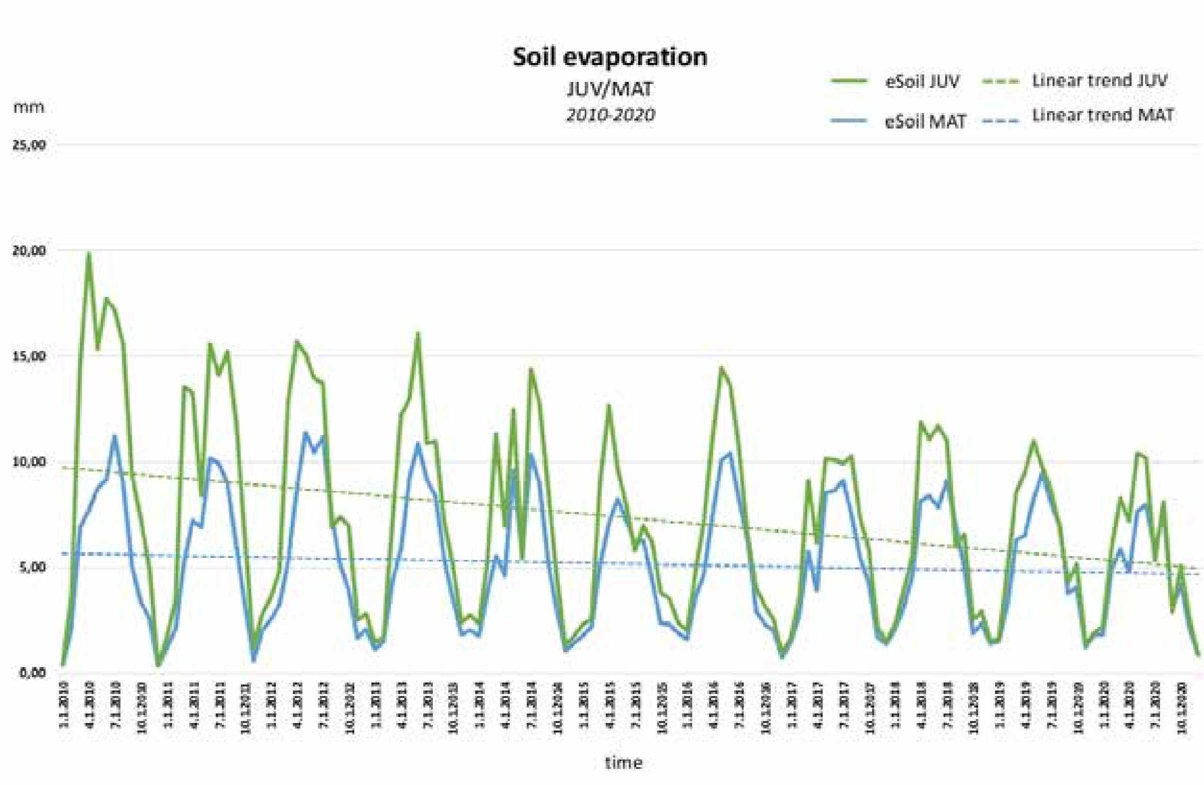

Figure 67: Soil evaporation (eSoil) performance of juvenile (JUV) and mature (MAT) stocks within the simulation period 2010-2020 based on monthly values, with linear trends indicating a progressive decline in soil evaporation for JUV due to the gradual transition to canopy closure as trees grow up.

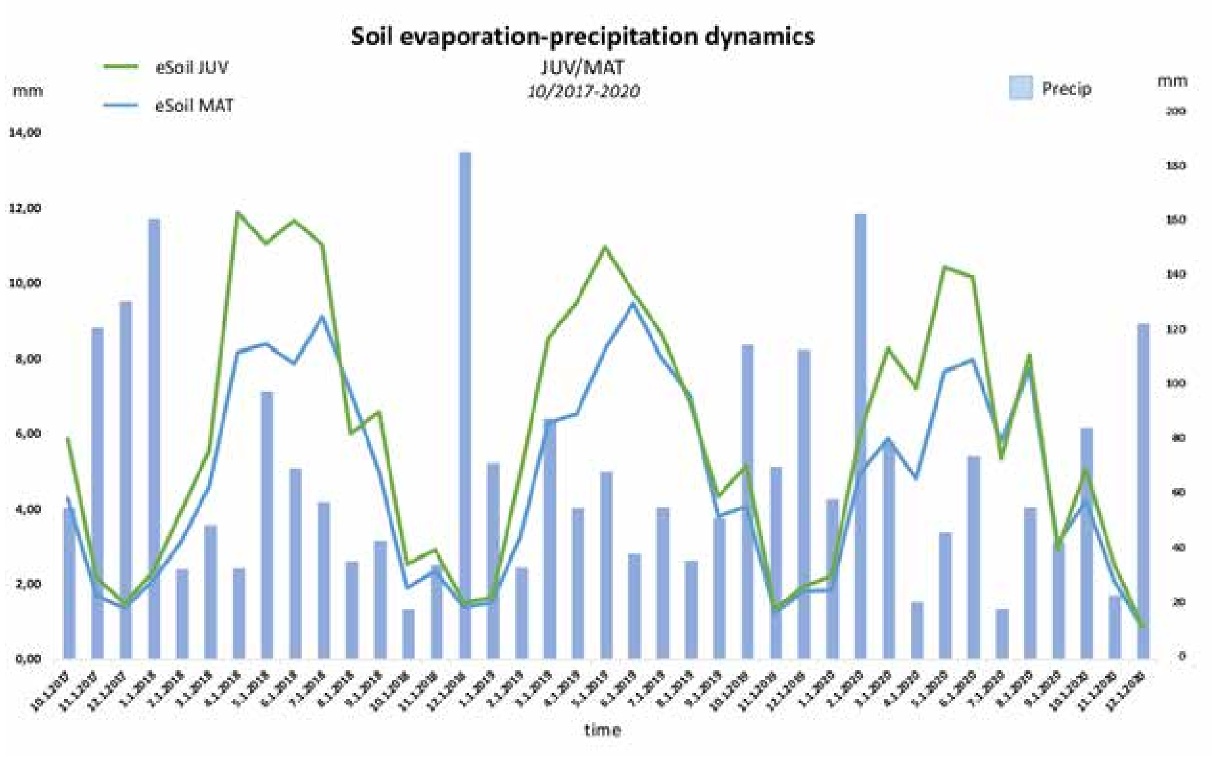

Figure 68: Soil evaporation (eSoil) dynamics on juvenile (JUV) and mature (MAT) stocks and their interrelation with precipitation, depicting seasonal soil water variability, for the timeline 10/2017 to 2020, based on monthly values.

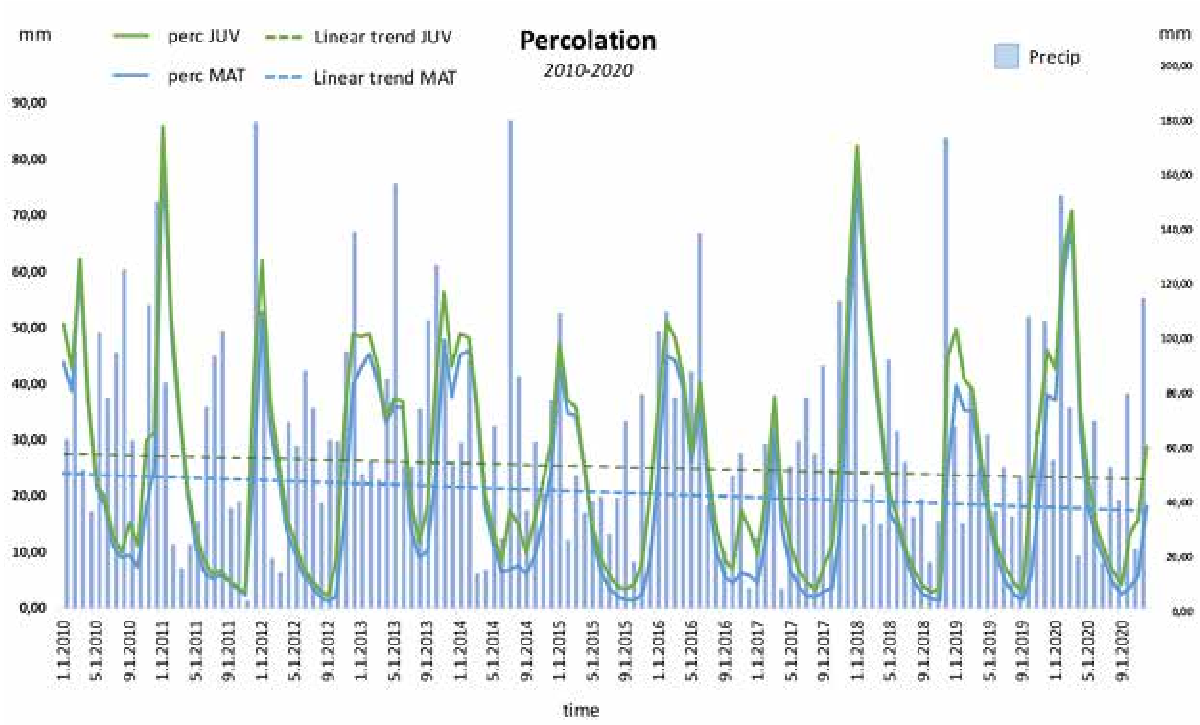

Figure 69: Percolation (perc) performance on watershed level after age-related plant modification for scenario JUV (juvenile) and MAT (mature), combined with precipitation (precip) for the period 2010 to 2020 based on monthly values.

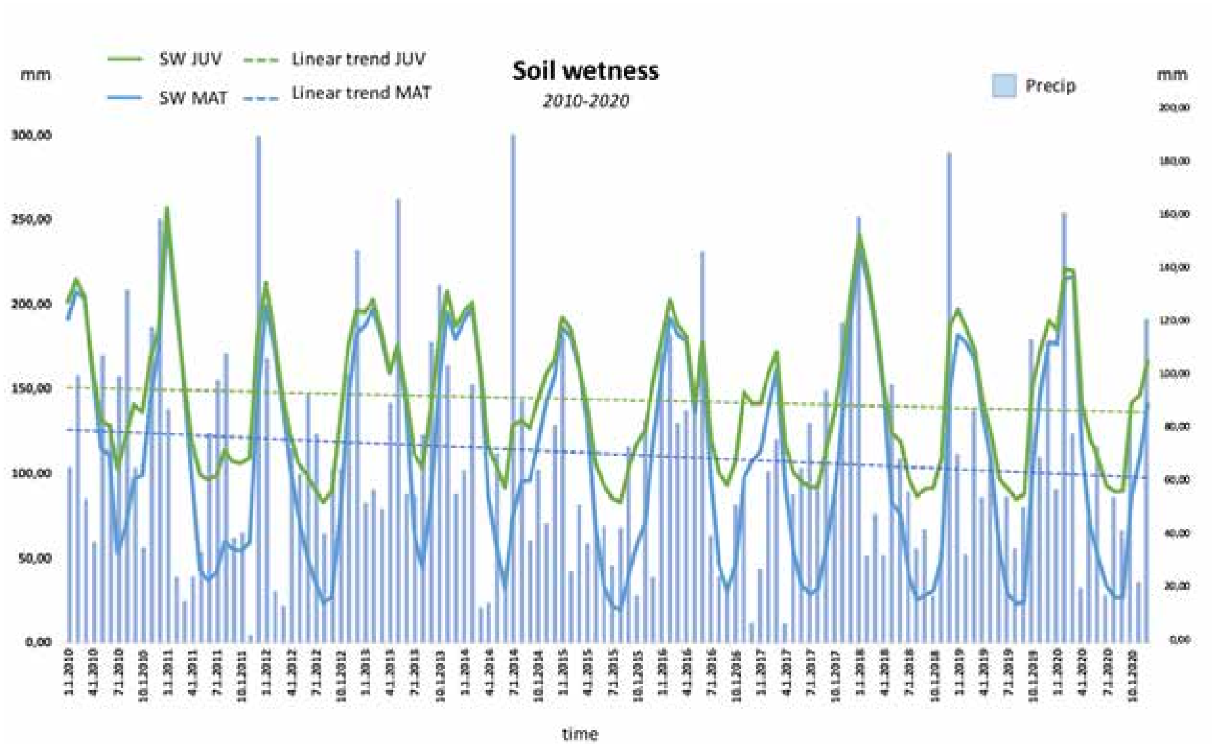

Figure 70: Average soil wetness (SW) performance on watershed level after age-related plant modification for scenario MAT (mature) and JUV (juvenile), compared with precipitation (precip) for the period 2010 to 2020, based on monthly values.

Regarding the effects on water-related ES with respect to runoff generation and quantitative groundwater formation, both water balance components increased only slightly under scenario JUV (**fig. 71** and **72**). The average annual deep groundwater formation for scenario MAT for the period 2010 to 2020 was 194 mm, whereas under scenario JUV, it was 217 mm, which is a marginal increase of 12 % under juvenile growing conditions. The shallow aquifer accounted for 444 mm/a in case of MAT, and 528 mm/a in case of JUV. The trendlines for the time period suggested, that groundwater depletion in the course of climate change can be expected to aggravate slightly more pronounced in case of the shallow aquifer on mature stocks due to higher extractions for plant water consumption.

Nevertheless, both scenarios showed a decline in shallow groundwater recharge throughout the time period. A rather slight decrease, and a less pronounced difference between the age-scenarios, was shown for the deep aquifer. But still a more pronounced dynamic reaction to precipitation inputs can be determined for the JUV scenario in both aquifers. This can be explained by the lacking balancing and flow retarding function of the crown cover.

The mean annual surface runoff increased slightly under scenario JUV from 8 mm (MAT) to 8.3 mm (3.2 % increase in case of JUV). In this case, the temporal distribution in the event of storms needs to be accounted for. As can be inferred from **fig. 73**, scenario JUV contributed to a rise in distinct runoff peaks with higher amounts of precipitation: In the dormant period 2017/2018 relative high precipitation values (118 to 157 mm) were detected three months in a row, which lead to more pronounced runoff peaks, and an increase in streamflow by up to 167 % (December 2017) for JUV compared to MAT due to the short circuit drain reaction to increased amounts and duration of input water.

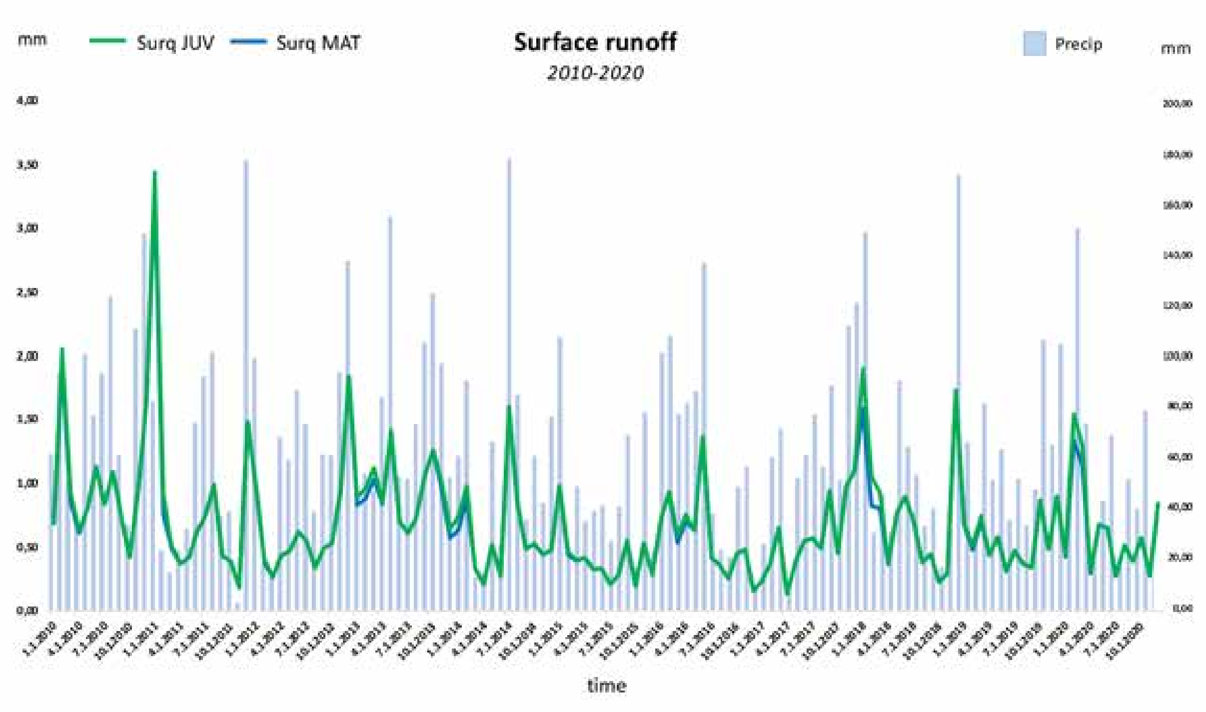

Figure 71: Surface runoff (Surq) performance on watershed level for age-scenario MAT (mature) and JUV (juvenile), compared with precipitation (Precip) for the period 2010 to 2020, based on monthly values.

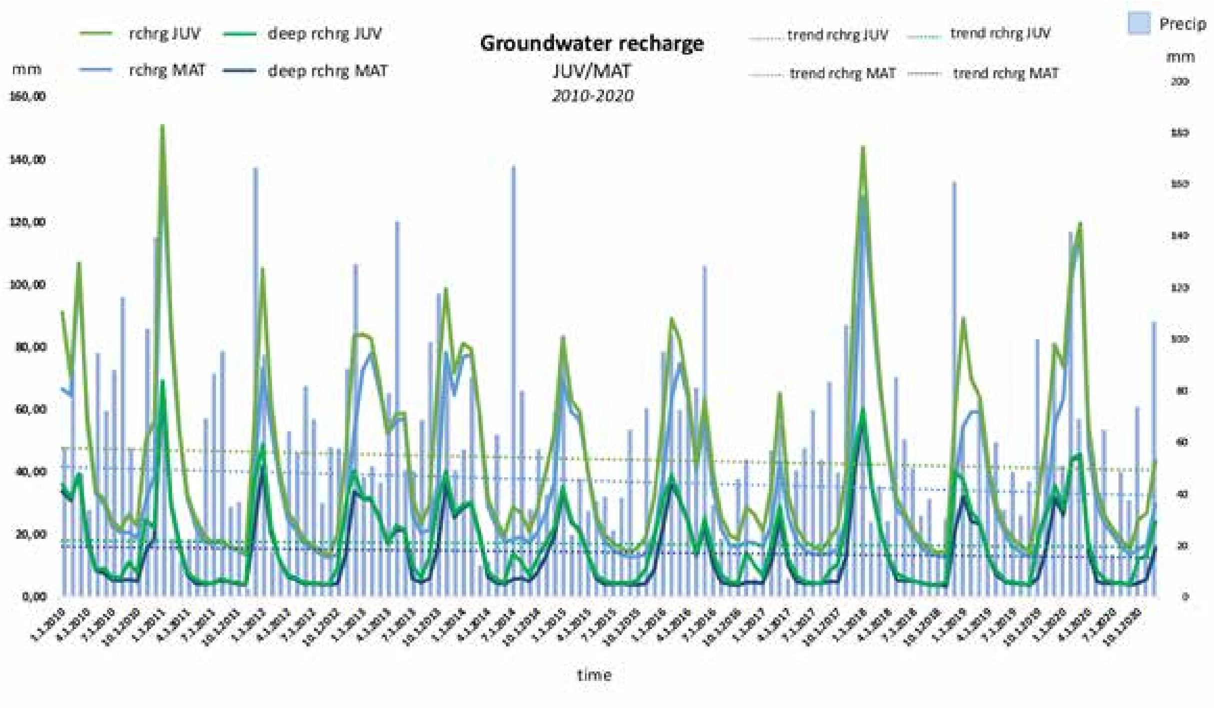

Figure 72: Groundwater recharge for shallow aquifer (rchrg), and deeper aquifer (deep rchrg) on watershed level after age-related plant modification for scenario MAT (mature) and JUV (juvenile) for the baseline period from 2010 to 2020, based on monthly values.

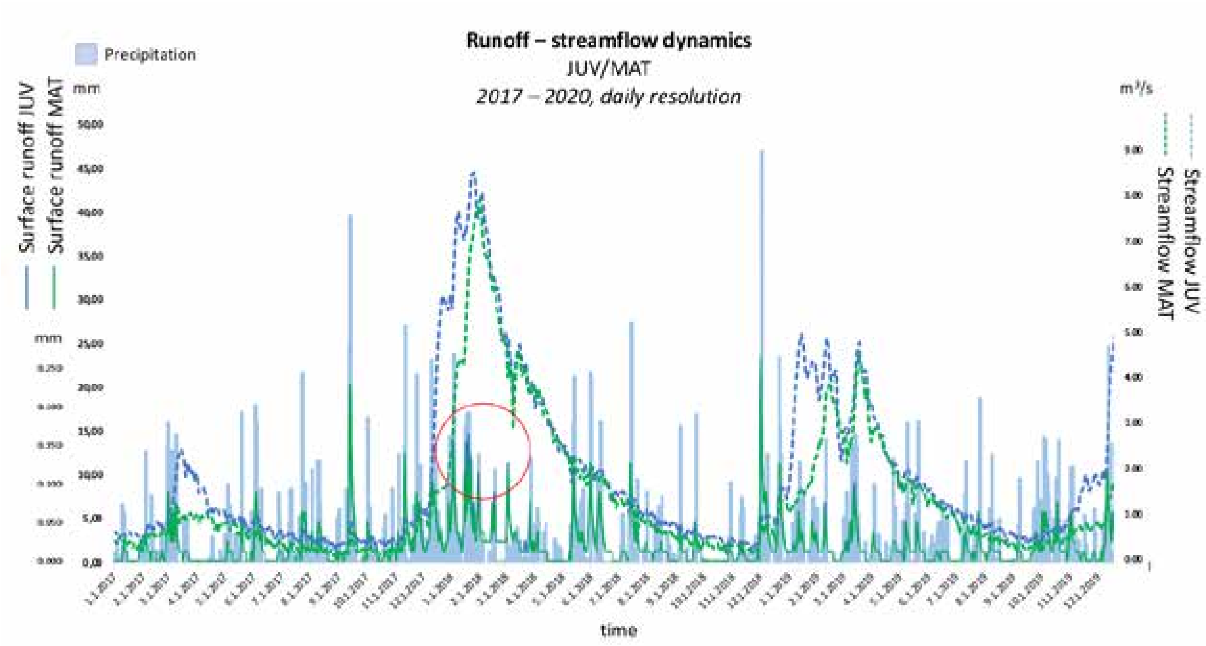

Figure 73: Interplay of surface runoff (surq) [mm], streamflow (stream) [m³/s], and precipitation (precip) [mm] on watershed level after age-related plant adaption for scenario MAT (mature) and JUV (juvenile) for the period 2017 to 2020, based on daily values.

In case of scenario MAT, the average annual lateral flow was 167 mm, whereas for JUV it was 209 mm (25 % increase in case of JUV). Both, surface runoff and lateral flow, contributed to a rise in water yield of averaged annual 24 % in the case of scenario JUV (217 mm/aa) compared to MAT (175 mm/aa). The resulting increase in streamflow in case of scenario JUV of averaged 27 % can be considered effective for flood generation as a potential cumulative factor in single peaks, when considering the temporal patterns of precipitation and the short circuit drain reaction. Nevertheless, in the evaluation of these results, it must be considered that the scenario setup is artificial. Under real conditions, only a small spatial extent of areas with juvenile stocking level exists, so that their contribution to rising water yield, as well as to rising groundwater recharge, must be presumed very small.

In order to assess possible causal relations in the differences between JUV and MAT with regard to water balance components, the period from 2010 to 2020, which was characterized by relatively low precipitation inputs (816 mm/aa) with at the same time rising atmospheric evaporative demand (825 mm/aa), was compared to a period with relatively high precipitation inputs, and lower evaporation impetus. These conditions were found in 1961 to 1971, with 1195 mm/aa precipitation, and 774 mm/aa pET. **Figure 74** shows selected water balance components for that period. Regarding the differences in water balance components, the period from 1961 to 1971 showed the following: 14 % higher soil water content in average annual values for scenario JUV compared to MAT (32 % from 2010 to 2020), approximately 6.2 % rise in surface runoff (3.2 % from 2010 to 2020), 14 % higher recharge for both, the shallow and deep aquifer (compared to 23 % for the shallow, and 12 % higher recharge for the deep aquifer for JUV from 2010 to 2020), and 15 % increase in lateral flow (25 % in 2010 to 2020). The flow dynamics lead to 14 % increase in streamflow for JUV compared to MAT (27 % from 2010 to 2020). For soil evaporation, juvenile stocks showed 8 % higher values than mature (42 % in 2010 to 2020). For actual *ET* the average annual within the period 1961 to 1971 on juvenile stocks was -10.9 % lower than in mature (-13.4 % from 2010 to 2020).

With higher precipitation inputs to the system but at the same time lower evaporative demand, as given in 1961 to 1971, the differences between JUV and MAT tended to level off, which can be explained by a lower interception storage with rising precipitation intensity, as well as with a lower saturation capacity of the air, as the relative humidity rises (Baumgartner & Liebscher 1990; Rakei et al. 1992). Hence, more input water is provided to the system to meet the water consumption in both cases. Lower inputs of precipitation water on the other hand lead to relatively higher infiltration with poor canopy cover given. Surface runoff on the other hand showed an incline in the deviation between the scenarios with higher precipitation amounts. When the average annual value was 14 mm/aa in case of MAT in 1961 to 1971 (15 % for JUV), it was only 8 % in 2010 to 2020 (8.3 % for JUV). A higher deviation between the age-scenarios (6.5 %) was thus found with higher amounts of precipitation as in the farer past (3 %), since the softening of the crown cover is less effective in case of more intense rainfall.

Equivalent to the increase in plant demand from rising potential *ET*, being most effective regarding soil evaporation with poor canopy cover, the deviation between MAT and JUV was higher in 2010 to 2020, with 42 %, compared to only 8 % in 1961 to 1971. But due to the decrease in total water input, the absolute values declined from 100 mm/aa for MAT in 1961 to 1971 (108 mm/aa for JUV) to 62 mm/aa in 2010 to 2020 (88 mm/aa for JUV). As **table 21** shows, when comparing the timelines, the relative decline on juvenile stocks was smaller compared to

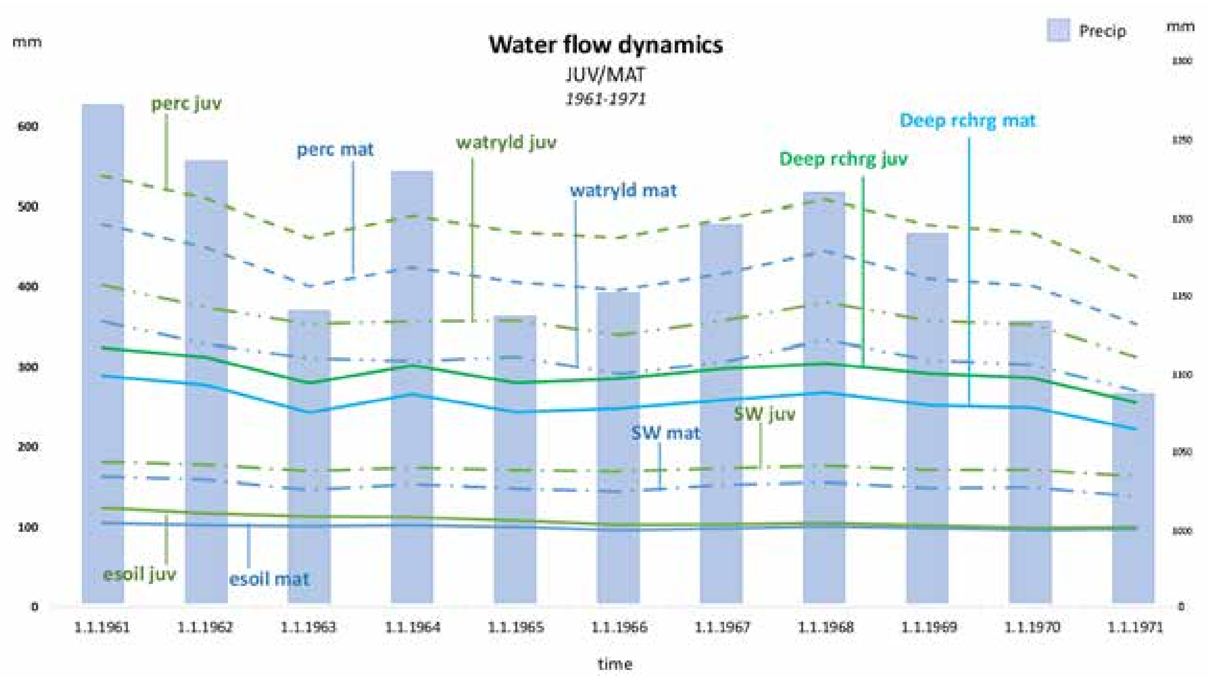

Figure 74: Water balance components of the Bobenthal2 catchment within the period 1961 to 1971, based on average annual values. precip = precipitation, watryld = water yield, SW = soil wetness, perc = percolation, Deep rchrg = deep groundwater formation, esoil = soil evaporation, mat = MAT scenario (mature), juv = JUV scenario (juvenile), based on average annual values.

mature, due to an elevated overall impetus for soil evaporation with close to open field conditions given. Also, with scarcer soil water availability, relatively more soil water is consumed by plant demand, leaving less water for evaporation from the soil, the more pronounced, the higher the consumption, as on mature stocks. This explains the deviation between JUV and MAT to rise with depleted soil water storage, whereas with sufficient water availability given to meet evaporative and plant demand, the conditions on both stocking types converged more closely, and the differences leveled out to some extent.
Accordingly, the higher water inputs due to increased precipitation and less evaporative demand also promoted an increase in soil wetness, and thus decreased the deviation between JUV and MAT in 1961 to 1971 (14 % difference between the scenarios) compared to 2010 to 2020 (32 % difference) based on absolute mean values.

Regarding groundwater recharge, there was an overall pronounced decrease in 2010 to 2020 compared to the farer past. When the mean annual value of shallow aquifer recharge was 691 mm/aa in 1961 to 1971 in case of MAT (788 mm/aa for JUV), it declined to 444 mm/aa in 2010 to 2020 (528 mm/aa for JUV). Regarding deep groundwater formation, the farer past showed 256 mm/a for MAT, and 292 mm/a for JUV. Regarding the change in % of JUV compared to MAT, the deviation between the scenarios was found slightly bigger with more scarce inputs to the system with respect to shallow aquifer recharge. This was also reflected in a higher difference between the timelines in case of scenario MAT with -35 % decline in 2010 to 2020 compared to 1961 to 1971, when JUV showed 33 %. Regarding deep groundwater formation, the deviation between the scenarios decreased from 14 % in 1961 to 1971 to 12 % in 2010-2020.

Table 21:

Change signal in % of differences between JUV and MAT for the periods 1961 - 1971 and 2010 - 2020, as well as the difference in change signal between the two contrasting periods.

	Change % JUV of MAT		**Change % 2010-2020 of 1961-1971**		
Period	*1961-1971*	*2010-2020*	*Scenario*	*JUV*	*MAT*
Actual *ET*	-11	-13		-21	-23
Soil *ET*	8	42		-18	-38
Soil wetness	14	32		-18	-30
Shallow GW recharge	14	18		-33	-35
Deep GW recharge	14	12		-25	-24
Percolation	15	27		-40	-45
Surface runoff	6.5	3		-45	-43
Lateral flow	15	25		-39	-43
Water yield	15	24		-39	-43
Streamflow	14	27		-40	-46

A possible explanation could be that the difference in baseflow between JUV and MAT was higher (24 % higher baseflow in case of JUV) in 2010-2020 than in 1961-1971 (14 % higher baseflow for JUV compared to MAT), as shown in **figure 75**. As consequence of the higher baseflow dynamics under juvenile stocks in the period with scarcer precipitation inputs, more losses to deep recharge occurred, which softened the deviation of JUV and MAT deep groundwater formation in that period compared to the farer past.

Equivalent to the groundwater situation, percolation was 45 % higher in 1961 to 1971 compared to 2010 to 2020 for MAT, (40 % in case of JUV), with a smoothed deviation between the age-scenarios of only 15 % compared to 27 % from 2010 to 2020. This indicated, that with less water inputs, the characteristics of stand precipitation versus close to open field conditions slightly promoted deep leeching in case of JUV.

For streamflow, as for lateral flow and water yield, the differences between JUV and MAT also seemed to level off as precipitation rose. All three parameters showed a deviation of 15 % between JUV and MAT for the period 1961 to 1971, whereas 27 % difference was simulated for streamflow (25 % for lateral flow) in 2010 to 2020. Water yield showed a deviation of 24 % between the scenarios, considering the relatively smaller amounts of surface runoff in 2010 to 2020. A relatively higher infiltration with poorer precipitation on juvenile stocks presumably caused juvenile stocks to be more effective in leachate, and thus to generate relatively higher amounts of yields in lateral flow and base flow, contributing to a rise in streamflow. Whereas with high precipitation amounts, stand precipitation and open field precipitation leveled out.

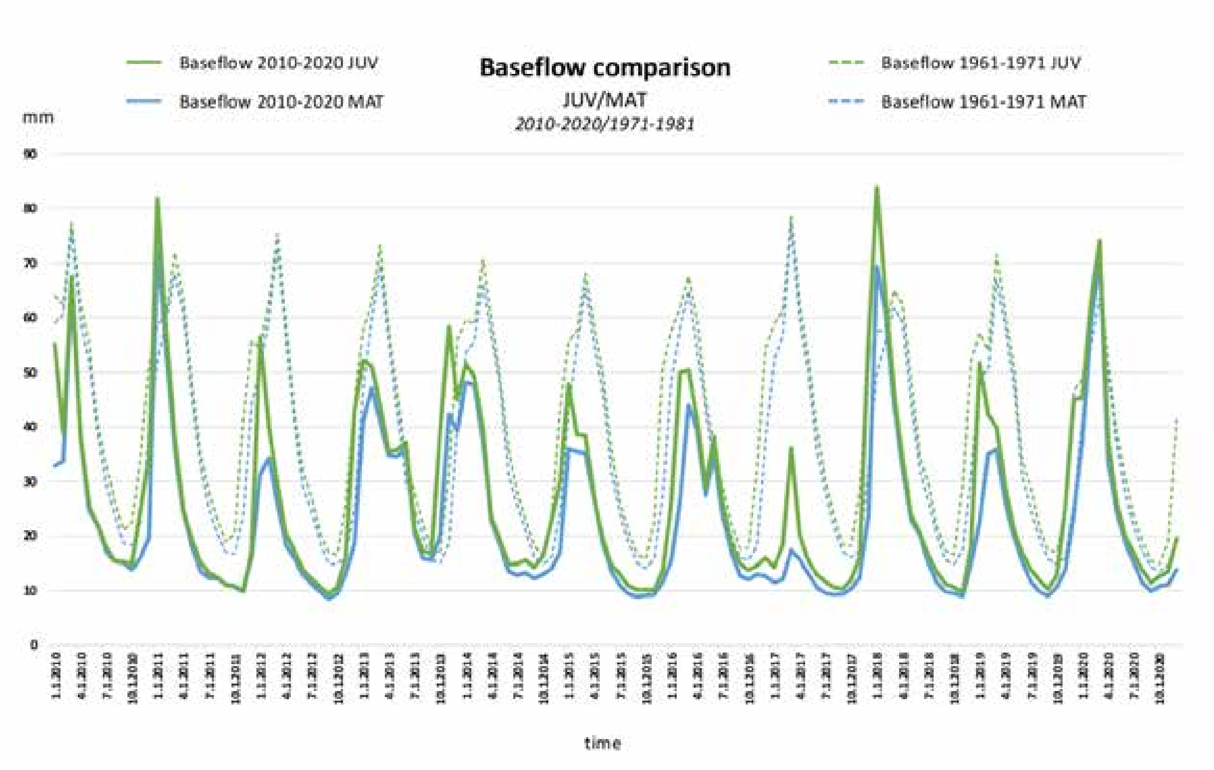

Figure 75: Baseflow dynamics for JUV and MAT scenario for the timelines 2010 to 2020 and 1961 to 1971, depicting a higher dynamic reaction in case of juvenile stocks in 2010 to 2020.

6 DISCUSSION

6.1 Plant parameter modification

In this model setup, the plant parameters were modified in order to approximate the model simulation to the field conditions of protected, permanent forests in the Palatinate Biosphere Reserve. The attempt pursued here was to meet the plant parameters as close to measured, and literature-based field data, analyze the model simulation with regard to plant growth and evapotranspiration performance, and detect possible improvements compared to the default model settings. Although the results showed only small enhancements for both quantities, SWAT+ was proven to be sensitive to the plant-water-cycle-interactions in the forest, with respect to LAI development and response to water stress at soil water contents with critical AWC. In the simulation of forest communities, whose phenological properties are tightly bound to the water cycle, the approximation to an adequate depiction of those interactions is of importance for the further use of SWAT+ in the forest.

6.1.1 SWAT+ ET estimates in forested areas

The default plant setup was found to show an overestimation of ET performance compared to literature values (Peck & Meier 1996), which is also suggested by Yang & Zhang (2016) in forested watersheds. Nevertheless, it must be noticed, that the literature values are based on the Penman-Monteith method. Neither are they suitable for a direct comparison, as they do not reflect hard data estimations in the specific area, nor did the model calibration aim for the target ET performance. In the context of the evaluation of plant parameter modification effects, they must be considered as a rough orientation towards improvement. Furthermore, it must be emphasized that when using a model run optimized for Penman-Monteith the overestimation was reduced significantly, and the values rather approximated stated values (modified oak resulted in 564 mm/aa, beech resulted in 552 mm/aa). But as the flow duration and statistical indices deteriorated, using the Hargreaves method was clearly recommended with regard to the objective targets (see **tab. 25**, **fig. 86**, *app*.). Consequently, three parameters identified to be sensitive with respect to ET, such as stomatal conductance, VPD, as well as canopy height were enabled, and their influence on performance improvement was not covered by the evaluation.

The modification resulted in a slight decrease of aET performance on watershed level by approximately -5 % based on yearly values, which indicated an improvement, considering stated literature values. In case of deciduous tree species, the overestimation was reduced to an acceptable extent after the plant database modification, showing a deviation of -113.4 mm/a in case of oak, and -85.6 mm/a in case of beech after modification, presumably caused by lower LAI in the dormant state. When analyzing the data on monthly basis, it was shown that the performance of actual ET within the dormant period was enhanced for both, coniferous and deciduous trees, taking leaf shedding in case of deciduous trees into account.

In case of coniferous tree species, the modification approximated stated values in case of douglas fir. Values for pine even exceeded the overestimation of the default settings by 3 % after modification, with significantly higher modified dormant LAI, and at the same time much lower modified LAI throughout the vegetation period, though still ranging above LAI 3.0. Spruce showed an overestimation in the default setup with only slight changes after modification, since the absolute change in LAI was small, and exceeded LAI 3.0 in any case. The minimum LAI settings were found to play the major role in changed aET performance, as maxima in LAI above 3.0 have no significance for aET based on formula **5.1.2**. Thus, SWAT+ does not account for tree specific differentiations of fully developed LAI throughout the vegetation period with regard to aET performance. Regarding the LAI development curves at the beginning and end of the growing season, the modifications showed improvements compared to the default setup

with respect to rise and decline, mature stocks and phenology data taken as a basis, so that the modifications resulted in enhanced *aET* performance with respect to *LAI* development.
Besides the rough orientation towards stated *aET* values, overestimated *aET* performances simulated by SWAT+ in forested areas is supported by two aspects, one of which is related to using the Hargreaves method instead of Penman-Monteith, and the other diagnosed to not be reflected in SWAT+ at all. The first aspect points to the lacking species-specific distinction in transpiration resistance factors, such as atmospherically driven stomatal closure and the general resistance of leaf conductance. In tree physiology, transpiration resistance is related to water supply, energy balance, daytime and seasonal variation (Monteith 1965; cf. Liebscher & Baumgartner 1990:362; Koch 1957), which cause *aET* to never meet *pET* in reality, and furthermore to be tree specific: The cuticle thickness and structure in the leaf surface and within the stomatal pore are found to differ significantly between species, which effects surface contact and transport processes across the cuticle (cf. Fernandéz et al. 2017: 5294). Considering the characteristics of the needle structure in conifers with a higher thickness of the epidermis, conifers show a lower cuticular permeance, and therefore request a higher driving force in transpiration impetus (Kertiens 1996; Riederer & Müller 2006; Riederer & Schreiber 2001), resulting in a generally larger deviation between *pET* and *aET* compared to deciduous trees. When using the Hargreaves method for *ET* calculation, the underlying formula for the calculation of transpiration (formula 5.1.2) promotes *aET* overestimations due to equaled maximum transpiration and *pET* (when $E'_o = pET - E_{can}$, and $E_{can} = 0$) above *LAI* 3.0 in case of dry conditions, as atmospherically driven stomatal closure is not accounted for. Furthermore, a lacking representation of tree specific hydraulically-induced stomatal closure affects the simulation of responses to soil water deficiency: Tree species exhibit individual strategies to cope with water stress by stomatal closure prior to critical soil water contents in order to prevent xylem carvitation (Matyssek & Herppich 2019; Brunold & Rüegesegger 1996; Köstner & Clausnitzer 2011; Hesse et al. 2018; Rukh et al. 2020; Tomasella 2017; Cochard et al. 1996; Nardini et al. 2015; McDowell et al. 2008; Maherali et al. 2004). Spruce, for instance, is observed to be very susceptible to short water supply, and therefore copes soil water scarcity with an isohydric strategy, showing early stomatal closure as response to drought (Lyr et al. 1992 in Pretzsch et al. 2014). Pine, on the other hand, is observed to show a wide range of distribution patterns (Kindel 1995), and is generally considered to follow an isohydric strategy, avoiding water stress by strict stomatal closure (Irvine et al. 1998, Leo et al. 2014, Salmon et al. 2015 in Martinez-Sancho et al. 2017). But, despite its high cuticula transpiration rate, pine was also shown to be varying between isohydric and anisohydric behavior depending on different pine species and their specific stress-acclimation (Poulos et al. 2012). Beech is also considered to vary between the anisohydric and isohydric strategy (Nguyen 2016), but is found to be very susceptible to drought, as it transpires considerably even with induced hydrostatic failure, which rather indicates anisohydric stomatal behavior (Walther et al. 2021). Oak trees on the other hand are considered isohydric, as they are less sensitive to higher stand temperatures, and show a higher PAR canopy transmissivity (about 10 % of incident radiation), higher *VPD* (20 % - 34 % compared to beech) and thus a more xeric distribution envelope (Hohnwald et al. 2020). Numerous studies suggest that tree species react with decline in transpiration prior to critical soil water contents, following the respective species-specific strategy (Walther et al. 2021; Irvine et al. 1998; Ewers et al. 2001; Grassi & Magnani 2005). Duursma et al. (2008) simulated the decline in relative daily maximum transpiration rate as a function of soil water content to start at 0.25 m3m-3 and progress rapidly with further drop in soil water content. **Figure 76** visualizes species-specific starts in transpiration decline induced by stomatal closure as response to decreasing soil water content way ahead of SWAT+ estimates: Underlying formula 5.1.2, and the results shown in **table 11**, SWAT+ calculated

a steep decline in aET for soil water contents of 0.11 Vol.-% (2.2 mm), and 0.32 Vol.-% (6.3 mm), whereas 2.3 Vol.-% (47.3 mm) or 4.5 Vol.-% (89.8 mm) showed no drop in aET[19]. The general assumption for water stress to occur once the evaporative demand exceeds the plant available soil water, expressed by the ratio between aET and pET, is supported by other model application, e.g. the forest growth model BALANCE. It is, though, enhanced in that case by implementing a threshold, which determines drought stress for photosynthesis based on a species-specific water deficiency coefficient (Rötzer et al. 2017). Eder (1984) assumes the lower limit of FC for sand soils in the Palatinate Forest (pore size 50 µ) at pF 1.7 (0.004 MPa), below which he concludes a rapid decrease in the flow rate with increasing suction tension, since the conductivity of the sandy soil decreases sharply with prolonged drought. The decreasing suction tension at 0.004 MPa is presumed to hydraulically induce the stomatal closure, as also supported by Irvine et al. (1998), who found a linear decline in stomatal conduction for pine between 12 % and 5 % volumetric water content. Tree species, that follow a rather isohydric strategy, such as oak and spruce, are even shown to induce stomatal closure earlier: Ewers et al. (2001) state spruce to decline in stomatal conductance linearly from 0.3 m^3m^{-3} soil water content downwards, which is also supported by Clausnitzer et al. (2011), stating the critical threshold value (tipping point) to be 9.5 Vol.-% soil water content in the upper 40 cm for transpiration to fall linearly with further decrease in soil water content. Grassi & Magnani (2005) found oak trees to exhibit limited photosynthetic activity below 30 % of soil water content.

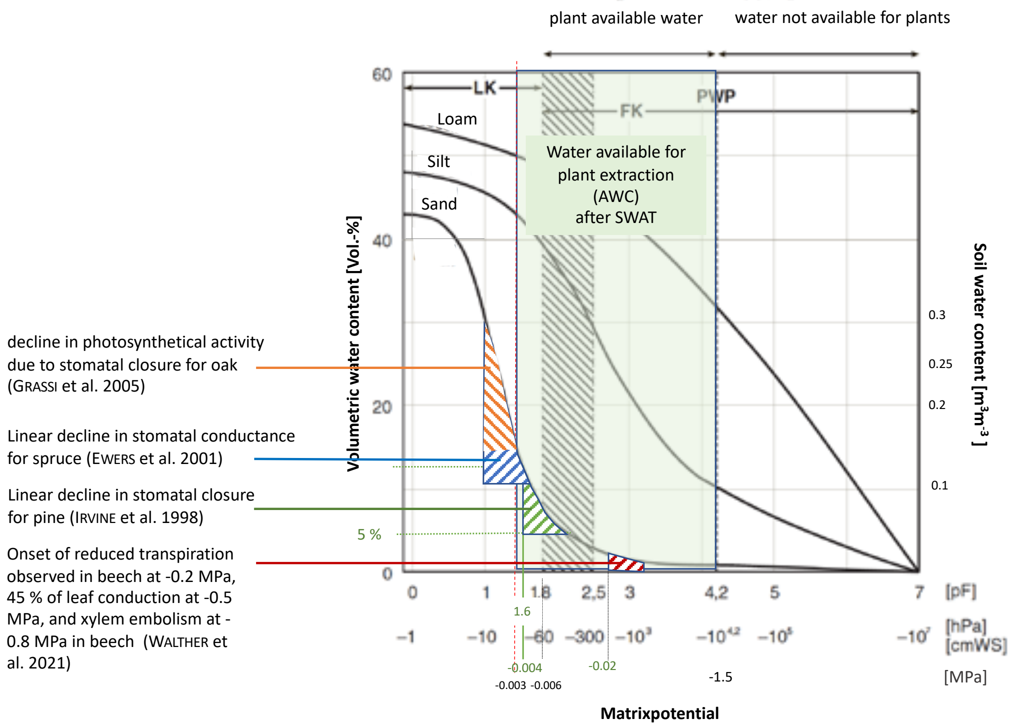

Figure 76: Species-specific response to decreasing soil water content. Modified after Scheffer & Schachtschabel (2010:228), Walther et al. (2021), Irvine et al. (1998), Ewers et al. (2001), Grassi & Magnani (2005), and Neitsch et al. (2011).

[19] The estimates of Vol.-% soil water content are calculated based on a converted equation by Hartge & Horn (1992), SWAT+ outputs for average soil wetness, and the used total soil layer depth of 2000 mm given.

Besides the hydrological driver soil moisture, the expression of stomatal opening and closure, described by stomatal conductivity, is also driven atmospherically by the vapor pressure deficit of the air surrounding the leaves, and therefore directly responds to increases in temperature, triggering the evaporative demand (pET) (Anderson & McDonnell 2005), so that with incline in air temperature, the deviation between aET and pET is supposed to increase. Although VPD, as well as stomatal conductance are modifiable in SWAT+, these transpiration-relevant parameters were disabled using the Hargreave´s method. From the unsatisfactory depiction of the relation between simulated aET and pET, the conclusion must be drawn, that using the Penman-Monteith method might be more expedient for simulating tree specific stomatal permeance with SWAT+, and thus improve model aET overestimations alongside. It must nevertheless be noticed, that using the Penman-Monteith method lead to a loss in flow duration accuracy, which was found in this model setup to cause unplausible soil water contents, and was therefore considered unsuitable to depict stress indication to drought, either. Since the target objective determines the calibration focus, the current study was limited in evaluating transpiration-related factors inducing stomatal closure in SWAT+, as it was calibrated with respect to groundwater recharge and runoff behavior, and did not aim the assessment of stress indication to drought in forests. For such interest, it is found to be suggested, to calibrate the model with regard to the target issues related to transpiration factors, using the Penman-Monteith method, in order to enhance tree specific aET, and derive adequate, model specific values for leaf conductance.

6.1.2 SWAT+ biomass performance in forested areas

The very small improvements regarding plant growth of 0.17 % to 3.8 % with the modified plant setup indicate that the changes in parameters governing plant growth in SWAT+ were too cautiously estimated, relying on literature-based field data. Regarding RUE, Yang & Zhang (2016) identified an average of 17 to 28.2 kg/biomass/ha/(MJ/m²), which exceeds the values used here, and stated in literature for the tree species. This gives incidence, that the identification of model specific parameter values must be pursued in order to enhance the coupling between forest growth and water cycling within the given limitations of the EPIC growth model.

Trees show an age-related decline in diameter growth associated with the relationship between assimilation (anabolism) and respiration (catabolism), since the maintenance costs increase with increasing tree size (Pretzsch 2003; Rubner 1931 in Pretzsch 2003; Mitscherlich 1948). Also, age-related constraints due to hydraulic resistance, reduced allocation of resources to stem growth, photosynthesis-respiration imbalance, and the degradation of suppression-release response are important factors (Smith & Long 2001; Weiner & Thomas 2001, Binley 2004 in Matsushita et al. 2015). Next to the growth degressive effect of age, size is another driver in forest growth, as with increase in size, more biomass is produced, and advantages for resources, such as light, arise (Pretzsch 2003; Matsushita et al. 2015; Matyssek et al. 2010). Fundamental processes in forest growth, such as the intrinsic factors of individual variation, and genetic configuration, as well as the extrinsic factors of intra- and interspecific competition, stand density, crowding and mixing effects (social status, compensation, substitution, strengthening) are not accounted for in SWAT+. Nor are heterogenous age patterns, as they usually occur in forests in which natural succession is established, and which significantly affect actual growth due to the dominant effect of age for tree growth development (Pretzsch 2003). By underlying stressors, with the growth limiting factors being water, nitrogen, phosphorus, temperature and aeration (Williams et al. 1989), the EPIC plant growth model does, though, reflect extrinsic growth factors such as resources and stand conditions, which matches with the doseresponse-principle suggested by Mitscherlich (1948)[20] . The limits the EPIC plant growth model shows towards forest growth were emphasized in the comparison to yield tables, based on the forest growth model SILVA. Since plant growth is tightly linked to the water cycle of forest ecosystems, further efforts might include the implementation of an unimodal, multifactorial tree growth concept into SWAT+, accounting for e.g. compensation effects. The new option SWAT+ provides regarding stand compilation does, though, allow for age and species differentiation on stand level, which should be pursued in future attempts following from this study, again tailored to the respective objective by targeted calibration. Nevertheless, it must be noticed, that the strengths of SWAT+ are clearly focused on hydrological modelling, so that addressing provisioning ES with regard to biomass appears limited, and model improvements regarding timber production/quantification or carbon sequestration would be mandatory for such interest.

The results underline the capability of SWAT+ to reflect the interlink between water cycling and plant growth in forested areas, which confirms it to be considered reliable for further investigations in forest hydrology modelling. Although the differences in plant growth and ET between the default and the modified simulations were small in total values, the results indicate a slight improvement, but also point to future challenges in further model development considering plant parameter adaption/calibration aiming the improvement of forest growth and aET performance. Sticking to accuracy in field-data-based values as basis for parametrization was shown successful with regard to LAI development curves based on phenology data. For plant growth, however, the approach was not confirmed expedient. Other studies showed more significant impacts, when calibrating the model to this specific interest (e.g. Yang & Zhang 2016). Regarding aET performance, improvements were identified to be related to enhanced LAI performance, but the approach was limited with regard to atmospherically driven transpiration factors, which are restricted to the Penman-Monteith method, so that the corresponding parameter adjustments could not be tested. Since in this study, the objective criterion was groundwater recharge and the water flow regime, the calibration was consequently focused on these targets. In order to enhance forest performance in SWAT+, future efforts are needed to carry on the search for model internal optimizations with regard to a better depiction of forest-growth-water-cycle-interactions.

6.2 Water balance and water-related ES of the forest

The SWAT+ simulations for both watersheds, Palatinate Biosphere Reserve and Bobenthal2, were shown to capture the hydrologic dynamics in the forested area sufficiently.

Regarding actual evapotranspiration, SWAT+ estimated a long-term average annual of 635.7 mm in the Palatinate Biosphere Reserve catchment, which is 77.4 % of the average annual precipitation. Overestimations by SWAT regarding aET in forested watersheds were reported by other studies (e. g. Yang & Zhang 2016). For Bobenthal2 on the other hand, only 51 % of the average annual precipitation was calculated to be lost through evapotranspiration. Reasonable estimations for aET can hardly be judged based on model calculations, as they require hard data, which is rarely available. In comparison to other water balance components, measuring evapotranspiration encounters difficulties, because it depends on so many factors. A direct metrological determination of aET of an entire catchment area is almost impossible and therefore usually performed using

[20] According to Mitscherlich (1948), the change in growth, which is bound to the supply with a certain growth factor (e.g. nutrients, water), is proportional to the difference between the actual growth and the potential maximum growth, and therefore decreases exponentially (cf. Pretzsch 2003: 147).

hydrological models. As this model setup was calibrated based on discharge, and aimed on the evaluation of runoff behavior and groundwater recharge, the total climatic water balance must be used as indicator for propriate aET estimations with respect to the specific interest. As models always simplify natural processes, the best possible accurate depiction of the target of interest is achieved with the cost of accuracy regrading other estimates, not aimed through calibration.

Nevertheless, the modifications in plant parameters were shown to slightly improve the SWAT+ performance regarding aET, as they reduced the overestimation by almost -5 % on watershed level, and by 13 - 15 % in case of deciduous tree species. SWAT+ was further proofed capable of depicting the seasonal variability in evapotranspiration patterns, as well as general plant response to soil water scarcity on watershed level, and thus the response to climate change. It was shown that with increasing evaporative demand due to rising mean air temperatures (see **Fig. 10**, section **2.3.3.1**), in addition to more frequent drought periods due to decreasing rainfall (**Fig. 77**), as observed in the dry years 2018, 2019, 2020, the interval between increased potential ET, and actual ET enlarged due to plant water stress induced by scarce soil water contents.

The lower water volume might result in dried out soils less capable of water absorption during heavy rain events, so that increased surface runoff and the risk of erosion must be concluded to occur more frequently in the course of such development. This is, however, not depicted in the model, since SWAT+ does not account for water repellency as a consequence of dried out soils, and the rainfall data has a daily resolution, whereas heavy storm events occur hourly (Neitsch et al 2011).

Regarding surface runoff, the simulation accounted 1.5 % (12.5 mm/aa) of the average annual precipitation leaving the Palatinate Biosphere Reserve watershed as overland flow (1.2 % in case of the Bobenthal2 catchment). The results reflected the very good retarding and softening

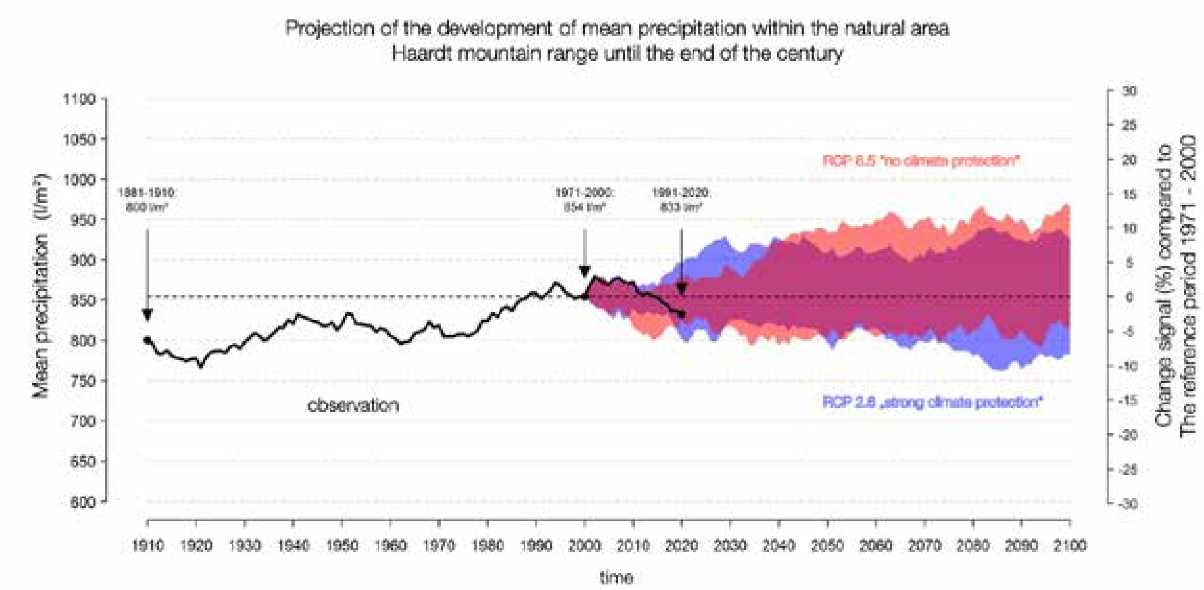

Figure 77: Development of mean precipitation from 1910 to 2100 in the study area (source: Competence center for climate change impacts, www.kwis-rlp.de). Blue area = RCP2.6 corridor ("strong climate protection"), red = RCP8.5 corridor ("no climate protection"), pink = overlap area of both corridors.

effect of the forested watershed on overland flow generation, and therefore indicated the good retention potential of forested land cover on Red Sandstone, whose soil and geological properties favor infiltration processes. The short circuit drain reaction as a response to occasional peaks in precipitation was, however, shown to be effective in a rise in total water yield and streamflow. Therefore the identification of critical source areas (CSA) for surface runoff generation should be put into focus of forest management in order to maintain and improve the good retention potential with respect to future developments with heavy storm events to happen more frequently, and increase in intensity and duration. In this context it must be emphazised that for an accurate simulation of overland flow generating processes at the space and time scale relevant for each process, fully distributed hydrological models are required, that provide a high resolution of temporal and spatial variability. As the results discussed here are founded in a semi-distributed model simulation on macroscale level, they lack the depiction of complex interactions on single event level and their small-scale variability necessary to identify CSAs. In the runoff behavior of the watershed, lateral flow, however, was shown to be the dominant factor, accounting for 93 % of water yield (96 % in case of Bobenthal2). The lateral flow from the aquifer was found to contribute the largest amount, whereas lateral flow from the soil was relatively lower (Tigabu et al. 2021). These results reflect a sufficient depiction of groundwater-related geological properties of the catchment area subsoils, with high permeability values, and a mainly retarding layer sequence of lower conductors in the shallow aquifer, as investigated by LGB & LFW (2004), albeit strongly simplified in SWAT+. The simulation provided the information that the majority of the seepage water contributes to the enrichment of the deep, extensively connected aquifer, with 177 mm/aa deep groundwater recharge in the Palatinate Biosphere Reserve catchment, and 231 mm/aa in the Bobenthal2 catchment, which is equivalent to 21 % of the average annual precipitation, 26 % for Bobenthal2 respectively. Since the modelled values match very well with other studies (LGB & LFU 2004), SWAT+ were shown capable of depicting the groundwater situation in the study area. For groundwater-driven watersheds, the applied equations used in the SWAT+ groundwater module were, though, reported to yield poor results due to their simplification, especially in the assessment of nutrient management or ecosystem services, as addressed with this study (Peterson & Hamlet 1998, Spruill et al. 2000, Srivastava et al. 2006, Gassman et al. 2007, Deb et al. 2019a in Bailey et al. 2020), which was not confirmed here in terms of quantities. The approach to implement a second groundwater layer, as well as extensive calibration of groundwater-related model variables, appeared expedient in achieving model improvements compared to the default setup (Tigabu et al. 2022). In accordance with the negative trend in the climatic water balance, aggravating since 2010, the SWAT+ simulation also indicated decreasing trends in groundwater formation, as reported by MUVF (2007), and Kopp et al. (2018). These decreasing trends also proved valid for the simulation of soil moisture conditions. Even though the average soil water storage was found to replenish in autumn and winter months, a pronounced depletion throughout the vegetation period was simulated for the dry years 2018, 2019 and 2020, associated with poor water inputs due to a decrease in precipitation in addition to higher air temperatures, and thus high plant water demand, at the same time. This becomes particularly evident in the model simulation, when comparing the development of pET, aET and soil moisture content in years with sufficient water supply throughout the vegetation period to drought dominated years: With sufficient water inputs, as in 2014, the deviation between pET and aET remained constantly small, but increased significantly in dry years, as the soil water content depleted from lacking precipitation with at the same time high evaporative demand, which ultimately provokes transpiration decline due to scarce plant water availability of the soil zone, indicating plant water stress (Tyree & Sperry 1988; Sperry et al. 1998 in Ewers et al. 2005; Rakei 1991). The general assumption, that drought periods throughout the growing season induce severe plant water stress the more pronounced, the lower the soil water content with at the same time high plant water demand, was found well captured by the model on watershed level, although the implemented algorithms suggested limitations in the depiction of tree response to drought, as shown in section **5.1.1** on HRU level. Especially with coarse textured, highly water permeable soils, showing a low water holding capacity, as given in the study area, the results suggest that trees will progressively be affected by water stress, as drought periods happen to occur more frequently in the future. Consequences in the form of drought stress, a decline in vitality and increased susceptibility to pathogenic pathogens, are already recorded for drought-sensitive species such as spruce and beech, the latter being dominant in the Palatinate Forest (MUEEF 2019). The proportion of trees showing no drought stress signals was 18 % in 2019 (ibid.). Further research on the impacts resulting from disturbances in the climatic water balance of forested watersheds is vital to understanding the basic requirements for the preservation of intact forest ecosystems, and in order to trace down tipping points in forest ecology, as climate change advances.

The provisioning and regulative ES forest provide regarding water flux regulation, and thus quantitative groundwater formation, and overland runoff control, bringing about benefits for human society in the form of drinking water supply, and flood control, were shown to be highly effective in the study area. Nevertheless, current and future decreasing trends in groundwater recharge, as well as a short circuit drain reaction resulting in peaks in water yield as a consequence of elevated precipitation amounts underline the importance of preserving functional processes related to intermediate components in the provision of those ES of the forest.

To also cover the qualitative aspect of groundwater formation, a nitrate calibration of the built model should be executed in a next step. This is required to also depict ES regarding nutrient cycling and water purification. To highlight the consequences for other levels of ES, such as e.g. health and recreation, or monetary values related to forest hydrology, a socio-economic evaluation would be necessary to pick up the topic.

6.3 Climate projections

According to the IPPC 5th Assessment Report (2014), an increase in surface temperature is projected by 2100 for all emission scenarios. For RCP8.5 ("no climate protection"), an increase in global earth temperature of more than 2 °C is predicted compared to the period 1850-1900. Under this scenario, an increase in the annual mean temperature of between 2.5 and 4.5 °C compared to the reference period 1971-2000 is assumed for Rhineland-Palatinate (Reiter et al. 2020). For the RCP2.6 scenario ("strong climate protection"), on the other hand, the forecasts predict an increase of 1.0 to 1.5 °C compared to the reference period. Both scenarios show a higher occurrence of heat waves per year (ibid.). There are, however, uncertainties in forecasting precipitation for Rhineland-Palatinate: The majority of climate projections show an increase in precipitation levels by the end of the century, with decreasing trends evident for the summer months. Under the conditions of "strong climate protection", the number of heavy storm events remains the same, whereas with RCP8.5, an increase in number from currently 2 - 3 to 3 - 4 heavy storm events per summer half-year is predicted. First indications of newly developed high-resolution climate projections, with a grid spacing of < 3 km, point to a rise in intensity of these events with a duration of even a few hours (ibid.). Additionally, to the ecological, social and economic dimensions of the global impact of the rapidly progressing, anthropogenic climate change, the potential degradation of forest ecosystems associated with it results in the deterioration of water-related ES, as the harmonization of the water cycle is interlinked with complex functional structures of the forest.

To determine potential effects of climatic changes on dynamics in the water cycle of the forest, high-resolution statistical and dynamic regional models were used on the basis of the

BIAS-adjusted REKLIES and EURO-CORDEX simulations RCP2.6 and RCP8.5 over the HYRAS area using downscaling methods (CCLM4.8.17, RACMO22E, RCA4, CLM, WRF361H). The processed 6 climate projections for RCP2.6 and RCP8.5 were then combined with the water balance model SWAT+, compared to the baseline period from 1961 to 1990, and analyzed with respect to hydrological quantities of interest: Evapotranspiration, flow dynamics (lateral flow, surface runoff, water yield), soil water content, and groundwater recharge, in order to conclude inherent functional processes relevant for water-related ES, and their development. The baseline period was characterized by a pronounced homogeneity of water balance dynamics, as can be inferred from **fig. 47**, whereas the current development is strongly affected by hydrological conditions of high dynamic character. The more balanced conditions of the far past are therefore very well suited as a reference for changes in the climatic system, which already prevail in current developments.
Regarding the water-cycle regulating ES of the forest, the future climate projections gave incidence, that the overall input in precipitation to the hydrological system will decrease in the future, with respect to streamflow quite constantly by mean values of -37 % in case of RCP2.6, and -30 % for RCP8.5 until the end of the century, with the most decrease predicted for RCP2.6 in minimum values (-59 %). Only RCP8.5 showed a slight increase in maximum values of 0.12 % for this period, correlated with elevated precipitation. For the middle of the century, minima and maxima for both scenarios ranged between approximately -14 % to -55 %. The decline in water yield was equivalent, with the most pronounced loss (-67.5 %) also for minimum values of RCP2.6 from 2071 to 2099, and a slight increase of 4 % for RCP8.5 in the same period, increasing precipitation given in that case. For surface runoff, the minima range around -60 % in all cases, and the maxima showed a decrease by -13.5 % for RCP2.6, but an increase of almost 29 % for RCP8.5, which is equivalent to 38.7 mm/aa in absolute values compared to 30 mm/aa within the baseline period. In the context of surface runoff being relevant for flash flood generation, two aspects are of high interest: processes that affect the infiltration capacity, and the spatial/temporal distribution of rainfall, especially in the event of heavy storms. With extreme rainfall intensity, the large volumes of water cannot be completely absorbed by the ground within given time intervals (Baumgartner & Liebscher 1990), so that critical source areas of overland flow generation are very likely to contribute to the generation of kinematic waves. According to Reiter et al. 2020, heavy storm events are predicted to occur more frequently in Rhineland-Palatinate in the future, especially for RCP8.5 by the end of the century (see **fig. 78**), so that with the higher water inputs in that case, the contribution of surface runoff to flash flood generation is relevant for water management. With respect to infiltration capacity, degraded soils, be it due to compaction or drying out, show reduced infiltration rates. In the context of climate change, drought periods promote soil desiccation, with the described consequences of water repellency. The impaired absorption capacity of desiccated, hydrophobic soils can lead to significant runoff peaks in response to flash flood generation (Schüler 2006). With scarce precipitation during the vegetation period, as predicted in the course of climate change (see **fig. 79**), in addition to higher mean air temperatures (see fig. 10, p. 41), and consequently droughts to happen more frequently, water repellency is very likely to aggravate overland flow generation as a result of heavy storms within the growing season.

Regarding deep groundwater recharge, both RCP2.6 and RCP8.5 projected minima and maxima to range between around -39 % (173 mm/aa) and 2 % (291 mm/aa). Until the end of the century, the scenario “no climate protection” showed change signals between still -35 % (183 mm/aa) to 2 % (291 mm/aa), equivalent to the increase in precipitation forecasted within this period. For RCP2.6, the decreasing trend even continued until the end of the century with minima and maxima raging between -41 % (168 mm/aa) and approx. -8 % (263 mm/aa), as precipitation was projected to further decrease by 3.5 % in mean values compared to the middle of the century.

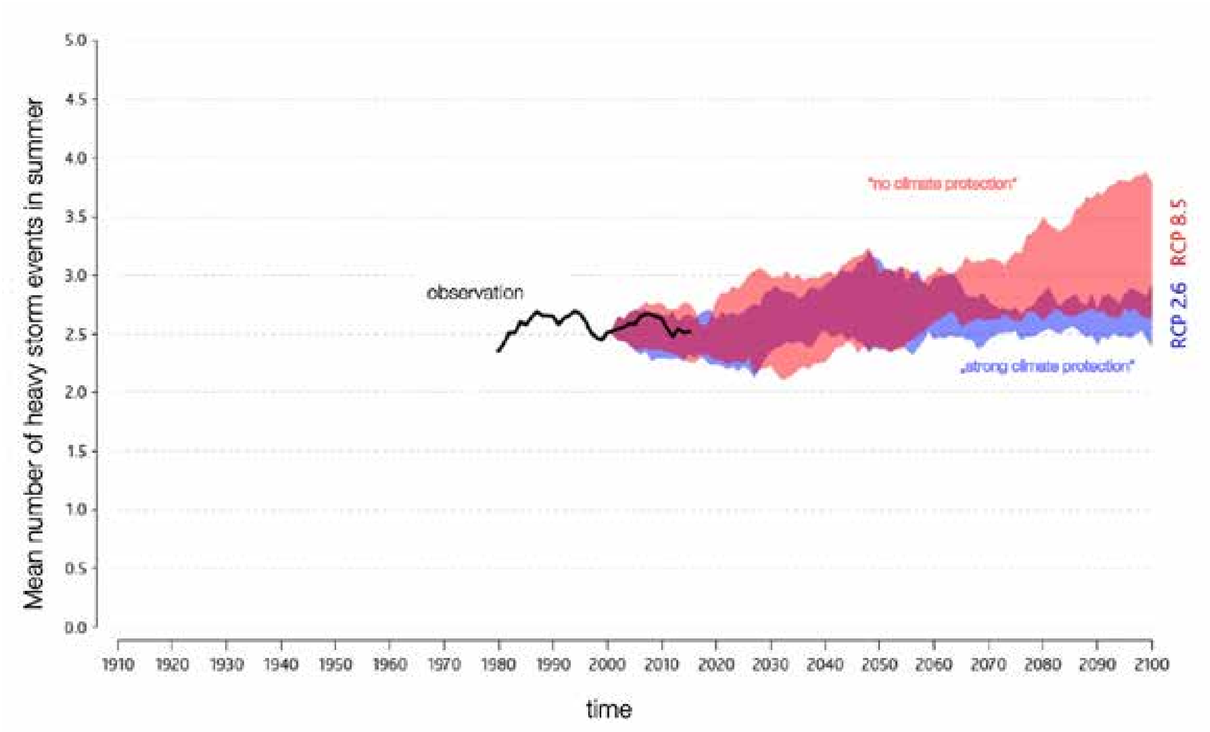

Figure 78: Projection of the future average number of heavy rain events in summer (Reiter et al. 2020). Blue area = RCP2.6 corridor ("strong climate protection"), red = RCP8.5 corridor ("no climate protection"), pink = overlap area of both corridors.

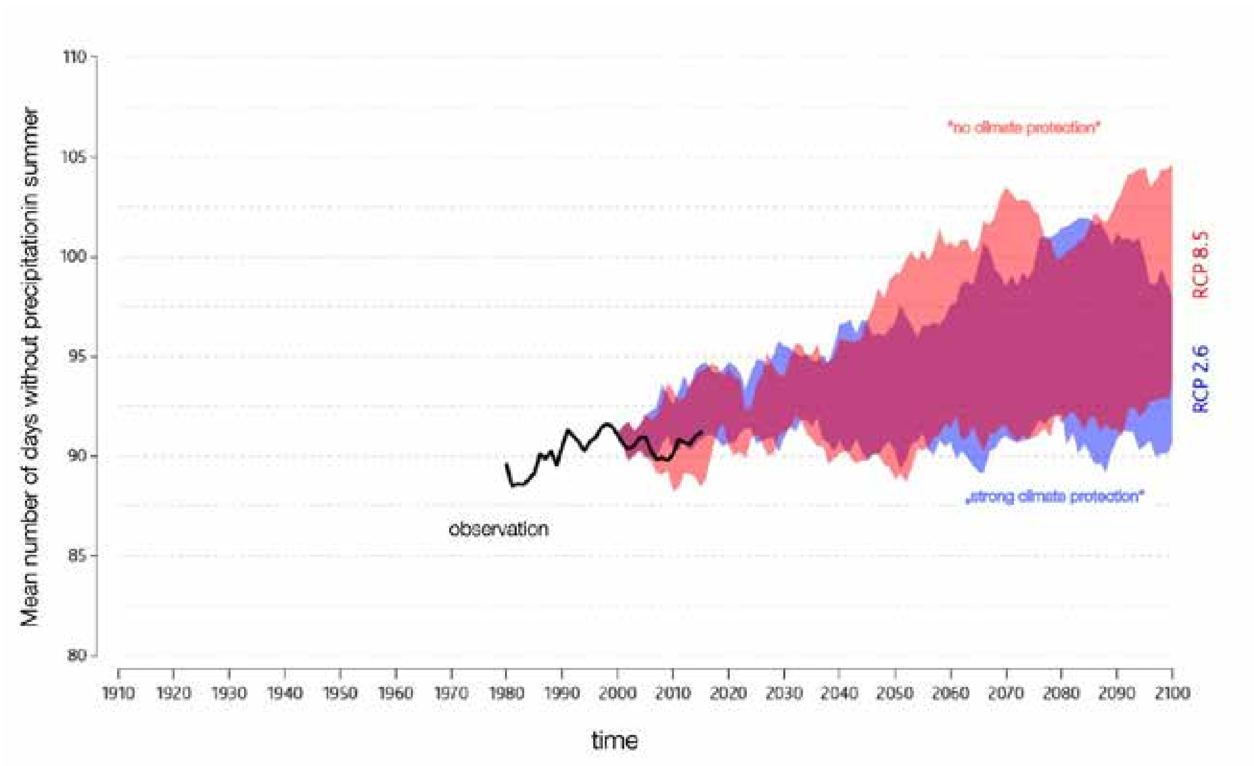

Figure 79: rojection of the mean number of days without precipitation in summer (Reiter et al. 2020). Blue area = RCP2.6 corridor ("strong climate protection"), red = RCP8.5 corridor ("no climate protection"), pink = overlap area of both corridors.

In this context it must be emphasized, that the current development aggravates more rapidly than captured by climate projections: As can be seen in **figure 77** and **10**, the present day developments for precipitation and mean air temperature partly almost outpace the climate projections already, which was also reflected in absolute values of simulated current and projected groundwater recharge: When in 1961 to 1990 the long-term deep groundwater formation was 285 mm/aa, it was simulated to be 177 mm/aa in 2000 to 2020. But neither RCP2.6 nor RCP8.5 reached such low mean average values in any timeline. Only minimum values under RCP2.6, with the highest projected loss of recharge until the end of the century, with 173 mm/aa by the middle, and 168 mm/aa by the end of the century, undercut todays recharge amounts. Only RCP8.5, with increased precipitation by the end of the century, was projected to match the baseline amounts of groundwater formation. An extension of the vegetation period, as already diagnosed for the last decade, which shortens the phase of groundwater replenishment, can also be concluded from the SWAT+ simulations, when comparing the deep groundwater formation of 2010 to 2020 with the past: As **figure 80** reveals, the replenishment tended to start later in the year compared to 1961 to 1971, when the depleted soil water storage first refilled to field capacity before deep percolation was promoted. Also the seasonal decline in groundwater formation started earlier in the year due to the accelerated growing season[21].

Although the broad corridor ranges of climate projections emphasize the high degree of uncertainty related with future scenario forecasts, the

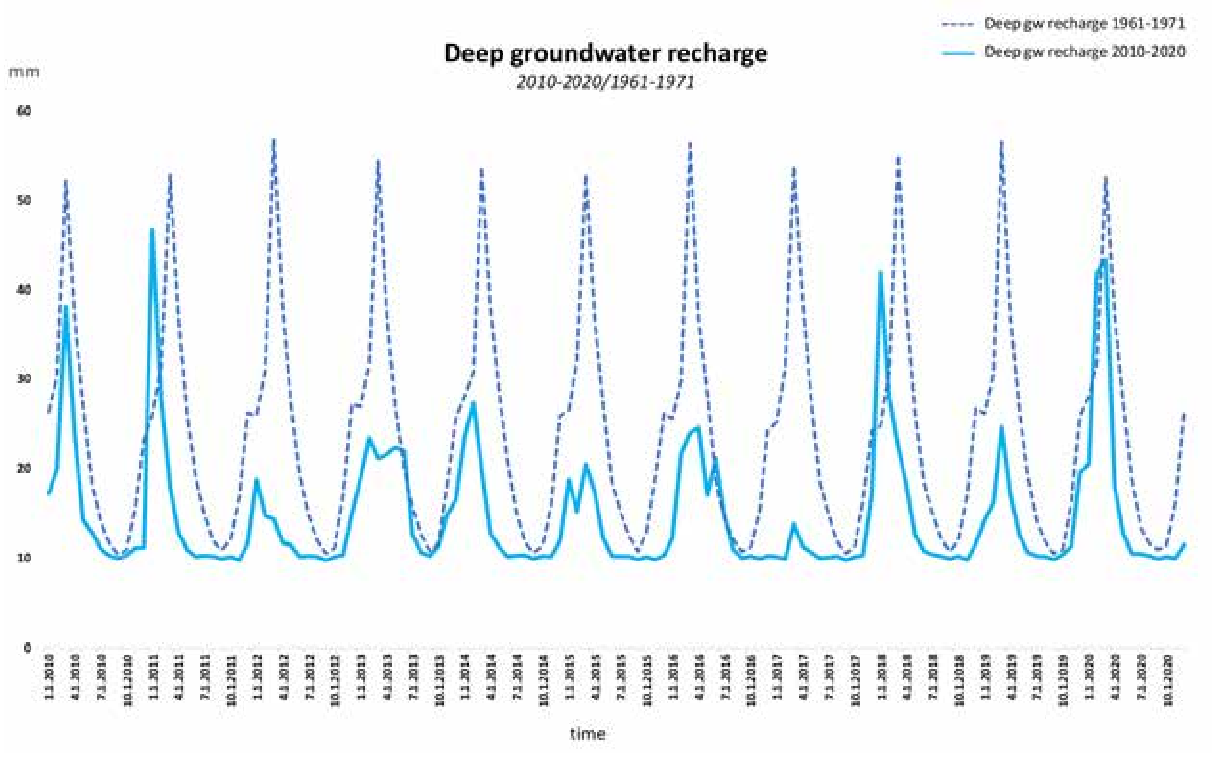

Figure 80: Comparison of deep groundwater recharge between the time periods 1961 to 1971 and 2010 to 2020, showing a decline in volumes and a shortening of the recharge period for 2010 to 2020 compared to the farer past.

[21] https://www.kwis-rlp.de/daten-und-fakten/phaenologie/

SWAT+ simulations depict an overall decreasing trend for groundwater recharge for current and future times compared to past times. Maximum values under the scenario "no climate protection" that indicate a possible tipping point regarding groundwater storage recovery, must not be considered an easing for ecosystem pressure, as deep groundwater recharge predominantly occurs in winter months. Soil water depletion throughout the growing season was still indicated by the projections.

Aggravating factors are also the lengthening of the growing season, as shown in **figure 81**, and the projected increase in heat waves within the vegetation period (Reiter et al. 2020). Both promote extended soil water depletion and a shortened period of replenishment, as percolation into deeper soil layers only occurs, when the soil water storage has filled again (Hermann et al 2014, see section **2.3.2**).

According to IPCC studies, climate models do not adequately reflect the sensitivity of extreme precipitation events to global temperature changes (IPCC 2013). Consequently, with assumed uniform distribution patterns of precipitation, periods of drought or heavy rain events that occur with decadal variability are underestimated in the model projections. In this context, the combination of periods of drought and heavy storm events promote higher surface runoff, since dried out soils have a reduced infiltration capacity for water. If the vegetation period extends at the same time, the overall losses can have a negative effect on groundwater recharge. Such developments have already been observed in the dry years of 2018 and 2019 in regions of Germany with rather low groundwater yields: pressure of use and severe summer drought led to an extreme lowering of the groundwater level in Lower Saxony in 2018 and 2019 (NLWKN 2020).

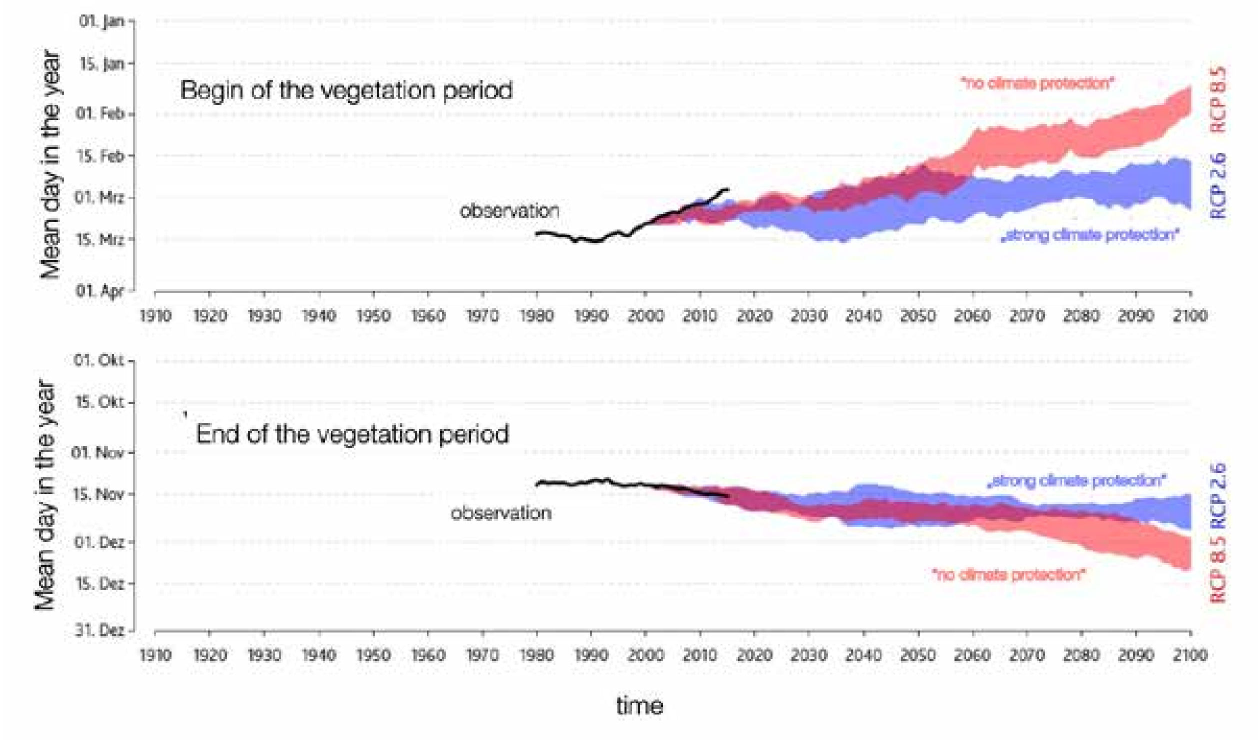

Figure 81: Projection of future change in the growing season (Reiter et al. 2020). Blue area = RCP2.6 corridor ("strong climate protection"), red = RCP8.5 corridor ("no climate protection"), pink = overlap area of both corridors.

The mean annual lows in 2018 were 0.23 meters below the record lows measured up to then (1988-2017).
Nevertheless, the broad minima and maxima corridors, ranging from -41 % to 2 % give an ambiguous picture for the projection of groundwater, which corresponds to other studies (KLIWA 2012; Hermann et al. 2014). With current limitations of climate models with regard to cloud formation and precipitation distribution patterns given, the hydrological modeling of groundwater recharge, strongly correlated to precipitation, is only limited in significance up to the end of the century (Bates et al. 2008 in Riedel & Weber 2020). Possible tipping points, as identified for deep groundwater recharge for RCP8.5 by the end of the century, most probably promote climatic conditions of more and more chaotic character, which are therefore even less predictable.

Furthermore, it must be pointed out that the future projections are based on constant soil and vegetation conditions. Changes in the vegetation cover, as consequence of increasing forest dieback due to a limited adaption capability, are not accounted for, nor are changes in the soil that can be brought about by a changed vegetation cover. However, predicted increase in winter precipitation (Reiter et al. 2020) may compensate for the effects of a lengthening of the vegetation period (water loss due to higher evaporation capacity), summer drought, and the resulting soil water depletion on the long-term average. Loss of vitality within the forest stocks, for example as a result of climatic or biotic catastrophes, such as storm events or damage by bark beetles, cannot be ruled out in the future and are associated with changes in material and energy flows. The release of humus-bound nutrients can lead to a deterioration in groundwater quality through leaching into deeper soil layers and deep seepage. Against the background that almost 50 % of the groundwater bodies in Germany are already considered polluted (UBA 2017b), this is of great water management relevance for the security of supply, and ought to be the matter of a future survey with a nitrate-calibrated SWAT+ model.

When dealing with climate projections, it must be assumed that they depict a framework of mean frequencies of weather conditions and their probability of occurrence (Kraus et al. 2013). Consequently, events with high temporal and spatial resolution, such as increased surface runoff subsequent to heavy storm events, are poorly captured. Basic insufficiencies in modelling of lumped landscape characteristics with assumed homogeneity, that can hardly predict flow volumes realistically, in addition to the uncertainty in climate models regarding precipitation distribution patterns as a result of the relationship between atmosphere and ocean circulation (Beven 2005 in Anderson & McDonnell 2005), makes the prediction of both, surface runoff and groundwater recharge still remain vague. Furthermore, SWAT+ assumes constant land use conditions, and thus does not simulate loss in forest cover due to climatic changes. To comprehend forest die-off in the course of climate change, changes in land use cover need to be applied to the model. Since there is scarce knowledge about tipping points in forest resilience to climatic stress, the development of land use changes in the future is hardly predictable. Further efforts on the assessment of such tipping points is needed, in order to gain input data for modelling drought induced forest die-off and its effect on future water balance developments.

6.4 Soil Compaction

For the SWAT+ simulation of impacts of soil compaction due to the forest pathway system and driving with heavy machinery in the course of harvest operations on water balance components, the followed approach included the alteration of soil properties with regard to bulk density, and the adaption of SCS Curve Number values representing infiltration rates. Both were modified according to driving test data collected in the study area by Reichardt (2002) and Schneider (2015). The SWAT+ model was shown to sufficiently depict expected impacts of changed soil conditions due to compaction on watershed level, and furthermore allowed for a differentiation of individual effects on different soil classes on HRU level.

Water flow regulation function/ flood protection

The results indicated, that the pathway system (C1) contributed to an average rise in surface runoff of 36 % compared to uncompacted conditions (C0) on watershed level, which consequently increased the water yield by averaged 12 %. With a share of approximately 11 % in total of the watershed´s spatial area, the impact of the pathway system on the water flow regulative function of the forested area, and thus on water-related ES related to it, seemed moderat when considering annual average values. The evaluation on daily basis, however, resulted in a significant rise in surface runoff in distinct peaks of up to 242 % (7.5 mm) of the undisturbed scenario (3.1 mm) as response to elevated single precipitation events, indicating a more pronounced effect on the water flow regulation function than suggested by average annual values. The elevated surface runoff from compacted soil conditions consequently lead to equivalent peaks in streamflow of up to 110 % on daily event level due to the short circuit drain reaction in the catchment. Such rises are in the risk of contributing significantly to the generation of flash floods, especially with heavy storm events with very high amounts of precipitation in a single hourly event to occur more frequently in the course of climate change, and furthermore considering the line structure of paths and wayside ditches, generating high flow velocities. The daily resolution of simulated effects of pathway compaction on the water-related ES water flow regulation therefore calls for actions with regard to improvements in the retention potential of the forest area. Forest roads have little or no retention capacity for water (Grunert & König 2000). According to Bott (2002), the water runoff can be decisively controlled via the path density and the type of path drainage. In order to direct the surface runoff water away from the paths, rounded cross profiles can be created, which drain into lateral ditches and from there over a wide area back into the adjacent forest areas (Peichl 1998). Infiltration drains of coarse crushed rocks in the substructure of forest roads, instead of throughs and culverts, let lateral water flow seep through the deeper road bodies (Backes et al. 2007).

For soil compaction from harvest operations (C2) the magnitude of impacts reflected the applied changes in bulk density and CN values: With SS being the dominant soil class in the area (82.4 %), which still allowed for infiltration after compaction due to the applied CN values (CN 57/71) reflecting its coarse texture, (C2) showed significantly lower impacts due to soil compaction than (C1). With 13 % share of the spatial catchment area, skid trails and preloaded areas were thus simulated to increase surface runoff by approximately 1 %. This reflects, that the retention capacity of the sandy soils was simulated to be still maintained after compaction, which is plausible, considering the high proportion of hydraulically conductive macro- and meso-pores, the number of which decreases, though, under compaction, but still a sufficient amount is preserved to maintain hydraulic conductivity. Water yield, contributing to streamflow, was increased by a small percentage of 0.5 %, lateral flow by 0.4 % in averaged annual values on watershed level.

It must be emphasized that the values for (C2) on catchment level are arithmetic in character, as they were derived from calculating the 4.1 % area cover of tracking data on skid trails to 13 % coverage according to the instructions of the forestry development plan, and the area extent of cultivated forest in the area. This neither depicts a realistic distribution of skid trails in the area, nor accounts for a realistic depiction of the distribution of site-specific soil conditions. In order to reflect the impacts of soil compaction due to harvest operations on HRU level, a more detailed evaluation was conducted, which also included the differentiation on soil classes. The results implied a clear interrelation between the magnitude of impact and the soil class: When for sand dominated soils (SS, LS) the retention potential was shown to be disturbed to a small extent, and also showed to maintain aeration, soils with higher clay and silt content, as for soil class L and SU, infiltration, percolation and aeration became inhibited more profoundly. The latter primarily for the soil class SU, with an increase in soil evaporation by approx. 3 %, which is considered an indication of potential water-logging. An increase in surface runoff by 46 % in mean values for all HRUs with soil class L in the catchment, covered by tracking data, was indicated (126 % for SU), as well as losses to percolation of -5.5 % (-1.4 % for SU). With a decrease of -2 % in lateral flow (-17 % for SU), it must be assumed that a part of the precipitation water still infiltrated, but was limited in percolating into deeper layers, and thus contributed to a rise in water yield by approx. 9 % for both, L and SU. These results need to be put into relation to the area extent of the respective HRUs for each soil class given through tracking data. On forest site level, examining one HRU with a high percentage of tracked skid trails and preloaded area, pure sands (SS) were found to generally maintain their hydrological conductive pore size distribution providing retention capacity, though decreased to an extent: Although there was no surface runoff simulated in the selected HRU for the given time period, decreases in percolation by 10 %, in soil wetness by 1.3 %, and small increases in water yield by 3 % indicated some deterioration of the soil retention function, which was similar for more clayey sand dominated soils (LS). Soil classes with higher proportions of meso- and micropores, as SU and L, showed a very pronounced response to compaction, reflected in significant peaks in surface runoff after compaction. When soil class SU showed 1.3 mm/aa surface runoff for undisturbed conditions, 27 mm/aa were simulated after compaction. For soil class L, surface runoff increased from 5.7 mm/aa to 32 mm/aa. These results confirm the attempt to compute inhibition of infiltration by appropriate adaption of CN values in SWAT+, especially when considering soil physics with regard to pore size distribution of the respective soil classes: Soils with great heterogeneity in terms of grain size distribution are considered more vulnerable to compaction due to their higher number of grain contact points (Terzaghi 1943). Due to the higher proportion of meso- and micropores in silt and loam dominated soils, their relative proportion of conductive meso- and macropores is reduced to a larger extent than in sand dominated soils, so that the hydraulic conductivity is limited more severely, resulting in lower infiltration capacity, and lower seepage, with at the same time higher surface runoff, and subsequent contribution to water yield. The retention function is therefore disturbed more sensitively on such soils. Internal FAWF monitoring data (unpublished) on pore degradation also confirms the general assumptions found reflected in the simulations, as shown in **table 22**. Furthermore, vulnerability of the soil with regard to compaction also increases with increasing soil water content, since the water film between the micropore soil particles is accompanied by a reduction in frictional resistance, which causes plastic flow under mechanical action and leads to kneading and destruction of the soil structure (Bolling 1986, Hildebrand & Wiebel 1986, Seifert & Seufert 1986, Terzaghi & Peck 1961 in Reichhardt 2002; Zenner et al. 2007; Terzaghi et al. 1996; McNabb et al. 2001). The simulated increasing impact of soil compaction with increasing proportion of micropores in the soil class is therefore considered to sufficiently depict specific soil class vulnerability in accordance with soil physics. It must, though, be noticed, that soil class L already showed the lowest hydraulic conductivity under undisturbed conditions due to the highest percentage of initial micropores. This was also reflected in the simulated highest amount of surface runoff for the uncompacted scenario, and an equivalent lowest share of lateral flow on water yield, which was both found distinctively increased after compaction. The effect of reduced macropores in the course of soil compaction from heavy machinery was simulated to be most pronounced, however, for soil class SU, resulting in distinct runoff peaks after compaction, when undisturbed conditions did not induce overland flow at all.

Table 22:

Soil compaction for selected substrates, and their derived pF-curves based on monitoring data of forest sites in the Palatinate Biosphere Reserve in the 1990ies, evaluated by the soil physics laboratory of the FAWF (unpublished).

	Change (absolute values) in bulk density	
	From <1,45 g/cm³ to >1,65 g/cm³	From <1,45 g/cm³ to >1,65 g/cm³
Soil type	Hydraulically conductive meso/macro pores (%) > 50 µm to > 0,2 µm (pF 0,8 to 4,2)	Micro pores (%) < 0,2 µm (pF > 4,2)
S	38 % to 28 %	7 % to 5 %
LS	37 % to 26 %	9 % to 7 %
SU	32 % to 24 %	15 % to 12 %
L	21 % to 12 %	28 % to 23 %

For the entire catchment area, showing only a small percentage of L (4.6 %) and SU (2 %), this may not have a large impact. But it can be concluded from the simulation results, that in catchments with higher amounts of clay and silt dominated soils, infiltration inhibition with all negative consequences of elevated surface runoff, lower soil aeration and losses to percolation, intensifies in the course driving with heavy machinery. Therefore, the development and provision of vulnerability maps with regard to soil properties for the forest practice is recommended, that also include soil moisture conditions. Although there are only slight signs of deterioration to the water flow regulation function as consequence of soil compaction from harvest operations in mean values on catchment level, even the sand dominated soil classes showed changes in the distribution of input water. With view on the high priority of maintaining the hydrologic continuity of forest stands in order to enhance their resilience to future challenges, traffic intensities should be reduced to a minimum. Where possible, soil-conserving harvesting methods should be given preference. Machine movements should therefore be spatially concentrated, which means that a higher driving intensity is accepted for a concentrated area, but the number of deformed areas can be limited (Müller & Schüler 2021).

<u>Habitat function</u>

The silt dominated soil class SU furthermore showed a rise in soil evaporation by approximately 3 %, which gives incidence of secondary waterlogging from which evaporation ascends. The indicated potential waterlogging also allows for the conclusion, that soil aeration becomes inhibited, which affects soil biota negatively. Regarding the habitat function, changes in soil properties affecting aeration and water supply result in a degradation of habitat conditions for edaphic organisms. This not only goes along with a loss in biodiversity, but also reduces soil functions related to regulative ES with respect to water purification, as the filter function becomes inhibited as a consequence of loss in aggregate stability, and exchangeable charged surfaces. This also includes the development of the secondary pore system (Bayer & Schrader 1997; Kaiser et al. 1994; Larink et al. 1994): Higher resistance to penetration and poor oxygen supply has a particularly negative effect on the macro and mesofauna. In the study area, however, due to the predominantly acidic soil environment (pH Ø 4.3), there is hardly any macrofauna, which is largely involved in the formation of the secondary pore system (Weber 1996; Kolk 1994; Fass 1995). As a result, the regeneration capacity of the soil with regard to dynamic pore formation is limited to the development of the root system as a result of natural succession. Since root growth strengthens the soil's natural regeneration capacity through loosening, ground vegetation and succession on compacted areas contribute to the recovery of soil properties. However, the germination bed function for tree seedlings is also impaired by a reduced air capacity due to the reduced coarse pore volume and the decrease in pore continuity (Hildebrand 1983). Fine root growth in particular is impaired by high bulk densities. Furthermore, Hildebrand (1983) gives 11 % by volume of air capacity as the limit value for undisturbed root growth. Another aspect of the limited air capacity of compacted soils is the reduction in gas exchange capacity. A lower gas exchange capacity of the soil results in a changed CO_2 disposal rate and a shortage of oxygen in the lower soil horizons. Due to the latter, the root area shifts to higher horizon layers (ibid.).

Groundwater recharge

The infiltration process along the line-structured pathways was simulated to be marginally inhibited considering average annual values on watershed level: Lateral flow and percolation were decreased by around 2 %. The impact on groundwater recharge in the watershed was calculated to be negligible, with a decrease of -2 % for the shallow, and -1.7 % for the deeper aquifer. Thus, regarding the water related ES groundwater recharge, there were no significant impacts computed by the model, neither for the simulation of the pathway system (C1), nor for skid trails and preloaded areas (C2). The latter even showed less impact, with negligible 0.2 % decrease of recharge for both aquifers. Also, the subsoil processes related to seepage water volumes changed only in small degrees in case of (C2): percolation was found inhibited by -0.2 %, so that consequently, also groundwater recharge was reduced by negligible -0.2 % on watershed level. The impact of soil compaction on the forest-specific ES groundwater recharge in the study area can therefore be considered marginal due to the infiltration favorable conditions, and low susceptibility to compaction of dominating Red Sandstone in the area. Furthermore, the spatial extent of pathway compaction of 11 % compacted area of the watershed predominantly forms line structures (as do skid trails, accounting for a similar spatial extent), which limit the spatial area with effective inhibition of infiltration relevant for areal seepage to small degrees.

It must be emphasized that the results are founded in model simulation, and furthermore, that both, average values as well as model simulations, lack the depiction of complex interactions on single event level in terms of small-scale variability. Bieger et al. (2016) conclude, that SWAT+ still shows weaknesses in representing runoff generating areas within a watershed sufficiently enough in terms of temporal variability in location and size (cf. Bieger et al. 2016:13). The parameter for estimating direct runoff depth from storm rainfall depth, Curve Number (CN), does, for instance, not account for spatial and temporal variabilities in infiltration into, but calculates the total depth loss of infiltration through aggregation (Ponce et al. 1996). The fact that a lumped model for infiltration is calculating an averaged infiltration rate that disregards the variability of real nature phenomena must be considered as both, an advantage in terms of simplicity and stability, as well as a disadvantage when it comes to variability and accuracy for geomorphological heterogenous environments (ibid.). In watershed modelling on meso or macro scale level, lumping becomes, however, necessary due to the extensive volume of spatial data. Furthermore, for the impact of slope on surface runoff, the model is reported to have further weaknesses: The SWAT+ internal algorithms account for increasing lateral flow with increasing slope, which leads to underestimations of surface runoff due to the interlink between lateral flow and soil water content (Bieger et al. 2015). If the identification of surface runoff generating areas and the derivation of related recommendations of action in the field of management practices is the predominant interest, catchments with high differentiation in slope are therefore suggested to be modified in key algorithms and parameters with regard to this requirement (ibid.). From this the conclusion is drawn, that the simulation of compaction effects on the water flow regulation function of forested areas should be developed further in future attempts, with a sufficient spatial coverage of tracking data on skid trail distribution provided. Also, it must be pointed out, that accelerative effects of flow rates on line-structured flow paths (pathway network and skid trails) increase the kinematic wave character of overland flow processes, which is not accounted for in SWAT+ either. Therefore, as suggested by Bieger et al. (2016), in the routing of water between different HRUs, the implementation of algorithms to adequately differentiate runoff processes, such as sheet flow and canalized flow, would improve the model´s representation of management operation effects, such as soil compaction in the course of driving with heavy machinery in more detail (cf. Bieger et al. 2016). With heavy storm events to be expected more frequently in the course of climate change, the most significant disadvantage of the SCS-CN approach might be the lack of expression of time, impact of rainfall intensity and its temporal distribution (ibid.). This inevitably leads to an insufficient performance in the context of runoff generation in the event of heavy storms coupled with very dry, hydrophobic soil conditions. The effect of water repellency is not accounted for in SWAT+ at all, it is rather assumed, that the dryer a soil, the higher the infiltration rate according to the respective soil characteristics, and the wetter the soil becomes, the more the infiltration rate decreases (Neitsch et al. 2011). Since the objective of this study was to assess the impact of anthropogenic pressure on water-related ES of the forest on catchment level, a lumped approach on macroscale level is legitimate. Also, the results were shown to be in accordance with soil physics. Nevertheless, for a precise forecast of flood waves with temporal, spatial and quantitative accuracy, the small-scale variablility of the geomorphilogically heterogenuous landscape must be captured. This can rather be accomplished by using a fully distributed model for selected parts of the catchment area.

6.5 Disrupted areas with rejuvenation

The assessment of influences of forest cover and canopy expression on the hydrologic cycle is subject of many studies, going back to the first catchment experiments initiated at the beginning of the last century (Hewlett et al. 1969). The general assumption, that reduced canopy cover in the course of bare fallen sites or as consequence of forest establishment, leads to increase in water yield (Hibbert 1967; Bosch & Hewlett 1982), was tested here through hydrological modelling based on an artificial catchment approach. The model simulation of rejuvenated stocks in comparison to mature, permanent stocks indicated that age-related stocking patterns affect the water balance of forested areas with respect to the targets of interest, water-related ES of the forest, to a small extent. The results showed that the SWAT+ model is capable of simulating age-related differences in forest stocks under the used model settings.

Regarding the soil water content, the overall simulated increase of 32 % on juvenile stocks compared to mature, primarily concentrated on the vegetation period, did not apply to the upper soil layer throughout the early age stages. This can be explained by the concentration of root penetration, and thus water extraction, in the upper 0.5 m (1 m in case of oak), as set for plant parametrization based on literature, and additionally by enhanced soil evaporation under juvenile growing conditions. Soil evaporation, accounting 42 % difference between JUV and MAT, was the most significant change signal between the two age-scenarios. As SWAT+ assumes no ground vegetation, the bare soil between saplings was exposed to incident light, which increased not only the stand temperature, but also soil evaporation (Vestin et al. 2020; Hedwall et al. 2013; Cermak et al. 1993). Furthermore, uncovered soils are more susceptible to soil erosion, as well as to enhanced mineralization of the humus layer. With increase in soil temperature enhanced N mobilization occurs, while at the same time the nutrient uptake by the young trees is lower, which can lead to N seepage into deeper soil layers, or, depending on the intensity of precipitation and the corresponding overland runoff processes, to discharge into adjacent surface waters (Block 2006; Block et al. 2016; Lee & Samuel 1976 in Keenan & Kimmis 1993). Considering a higher droplet energy from precipitation water on the soil surface, detachment of soil particles might also result in a higher erosive potential under juvenile growing conditions, affecting stand nutrient supply and water bodies qualitatively.

With 23 % higher groundwater recharge in average, juvenile stands were found to slightly promote groundwater formation quantitatively. In the provision of the benefit "clean drinking water" forest ecosystems provide, the qualitative aspect cannot be neglected, though, which in turn is in the risk of deterioration due to higher loads of mobilized nitrate as a result of enhanced mineralization processes on juvenile stocks. To assess differences in qualitative groundwater formation between the stocking types, a nutrient cycle focused evaluation of the area should be conducted based on the built SWAT+ model. Building on this study, a nitrate calibration of the catchment could therefore be carried out in a next step.

With regard to the provisioning ES quantitative groundwater recharge, the data suggested that the evaporative demand was the ruling factor in differences between juvenile and mature stocks: The higher the demand, the more pronounced was the deviation between the stocking types, due to the higher stand transpiration under mature conditions, when in total more water was extracted from deeper soil layers.

With close to open field conditions, less precipitation is held back and stored for interception by the canopy (Rakei et al. 1992). By buffering and retarding the precipitation water, fully developed canopies soften the flow regime, and thus water contribution to streams and groundwater in magnitude and time. The simulation showed the contrary effect with poorly developed canopies in case of very young tree ages: The contribution to streamflow slightly increased under the JUV scenario. With regard to the regulative ES water regulation, bringing about the benefit of flood protection, the differences in surface runoff remained quite constant between the scenarios in annual mean values. Although the absolute change in surface runoff is not considerably high in average, the short circuit of response to drainage indicated the potential of promoted overland flow generation from juvenile areas. Due to the detected short circuit drain reaction in the instance of elevated precipitation intensity and duration, and the kinematic wave character of overland flow, the spatial and temporal distribution patterns of the water inputs were found to rather rule the deviation here. The simulation suggests that with heavy storm events to occur more frequently in the future, the stocking type might make a difference in the generation of critical source areas for overland flow generation, contributing to a rise in the hydrograph of receiving waters to a certain degree. This particularly applies in case of additional soil compaction on juvenile stocks, considering the results shown in section 5.4, which is expected to result in a cumulative increase in surface runoff peaks.

In combination with the period from 1961 to 1971, the simulation revealed basic hydrological and climatic controlling factors, governing the magnitude of hydrological differences between juvenile and mature forest stocks. The interval between JUV and MAT was found to be the most pronounced with high evaporative demand due to rising air temperature, and at the same time less water inputs due to decreasing precipitation, as in 2010 to 2020. Interrelations between these drivers and the water balance parameters of nonlinear character are presumed. Generally, more precipitation levels out the retarding and storage effect of the canopy cover, and so does the gain

in infiltration of uncovered soil, as stand precipitation and outdoor precipitation approximate (Baumgartner & Liebscher 1990). With poor evaporative demand, as in case of the period from 1961 to 1971, softening the driver of hydrological circulation due to low temperatures, the scenarios converged. Besides the hydrological drivers precipitation and air temperature, the plant physiological factors canopy and root expression were found effective: The differences in water balance between both scenarios appeared to be the most significant, the younger the juvenile stock, the less dense the canopy cover has grown, and the less pronounced the roots have developed.
The artificial attempt is, though, not directly transferable to the given field conditions, since the proportion of juvenile stand areas in the total area is negligibly small (112 ha in total, compared to 22336.9 ha size of the entire Bobenthal2 catchment), and their distribution is irregularly embedded in permanent stocking areas (see **fig. 82**), so that cumulative effects of surface runoff volumes are less effective.

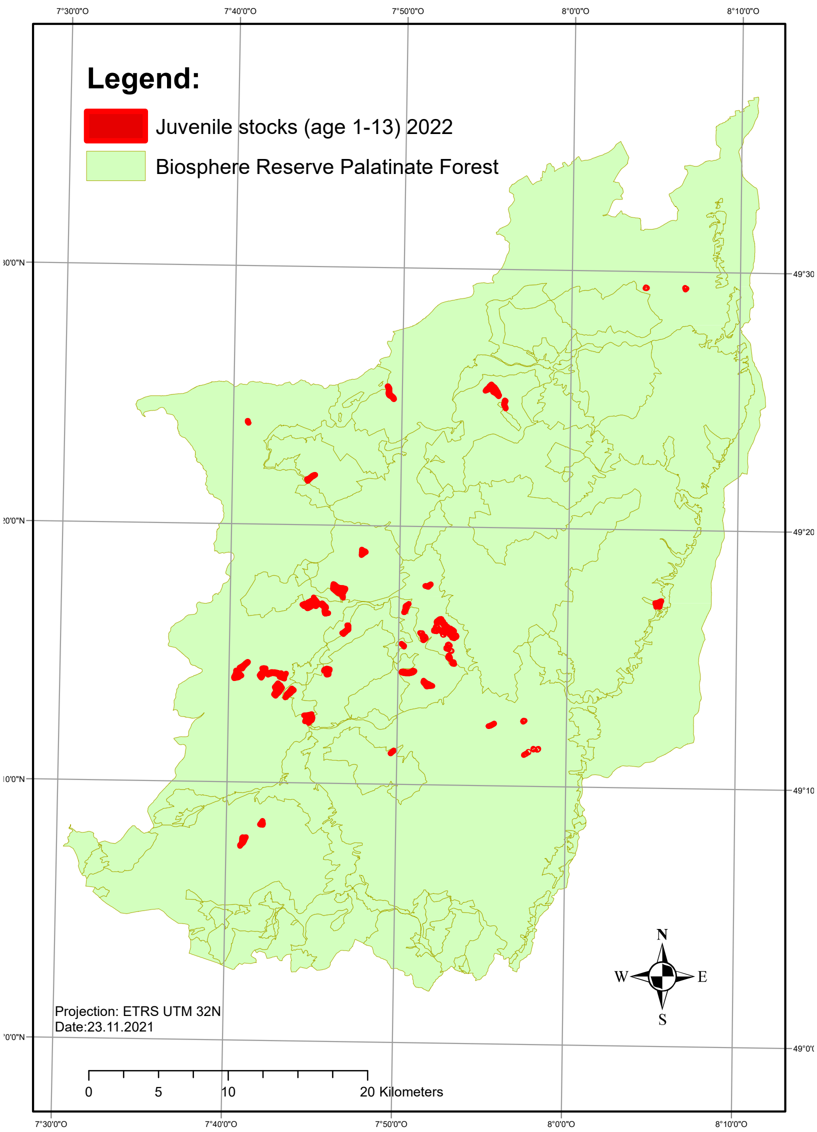

Figure 82: Distribution of juvenile stocks (age 3-13) in the Biosphere Reserve Palatinate Forest in 2019.

Furthermore, in reality, the growing ground vegetation rapidly competes with tree saplings for water, nutrients, and light (Urban Nilsson & Hällgren 1996; Craine & Dypzinski 2013; Kompa 2004), and also leads to quick closure of soil cover, as well as enhanced total stand ET (Pretzsch 2019; Schmaltz 1969 in Peck & Mayer 1969). During drought episodes, the understorey vegetation is even reported to be a main source of water depletion, while tree transpiration declines due to occasional stomatal closure (Gobin et al. 2015). Modeling the effects of rejuvenation under realistic conditions must therefore include the simulation of ground vegetation. This attempt can be pursued with SWAT+, using the incorporated plant community compilation application (Bieger et al. 2016), which allows for different plant types growing on the same stock, parametrized separately, so that a herb layer could be included, required plant data for parametrization given. Still, proofing the model sufficiency in simulating age-related differences in water balance lays the foundation, not only for further assessments of rejuvenation effects on a more realistic level in areas with a significant percentage of bare fallen sites. Also, an adaption aiming the evaluation of water-related effects of other forest management measures associated with gaps in canopy cover, such as thinning, can potentially be conceptualized. Although the approach followed here was artificial, the probability of bare falling areas with developing natural succession equivalent to the juvenile scenario is more likely to increase in number and spatial extent with aggravating conditions for pest and calamity development, windthrow, wild fires, and die off due to drought stress in the course of climate change. Changing climatic conditions, that affect the hydrological drivers described above, also influence the magnitude of differences between the stocking types: For a developing future with high expression in evaporative demand due to increasing air temperature, combined with scarce water availability and promoted drought phases throughout the vegetation period, as projected in the climate scenarios for RCP8.5 in the middle of the century (section **5.3**), the hydrological effect, or change signal, juvenile conditions show compared to mature is suggested to be most distinct. With both factors given, high precipitation and high evaporative demand, as predicted in the climate scenarios for the end of the century (section **5.3**), the leveling out effect is presumed to be counteracted by a rise in soil evaporation on juvenile stocks. With more water available for evaporative extraction at high demand, the deviation between the scenarios JUV and MAT is expected to increase again.

Besides reinforcing anthropogenic factors, rejuvenation is a viable natural phenomenon, which brings about evolutionary dynamics, such as genetic plasticity and adaptation, which also potentially enhance the response to changing climatic conditions and geographical distribution limits (Fady et al. 2016; Parmesan et al. 2003), and the progression of reorganization and renewal (Gunderson & Holling 2001). Due to the longevity of tree species, and the resulting disequilibrium with the rapid progression of climate change, maladaptation endangers not only the preservation of the forest itself, but also the provision of ES related to it. The strong selection during early life stages in the establishing phase is found to promote quicker genetic adaptation (Jump et al 2006; Muffler et al. 2021). In this regard, the catalyzing effects of rejuvenation on in-situ adaptation of forest composition to climate change can reduce the disequilibrium between tree species composition and changing climatic factors (Thom et al. 2018). The mitigation of negative consequence on water regulation of juvenile stand conditions in terms of increased runoff peaks with heavy storm events, especially when increasing in spatial extent, must be discussed with respect to silvicultural measures to enhance the retention potential of forest areas. The assessment of critical source areas (CSA) of overland flow generation must therefore move into focus to implement appropriate measures.

7 CONCLUSIONS

This study strived to assess water-related regulative and provisioning ES related to runoff regime and groundwater recharge in the Palatinate Forest Biosphere Reserve in south-west Germany using hydrological modelling with SWAT+. In order to depict the conditions of the study area, the SWAT+ model was modified regarding permanent forest specific plant parameters, calibrated and validated targeting the runoff regime (discharge), and adapted to the respective objectives.

The model setup for the meso-scale watershed confirmed SWAT+ capable of simulating the target issues of regulative and provisioning ES of the forest, based on their intermediate components related to water flow regulation, though development potential was identified pointing to future tasks in model adaption.

As indicators for the respective intermediate components, model internal parameters regarding water storage and buffer (retention), soil functions and stand structure were adjusted according to the given catchment conditions, and with regard to impacts of anthropogenic factors related to forest management, and climate change. SWAT+ was shown sensitive to the applied changes of the respective indicators, so that its capability to assess possible inductors of ES degradation is confirmed through the study. According to Ives & Messerli (1989), meso-scale watersheds are particularly vulnerable to anthropogenically induced ecosystem degradation. In this study, soil compaction due to driving with heavy machinery in the course of harvest operations, disrupted areas with rejuvenation as a result of either silvicultural management practices, or due to windthrow, pests and calamities in the course of climate change (also considered anthropogenic), as well as climate change itself as a major stressor for forest ecosystems were considered as potential risk factors for the degradation of water-related ES in the forest. For each of those influencing factors, separate scenarios were created and compared to the calibrated baseline model, representing current conditions based on field data (soil condition survey, forest inventory). All three influencing factors were found effective on the water balance of the forest, and thus on derived water-related ES.

The simulations revealed the sensitive character of forest-water-cycle-interactions, with regard to age-patterns related to differences in canopy expression, climate change, as well as deteriorated soil functions to a certain extent and spatial distribution. The sensitivity, and thus susceptibility for deterioration, of forests to the ecosystem conditions allows for the conclusion, that maintenance of the complex structure and intactness of its interrelations, especially with the given challenge climate change, urges for carefully adapted measures of conservation, efforts in the identification of CSA and their disposal, as well as preservation and reestablishment of the hydrological continuity in forest stands.

Overall, the simulation confirmed the favorable conditions forest provide for deep groundwater formation, and thus the provision with clean drinking water. With 177 mm/aa deep groundwater recharge (21.6 % of the average annual precipitation), the Palatinate Forest contributes significantly to the supply with drinking water for surrounding municipalities. Besides the favorable conditions of forests regarding water retention, water flow regulation, and undisturbed soil functions, the geological conditions of the Red Sandstone in the area favor rapid deep seepage of infiltration water, contributing to new groundwater formation.

Related to the high infiltration capacity of the pedological and geological properties of the Red Sandstone, as well as to the retarding and buffering influence of forest canopy cover on precipitation water, the forest was simulated to exhibit a significant mitigation effect on runoff generation: With 12.5 mm/aa (1.5 % of the average annual precipitation being transported overland), the forest has a strongly pronounced softening effect on area runoff volumes of kinematic character. As lateral flow accounts for 169 mm/aa, which is 20.6 % of the long-term average annual precipitation, the flow regime is dominated by a retarded discharge, and thus exhibits a profound contribution to decentral flood protection in magnitude and time. Nevertheless, elevated amounts of precipitation, exceeding the infiltration capacity of the sandy soils, were found to result in pronounced peaks in surface runoff in a short circuit drain reaction. Consequently, in the evaluation of enhancement measures for decentralized flood control, critical source areas for runoff generation in the forest are recommended to move into focus of forest management. It must be noticed, that this study did not cover chemical aspects of water-related ES, assessing the intactness of related intermediate components such as water purification, and nutrient regulation. In order to gain the complete picture of qualitative water-related ES of the forest, the indicators control of chemical compounds, their recycling, metabolization and storage, as well as absorption and filtering should be addressed in further attempts. Especially the fact of persisting inputs of excess nitrogen via air deposition in forest ecosystems urges for the assessment of consequences for related regulative and provisioning ES in qualitative terms.

Future climate projections

The international group of experts of the United Nations on climate change (Intergovernmental Panel on Climate Change, IPCC 2013, 2018), leaves no doubt about the influence of human activity on global climate development. In order to assess changes in the climate and their impact on human societies in the future, predictions about the future development of climate are sought through climate models, but their predictions are subject to uncertainties (Becker et al. 2008; Krähenmann 2019). In order to take account of the uncertainties, global climate models (GCMs) are combined with parametrized regional climate models (RCMs), but still important processes relevant to the climate, such as the formation of showers and thunderstorms (extensive convection with rapid vertical transport of heat and water vapor) or convective exchange processes between the atmosphere and the ocean pose challenges[22] . Furthermore, the SWAT+ model setup does not account for changes in the vegetation, as consequence of forest dieback due to changed climatic conditions, nor for changes in the soil properties that can be brought about by a changed vegetation cover.
Against this background of uncertainties, the results of hydrological modelling in the area must be considered limited in the representation of future developments. Nevertheless, basal hydrological interrelations and their effects on water-related ES of the forest can be concluded from the climate scenarios. They give incidence of potential fields of action for nowadays forest management, aiming the adaption of silviculture to the challenges the longevity of forest ecosystems brings about.

With forecasted higher evaporative demand and an extension of the vegetation period, resulting in elevated vegetation water consumption, and at the same time drought periods to occur more frequently, a negative water balance is reached far earlier in the year, and thus soil water depletion is expected to aggravate throughout the growing season. This does not only affect a shortening in water supply for trees, struggling with promoted drought stress and potential vitality decline alongside, but also shortens the period of groundwater replenishment, resulting in a decline in the provisioning ES groundwater formation, as forecasted for the middle of the century in both, RCP2.6 and RCP8.5 scenarios. With a rise in precipitation, as projected in case of RCP8.5 by the end of the century, groundwater storage depletion is predicted to recover, but still approximately equals groundwater formation volumes of the past only when considering maximum values.

[22] Efforts are intensified on statistical correction methods to minimize model errors using suitable, high-quality data sets Hyras; e.g. Rauthe et al., 2013; https://rcccm.dwd.de/DE/leistungen/hyras/hyras.html

Regarding the provisioning ES decentralized flood protection, the future scenarios simulated surface runoff to correlate with precipitation amounts, so that with a decreasing trend in precipitation, less surface runoff occurred, and with elevated rainfall by the end of the century (RCP8.5), a gain in surface runoff was predicted again. With heavy storm events to occur more frequently, and desiccated soils, exhibiting water repellency in drought periods, the contribution of overland flow to sudden rises in the hydrograph of receiving water bodies is expected to increase alongside. Considering the additional gain in surface runoff from current soil compaction, showing a slow regeneration potential, measures to increase the retention potential are indicated in order to maintain the high quality of water flow regulation in the forest.

Ultimately, a limited adaption capability of forest ecosystems to the rapidly progressing changes in global climate brings about the risk of forest die-back, with tremendous consequences for water-related ES. Consequently, in order to adapt silviculture to future challenges, forestry efforts must focus on strengthening the stand resilience (Landesforsten Rheinland-Pfalz 2020), as well as the hydrological continuity. Diversification in the form of a mixture of tree species tailored to the location and built upon the natural forest community, cushions the risks caused by climate change as broadly as possible (Cavers & Cottrell 2015, Hussendörfer 1996, Roloff & Grundmann 2008 in BfN 2020b). In accordance with current basic instructions (Landesforsten Rheinland-Pfalz 2020), natural succession should be complemented by point-effective plantings on damaged or bare areas, when natural regeneration does not perform sufficiently. Variability is an indispensable feature of the dynamics of biological systems that lead to adaptive change (cf. Mitchell 2008:55).

Despite all measures that are realized in current guideline, efforts for the improvement of the hydrological continuity with focus on maintaining the internal forest climate need to be intensified, in order to mitigate drought impacts (Müller & Schüler 2021).

Soil compaction

Modelling soil compaction with SWAT+ in a forested watershed was found to match the general expectations with regard to the magnitude of impacts on water balance components, water flow regulation, and derivable water-related ES, especially with respect to soil class differentiation in accordance with soil physics. The attempt to adjust soil bulk density in addition to the SCS Curve Number, which governs the infiltration process in SWAT+, was found expedient for a proper depiction of changed soil water flow response to compacted conditions. The favorable infiltration conditions of Red Sandstone given in the entire area were found to dominate the magnitude of impact on watershed level, resulting in moderate signs of deterioration for water-related ES as consequence of soil compaction.

Nevertheless, daily resolutions of contributions to streamflow from elevated amounts of surface runoff due to high precipitation inputs from pathways, as well as from skid trails and preloaded areas with clay and silt dominated soils, suggest actions to improve the retention potential. This can be achieved by directing the surface water away from the paths in order for it to reinfiltrate into the adjacent forest stands. Re-draining measures that help the runoff water from compacted areas to flow back into stocks are indicated for the skid trail system, as well as alternative, more soil-conserving harvesting methods such as cable crane routes, particularly on vulnerable areas (Gaumitz 1991; Gallus et al. 2007). Further flood contributing processes, such as direct runoff from water-bearing skid trails promoted by heavy machinery, need to be avoided and redraining measures, that help direct the excess water back into the adjacent forest stock, should be initialized (Landesforsten Rheinland-Pfalz 2018). Since ruts show a strong relationship with decreased forest productivity, their formation ought to be kept at a minimum (Schönauer et al. 2021). Also, felling practices that support residues to remain in the stock, help maintaining the basic habitat requirements of the soil biota, and the protection

of the mineral soil and organic matter.
This analysis supports the assumption that the vulnerability of soils to compaction increases with the percentage of silt and clay soil particles, which must be reflected in suitability maps for traffic. The use of forest machines should account for the pedological vulnerabilities in order to keep the traffic below an ecologically degenerative threshold. In addition to the substrate and previous load, this also includes the water content of the soil. From a hydrological, pedological and ecological point of view, priority must be given to concentrating on as few skid trails as possible. The accurate prediction of trafficability based on actual operating conditions, taking preloads and soil vulnerability into account, can minimize the negative impacts. It can be concluded, that driving with heavy harvest machinery should strictly follow the guidelines from the forest development handbook with respect to sandy substrates from weathered Red Sandstone. With increasing micro pores, as given in loamy and silty substrates, the use of heavy machinery must be restricted to the lowest possible level to no driving at all, especially in the case of high moisture soil conditions. In order to obtain predictability in the operational process and to keep the traffic below an ecologically degenerative threshold, trafficability maps that include cartographic knowledge of moist and therefore sensitive areas can be a supporting tool (Schönauer et al. 2021), and should be developed further. Substrate, pre-load and slope incline should also be implemented in a decision support system, as is currently being developed in an ongoing dissertation project at the FAWF[23] .

Disrupted areas with rejuvenation

The simulation allowed for the assumption that with undeveloped canopy cover, stand conditions suffer losses in their retarding effect on water flow regimes, which favors the generation of overland flow, and promotes higher leaching in quantitative terms. The latter is potentially counteracted by a deterioration of leachate in qualitative terms, as on unshaded forest floors the mobilization of excessive nutrients and their wash out enhances with direct exposure to sunlight. As an indication for rising soil temperatures on rejuvenated stocks, soil evaporation was shown to increase, the more profound, the less developed the crown cover, and the higher the evaporative demand of the atmosphere. The hydrological differentiation between closed canopy stands and close to open field conditions was found to be governed by the dominant factors atmospheric evaporative impetus and precipitation amounts, so that the following interrelations were identified: The higher the evaporative demand, the more scarce the water inputs to the system, and the less covered the canopy cover, the more pronounced is the hydrological impact of rejuvenated forest stands compared to mature stocking structures.
Though persistently dense areas that lead to a decoupling of the spreading rate are unfavorable (Block et al. 2016), closed stands and the maintenance of an intact inner forest climate are hydrologically of high priority, especially in stands with shade tree species such as beeches. Furthermore, growing herb layers increase the total stock transpiration. The additional water consumption can lead to a reduction of available soil water in dry periods within the vegetation period. At the same time, incident light on the forest floor increases not only the stand temperature, but also the water losses through soil evaporation (Müller & Schüler 2021). Especially in the course of climate change, species-specific demands on atmospheric moisture conditions need to be accounted for. In order to maintain a favorable water balance for beech stands, Hohnwald et al. (2020) suggest that they should be excluded from sites with current oak dominance, and conditions of shaded, closed canopies should be respected. When rejuvenating light tree species, such as oak, areas that meet the light-ecological requirements of these tree species should be limited to a sufficient extent.

[23] Contact person: I. Siebert

Additionally, for a future development with aggravating windthrow, pests and calamity pressure, bare falling areas may grow in number and extent, which urges for measures to increase the retention potential in the area.
In rejuvenation, the establishment of small-scale vertical structures, as well as temporal horizontal structures, with a high proportion of serving, regrowing trees (under and middle class) increases the hydrological effectiveness (Müller & Schüler 2021).
(Pre-) rejuvenation and mixed stands rich in deciduous trees fulfill their water protection functions over the long term, since the natural soil fertility, soil structure and biological activity (especially the macro pore promoting macrofauna) are preserved, and thus infiltration and retention capacity are enhanced (ibid.).

Due to their high genetic diversity, it is assumed that natural regeneration offers better conditions for the establishment of adapted tree individuals than artificial regeneration processes (Cavers & Cottrell 2015, Hussendörfer 1996, Roloff & Grundmann 2008 in BfN 2020b).

In all silvicultural interventions, special attention must be paid to maintaining or improving the forest interior climate and the soil water supply in order to buffer temperature extremes and reduce competition for water (Bolte & Ibisch 2007; Ellison et al. 2017, Vose et al. 2016 in BfN 2020b).

VI BIBLIOGRAPHY

AG Geologie (2021): Geologische Kartieranleitung. Available: https://www.geokartieranleitung.de/Fachliche-Grundlagen/Stratigraphie-Kartiereinheiten/Stratigraphie-der-Bundesrepublik/Tabellen-der-Bundesl%C3%A4nder/Rheinland-Pfalz/Perm (16.9.2021)

Albert, C., Burkhard, B., Daube, S., Dietrich, K., Engels, B., Frommer, J., Götzl, M., Gret-Regamey, A., Job-Hoben, B., Keller, R., Marzelli, S., Moning, C., Müller, F., Rabe, S.-E-, Ring, I., Schwaiger, E. Schweppe-Kraft, B., Wüstemann, H. (2015): Empfehlungen zur Entwicklung bundesweiter Indikatoren zur Erfassung von Ökosystemdienstleistungen – Diskussionspapier. BfN-Skripten, Bonn, Bad Godesberg. ISBN 978-3-89624-145-0

Amatya, D. M., Skaggs, R. W., & Gregory, J. D. (1995): Comparison of methods for estimating REF-ET. J. Irrig. Drain. Eng., DOI:10.1061/(ASCE)0733-9437(1995)121:6(427), 427–435.

Amatya, D.M. & Harrison, C.A. (2016): Case Study Grass and Forest Potential Evapotranspiration Com-parison Using Five Methods in the Atlantic Coastal Plain. J. Hydrol. Eng., 05016007, American Society of Civil Engineering, 2016. DOI: 10.1061/(ASCE)HE.1943-5584.0001341.

Ampoorter, E., de Schrijver, A., van Nevel, L., Hermy, M., Verheyen, K. (2012): Impact of mechanized harvesting on compaction of sandy and clayey forest soils: results of a meta-analysis. Annals of Forest Science (2012) 69:533-542; DOI: https://doi.org/10.1007/s13595-012-0199-y

Anderson, M.G., McDonnell, J.J. (2005): Encyclopedia of Hydrological Science. John Wiley & Sons Ltd., ISBN 13: 978-0-471-49103-9

Arbeitskreis Standortkartierung in der Arbeitsgemeinde Forsteinrichtung (1980): Forstliche Standortaufnahme. Landwirtschaftsverlag, 4th edition, 188 p.

Arnáez, J., Larrea, V., Ortigosa, L. (2004): Surface runoff and soil erosion on unpaved forest roads from rainfall simulation tests in northeastern Spain. Catena 57 (2004) 1-14

Arnold, J.G., Srinivasan, R., Muttiah, R.S., Williams, J.R. (1998): Large area hydrologic modeling and assessment part I: model development 1. JAWRA Journal of the American Water Resources Association, 34(1), pp.73-89.

Arnold, J.G. & Fohrer, N. (2005): SWAT2000: Current Capabilities and Research Opportunities in Applied Watershed Modelling. Hydrological Processes 19:563-572

Arnold, J., Chinnasamy, S., Di Luzio, M., Haney, E. B., Kannan, N., White, M. (2010): The HUMUS/SWAT National Water Quality Modeling System.

Arnold, J.G., Moriasi, D.N., Gassman, P.W., Abbaspour, K.C., White, M.J., Srinivasan, R., Santhi, C., Harmel, R.D., van Griensven, A., Van Liew, M.W., Kannan, N., Jha, M.K. (2012): SWAT: Model use, calibration, and validation. Trans. ASABE 55(4), 1491-1508.

Arnold, J.G., Youssef, M.A., Yen, H., White, M.J., Sheshukov, A.Y., Sadeghi, A.M., Moriasi, D.N., Steiner, J.L., Amatya, D.M., Skaggs, R.W., Haney, E.B., Jeong, J., Arabi, M., Gowda, P.H. (2015): Hydrological Processes and Model Representation: Impact of Soft Data on Calibration. Transactions of the ASABE 58 (6):1637-1660, DOI:10.1111/1752-1688.12524

Assmann, A. & H. Gündra (1999): Die Bedeutung integrierter Planungsverfahren für die Umsetzung dezentraler Hochwasserschutzmaßnahmen. Hydrol. u. Wasserbewirtsch., 43, pp. 160-164

Auerswald, K., Fiener, P., Dikau, R. (2009): Rates of sheet and rill erosion in Germany – A meta-analysis. Geomorphology 111 (2009) 182-193

Backes, C., Gallus, M., Schubert, G., Schüler, G., Vasel, R. (2007): Entschärfung von linearen Abflüssen durch vorsorgende Waldwegebautechnik. In: Schüler, G., Gellweiler, I. & Seeling, S. (eds.): Dezentraler Wasserrückhalt in der Landschaft durch vorbeugende Maßnahmen der Waldwirtschaft, der Landwirtschaft und im Siedlungswesen. Comm. from Research Institute for forest ecology and forestry (FAWF), No 64/07, 51-60.

Baffaut, C., John Sadler, E., Ghidey, F. & Anderson, S.H. (2015): Long-term agroecosystem research in the Central Mississippi River Basin: SWAT simulation of flow and water quality in the Goodwater Creek Experimental Watershed. J. Environ. Qual. 44, 84. DOI: http://dx.doi.org/10.2134/jeq2014.02.0068

Bailey, R.T., Park, S., Bieger, K., Arnold, J.G., Allen, P.M. (2020): Enhancing SWAT+ simulation of groundwater flow and groundwater-surface water interactions using MODFLOW routines. Environmental Modelling & Software, 126, p.104660.

Balazs, A. (1983): Interzeptionsverdunstung des Waldes im Winterhalbjahr als Bestimmungsgröße des nutzbaren Wasserdargebots. Contrib. Hydrology, special issue 4, pp. 79-102.

Barnard, J.D. (1948): Heat units as a measure of canning crop maturity. The Canner 106:28

Bartelink, H.H., Kramer, K., Mohren, G.M.J. (1997): Applicability of the radiation-use efficiency concept for simulating growth of forest stands. Agricultural and Forest Meteorology 88 (199), p. 169-179, DOI:10.1016/S0168-1923(97)00041-5

Bartsch, N. & Röhrig, E. (2016): Waldökologie. Einführung für Mitteleuropa. Springer Spektrum, 2nd edition, ISBN 978-3-662-44267-8.

Bateman, I.J., Mace, G.M., Fezzi, C., Atkinson, G., Turner, K. (2011): Economic analysis for ecosystem service assessments. Environmental and Resource Economics 48(2): 177–218.

Bauer, C. (2019): Anomalie Wasser. Diploma thesis, Institute for Experimental Physics, Karl-Franzens-University Graz.

Baumbach, G. (1993): Luftreinhaltung: Entstehung, Ausbreitung und Wirkung von Luftverunreinigungen; Messtechnik, Emissionsminderung und Vorschriften. Springer-Verlag Berlin Heidelberg GmbH, 3rd edition. ISBN 978-3-540-56823-0

Baumgartner, A. (1990): Verdunstung. In: Baumgartner, A. & Liebscher, H.-J. (1990): Lehrbuch der Hydrologie, Band 1: Allgemeine Hydrologie – Quantitative Hydrologie. Gebrüder Borntraegger, Berlin Stuttgart. ISBN 3-443-30001-4

Baumgartner, M., Hesse, B. D., Augustaitiene, I., Marozas, V., Mozgeris, G., Bycenkiene, S., Mordas, G., Pivoras, A., Pivoras, G., Juonyte, D., Ulevicius, V., Augistaitiene, A., Matyssek, R. (2019): Re-sponses of species-specific sap flux, transpiration and water use efficiency of pine, spruce and birch trees to temporarily moderate dry periods in mixed forests at a dry and wet forest site in the hemi-boreal zone; Journal of Agricultural Meteorology No 75, p. 13-19.

Baumgartner, A. & Liebscher, H.-J. (1990): Lehrbuch der Hydrologie, Band 1: Allgemeine Hydrologie – Quantitative Hydrologie. Gebrüder Borntraegger, Berlin Stuttgart. ISBN 3-443-30001-4

Bayer, B. & Schrader, S. (1997): Auswirkungen der Bodenbearbeitung und mechanischen Belastung im Ackerboden auf Milben und die biologische Bodenaktivität. Comm. German Soil Science Society 85 II, 469-472

Becker, P., Deutschländer T., Kossmann, M., Namyslo, J., Knierim, A. (2008): Klimaszenarien und Klimafolgen. Information on spatial development, Issue 6/7.2008

Beeger, H. et al., (1989): Die Landschaften von Rheinhessen-Pfalz – Benennung und räumliche Abgrenzung. In: Berichte zur deutschen Landeskunde (reports on German regional studies), Volume 63, Issue 2, pp. 327–359

Bennecke, P. (1992): Vorhersagbarkeit der Wasserbindungs- und Wasserleitfähigkeitsfunktion an bodenkundlichen Substratmerkmalen. In: Regionalisierung der Hydrologie (ed.: DFG), Ann. XI of Senate comm. Water research, VCH, Weinheim, pp. 221-239

Beven, K. (1981): Kinematic Subsurface Stormflow. Water Resources Research, Vol. 17, No 5, pp. 1419-1424. DOI: https://doi.org/10.1029/WR017i005p01419

Beven, K. (1982): On subsurface stormflow: an analysis of response times. Hydrol. Sci. J. 4: 505-521. DOI:10.1080/02626668209491129

Beven, K. (2012): Rainfall-Runoff Modelling - The Primer. John Wiley & Sons, Ltd, 2nd Edition. ISBN 978-0-470-71459-1

BfN - Federal Agency for Nature Conservation (2020a): Fachkonzept Biotpoverbund Gewässer und Auen. Background documents catalog of measures „Biotopverbund Blaues Band Deutschland“ and profile of measures „Biotopverbund Blaues Band Deutschland“ for the „Fachkonzept Biotopverbund Gewässer uns Auen“ in the federal program „Blaues Band Deutschland“. Specialist group, authors: Ehlert, T., Hees, M., Neikirchen, B., Riecker, T., Ritz, S. (BfN), Anlauf, A., Krempel, C., Lütz, M., Ondruch, P., Schuler, J. (BfG). Available: https://www.bfn.de/fileadmin/BfN/wasser/Dokumente/Blaues_Band/Blaues_Band_3_Massnahmen_Katalog_Steckbriefe_bf.pdf (3.4.2021)

BfN - Federal Agency for Nature Conservation (2020b): Wälder im Klimawandel: Steigerung von Anpassungsfähigkeit und Resilienz durch mehr Vielfalt und Heterogenität. Ein Positionspapier. 2nd corrected version, Bonn – Bad Godesberg, April 2020

Bieger, K., Hörmann, G., Fohrer, N. (2015): Detailed spatial analysis of SWAT-simulated surface runoff and sediment yield in a mountainous watershed in China. J. Hydrol. Sci., 60 (5) 2015. DOI: http://dx.doi.org/10.1080/02626667.2014.965172

Bieger, K., Arnold, J.G., Rathjens, H., White, M. J., Bosch, D.D., Allen, P.M., Volk, M., Srinivasan, R. (2016): Introduction to SWAT+, a Completely Restructured Version of the Soil and Water Assessment Tool. Journal of the American Water Resources Association (JAWRA) 53(1): 115– 130. DOI: doi.org/10.1111/1752-1688.12482

Biosphärenreservat Pfälzerwald-Nordvogesen (2021): https://www.pfaelzerwald.de (17.9.2021)

Block, J. (2006): Stickstoffbelastung der rheinland-pfälzischen Wälder. Comm. FAWF, 60, pp. 1-27

Block, J., Dieler, J., Gauer, J., Greve, M., Mosham-mer, R., Schuck, J. Schwappacher, V., Wunn, U. (2016): Gewährleistung der Nährstoffnachhaltigkeit der Nährstoffversorgung bei der Holz- und Biomassenutzung im Rheinland-Pfälzischen Wald. Comm. FAWF, Trippstadt No 79/16, 230 p. Available: http://www.fawf.wald-rlp.de/index.php?id=2601 (14.5.2021)

BMI - Federal Ministry of the Interior (2013): Bericht zur Flutkatastrohe 2013: Katastrophenhilfe, Entschädigung, Wiederaufbau. StabFH-51004/24#2.

BMU - Federal Ministry for the Environment, Nature Conservation and Reactor Safety (ed.) (2006): Wasserwirtschaft in Deutschland. Teil 2 - Gewässergüte. Berlin: BMU.

BMU - Federal Ministry for the Environment, Nature Conservation and Reactor Safety (ed.) (2008): Grundwasser in Deutschland. Reihe Umweltpolitik. Authors: C. Bannick, B. Engelmann, R. Fendler, J. Frauenstein, H. Ginzky, C. Hornemann, O. Ilvonen, B. Kirschbaum G. Penn-Bressel, J. Rechenberg, S. Richter, L. Roy, R. Wolter (UBA – Federal Environment Agency)

BMU & BfN - Federal Ministry for the Environment, Nature Conservation and Reactor Safety & Federal Agency for Nature Conservation (ed.) (2021): Auenzustandsbericht 2021.DOI 10.19217/brs211

BNatSchG – Bundesnaturschutzgesetz (2009): Gesetz über Naturschutz und Landschaftspflege. Bundesnaturschutzgesetz vom 29. Juli 2009 (BGBl. I S. 2542), last changed through Article 1 of the law from 18. August 2021 (BGBl. I S. 3908). Available: https://www.gesetze-im-internet.de/bnatschg_2009/BNatSchG.pdf (2.3.2021)

Bolte, A., & Ibisch, P.L. (2007): Neun Thesen zu Klimawandel, Waldbau und Naturschutz. AFZ-Der Wald 11/2007

Bordt, M., Saner, M.A. (2018): A critical review of ecosystem accounting and services frameworks. One Ecosystem 3: e29306. DOI: https://doi.org/10.3897/oneeco.3.e29306

Bosch, J.M. & Hewlett, J.D. (1982): A review of catchment experiments to determine the effect of vegetation changes on water yield and evapotranspiration. J. Hydrol. 55, 3–23. DOI: https://doi.org/10.1016/0022-1694(82)90117-2

Boswell, V.R. (1926): The influence of temperature upon the growth and yield of garden peas. Proc. Amer. Soc. Hort. Sci. 23:162-168

Bott, W. (2002): Prozessorientierte Modellierung des Wassertransports zur Bewertung von Hochwasserschutzmassnahmen in bewaldeten Entstehungsgebieten. Ph.D.-thesis, University Mainz. 114 pp.

Bottinelli, N., Hallaire, V., Goutal, N., Bonnaud, P., Ranger, J. (2014): Impact of heavy traffic on soil microporosity of two silty forest soils: Initial effect and short-term recovery. Geoderma 217-218 (2014) 10-17.

Boyd, J. & Banzhaf, S. (2007): What are ecosystem services? The need for standardized environmental accounting units. Ecological Economics 63(2–3): 616–626.

Brechtel, H.M. (1990): Interzeption. In: Baumgartner, A. & Liebscher, H.-J. (eds.) (1990): Lehrbuch der Hydrologie, Part 1, Berlin, Gebrüder Borntraeger, p. 313-326

Bréda, N., Huc, R., Granier, A., Dreyer, E. (2006): Temperate forest trees and stands under severe drought: a review of ecophysiological responses, adaptation processes and long-term consequences. Annals of Forest Science 63: 625-644.

Bredemeier, M., Cohen, S., Godbold, D.L., Lode, E., Pichler, V., Schleppi, P. (eds.) (2011): Forest Management and the water cycle. An Ecosystem-Based Approach. Ecological Studies 212. Springer Science+Buisness Media B.V. 2011. ISBN 978-94-007-1785-5

Brockerhoff, E.G., Barbaro, L., Castagneyrol, B., Forrester, D.I., Gardiner, B., Gonzalez-Olabarria, J.R., Lyver, P. O´B., Meurisse, N., Oxbrough, A., Taki, H., Thompson, I.D., van der Plas, F., Jactel, H. (2017): Forest biodiversity, ecosystem functioning and provision of ecosystem services. Biodivers Conserv, Springer Science+Buisness Media B-V. DOI:10.1007/s10531-017-1453-2

Brodribb, T. (1996): Dynamics of changing intercellular CO_2 concentration (ci) during drought and determination of minimum functional ci. Plant Physiol. (1996) 111:179-185

Broughton, W.C. (1989): A Review of the USDA SCS Curve Number Method. Aust. J. Soil Res., 1989, 27, 511-23

Brown, P.W. (2013): Heat Units. College of Agriculture and Life Science, AZ1602, 7 p.

Brumme, R. & Khanna, P.K. (eds.) (2009): Functioning and Management of European Beech 265 Ecosystems Ecological Studies 208, Springer-Verlag Berlin Heidelberg 2009. DOI:10.1007/978-3-642-00340-0_15

Brunet, J., Fritz, Ö. & Richnau, G. (2010): Biodiversity in European beech forests – A review with recommendations for sustainable forest management. Ecol. Bull. 53, 77-94.

Brunold, C., Rüegsegger, A., Brändle, R. (eds.) (1996): Stress bei Pflanzen. UTB Stuttgart, ISBN 978-3825281250.

BUMB - Federal Ministry for the Environment, Nature Conservation, Building and Nuclear Safety (2015): Den Flüssen mehr Raum geben. Renaturierung von Auen in Deutschland. Available: https://www.bmu.de/fileadmin/Daten_BMU/Pools/Broschueren/auen_in_deutschland_bf.pdf (4.6.2021)

Burschel, P. & Huss, J. (1997): Grundriß des Waldbaus: ein Leitfaden für Studium und Praxis. 487 p. 2nd, revised. and ext. edition Berlin. ISBN 978-3-8263-3045-2

Buscot, F., Varma, A. (2005): Microorganisms in Soils: Roles in Genesis and Functions. Springer Berlin Heidelberg New York. ISBN 3-540-22220-0

Butzen, V., Seeger, M., Wirtz, S., Huemann, M., Mueller, C., Casper, M., Ries, J. B. (2014): Quantification of Hortonian overland flow generation and soil erosion in a Central European low mountain range using rainfall experiments. Catena 113 (2014) 202-212.

Canessa, R., van den Brink, L., Saldana, A., Rios, R.S., Hättenschwiler, S., Mueller, C.W., Prater, I., Tielböger, K., Bader, M.Y. (2020): Relative effects of climate and litter traits on decomposition change with time, climate and trait variability. Journal of Ecology, 2021;190:447-458

Cermák, J., Matyssek, R., Kučera, J. (1993): Rapid response of large, drought-stressed beech trees to irrigation. Tree Physiol 12:281–290.

Chen, J., Saunders, S. C., Crow, T. R., Naiman, R. J., Brosofke, K. D., Mroz, G. D., Brookshire, B. L., Franklin, J. F. (1999): Microclimate in Forest Ecosystem and Landscape Ecology Variations in local climate can be used to monitor and compare the effects of different management regimes. BioScience Vol. 49 No 4

Chicharo, L., Müller, F., Fohrer, N. (2015): Ecosystem Services and River Basin Ecohydrology. Springer Dordrecht Heidelberg New York London. ISBN 978-94-017-9845-7, DOI 10.1007/978-94-017-9846-4

Choat, B., Jansen, S., Brodribb , T.J., Cochard, H., Delzon, S., Bhaskar, R., Bucci, S.J., Feild, T.S., Gleason, S.M., Hacke, U.G., Jacobsen, A.L., Lens, F.; Maherali, H., Martinez-Vilalta, J., Mayr, S., Mencuccini, M., Mitchel, P.J., Nardini, A., Pittermann, J., Pratt, R.B., Sperry, J.S., Westoby, M., Wright, I.J., Zanne, A.E. (2012): Global convergence in the vulnerability of forests to drought. Nature 491: 752-755.

Clausnitzer, F., Köstner, B., Schwärzel, K., Bernhofer, C. (2011): Relationships between canopy transpiration, atmospheric conditions and soil water availability—Analyses of long-term sap-flow measurements in an old Norway spruce forest at the Ore Mountains/Germany. Agricultural and Forest Meteorology 151 (2011) 1023–1034. DOI:10.1016/j.agrformet.2011.04.007

Chow, V. T. (1959): Open-channel Hydraulics, Mc-Graw Hill, New York, p. 607.

Cochard, H., Bréda, N., Granier, A. (1996): Whole tree hydraulic conductance and water loss regulation in Quercus during drought: evidence for stomatal control of embolism? Annales des sciences forestières, INRA/EDP Science, 1996, 53 (2-3), pp. 197-206. Available: https://hal.archives-ouvertes.fr/hal-00883043 (6.8.2021)

Collet, C., Löf, M., Pages, L. (2005): Root system development of oak seedlings analysed using an architectural model. Effects of competition with grass. Plant and Soil (2006) 279:367-383. DOI:10.1007/s11104-005-2419-9

Costanza, R., dArge, R., de Groot, R., Farber, S., Grasso, M., Hannon, B., Limburg, K., Naeem, S., Oneill, R.V., Paruelo, J., Raskin, R.G., Sutton, P., van den Belt, M. (1997): The value of the world's ecosystem services and natural capital. Nature 387 (6630), 253–260.

Costanza, R. de Groot, R., Braat, L., Kubiszewski, I., Fioramonti, L., Sutton, P., Farber, S., Grasso, M. (2017): Twenty years of ecosystem services: How far have we come and how far do we still need to go? Ecosystem Services 28, 1-16, Elsevier B.V. 2017

Craine, J. M., Dybzinski, R. (2013): Mechanisms of plant competition for nutrients, water and light. Functional ecology, British Ecology Society. DOI:10.1111/1365-2435.12081

Croke, J. C., Hairsine, P. B. (2006): Sediment delivery in managed forests: a review. Environ. Rev. 14: 59-87 (2006). DOI:10.1139/A05-016

Czihak, G., Langer, H. & Ziegler, H. (eds.) (1996): Biologie. Ein Lehrbuch. 6th unchanged edition, Springer, Berlin – Heidelberg – New York 1996, S. 420–424.

Danacova, M., Valent, P., Vyleta, R., Hlavcova, K. (2017): The effects of rainfall on surface runoff and soil erosion from forested areas. Conference paper, Section Forest Ecosystems.

Daily, G.C. (1997): Nature's Services: Societal Dependence on Natural Ecosystems. Island Press, Washington D.C.

Davie, T. (2002): Fundamentals of Hydrology. Routledge London and New Yorl, 2nd edition. ISBN13: 978–0–415–39986–9

Dehner, U., Renger, M., Bräunig, A., Lamparter, A., Bauriegel, A., Burbaum, B., Hartmann, K.-J., Hennings, V., Idler, F., Krone, F., Martin, W., Meyer, K., Waldmann, F. (2015): Neue Kennwerte für die Wasserbindung in Böden. Contribution to the annual conference of the DBG (German Soil Society) "Unsere Böden - Unser Leben". Available: http://www.dbges.de (5.6.2021)

Delphis, F.L., Carlyle-Moses, D., Tanaka, T. (eds.) (2011): Forest Hydrology and Biogeochemistry. Synthesis of Past Research and Future Directions. ISBN 978-94-007-1362-8, DOI 10.1007/978-94-007-1363-5

del Rio, M., Schütze, G., Pretzsch, H. (2014): Temporal variation of competition and facilitation in mixed species forests in Central Europe. Plant Biology 16 (2014) 166–176. DOI:10.1111/plb.12029

Dixon, R.K., Solomon, A.M., Brown, S., Houghton, R.A., Trexier, M.C., Wisniewski, J. (1994): Carbon Pools and Flux of Global Forest Ecosystems. Science 263, 185–190. DOI: http://dx.doi.org/10.1126/science.263.5144.185.

Dobler, L., Hinterding, A., Gerlach, N. (2004): INTERMET – Interpolation stündlicher und tagesbasierter meteorologischer Parameter. Complete documentation. State Office for Water Management Rhineland-Palatinate.

Doerr, S. H., Shakesby, R. A., Walsh, R. P. D. (2000): Soil water repellency: its causes, characteristics and hydro-geomorphological significance. Earth-Science Reviews 51 (2000) 33-65. DOI: https://doi.org/10.1016/S0012-8252(00)00011-8

Duursma, R.A., Kolari, P., Perkämäki, M., Nikinmaa, E., Hari, P., Delzon, S., Loustau, D., Ilvesniemi, H., Pumpanen, J., Mäkelä, A. (2008): Predicting the decline in daily maximum transpiration rate of two pine stands during drought based on constant minimum leaf water potential and plant hydraulic conductance. Tree Physiology 28, pp. 265-276

DWD – German Weather Service (ed.) (1957): Klima-Atlas von Rheinland-Pfalz. Verlag Deutscher Wetterdienst, Bad Kissingen 1957, pp 6 f.

EASAC – European Academies Science Advirory Council (2017): Multi-functionality and sustainability in the European Union´s forests. German National Academy of Science Leopoldina 2017. ISBN 978-3-8047-3728-0

Eastaugh, C. S., Rustomji, P. K., Hairsine, P. B. (2007): Quantifying the altered hydrologic connectivity of forest roads resulting from decommissioning and relocation. Hydrological Processes 22, 2438-2448 (2008).

Eder, W. (1984): Quantification of pedological site factors as a basis for performance-related site mapping, especially on Buntsandstein sites in the Palatinate. Mainz, 1980. 263 p. Notifications from forest management and silviculture (23). Approved. Dissertation. Göttingen.

Eder, W. & Dong, P.H. (2003): Vorläufige Referenztafeln für die Forsteinrichtung. Institute of forest ecology and forestry (FAWF), unpublished.

EEA – European Environmental Agency (2015): Water-retention potential of Europe's forests. A European overview to support natural water-retention measures. EEA Technical Report No 13/2015, ISSN 1725-2237

Ehleringer, J.R. & Cerling, T.E. (1993): Atmospheric CO_2 and the ratio of intercellular to ambient CO_2 concentrations in plants. Tree Physiology 15, 105-111, Heron Publishing, Victoria, Canada

Ehrlich, P.R. & Mooney, H.A. (1983): Extinction, substitution, and ecosystem services. Bioscience 33 (4), 248–254.

El-Khoury, A., Seidou, O., Lapen, D.R., Que, Z., Mohammadian, M., Sunohara, M., Bahram, D. (2015): Combined impacts of future climate and land use changes on discharge, nitrogen and phosphorus loads for a Canadian river basin. J. Environ. Manag. 151, 76–86. DOI: http://dx.doi.org/10.1016/j.jenvman.2014.12.012.

Ellenberg, H. (1996): Vegetation Mitteleuropas mit den Alpen in ökologischer, dynamischer und historischer Sicht. 5th strongly revised edition, Ulmer, Stuttgart.

Ellenberg, H. & Leuschner, C. (2010): Vegetation Mitteleuropas mit den Alpen. 6th edition, Eugen, Ulmer, Stuttgart. ISBN 978-3-8252-8104-5

Engman, E.T. (1983): Roughness coefficient for routing surface runoff. Proc. Spec. Conf. Frontiers of Hydraulic Engeneering.

EPA – United Staes Environmental Protection Agency (2009): Guidance on the Development, Evaluation, and Application of Environmental Models. Office of the Science Advisor, Council for Regulatory Environmental Modelling, EPA/100/K-09/003 I March 2009.

Erdmann, K.-H. (1995): Biosphärenreservate in Deutschland – Leitlinien für Schutz, Pflege und Entwick-lung. Springer, 377 p.

Ernstberger, H. (2000): Fernerkundung sensibler Niederschlagsflächen im Einzugsgebiet der Nahe auf der Grundlage der Niederschlags-Abflussgleichung. Report IRMA II A3, self-publishing of the State Office for Water Management Rhineland-Palatinate, 17 p. + App.

Eser, U., Neureuther, A.-K., Seyfang, H., Müller, A. (2014): Prudence, justice and good life. A typology of ethical reasoning in selected European national biodiversity strategies. Bfn, Bonn 2014. ISBN 978-3-944811-00-0, (19.3.2020)

EU - European Commission (2011): Our life insurance, our natural capital: an EU biodiversity strategy to 2020. Communication from the Commission to the European Parliament, the Council, The Economic and Social Committee and the Committee of the Regions (COM (2011) 244 final). (ENBS). (7.3.2021).

EU – European Union (2014): Study on Economic and Social Benefits of Environmental Protection and Resource Efficiency Related to the European Semester. Final Report, February 2014, ENV.D.2/ETU/2013/0048r. Authors: Fenn, T., Fleet, D., Garrett, L., Daly, E., Elding, C., Hartman, M., Udo, J.: J834/EU Semester; DOI:10.2779/76964

Eugster, W, & Haeni, M. (2013): Nutrients or Pollutants? Nitrogen Deposition to European Forests. Department of Environmental Systems Science, Institute of Agricultural Sciences, ETH Zürich, Zürich, Switzerland. Available: http://homepage.usys.ethz.ch/~eugsterw/publications/pdf/Eugster-Haeni-COST-Book-FINAL.pdf (25.2.2021)

Ewers, B.E., Oren, R., Phillips, N., Strömgren, M., Linder, S. (2001): Mean canopy stomatal conductance responses to water and nutrient availabilities in Picea abies and Pinus taeda. Tree Physiology 21, pp. 841-850.

Fabiánek, T., Mensík, L., Tomásková, I., Kulhavý (2009): Effects of spruce, beech and mixed commercial stand on humus conditions of forest soils. Journal of Forest Science, 55, 2009 (3): 119–126.

Fady, B., Aravanopoulos F.A., Alizoti P., et al. (2016): Evolution-based approach needed for the conservation and silviculture of peripheral forest tree populations. Forest Ecology and Management (2016), 375:66 – 75. DOI: http://dx.doi.org/10.1016/j.foreco.2016.05.015

FAO - Food and Agriculture Organization of the United Nations (2015): Global forest resources assessment 2015. FAO, Rome

Faramarzi, M., Srinivasan, R., Iravani, M., Bladon, K.D., Abbaspour, K.C., Zehnder, A.J., Goss, G.G. (2015): Setting up a hydrological model of Alberta: data discrimination analyses prior to calibration. Environ. Model. Softw. 74, 48–65.

Fass, H. J. (1995): Streuabbau – Waldkalkung. Diploma Thesis Univ. Trier, 127 S., Trier

FAWF – Forschungsanstalt für Waldökologie und Forstwirtschaft (2012): Waldbodenzustand in Rheinland-Pfalz. Ergebnisse der zweiten landesweiten Bodenzustandserhebung BZE II. Ann. o. FAWF Rhineland-Palatinate, No 70/12

Fernández, V., Bahamonde, H.A., Peguero-Pina, J.J., Gil-Pelegrin, E., Sacho-Knapik, D., Gil, L., Goldbach, H.E., Eichert, T. (2017): Physico-chemical properties of plant cuticles and their functional and ecological significance. Journal of Experimental Botany, Vol. 68, No 19 pp. 5293–5306. DOI:10.1093/jxb/erx302

Fiedler, H.J. (2001): Böden und Bodenfunktionen in Ökosystemen, Landschaften und Ballungsgebieten. Expert Verlag, ISBN 3-8169-1875-1

Fisher, B., Turner, R.K., Morling, P. (2009): Defining and classifying ecosystem services for decision making. Ecological Economics 68(3): 643–653.

Fohrer, N. (ed.), Bormann, H., Miegel, K., Casper, M., Bronstert, A., Schumann, A., Weiler, M. (2016): Hydrologie. Utb. ISBN: 978-3-8252-4513-9

Forest Site Survey (1980): Forstliche Standortaufnahme: Begriffe, Definitionen, Kennzeichnungen, Erläuterungen. Landwirtschaftsverlag, 4th edition. Münster-Hiltrup, 188 p.

Forest Site Survey (2016): Forstliche Standortaufnahme: Begriffe, Definitionen, Kennzeichnungen, Erläuterungen. 7th edition, IHW-Verlag, 400 p., ISBN 9783930167807

Francesconi, W., Srinivasan, R., Perez-Minana, E., Willock, S.P., Quintero, M., (2016): Using the soil and Water Assessment Tool (SWAT) to model ecosystem services: A systematic review. Journal of Hydrology 535, p. 625-636. DOI: http://dx.doi.org/10.1016/j.jhydrol.2016.01.034

Frossard, E., Blum, W. E. H., Warkentin, B. P. (2006): Function of Soils for Human Societies and the Environment. Geological Society Special Publications No 266, London. ISBN 13: 978-1-86239-207-6

Fründ, H.-C. & Averdiek, A. (2016): Soil aeration and soil water tension in skidding trails during three years after trafficking. Forest Ecology and Management 380 (2016) 224–231.

Gallus, M., Ley, M., Schubert, D., Schüler, G., Segatz, E. & Werner, W. (2007): Renaturierung von Hangbrüchern im Hunsrück zur Glättung von Abflussspitzen. In: Schüler, G., Gellweiler, I. & Seeling, S. (eds.): Dezentraler Wasserrückhalt in der Landschaft durch vorbeugende Maßnahmen der Waldwirtschaft, der Landwirtschaft und im Siedlungswesen. Comm. from Research Institute for Forest Ecology and Forestry (FAWF), No 64/07, 337 p.

Garamszegi, B. & Kern, Z. (2014): Climate influence on radial growth of Fagus sylvatica growing near the edge of its distribution in Bükk Mts., Hungary. Dendriobiology, Okt. 2014; DOI: 10.12657/denbio.072.008

Garbulsky, M.F., Penuelas, J., Papale, D., Ardö, J., Goulden, M.L., Kiely, G., Richardson, A.D., Rotenberg, E., Veendaal, E.M., Filella, I. (2010): Patterns and controls of the variability of radiation use efficiency and primary productivity across terrestrial ecosystems. Global Ecol. Biogeogr. (2010) 19, pp. 253-267. DOI: https://doi.org/10.1111/j.1466-8238.2009.00504.x

Gassman, P.W., Reyes, M., Green, C.H., Arnold, J.G. (2007): The Soil and Water Assessment Tool: Historical development, applications, and future directions. Trans. ASABE 50(4), 1211-1250.

Gaumitz, B. (1991): Festlegung von Seil(kran) trassenabständen bei der Walderschließung. Contr. f. Forestecol., 25, 185-188

Geiger, M. (ed.) (1987): Der Pfälzerwald, Portrait einer Landschaft. Landau i.d. Pfalz, Verl. Pfälz. Landeskunde. ISBN 978-39801-1471-4.

Gilman, E.F. (1990): Tree growth and development. I. Form, Spread, Depth and Periodicity. J. Environ. Hort. 8(4):215-2020. DOI:10.24266/0738-2898-8.4.215

Glaser, R., Hauter, C., Faust, D., Glawion, R., Saurer, H., Schulte, A., Sudhaus, D. (2017): Physische Geographie kompakt. Springer Spektrum. ISBN 978-3-662-50460-4

Gobin, R., Korboulewsky, N., Dumas, Y., Balandier, P. (2015): Transpiration of four common understorey plant species according to drought intensity in temperate forests. Annals of Forest Science (2015) 72:1053–1064, DOI:10.1007/s13595-015-0510-9

Godbold, D.L., Hüttermann, A. (1994): Effects of acid rain on forest processes. Wiley-Liss, a John Wiley & Sons, Inc., Publication.

Goulden, M.L. & Bales, R.C. (2019): California forest die-off linked to multi-year deep soil drying in 2012–2015 drought. Nature Geoscience, 12. DOI: 10.1038/s41561-019-0388-5

Gower, S.T., Kuchari, C.J., Norman, J.M. (1999): Direct and indirect estimation of leaf area index, ƒAPAR, and net primary production of terrestrial ecosystems. Remote Sens. Environ. 70:29-51, DOI: https://doi.org/10.1016/S0034-4257(99)00056-5

Grant, G.E. (2005): The role of forests and forest harvest on floods: myths and realities. Presentation at the XXII IUFRO World Congress, Brisbane, Australia. Int. For. Rev. 7, 5: 311

Grassi, G. & Magnani, F. (2005): Stomatal, mesophyll conductance and biochemical limitations to photosynthesis as affected by drought and leaf ontogeny in ash and oak trees. Plant, Cell and Environment (2005) 28, pp. 834-849.

Green, W.H. & Ampt, G.A. (1911): Studies on soil physics — 1: The flow of air and water through soils. J. Agric. Sci. 4: 11–24.

Greiffenhagen, A. (2005): Einfluss der Humusauflage auf das Benetzungsverhalten und den Wasserhaushalt von Kiefernstandorten. Dissertation TU Berlin, ISSN 0930-7787

Grigal, D.F. & Vance, E.D. (2000): Influence of soil organic matter on forest productivity. New Zealand Journal of Forestry Science 30(1/2): 169-205

Groan, T. (2008): https://de.wikivoyage.org/wiki/Pf%C3%A4lzerwald#/media/Datei:Karte_Pf%C3%A4lzerwald.png (3.4.2021)

Gruba, P. & Mulder, J. (2014): Tree species affect cation exchange capacity (CEC) and cation binding properties of organic matter in acid forest soils. Science of the Total Environment 511 (2015) 655–662. DOI: http://dx.doi.org/10.1016/j.scitotenv.2015.01.013

Grunert, J. & D. König (2000): Hochwassermanagement in Entstehungsgebieten – Vorsorge aus forstlicher und wasserwirtschaftlicher Sicht. Hier: Empirische Untersuchungen im Testgebiet „Thiergarten/Reichenbach“. Interim report Univ. Mainz, Forest Laboratory (Forstl. Versuchsanstalt) Rhineland- Palatinate, 5 p. (unpublished)

GTOS - Global Terrestrial Observing System (2009): LAI. Assessment of the status of the development of the standards for the terrestrial essential climate variables. GTOS 66.

Gunderson, L.H., Holling, C.S. (2001): Panarchy: Understanding Transformations in Human and Natural Systems. Island Press; Washington, Covelo, London.

Guse, B., Kiesel, J., Pfannerstill, M. and Fohrer, N. (2020): Assessing parameter identifiability for multiple performance criteria to constrain model parameters. Hydrological Sciences Journal, 65(7), pp.1158-1172.

Haas, M.B., Guse, B., Pfannerstill, M. and Fohrer, N. (2016): A joined multi-metric calibration of river discharge and nitrate loads with different performance measures. Journal of Hydrol., 536, pp.534-545.

Hager, H. (1988): Stammzahlreduktion: Die Auswirkungen auf Wasser-, Energie- und Nährstoffhaushalt von Fichtenjungwüchsen. Forest publication series, Univ. Vienna, soil science, Vol. 1.

Hahn, H.J., Bauer, A., Friedrich, E. (eds.) (2000): Wasser im Biosphärenreservat Naturpark Pfälzerwald. Results of the interdisciplinary conference from July 10th to 12th, 1999 at the University of Landau. Institute for regional environmental research and environmental education (IFU), Landau. ISBN 3-9807170-0-3

Hailer, N. (1971): Die natürlichen Vegetationsgebiete. In: Alter, W.: Pfalzatlas, Text band II. Speyer

Haines-Young, R. & Potschin, M. (2010): The links between biodiversity, ecosystem services and human well-being. In: Raffaelli, D.G. & Frid, C.L.J. (eds.): Ecosystem ecology: a new synthesis. Cambridge University Press, Cambridge, pp 110–139

Hammel, K. & Kennel, M. (2001): Charakterisierung und Analyse der Wasserverfügbarkeit und des Wasserhaushalts von Waldstandorten in Bayern mit dem Simulationsmodell Brook90. Forest Research Report, München, 185

Haneke, J. & Weidenfeller, M. (2010): Die geologischen Baueinheiten der Pfalz. In: Geiger, M. et al. (eds.): Geographie der Pfalz. Verlag Pfälzische Landeskunde, Landau/Pf., 81 p.

Hansen, J., Mki. Sato, R., Ruedy, K., LoD. W. Lea, Medina-Elizade, M. (2006): Global temperature change. Proc. Natl. Acad. Sci. 103, S. 14288-14293.

Hansjürgens, B., Nesshöver, C., Schniewind, I. (2012): Der Nutzen von Ökonomie und Ökosystemdienstleistungen für die Naturschutzpraxis. Workshop I: Einführung und Grundlagen. BfN-Skripten 318, Bonn-Bad Godesberg 2012, ISBN 978-3-89624-053-8, 2nd edition

Hargreaves, G.H. & Samadi, Z.A. (1982): Estimating potential evapotranspiration. J. Irrig. Drain. Div., 1982, Vol. 108, Issue 3, pp. 225-230

Hargreaves, G.L., Hargreaves, G.H., Riley, J.P. (1985): Agricultural benefits for Senegal River Basin. J. Irrig. Drain. Eng. 111(2): 113–124. DOI: http://dx.doi.org/10.1061/(ASCE)0733-9437(1985)111:2(113)

Hartge, K.H. & Horn, R. (1992): Die physikalische Untersuchung von Böden. Stuttgart, 177 p., 3rd edition. ISBN 9783432821238.

Hayes, F. & Bangor, C.E.H. (2017): Mapping critical levels for vegetation. UNECE International Cooperative Program on Effects of Air Pollution on Natural Vegetation and Crops. Available: https://unece.org/fileadmin/DAM/env/documents/2017/AIR/EMEP/Final__new_Chapter_3_v2__August_2017_.pdf (6.3.2021).

Heath, R. (1983): Basic Ground-Water Hydrology. U.S. Geological Survey Water-Supply Paper 2220, 86 p.; ISBN 0-607-68973-0

Hedwall, P.-O., Grip, H., Linder, S., Lövdahl, L., Nilsson, U., Bergh, J. (2013): Effects of clear-cutting and slash removal on soil water chemistry and forest-floor vegetation in a nutrient optimised Norway spruce stand. Silva Fennica vol. 47 No 2, article id 933, 16 p.

Heitele, H. (1993): Das Buntsandsteinprofil bei Landstuhl und seine Gliederung in Grundwasser-stockwerke. Mainz geoscience announcements 22, pp. 39-56, Mainz

Helvey, J.D. (1964): Rainfall interception by hardwood forest litter in the southern Appalachians. U.S. Forest Service Reseach Paper SE-8, Department of Agriculture, Forest Service, North Carolina.

Hesse, B., Goisser, M., Hartmann, H., Grams, T.E.E. (2018): Repeated summer drought delays sugar export from the leaf and impairs phloem transport in mature beech. Tree Physiology OO, 1-9

Hewlett, J.D., Lull, H.W., Reinhart, K.G. (1969): In defence of experimental watersheds. Water Resour. Res., 5(1): 306--316. DOI:10.1029/WR005I001P00306

Hermann, F., Chen, S., Kunkel, R. und Wendland, F. (2014): Auswirkungen von Klimaänderungen auf das nachhaltig bewirtschaftbare Grundwasserdargebot und den Bodenwasserhaushalt in Nordrhein-Westfalen. Research Center Jülich Institute for Bio- and Geosciences (IBG-3: Agrosphere)

Hibbert, A.R. (1967): Forest treatment effects on water yield. In: W.E. Sopper & H.W. Lull (eds), Int. Syrup. For. Hydrol., Pergamon, Oxford, 813 pp.

Hiege, W. (1985): Wasserhaushalt von Forsten und Wäldern und der Einfluss des Wassers auf Wachstum und Gesundheit von Forsten und Wäldern: eine Literaturstudie. Water management Nature Forest and Landscape, Utrecht. Available: https://edepot.wur.nl/515294 (21.12.2021)

Hildebrand, E. E. (1983): Der Einfluß der Bodenverdichtung auf die Bodenfunktionen im forstlichen Standort. Forestry Scien. Cbl. 102/2, 111 – 125

Hildebrand, E.E. (1996): Forstliche Bodenbewirtschaftung. In: Handbuch der Bodenkunde, Loseblatt-Ausgabe, Landsberg/Lech, 1-20

HLUG - Hessian State Agency for Nature Conservation, Environment and Geology (2020): Gewässerkundlicher Jahresbericht 2020. Hydrology in Hessian, Issue 23. ISBN 978-3-89026-723-4.

Höll, K. (2002): Wasser – Nutzung im Kreislauf, Hygiene, Analyse und Bewertung. Walter de Gruyter Berlin, New York, 8th Edition. ISBN 3-11-012931-0.

Hörmann, G., Fohrer, N., Kluge, W. (2014): Modelle zum Wasserhaushalt. V - 3.2 Ökosystemare Modelle und Partialmodelle. In: Schröder, W., Fränzle, O., Müller, F. (eds.) (2014): Handbuch der Umweltwissenschaften. ISBN 9783527321445. Wiley-VCH Verlag GmbH & Co. KGaA.

Hoffmann, D. (1980): Der Einfluß von Bestockungsunterschieden (Baumart, Bestockungsdichte) auf den Wasserhaushalt des Waldes und seine Wasserspende an die Landschaft. Completion report to the DFG research project. 304 p., 3 pcs. (unpublished).

Hoffmann, H.-D. (1982): Die Interzeption einer Fichtenstreudecke im Freiland und im Bestand. In: Wasser aus dem Wald, Wasser für den Wald (eds.: De Haar, U. & Hoffmann, D.). Contribution to hydrology, Kirchzarten, pp. 103-116.

Hohnwald, S., Indreica, A., Walentowski, H., Leuschner, C. (2020): Microclimatic Tipping Points at the Beech–Oak Ecotone in the Western Romanian Carpathians. Forests 2020, 11, 919; doi:10.3390/f11090919

Holvoet, K., van Griensven, A., Gevaert, V., Seuntjens, P., Vanrolleghem, P.A. (2008): Modifications to the SWAT code for modelling direct pesticide losses. Environ. Model. Softw. 23, 72–81. DOI: http://dx.doi.org/10.1016/j.envsoft.2007.05.002

Horn, R., Doma, H., Sowiska-Jurkiewicz, A., Van Ouwerkerk, C. (1995): Soil compaction processes and their effects on the structure of arable soils and the environment. Soil Till Res 35:23–36

Horton, R.E. (1933): The Role of Infiltration in the Hydrologic Cycle. Transactions of the American Geo-physical Union, 14, 446-460. DOI: http://dx.doi.org/10.1029/TR014i001p00446

HUANG, C.-Y., ANGEREGG, W.R.L., ASNER, G.P. (2019): Remote sensing of forest die-off in the Anthropocene: From plant ecophysiology to canopy structure. Remote Sensing of Environment 231 (2019) 111233, Elsevier Inc. DOI: https://doi.org/10.1016/j.rse.2019.111233

IBISCH, P., KREFT, S., LUTHARDT, V. (eds.) (2012): Regionale Anpassung des Naturschutzes an den Klimawandel: Strategien und methodische Ansätze zur Erhaltung der Biodiversität und Ökosystemdienstleistungen in Brandenburg. Eberswalde University for Sustainable Development, ISBN 978-3-00-038210-9

IPCC – INTERGOVERNMENTAL PANEL ON CLIMATE CHANGE (1990): Climate Change – the IPPC Scientific Assessment. HOUGHTON, F.T., JENKINS, G.J., EPHRAUMS, J.J. (eds.); Cambridge University Press, Cambridge UK.

IPCC– INTERGOVERNMENTAL PANEL ON CLIMATE CHANGE (2007): Climate Change 2007: Impacts, Adaptation and Vulnerability. Contribution of Working Group II to the Fourth Assessment Report of the Intergovernmental Panel on Climate Change, M.L. PARRY, O.F. CANZIANI, J.P. PALUTIKOF, P.J. VAN DER LINDEN AND C.E. HANSON (eds.), Cambridge University Press, Cambridge, UK, 976pp.

IPCC – INTERGOVERNMENTAL PANEL ON CLIMATE CHANGE (2013): Climate Change 2013: The Physical Science Basis. Contribution of Working Group I to the Fifth Assessment Report of the Intergovernmental Panel on Climate Change [STOCKER, T.F., D. QIN, G.-K. PLATTNER, M. TIGNOR, S.K. ALLEN, J. BOSCHUNG, A. NAUELS, Y. XIA, V. BEX AND P.M. MIDGLEY (eds.)]. Cambridge University Press, Cambridge, United Kingdom and New York, NY, USA, 1535 pp.

IPCC – INTERGOVERNMENTAL PANEL ON CLIMATE CHANGE (2018): Global Warming of 1.5 °C. An IPCC Special Report on the impacts of global warming of 1.5 °C above pre-industrial levels and related global greenhouse gas emission pathways, in the context of strengthening the global response to the threat of climate change, sustainable development, and efforts to eradicate poverty [MASSON-DELMOTTE, V., P. ZHAI, H.-O. PÖRTNER, D. ROBERTS, J. SKEA, P.R. SHUKLA, A. PIRANI, W. MOUFOUMA-OKIA, C. PÉAN, R. PIDCOCK, S. CONNORS, J.B.R. MATTHEWS, Y. CHEN, X. ZHOU, M.I. GOMIS, E. LONNOY, T. MAYCOCK, M. TIGNOR, AND T. WATERFIELD (eds.)]. In Press.

IRVINE, J., PERKS, M.P., MAGNANI, F. & GRACE, J. (1998): The response of Pinus sylvestris to drought: stomatal control of transpiration and hydraulic conductance. Tree Physiology 18, pp. 393-402

IVERSEN, C.M., HOOKER, T.D., CLASSEN, A.T., NORBY, R.J. (2011): Net mineralization of N at deeper soil depths as a potential mechanism for sustained forest production under elevated [CO_2]. Global Change Biology, Vol. 17, Issue 2, pp. 1130-1139. DOI: https://doi.org/10.1111/j.1365-2486.2010.02240.x

IVES, J.D. & MESSERLI, B. (1989): The Himalayan Dilemma: Reconciling Development and Conservation. Psychology Press. DOI: http://dx.doi.org/10.4324/9780203169193

JASTROW, J.D. & MILLER, R.M. (1990): Methods for assessing the effects of biota on soil structure. Agriculture, Ecosystems and Environment, 34 (1991) 279-303, Elesevier Science Publishers B.V., Amsterdam

JM – MINISTRY FOR JUSTICE (2021): http://landesrecht.rlp.de/jportal/portal/t/16b2/page/bsrlpprod.psml;jsessionid=97BED506D1544DF549339A4F2F01E612.jp16;jsessionid=14E2C6E2FBB21A4205A62B4B61F281CB.jp16?doc.hl=1&doc.id=jlr-BRPf%C3%A4lzerwaldVRPrahmen&documentnumber=1&numberofresults=4&doctyp=Norm&showdoccase=1&doc.part=X&paramfromHL=true#jlr-BRPf%C3%A4lzerwaldVRPrahmen (17.9.2021)

Jürging, P. & Patt, H. (eds.) (2004): Fließgewässer- und Auenentwicklung. Grundlagen und Erfahrungen. Springer Berlin Heidelberg New York 2005. ISBN 3-540-21415-1

Jump, A. S., Hunt, J. M., & Penuelas, J. (2006): Rapid climate change-related growth decline at the southern range edge of Fagus sylvatica. Global Change Biology, 12, 2163–2174. DOI: https://doi.org/10.1111/j.1365-2486.2006.01250.x

Kaiser, E.-A., Walenzik, G. & Heinemeyer, O. (1994): Auswirkungen von Bodenverdichtung auf die mikrobielle Biomasse und bodenbiologische Prozesse. Agricultural Research (Landbauforschung) Völkenrode, Special Issue 147.

Kampf, J. (2021): Änderungen des Wasserhaushalts 1951 bis 2020. Presentation Mainz Environment Days ("Mainzer Umwelttage") (unpublished)

Keenan, R. & Kimmis, J.P. (1993): The ecological effects of clear-cutting. Environmental Reviews 1993; DOI: 10.1139/a93-010

Keesstra, S.D., Geissen, V., Mosse, K., Piiranen, S., Scudiero, E., Leistra, M. van Scheik, L. (2012): Soil as a filter for groundwater quality. Current Opnion in Environmental Sustainability, Volume 4. Sciencedirct, Elsevier. ISBN 1877-3435

Kerstiens, G. (1996): Cuticular water permeability and its physiological significance. Journal of Experimental Botany, Vol. 47, No 305, pp. 1813-1832.

Kindel, K.-H. (1995): Kiefern in Europa. Gustav Fischer Verlag Stuttgart. ISBN: 3827408512

Kirby, J.T. & Durrans, S.R. (2007): PnET-II3SL/SWAT: Modelling the combined effects of forests and agriculture on water availability. J. Hydrol. Eng. 12(3): 319–326. doi:10.1061/(ASCE)1084-0699(2007)12:3(319)

Kirchner, M (1986): Wirkungen unterschiedlicher Landnutzungen auf den Wasserhaushalt bayerischer Flussgebiete. Scientific communications Meteor. Inst., University of Munich, No 55.

Kirkham, M.B. (2005): Principles of soil and plant water relations. Elsevier Academic Press. ISBN 0-12-409751-0

Klein Tank, A.M.G., Wijngaard, J.B., Können, G.P., Böhm, R., Demarée, G., Gocheva, A., Mileta, M., Pashiardis, S., Hejkrlik, L., Kern-Hansen, C., Heino, R., Bessemoulin, P., Müller-Westermeier, G., Tzanakou, M., Szalai, S., Pálsdóttir, T., Fitzgerald, D., Rubin, S., Capaldo, M., Maugeri, M., Leitass, A., Bukantis, A., Aberfeld, R., van Engelen, A.F.V., Forland, E., Mietus, M., Coelho, F., Mares, C., Razuvaev, V., Nieplova, E., Cegnar, T., Antonio López, J.,Dahlström, B., Moberg, A., Kirchhofer, W., Ceylan, A., Pachaliuk, O., Alexander, L.V. et al. (2002): Daily Dataset of 20th-Century Surface Air Temperature and Precipitation Series for the European Climate Assessment. International Journal of Climatology, 22, 1441-1453. DOI: https://doi.org/10.1002/joc.773

Klimenko, D. E., Cherepanova, E. S., Khomyleva, A. A. (2020): Spatial Modeling of Maximum Capacity Values of Irrecoverable Rainfall Retention by Forests in a Small Watershed. Forests 2020, 11, 641; DOI:10.3390/f11060641

KLIWA – Klimaveränderungen und Wasserwirtschaft (2017): Entwicklung von Bodenwasserhaushalt und Grundwasserneubildung in Baden-Württemberg, Bayern, Rheinland-Pfalz und Hessen (1951-2015). Authors: Baumeister, C., Gudera, T., Hergesell, M., Kampf, J., Kopp, B., Neumann, J., Schwebler, W., Wingering, M. KLIWA-Report, No 21

Koch, W. (1957): Der Tagesgang der „Produktivität der Transpiration". Planta, Issue 48, pp. 418-452 (1957). DOI: https://doi.org/10.1007/BF01939353

Koehler, G. (1998): Erprobungs- und Entwicklungsvorhaben „Oster". Auswirkungen einer Bachrenaturierung auf Gewässer und Aue. Approx. i.e. specialist hydraulic engineering and water management i.e. University Kaiserslautern, No 7, 240 S.

Koehler, G., Frey, W., Schindler, H., Hauptlorenz, H. (2010): Konzept zur ökologischen Bewertung und Entwicklung der Wooge im Biosphärenreservat Pfälzerwald (Aktenzeichen: 23747-33/2). DBU- Final Report, German Federal Foundation for the Environment and Technical University Kaiserslautern.

Kõlli, R. (2017): Dynamics of annual falling debris decomposition and forest floor Accumulation. Applied Soil Ecology (2017), Elsevier B.V. DOI:10.1016/j.apsoil.2017.06.039

Köstner, B., & Clausnitzer, F. (2011): Die Transpiration eines Fichten- und Buchenbestandes unter Bodentrockenheit im Tharandter Wald. Waldökologie, Landschaftsforschung und Naturschutz (Forest ecology, landscape research and nature conservation), Issue 12, pp. 29-35

Kolk, A.G. (1994): Mehrjährige Untersuchungen zur Charakterisierung der mikrobiellen Biomasse und ihrer Aktivität in Waldböden zweier verschiedener Standorte unter dem Einfluß praxisüblicher Kompensationskalkungen. Dissertation, Technical University Kaiserslautern, Subject Area Biology.

Kolymbas, D. (2019): Geotechnik. 5th edition. Springer Verlag GmbH Deutschland. ISBN 978-3-662-58471-2

Kompa, T. (2004): Die Initialphase der Vegetationsentwicklung nach Windwurf in Buchen-Wäldern auf Zechstein- und Buntsandstein-Standorten des südwestlichen Harzvorlandes. Dissertation, Univ. Göttingen, 223 p.

Kopp, B., Baumeister, C., Gudera, T., Hergesell, M., Kampf, J., Morhard, A., Neumann, J. (2018): Entwicklung von Bodenwasserhaushalt und Grundwasserneubildung in Baden-Württemberg, Bayern, Rheinland-Pfalz und Hessen von 1951 bis 2015. HW 62. 2018, H.2, DOI:10.5675/HyWa_2018,2_1

Korpel, S. (1995): Die Urwälder der Westkarpaten. G. Fischer, Stuttgart, 310 pp.

Krähenmann, S. (2019): Statistisches Downscaling und BIAS-Adjustierung der EURO-CORDEX Simulationen über dem HYRAS-Gebiet. DWD/KU11, working concept of the BMVI expert network

Kraus, C., Zimmer, M. & Manger, R. (2013): Klima- und Landschaftswandel in Rheinland-Pfalz (KlimLandRP) – Klimamodelle und Klimaprojektionen. Topic sheet. Eds.: Competence center of climate change impacts Rhineland-Palatinate.

Krupa, S.V. (2002): Effects of atmospheric ammonia (NH_3) on terrestrial vegetation: a review. Environmental Pollution 124 (2003) 179–221. DOI:10.1016/S0269-7491(02)00434-7

Labelle, E.R. & Jaeger, D. (2011): Soil Compaction Caused by Cut-to-Length Forest Operations and Possible Short-Term Natural Rehabilitation of Soil Density. Soil Science Society of Am. Journal 75(6):2314. DOI:10.2136/sssaj2011.0109

Landesforsten Rheinland-Pfalz (2018): Handbuch Walderschließung, vs. 1.1 (Az. 64 250), 73 p.

Landesforsten Rheinland-Pfalz (2020): Grundsatzanweisung: Waldverjüngung im Klimawandel - Wiederbewaldung, Vorausverjüngung und Jungwaldpflege, vs. 1.0, 40 p.

Lange, O.L., Nobel, P.S., Osmond, C.B., Ziegler, H. (1982): Physiological Plant Ecology II – Water Relations and Carbon Assimilation. Springer-Verlag Berlin Heidelberg, ISBN 978-3-642-68152-3

Larink, O., Heisler, C., Söchtig, W., Lübben, B., Wickenbrock, L. (1994): Auswirkungen von Bodenverdichtung auf die Meso- und Makrofauna. Agricultural Research (Landbauforschung) Völkenrode, Special Issue 147

LAWA – Federal/State Working Group on Water (2016): Daten der Bund/Länderarbeitsgemeinschaft Wasser zum Bericht nach Art. 13 der EG-Richtlinie 2000/60/EG. Reporting portal WasserBLIcK/BfG, 23.03.2016

LAWA – Federal/State Working Group on Water (2019): LAWA-Arbeitsprogramm Flussgebietsbewirtschaftung 2019 - Aktualisierung und Anpassung der LAWA-Arbeitshilfe zur Umsetzung der EG-Wasserrahmenrichtlinie, Teil 3, Kapitel II.1.2 -Grundwasser. LAWA General Assembly, Jena 2019.

Lehmann, A. & Rilling, M.C. (2015): Understanding mechanisms of soil biota involvement in soil aggregation: A way forward with saprobic fungi?. Soil Biology & Biochemistry (2015), DOI: http://dx.doi.org/10.1016/j.soilbio.2015.06.006

Lehn, H., Flaig, H., Mohr, H. (1995): Vom Mangel zum Überfluß, Störungen im Stickstoffkreislauf. GAIA - Ecological Perspectives on Science and Society · January 1995, DOI: 10.14512/gaia.4.1.7

Leibundgut, H. (1984): Die natürliche Waldverjüngung. 2nd edition, Paul Haupt, Bern and Stuttgart, 115 p.

Lenhart, T., Eckhardt, K., Fohrer, N., Frede, H.-G. (2002): Comparison of two different approaches of sensitivity analysis. Physics and Chemistry of the Earth 27 (2002) 645-654. DOI:10.1016/S1474-7065(02)00049-9

Leonhardt, J. (2003): Wald und Forstwirtschaft in Rheinland-Pfalz. Forst und Holz 58 (17): pp. 491-493.

Leta, O.T., Nossent, J., Velez, C., Shrestha, N.K., van Griensven, A. & Bauwens, W. (2015): Assessment of the different sources of uncertainty in a SWAT model of the River Senne (Belgium). Environ. Model. Softw. 68, pp. 129–146. DOI: http://dx.doi.org/10.1016/j.envsoft.2015.02.010

Leuschner, C. (1998): Water extraction by tree fine roots in the forest floor of a temperate Fagus-Quercus forest. Ann. Sci. For., 55, pp. 141-157

Leuschner, C. (2009): Die Trockenheitsempfindlichkeit der Rotbuche vor dem Hintergrund des prognostizierten Klimawandels. Yearbook of the Academy of Sciences in Göttingen, Göttingen, pp. 281–296.

Leuschner, C. & Ellenberg, H. (2017): Ecology of Central European forests: Vegetation Ecology of Central Europe. Version 6th. Springer Nature: Cham Switzerland, Vol. I., 971 S.

Levin, S.A. (2000): Encyclopedia of Biodiversity. Academic Press, 1st Edition. ISBN 978-0122268656

Leyton, L., Reynold, E.R.C., Thompson, F.B. (1967): Rainfall interception in forest and moorland. In: Sopper, W.E. & Lull, H.W. (eds.), Forest Hydrology, Pergamon, Oxford, 163-178

LfU Bavaria – Bavarian State Office for the Environment (2008): Wasser in Bayern. Aquatic annual report 2007.

LGB & LfW RLP – State Office for Geology Rhineland Palatinate & State Office for Watermanagement Rhineland Palatinate (2004): Hydrogeologische Kartierung Kaiserslautern. 96 p., Mainz 2004.

LIGHTHILL, M.J. & WHITHAM, G.B. (1955): On Kinematic Waves. I. Flood Movement in Long Rivers. Proc. R. Soc. Lond. A 1955, 229, DOI: https://doi.org/10.1098/rspa.1955.0088

LUNG MV - STATE OFFICE FOR THE ENVIRONMENT, NATURE CONSERVATION AND GEOLOGY MECKLENBURG-WESTERN POMERANIA (n.d): Beiträge zum Bodenschutz in Mecklenburg-Vorpommern – Bodenverdichtung. https://www.lung.mv-regierung.de/dateien/bodenverdichtung.pdf (4.3.2021)

LWF AKTUELL (2003): http://www.waldwissen.net (13.8.2021)

LYR, H. & HOFFMANN, G. (1967): Growth rates and growth peridodicity of tree roots. In: ROMBERGER, J.A. & MIKOLA, P. (eds.). International Review of Forest Research, Vol. 2, 1st edition, p.181-236. ISBN 9781483224794

MACE, G.M., BATEMAN, I., ALBON, S., BALMFORD, A., BROWN, C., CHURCH, A., (2011): Conceptual Framework and Methodology. UK National Ecosystem Assessment, Technical Report. Cambridge: UNEP-WCMC

MAGOON, C. A. & CULPEPPER, C.W. (1932): Response of Sweet Corn to Varying Temperatures from Time of Planting to Canning Maturity. Technical Bulletins 163380, United States Department of Agriculture, Economic Research Service. DOI:10.22004/ag.econ.163380

MAHERALI, H., POCKMAN, W.T., JACKSON, R.B. (2004): Adaptive variation in the vulnerability of woody plants to xylem cavitation. Ecology, 85, pp. 2184–2199.

MAINZER, K. (ed.) (1999): Komplexe Systeme und nichtlineare Dynamik in Natur und Gesellschaft: Komplexitätsforschung in Deutschland auf dem Weg ins nächste Jahrhundert. Springer-Verlag Berlin Heidelberg. ISBN-13: 978-3-642-64240-1, 1st edition.

MALCHEREK, A. (2019): Fließgewässer. Hydraulik, Hydrologie, Morphologie und Wasserbau. Springer Vieweg. ISBN 978-3-658-26999-9; DOI: https://doi.org/10.1007/978-3-658-27000-1

MARGALEF-MARRASE, J., PÉREZ-NAVARRO, M.A., LLORET, F. (2020): Relationship between heatwave-induced forest die-off and climatic suitability in multiple tree species. Global Change Biology, Vol. 26, Issue 5. DOI: https://doi.org/10.1111/gcb.15042

MARSHALL, T.J., HOLMES, J.W., ROSE, C.W. (2001): Soil Physics. Cambridge University Press, third edition. ISBN 0-521-45766-1.

MARTINEZ-SACHNO, E., DORADO-LINAN, I., HACKE, U.G., SEIDEL, H., MENZEL, A. (2017): Contrasting hydraulic architectures of Scots Pine and Sessile Oak at their southernmost distribution limits. Frontiers in Plant Science, Vol. 8, Article 598. DOI:10.3389/fpls.2017.00598

MATSUSHITA, M., TAKATA, K., HITSUMA, G, YAGIHASHI, T., NOGUCHI, M., SHIBATA, M., MASAKI, T. (2015): A novel growth model evaluating Age Size effects on long-term trends in tree growth. Forest Tree Breeding Center, Forestry and Forest Products Research Institute, Japan. Dryad, DOI: https://doi.org/10.5061/dryad.7qc3s

MATYSSEK, R., FROMM, J., RENNENBERG, H., ROLOFF, A. (2010): Biologie der Bäume: Von der Zelle zur globalen Ebene. UTB GmbH, 1st edition, 349 p., ISBN 978-3825284503.

MATYSSEK, R. & HERPPICH, W. B. (2019): Experimentelle Pflanzenökologie – Grundlagen und Anwendungen, Springer Spektrum ISBN 978-3-662-53463-2

MCDOWELL, N., POCKMAN, W.T., ALLEN, C.D., BRESHEARS, D.D., COBB, N., KOLB, T., PLAUT, J., SPERRY, J.,WEST, A.,WILLIAMS, D.G., YEPEZ, E.A. (2008): Mechanisms of plant survival and mortality during drought: why do some plants survive while others succumb to drought? New Phytol. 178, 719–739.

McDowell, N.G. (2011): Mechanisms linking drought, hydraulics, carbon metabolism, and vegetation mortality. Plant Physiol 155:1051–1059.

McKeown, R.A., Putz, G., Arnold, J. & Di Luzio, M. (2005): Modifications of the Soil and Water Assessment Tool (SWATC) for streamflow modeling in a small, forested watershed on the Canadian Boreal Plain. In Proceedings of the 3rd International SWAT Conference, 13–15 July 2005, Zurich, Switzerland. R. Srinivasan, J. Jacobs, D. Day, & K. Abbaspour (eds.), pp. 189–199.

McNabb, D.H., Startsev, A.D., Nguyen, H. (2001): Soil Wetness and Traffic Level Effects on Bulk Density and Air-Filled Porosity of Compacted Boreal Forest Soils. Soil Sci. Soc. Am. J., Vol. 65. DOI: https://doi.org/10.2136/sssaj2001.6541238x

MEA - Millennium Ecosystem Assessment (2005): Ecosystems and Human Well-Being: Synthesis. Island Press.

Meynen, E. & Schmithüsen, J. (1960): Handbuch der naturräumlichen Gliederung Deutschlands. Federal Institute for regional studies, Remagen/Bad Godesberg.

Mills, G., Harmens H., Hayes F., Pleijel H., Buker P., González-Fernández I. (2017): Chapter 3: Mapping critical levels for vegetation. Manual on Methodologies and Criteria for Modelling and Mapping Critical Loads & Levels and Air Pollution Effects, Risks and Trends. IPC Vegetation. Available: https://icpvegetation.ceh.ac.uk/chapter-3-mapping-critical-levels-vegetation (9.7.2021)

Mishra, S.K., Vijay, P., Singh, P., Singh, P.K. (2018): Revisiting the Soil Conservation Service Curve Number Method. Springer Nature Singapore Pte Ltd. 2018 V. P. Singh et al. (eds.): Hydrologic Modeling, Water Science and Technology Library 81. DOI: https://doi.org/10.1007/978-981-10-5801-1_46

Mitchell, S. (2008): Komplexitäten: Warum wir erst anfangen, die Welt zu verstehen. Suhrkamp Verlag Frankfurt a. M. ISBN 978-3-518-26001-2

Mitscherlich, E.A. (1948): Die Ertragsgesetze. German academy of science Berlin, lectures and writing, Akademie-Verlag, Berlin (42 p)

Mitscherlich, G. & Moll, W. (1970): Untersuchungen über die Niederschlags- und Bodenfeuchtigkeitsverhältnisse in einigen Nadel- und Laubholzbeständen in der Nähe von Freiburg/Br. Teil I: Niederschlagsverhältnisse. AFJZ 141, 49-60.

Mitscherlich, G. (1971): Wald, Wachstum und Umwelt, Bnd. 2: Waldklima und Wasserhaushalt. Sauerländer´s, Frankfurt a.M.

Mohr, K., Meesenburg, Horváth, B., Meiwes, K.J., Schaaf, S., Dämmgen, U. (2005): Bestimmung von Ammoniak-Einträgen aus der Luft und deren Wirkung auf Waldökosysteme. Weser-Ems Chamber of Agriculture, Oldenburg Lower Saxony Forest Research Institute, Göttingen; Federal Research Institute for Agriculture, Institute for Agricultural Ecology, Braunschweig, final report on behalf of the Federal Environment Agency.

Mokany, K., Raison, R.J., Prokushkin, A.S. (2006): Critical analysis of root:shoot ratios in terrestrial biomes. Global Change Biology 12, 84-96, DOI: https://doi.org/10.1111/j.1365-2486.2005.001043.x

Monteith, J.L. (1965): Evaporation and the environment. In Proceedings of the 19th Symposia of the Society for Experimental Biology: The State and Movement of Water in Living Organisms. Cambridge University Press, London. pp. 205–234.

Monteith, J.L. (1985): Evaporation from land surfaces: Progress in analysis and prediction since 1948. pp. 4-12. In Advances in Evapotranspiration, Proc. National Conference on Advances in Evapotranspiration, Dec. 16-17, Chicago, IL, Am. Soc. Agric. Eng., St. Joseph, MI.

Moriasi, D.N., Arnold, J.G., Van Liew, M.W., Bingner, R.L., Harmel, R.D., Veith, T.L. (2007): Model evaluation guidelines for systematic quantification of accuracy in watershed simulations. Transactions of the ASABE, 50(3), pp.885-900.

MUEEF - Ministry for the Environment, Energy, Food and Forest (eds.) (2019): Waldzustandsbericht 2019. Autograph, 69 p.

MUEEF – Ministry for the Environment, Energy, Food and Forest (eds.) (2020): Waldzustandsbericht 2020. Autograph, 71 p.

Müller, J. (1996): Beziehung zwischen Vegetationsstrukturen und Wasserhaushalt in Kiefern- und Buchenökosystemen. Notifications from the BFH Hamburg, No 185, 112-128

Müller, J. (2011): Das Blaue Gold des Waldes. Research Report 1/2011, Wald und Holz.

Müller, E.V. & Schüler, G. (2021): Strategie mit Handlungsempfehlungen zur Verbesserung der Grundwasserqualität. Final report of the INTERREG-Ecoserv-Project, subproject Nutrient Cycling, 63 p.

Mueller, K.E., Eissenstat, D.M., Hobbie, S.E., Oleksyn, J., Jagodzinski, A.M., Reich, P.B., Chadwick, O.A., Chorover, J. (2012): Tree species effects on coupled cycles of carbon, nitrogen, and acidity in mineral soils at a common garden experiment. Biogeochenistry (2012) 111:601-614. DOI:10.1007/s10533-011-9695-7

Muffler, L., Schmeddes, J., Weigl, R., Barbeta, A., Beil, I., Bolte, A., Buhk, C., Holm, S., Klein, G., Klisz, M., Löf, M., Penuelas, J., Schneider, L., Vitasse, Y., Kreyling, J. (2021): High plasticity in germination and establishment success in the dominant forest tree Fagus sylvatica across Europe. Global Ecol Biogeogr. 2021;30:1583–1596, DOI:10.1111/geb.13320.

Munich Re (2000): Natural catastrophes – the current position, special millennium issue. Munich Reinsurance Co, Munich, Germany

MUVF – Ministerium für Umwelt, Forsten und Verbraucherschutz Rheinland Pfalz (2007): Grundwasserbericht 2007. ISBN 978-3-933123-18-3

MWKE-RLP – Ministry for economy, climate protection, energy and land planning Rhineland-Palatinate (2021): Klimawandelinformationssystem (kwis-rlp): http://www.kwis-rlp.de/index.php?id=6867 (09.09.2021).

Nagel, H.-D., Gregor, H.-D. (1999): Ökologische Belastungsgrenzen – Critical Loads & Levels. Ein internationales Konzept für die Luftreinhaltepolitik. Springer Berlin Heidelberg, 1-259

Nardini, A., Casolo, V., Dal Borgo, A., Savi, T., Stenni, B., Bertoncin, P., Zini, L., McDowell, N.G. (2015): Rooting depth, water relations and non-structural carbohydrate dynamics in three woody angiosperms differentially affected by an extreme summer drought. Plant Cell and Environment 39, 618–627. DOI: https://doi.org/10.1111/pce.12646

Nawaz, M.F., Bourrié, G., Trolard, F. (2012): Soil compaction impact and modelling. A review. Springer, Agron. Sustain. Dev. (2013) 33:291–309; DOI 10.1007/s13593-011-0071-8

Neary, D.G., Ice, G.G., Jackson, C.R. (2009): Linkages between forest soils and water quality and quantity. Forest Ecology and Management 258 (2009) 2269-2281. DOI:10.1016/j.foreco.2009.05.027

Neitsch, S. L., J. G. Arnold, J. R. Kiniry, J. R. Williams (2005): Soil and Water Assessment Tool Theoretical Documentation, Version 2005. Texas Water Resources Institute College Station, Available: https://swat.tamu.edu/media/1292/SWAT2005theory.pdf (2.4.2022)

Neitsch, S. L., J. G. Arnold, J. R. Kiniry, J. R. Williams (2011): Soil and Water Assessment Tool Theoretical Documentation, Version 2009. Texas Water Resources Institute Technical Report No. 406 Texas A&M University System College Station, Texas 77843-2118, Soil and Water Research Laboratory - Agricultural Research Service Blackland Research Center – Texas AgriLife Research. Available: https://swat.tamu.edu/media/99192/swat2009-theory.pdf (3.10.2021)

Nguyen, Ngoc Quynh (2016): Anatomical, physiological and molecular responses of European Beech (Fagus sylvatica L.) to drought. Dissertation, University of Göttingen, 121 p.

Nilgard, B. (1971): Pedological influence of spruce planted on former beech forest soils in Scania, south Sweden. Oikos, 21, pp. 302-314

NLWKN - Lower Saxony State Office for Water Management, Coastal and nature protection (2020): Grundwasserbericht Niedersachsen Sonderausgabe zur Grundwasserstandssituation in den Trockenjahren 2018 und 2019. http://www.nlwkn.niedersachsen.de/service/veroeffentlichungen_webshop/ (23.6.2021)

Nordmann, B. (2011): Einfluss der Forstwirtschaft auf den vorbeugenden Hochwasserschutz – Integrale Klassifizierung abflusssensitiver Waldflächen. Ph.D.-thesis, Techinal University Munich

Oldeman, L.R., Hakkeling, R.T.A., Sombroek, W.G. (1991): World Map of the Status of Human-induced Soil Degradation. Global Assessment of Soil Degradation (2. Ed.). ISRIC and UNEP, Wageningen.

Oppermann, J., Galloway, G.E., Fargione, J., Mount, J.F., Richter, B.D., Secchi, S. (2009): Sustainable Floodplains through large-scale reconnection to rivers. Science Vol. 326, published by AAAS, pp. 1487-1488

Osipov, V.I. (2015): The Terzaghi Theory of Effective Stress. In: Physicochemical Theory of Effective Stress in Soils. SpringerBriefs in Earth Sciences. Springer, Cham. DOI: https://doi.org/10.1007/978-3-319-20639-4_2

Ott, K., Dierks, J., Voget-Kleschin, L. (eds.) (2016): Handbuch Umweltethik. J.B. Metzler, Stuttgart, Springer-Verlag GmbH Deutschland. ISBN 978-3-476-02389-6

Page-Dumroese, D.S., Jurgensen, M.F., Tiarks, A.E., Ponder, F., Sanchez, F.G., Fleming, R.L., Kranabetter, J.M., Powers, R.F., Stone, D.M., Elioff, J.D., Scott, D.A. (2006): Soil physical property changes at the North American Long-Term Soil Productivity study sites: 1 and 5 years after compaction. Can. J. For. Res. 36: 551–564. Doi:10.1139/X05-273

Parmesan, C., Yohe, G. (2003): A globally coherent fingerprint of climate change impacts across natural systems. Nature 421, pp. 37-42.

Peck, A. & Mayer, H. (1996): Einfluß von Bestandesparametern auf die Verdunstung von Wäldern. Forstw Cbl 115, 1–9 (1996). DOI: https://doi.org/10.1007/BF02738580

Peichl, B. (1998): Hochwasser, Erosion und Waldstraßenbau. Allgem. Forstzeitschr., 53, pp. 992-994

Penka, M., Vyskot, M., Klimo, E., Vašíèek, F. (1985): Floodplain forest ecosystem: I. Before water management measures. Academia, Praha, 466 p.

Pfannerstill, M. Guse, B. Fohrer, N. (2014a): A multi-storage groundwater concept for the SWAT model to emphasize nonlinear groundwater dynamics in lowland catchments. Hydrological Processes 28 (22), pp. 5599–5612.

Pfannerstill, M. Guse, B. Fohrer, N. (2014b): Smart low flow signature metrics for an improved overall performance evaluation of hydrological models. Journal of Hydrology 510, pp. 447–458.

Pomeroy, J.W. & Schmidt, R.A. (1993): The use of fractal Geometry in Modelling intercepted snow accumulation and sublimation. 50th Eastern Snow Conference, Quebec City 1993, Honor Paper Award, 10 p.

Ponce, V.M. & Hawkins, R.H. (1996): Runoff Curve Number: Has it reached maturity? J. Hydrol. Eng, Jan 1996, 1 (1):11–19

Potschin, M. B. & Haines-Young, R. H. (2011): Ecosystem services: Exporting a geographical perspective. Progress in Physical Geography 35:575, DOI: 10.1177/0309133311423172

Potschin, M. B., Haines-Young, R. H. (2016): Defining and measuring ecosystem services. In: Potschin, M., Haines-Young, R., Fish, R. and Turner, R.K. (eds): Routledge Handbook of Ecosystem Services. Routledge, London and New York, pp. 25-44. Available: http://www.routledge.com/books/details/9781138025080/ (3.4.2021)

Pott, R., Hüppe, J. (2007): Spezielle Geobotanik. Pflanze – Klima – Boden. Springer Berlin Heidelberg New York. ISBN-13 978-3-540-49356-3

Poulos, H.M., Berly, G.P., Mills, S.A. (2012): Differential stress tolerance of four pine (Pinaceae) across the elevation gradient of the San Bernardino Mountains, Sothern California, USA. Journal of the Torrey Botanical Society 139(1), 2012, pp. 96-108. (2.2.2022)

Pretzsch, H. (2003): Grundalgen der Waldwachstumsforschung. 2nd revised edition, Springer Spektrum. ISBN 978-3-662-58154-4, DOI: https://doi.org/10.1007/978-3-662-58155-1

Pretzsch, H., Rötzer, T., Matyssek, R., Grams, T.E.E., Häberle, K.-H., Pritsch, K., Kerner, R., Munch, J.-C. (2014): Mixed Norway spruce (*Picea abies* [L.] *Karst*) and European beech (*Fagus sylvatica* [L.]) stands under drought: from reaction patterns to mechanism. Springer Berlin Heidelberg. DOI:10.1007/s00468-014-1035-9

Pretzsch, H. (2019): Grundlagen der Waldwachstumsforschung. Springer Spektrum, Berlin, Heidelberg, ISBN 978-3-662-58155-1

Priestley, C.H.B. & Taylor, R.J. (1972): On the assessment of surface heat flux and evaporation using large-scale parameters. Mon. Weather Rev. 100: 81–92. DOI: http://dx.doi.org/10.1175/1520-0493(1972)100<0081:OTAOSH>2.3.CO;2

Rakei, A. (1991): Wasserhaushalt eines Alt- und Jungkiefernbestandes auf Rostbraunerde des Grunewaldes (Berlin). Bodenökologie und Bodengenese. Self-published by the institute for Ecology, TU Berlin, 134 p.

Rakei, A., Renger, M., Wessolek, G. (1992): Wasserhaushalt eines Jungkiefernbestandes im Grunewald (Berlin). Allg. Forst- u. J.-Ztg., 163, Jg., 9: 169-172

Rauthe, M, Steiner, H, Riediger, U, Mazurkiewicz, A., Gratzki, A. (2013): A Central European precipitation climatology – Part I: Generation and validation of a high-resolution gridded daily data set (HYRAS). Meteorol. Magazine, Vol 22, No 3, 235–256, DOI:101127/0941-2948/2013/0436

Reichardt, M. (2002): Bodenwschäden durch Forstmaschinen: Erfassung von natürlichen Regenerationsprozessen auf einer befahrenen Fläche. Master's degree in pedology, University of Trier, FB VI: Geography / Geosciences - Applied Physical Geography.

Reiter, P., Sauer, T., Zimmer, M, Voigt, M. (2018): Klimawandel in Rheinland-Pfalz. Themenheft Klimawandel – Entwicklung bis heute. Rhineland-Palatinate Competence center for the Impacts of Climate Change at the Research Institute for Forest Ecology and Forestry, Trippstadt.

Reiter, P., Sauer, T., Voigt, M., Zimmer, M. (2020): Klimawandel in Rheinland-Pfalz. Themenheft Klimawandel – Entwicklungen in der Zukunft. Rhineland-Palatinate Competence Center for the Impacts of Climate Change at the Research Institute for Forest Ecology and Forestry Trippstadt in cooperation with the State Office for the Environment RLP.

Rehfuess, K.E. (1990): Waldböden, Entwicklung, Eigenschaften und Nutzung. Hamburg, Berlin

Riedel, T. & Weber, T.K.D. (2020): The influence of global change on Europe's water cycle and ground-water recharge. Hydrogeol J 28, 1939–1959 (2020). DOI: https://doi.org/10.1007/s10040-020-02165-3

Riederer, M. & Schreiber, L. (2001): Protecting against water loss: analysis of the barrier properties of plant curticles. Journal of Experimental Botany, Vol. 52, No 363 (plants under stress special issue), pp. 2023-2032.

Riederer, M. & Müller, C. (eds.) (2006): Biology of the Plant Cuticle. Blackwell Publishing Ltd., ISBN-13: 978-1-4051-3268-8

Ritchie, J.T. (1972): Model for predicting evaporation from a row crop with incomplete cover. Water Resources Research, Vol. 5, Issue 5, pp. 1204-1213. DOI: https://doi.org/10.1029/WR008i005p01204

Rötzer, T., Häberle, K.H., Kallenbach, C., Matyssek, R., Schütze, G. & Pretzsch, H. (2017): Tree species and size drive water consumption of beech/spruce forests - a simulation study highlighting growth under water limitation. Plant Soil. Springer International Publishing AG Switzerland 2017. DOI:10.1007/s11104-017-3306-x.

Rosenzweig, C., G. Casassa, D.J. Karoly, A. Imeson, C. Liu, A. Menzel, S. Rawlins, T.L. Root, B. Seguin, P. Tryjanowski (2007): Assessment of observed changes and responses in natural and managed systems. Climate Change 2007: Impacts, Adaptation and Vulnerability. Contribution of Working Group II to the Fourth Assessment Report of the Intergovernmental Panel on Climate Change. M.L. Parry, O.F. Canziani, J.P. Palutikof, P.J. van der Linden & C.E. Hanson, (eds.), Cambridge University Press, Cambridge, UK, pp. 79-131.

Roth, C.H. (1996): Physikalische Ursachen der Wassererosion. In: Blume, H.P., Frede, G.H., Fischer,W., Felix-Henningsen, P., Horn, R., Stahr, K. (eds.): Handbuch der Bodenkunde. Ecomed, Taunusstein, pp. 1–34.

Rukh, S., Poschenrieder, W., Heym, M., Pretzsch, H. (2020): Drought Resistance of Norway Spruce (*Picea abies* [L.] *Karst*) and European Beech (*Fagus sylvatica* [L.]) in Mixed vs. Monospecific Stands and on Dry vs. Wet Sites. From Evidence at the Tree Level to Relevance at the Stand Level. Forests 2020, 11, 639; DOI:10.3390/f11060639

Rust, S. (2009): Expertise Waldstruktur und Wasserhaushalt. Trinkwasserwald e.V. Available: http://docplayer.org/44084267-Waldstruktur-und-wasserhaushalt.html 21.9.2021

Ryan, M.G., Phillips, N., Bond, B.J. (2006): The hydraulic limitation hypothesis revisited. Plant, Cell & Environment 29 (3): 22-30.

Ryan, M.G. (2011): Tree Responses to Drought. Tree Physiol. 2011, 31, 237–239, DOI:10.1093/treephys/tpr022.

Sangrey, D.A., Harrop-Williams, K.O., Klaiber, J.A. (1984): Predicting Ground-Water Response to

Precipitation. J. Geotech. Engrg. 1984.110:957-975. https://doi.org/10.1061/(ASCE)0733-9410(1984)110:7(957), 20.10.2021

Saxton, K.E. & Rawls, W.J. (2006): Soil Water Characteristic Estimates by Texture and Organic Matter for Hydrologic Solutions. Soil Science Society of America Journal, 70, pp. 1569-1578. DOI: http://dx.doi.org/10.2136/sssaj2005.0117

Schabel, A. (2020): Arealveränderungen bei Buche und Eiche in Südwestdeutschland und damit einhergehende strukturelle und waldbauliche Auswirkungen. Presentation at the online conference of the BfN „Natura 2000 – Waldlebensraumtypen im Klimawandel".

Schäfer, B., Bens, O., Fischer, H., Hüttl, R.F. (2002): Einfluss des Baumartenwechsels auf die Wasserspeicherfähigkeit von sandigen Böden Nordost-Brandenburgs. Forst und Holz, 57, pp. 571-575

Schaich, H. (2009): Zukunftsfähige Auenlandschaften durch Wiedervernässung und Beweidung? Interdisziplinäre Analyse einer Renaturierungsmaßnahme am Beispiel des Syrtals (Luxemburg). Dissertation of the Faculty of Forestry and Environmental Sciences at the Albert-Ludwigs-University of Freiburg, 199 p.

Scheffer, F., Schachtschabel, P. (1998): Lehrbuch der Bodenkunde. 14th, revised and ext. Edition/ by P. Schachtschabel. Ferdinand Enke Verlag Stuttgart

Schenk, D., W. Bott & J. Grunert (2001): Wasserrückhalt in Wäldern – Hochwassermanagement in Entstehungsgebieten – Vorsorge aus forstlicher und wasserwirtschaftlicher Sicht. Research Report for the Research Institute for forest ecology and forestry (FAWF) Trippstadt (unpubl.), 30 p.

Schjønning, P., van den Akker, J. J.H., Keller, T., Greve, M.H., Lamandé, M., Simojoki, A. (2016): Soil threats in Europe: status, methods, drivers and effects on ecosystem services. A review report. JRC technical report, European Union. Stolte, J., Tesfai, M., Øygarden, L., Kværnø, S., Keizer, J., Verheijen, F., Panagos, P., Ballabio, C., Hessel, R. (eds.): Soil threats in Europe. DOI:10.2788/488054 (print); DOI:10.2788/828742 (online)

Schmaltz, J. (1969): Die Bedeutung des Waldes für den Wasserkreislauf. Forest archive, 40, p. 132-147.

Schmidt, J.P. (1993): Eine Einführung in die hydrologischen Untersuchungen von Waldökosystemen. Forest archive 64, pp. 158-163.

Schneider, R. (2015): Auswirkungen der Holzernte mit schweren Maschinen auf den Waldboden. Research report on forest research funding FAWF Trippstadt 2015

Schönauer, M., Maack, J., Hoffmann, S., Jensen, M. (2021): Comparison of Selected Terramechanical Test Procedures and Cartographic Indices to Predict Rutting Caused by Machine Traffic during a Cut-to-Length Thinning-Operation. Forests · January 2021, 12, 113; DOI: 10.3390/f12020113

Schröck H.-W. (2020): Praxisinformation der FAWF: Aktueller Trockenstress im Wald. 4 p. (unpublished)

Schröder, C.; Luthardt, V.; Jeltsch, F. (2012): Development of a holistic evaluation method for ecosys-tem services of peatlands. Contribution to the 14th International Peat Congress: Peatlands in Balance, June 3-8 2012, Stockholm, Sweden. Online available Theme I.5 Special session - Peatland ecosystem services No 196.

Schüler, G., Bott, W., Schenk, D. (2002): Hochwasservorsorge durch Waldbewirtschaftung. Forst und Holz, 57. No 1/2

Schüler, G. (2006): Identification of flood-generating forest areas and forestry measures for water retention. For. Snow Landsc. Res. 80, 1: 99–114 (2006)

Schüler, G., Schobel, S. Wilkinson, K., Schultze, B., Karl, S., Scherzer; J. (2016): The impacts of a changing climate on catchment water balance and forest management. Ecohydrology, (30.10.2021)

Schürz, C. (2019): SWATplusR: Running SWAT2012 and SWAT+ Projects in R. DOI: https://github.com/chrisschuerz/SWATplusR

Shierlaw, J. & Alston, A.M. (1984): Effects of soil compaction on root growth and uptake of phosphorus. Plant and Soil 77, pp. 15-28.

Sierra, C.A., Loescher, H.W., Harmon, M.E., Richardson, A.D., Hollinger, D.Y., Perakis, S.S. (2009): Interannual variation of carbon fluxes from three contrasting evergreen forests: the role of forest dynamics and climate. Ecology 90, pp. 2711–2723.

Singh, V.P. (2002): Is hydrology kinematic? Hydrol. Process. 16, pp. 667–716 (2002). DOI: https://doi.org/10.1002/hyp.306

Sloan, P.G., & Moore, I.D. (1984): Modeling subsurface stormflow on steeply sloping forested watersheds. Water Resour. Res. 20:1815–1822. DOI: https://doi.org/10.1029/WR020i012p01815

Smith, F.W., & Long, J.N. (2001: Age-related decline in forest growth: an emergent property. Forest Ecology and Management, 86, pp. 3048–3062.

Soetaert, K. & Petzoldt, T. (2010): Inverse modelling, sensitivity and Monte Carlo analysis in R using package FME. Journal of Statistical Software 33 (3), 1–28.

Solomon, S., Qin, D., Manning, M., Chen, Z., Marquis, M., Averyt, K.B., Tignor, M., Miller, H.L. (Eds.) (2007): Climate Change 2007: The Physical Science Basis — Contribution of Working Group I to the Fourth Assessment Report of the Intergovernmental Panel on Climate Change. Cambridge University Press, Cambridge, UK and New York, USA. Available: http://www.ipcc.ch/publications_and_data/publications_ipcc_fourth_assessment_report_wg1_report_the_physical_science_basis.htm (8.5.2020)

Spuhler, L. (1957): Einführung in die Geologie der Pfalz. Verlag der Pfälzischen Gesellschaft zur Förderung der Wissenschaften Speyer/Rh., Vol. 34

Spuhler, L. (1957): Einführung in die Geologie der Pfalz. Verlag der Pfälzischen Gesellschaft zur Förderung der Wissenschaften Speyer/Rh., Issue 34

SRU - Sachverständigenrat für Umweltfragen (1998): Flächendeckender Grundwasserschutz. Special Report, printed manner 13/10196.

SRU – Sachverständigenrat für Umweltfragen (2008): Umweltgutachten 2008 – Umweltschutz im Zeichen des Klimawandels, chapter 7: water protection.

Stahr, K., Kandeler, E., Herrmann, L., Streck, T. (2008): Bodenkunde und Standortlehre. Verlag Eugen Ulmer Stuttgart, 3rd edition. ISBN 978-3-8252-4687-7

StatLan RLP – State Statistical Office of Rhineland-Palatinate (2016): Statistisches Jahrbuch 2016. State Statistical Office of Rhineland-Palatinate, Bad Ems

Stoffels, J., Hill, J., Sachtleber, T., Mader, S., Buddenbaum, H., Stern, O., Langshausen, J., Dietz & G. Ontrup, J. (2015): Satellite-Based Derivation of High-Resolution Forest Information

Layers for Operational Forest Management. Forests, 6 (6): 1982-2013. DOI: https://doi.org/10.3390/f6061982

Stojanovic, D. B., Krzic, A., Mstovic, B., Orlovic, S., Duputie, A., Djurdjevic, V., Galic, Z., Stojnic, S. (2013): Prediction of the European beech (*Fagus sylvatica* L.) xeric limit usinga regional climate model: An example from southeast Europe. Agricultural and Forest Meteorology 176 (2013) 94-103, Elsevier B.V.

Stovall, A.E.L., Shugart, H., Yang, X. (2019): Tree Height Explains Mortality Risk during an Intense Drought. Nat. Commun. 2019, 10, 1–6, doi:10.1038/s41467-019-12380-6.].

Strasburger, E., Noll, F., Schenk, H., Schimper, A.F.W. (1967): Lehrbuch der Botanik. 29th edition, updated by von Denffer et al., Gustav Fischer-Vlg., Stuttgart, S. 87–90, pp. 217–218, 361 p.

Sukachev, V. & Dylis, N. (1964): Fundamentals of forest biogeocoenology. Oliver & Boyd, Edinburgh, 55 pp. of refs.

Tang, J., Bolstad, P.V., Ewers, B.E., Desai, A.R., Davis, K.J., Carey, E.V. (2006): Sap flux-upscaled canopy transpiration, stomatal conductance, and water use effieciency in an old growth forest in the Great Lakes region of United States. Journal of Geophysical Research, Vol. 111, doi:10.1029/2005JG000083

TEEB - The Economics of Ecosystems and Biodiversity (2010): Mainstreaming the Economics of Nature: A Synthesis of the Approach, Conclusions and Recommendations of TEEB. Earthscan, London and Washington.

Terzaghi, K. (1943): Theoretical Soil Mechanics. John Wiley & Sons, Inc.

Terzaghi, K., Reck, R.B., Mesri, G. (1996): Soil Mechanics in Engineering Practice. A Wiley-Intersience Publication, 3rd edition. John Wiley & Sons, INC.

TFEU – Treaty on the functioning of the European Union (2012): Consolidated versions of the Treaty on European Union and the Treaty on the functioning of the European Union (2012/C326/01); available: https://eur-lex.europa.eu/legal-content/EN/TXT/PDF/?uri=CELEX:12012E/TXT&from=EN (2.3.2021)

Thom, D., Rammer, W., Seidl, R. (2017): Disturbances catalyze the adaptation of forest ecosystems to changing climate conditions. Glob Chang Biol. 23(1): pp. 269-282. DOI:10.1111/gcb.13506

Tigabu, T., Wagner, P., Fohrer, N. (2021): Improvement of the plant growth model for forest and representation of skid trails in the hydrological model SWAT+. Project report 1 (unpubl.). Department of Hydrology and Water Ressources Management Kiel University.

Tigabu, T., Wagner, P., Fohrer, N. (2022): Mapping water balance components and the impact of skid trails. Project report 4 (unpubl.). Department of Hydrology and Water Ressources Management Kiel University.

Todd, D.K. & Mays, L.W. (2004): Groundwater Hydrology. John Wiley & Sons, 3rd edition. ISBN 978-0471452546

Tomasella, M., Häberle, K.-H., Nardini, A., Hesse, B., Machlet, A., Matyssek, R. (2017): Post-drought hydraulic recovery is accompanied by non-structural carbohydrate depletion in the stem wood of Norway spruce saplings. Sci Rep 7, 14308 (2017). DOI: https://doi.org/10.1038/s41598-017-14645-w

Trenberth, K. (2005): The Impact of Climate Change and Variability on Heavy Precipitation, Floods, and Droughts. National Center for Atmospheric Research, Boulder, CO, USA, John Wiley & Sons, Ltd.

Tüxen, R. (1986): Unser Buchenwald im Jahresverlauf. Supplements to the publications for nature conservation and landscape conservation in Baden-Württemberg 47, pp. 1-128.

Tyree M.T. & Sperry J.S. (1988): Do woody-plants operate near the point of catastrophic xylem dysfunction caused by dynamic water-stress – answers from a model. Plant Physiology 88, pp. 574–580.

UBA – Umweltbundesamt (2004): Daten aus dem Messnetz 2000 bis 2003. German Federal Environment Agency, Area of Expertise II 6.6, Langen

UBA – Umweltbundesamt (2013): Erfassung, Prognose und Bewertung von Stoffeinträgen und ihren Wirkungen in Deutschland. Summarizing final report, Texts 38/2011.

UBA – Umweltbundesamt (2017a): Quantifizierung der landwirtschaftlich verursachten Kosten zur Sicherung der Trinkwasserbereitstellung. Environmental research plan of the Federal Ministry of the Environ-ment, Nature protection, Building and Nuclear Safety (BfN), research code 3716 74 263 0 UBA-FB 002511. Texts 43/2017. Authors: Oelmann, M., Czichy, C., Scheele, U., Zaun, S., Dördelmann, O., Harms, E., Penning, M., Kaue, M., Bergmann, A., Steenpass, C.; ISSN 1862-4359

UBA – Federal Environment Institute (eds.) (2017b): Wasserwirtschaft in Deutschland. Grundlagen, Belastungen, Maßnahmen. Umweltbundesamt, Dessau-Roßlau

UBA – Federal Environment Institute (ed.) (2018a): Critical Load Daten für die Berichterstattung 2015-2017 im Rahmen der Zusammenarbeit unter der Genfer Luftreinhaltekonvention (CLRTAP). Texts 60/2018.

UBA – Federal Environment Institute (eds.) (2018b): PINETI-3: Modellierung atmosphärischer Stoffeinträge von 2000 bis 2015 zur Bewertung der ökosystem-spezifischen Gefährdung von Biodiversität durch Luftschadstoffe in Deutschland. Texts 79/2018.

Ulrich, B. (1983): Soil acidity and its relations to acid deposition. In: Effects of Accumulation of Air Pollutants in Forest Ecosystems. Reidel, Dordrecht, Springer: 127–146.

UN - United Nations Conference on Environment and Development (1992): Convention on Biological Diversity (CBD). (3.4.2020)

UNESCO - United Nations Educational, Scientific and Cultural Organization (2015): Water for a Sustainable World. The United Nations World Water Development Report 2015. Paris, UNESCO 2015.

UNESCO - United Nations Educational, Scientific and Cultural Organization (2019): Leaving no one behind. The United Nations World Water Development Report 2019. UNESCO 2019. ISBN 978-92-3-100309-7

Urban Nilsson, G.-Ö. & Hällgren, J.-E. (1996): Competition for water and nutrients between ground vegetation and planted picea abies. New Zealand Journal of Forestry Science 26(1/2): 99-117 (1996).

Venetis, C. (1969): A study on the recession of unconfined aquifers. Inernat. Assoc. o. Scientif. Hydrol. Bulletin, 14:4, 119-125. DOI: http://dx.doi.org/10.1080/02626666909493759

Vestin, P., Mölder, M., Kljun, N., Cai, Z., Hasan, A., Holst, J., Klemedtsson, L., Lindroth, A. (2020): Impacts of Clear Cutting of a Boreal Forest on Carbon Dioxide, Methane and Nitrous Oxide Fluxes. Forests 2020, 11, 961; DOI:10.3390/f11090961

Wagenbrenner, J. W., Robichaud, P. R., Elliot, W. J. (2010): Rill erosion in natural and disturbed forests: 2. Modeling Approaches. Water Resources Research Vol. 46, W10507, DOI:10.1029/2009WR008315

WAGENSCHEIN, D. (2006): Einfluss der Gewässermorphologie auf die Nährstoffretention - Modellstudie am Beispiel der mittleren Weißen Elster. Dissertation, Faculty of Environmental Sciences and Process Engineering at the Brandenburg Technical University, 122 p.

WALTHER, L. GANTHALER, A., MAYR, S., SAURER, M., WALDNER, P., WALSER, M., ZWEIFEL, R., VON ARX, G. (2021): From the comfort zone to crown dieback: Sequence of physiological stress thresholds in mature European beech trees across progressive drought. Science of the Total Environment 753 (2021) 141792. DOI: https://doi.org/10.1016/j.scitotenv.2020.141792

WATSON, B.M., COOPS, N., SELVALINGAM, S. & GHAFOURI, M. (2005): Improved simulation of forest growth for the Soil and Water Assessment Tool (SWAT). In Proceedings of the 3rd International SWAT Conference, 13–15 July 2005, Zurich, Switzerland. Edited by R. Srinivasan, J. Jacobs, D. Day and K. Abbaspour. pp. 142–152.

WATSON, B.M., MCKEOWN, R. A., PUTZ, G. & MACDONALD, J.D. (2008): Modification of SWAT for modelling streamflow from forested watersheds on the Canadian Boreal Plain. J. Environ. Eng. Sci. 7: S145–S159 (2008). Published by NRC Research Press. doi:10.1139/S09-003

WATTENBACH, M., HATTERMANN, F., WENG, R., WECHSUNG, F., KRYSANOVA, V., AND BADECK, F. (2005): A simplified approach to implement forest eco-hydrological properties in regional hydrological modeling. Ecol. Model. 187: 40–59. DOI:10.1016/j.jhydrol.2007.08.005

WEBER, M. (1996): Makrofauna - Waldkalkung. Dissertation University of Mainz.

WEIHE, J. (1968): Niederschlagszurückhaltung durch Wald.- Allgemeine Forstzeitschrift 23, 522-524.

WEISS, A. (1993): Pflege- und Entwicklungsplan Naturpark Pfälzerwald. Verein Naturpark Pfälzerwald e.V. (eds.), Bad Dürkheim, revised version 2002

WIGGERING, H. & MÜLLER, F. (eds) (2003): Umweltziele und Indikatoren. Springer, Berlin, Heidelberg/New York, 670 p.

WILHELM, G.J. & RIEGER, H. (2013): Naturnahe Waldwirtschaft - mit der QD-Strategie. Verlag Eugen Ulmer, ISBN 978-3800178582.

WILLIAMS, J.R. (1969): Flood routing with variable travel time or variable storage coefficients. Trans. ASAE, 12(1): 100–103.

WILLIAMS, J. R., JONES, C. A., KINIRY, J. R., SPANEL, D. A. (1989): The EPIC Crop Growth Model. Transactions of the ASAE. 32(2): 0497-0511. DOI:10.13031/2013.31032

WOHLRAB, B., ERNSTBERGER, H., MEUSER, A., SOKOLLEK, V. (1992): Landschaftswasserhaushalt. Verlag Paul Parey, Hamburg und Berlin. ISBN 3-490-19116-1

YANG, Q. & ZHANG, X. (2016): Improving SWAT for simulating water and carbon fluxes of forest ecosystems. Sci Total Environ, DOI: http://dx.doi.org/10.1016/j.scitotenv.2016.06.238

ZAMBRANO-BIGIARINI, M. (2014): hydroGOF: Goodness-of-fit functions for comparison of simulated and observed hydrological time series. R package version 0.3-8.

ZEMKE, J., ENDERLING, M., KLEIN, A., SKUBSKI, M. (2019): The Influence of Soil Compaction on Runoff Formation. A Case Study Focusing on Skid Trails at Forested Andosol Sites. Geoscience 2019, 9, 204; DOI: https://doi.org/10.3390/geosciences9050204

Zenner, E.K., Fauskee, J.T., Berger, A.L., Puettmann, K.J. (2007): Impacts of Skidding Traffic Intensity on SoilDisturbance, Soil Recovery, and Aspen Regeneration in North Central Minnesota. Society of American Foresters; NORTH. J. APPL. FOR. 24(3) 2007

Zhang, L., Dawes, W.R., Walker, G.R. (2001): Response of mean annual evapotranspiration to vegetation changes at catchment scale. Water Resources Research 37: 701–708.

Table 23:

New curve number (CN) values calculated for the different hydrologic soil groups based the degree of compaction, the soil physical properties, and different land use classes used in SWAT+. For (C2) soil class SS was increased by 58%, SL and SU by 26%, and L by 58%. For (C1) the maximum possible value for the respective land uses and hydrologic soil groups was assumed.

Scenario (C2)	**Hydrological soil group**							
	A		B		C		D	
Land use class	default	new	default	new	default	new	default	new
wood_f	36	57	60	76	73	95	79	95
rc_strow_g	67/	95	78	95	85	95	89	95
urban	98	98	98	98	98	98	98	98
wood_p	45/	71	66	83	77	95	83	95
sg_strow_g	63	95	75	95	83	95	87	95
Scenario (C1)								
wood_f	36	95	60	95	73	95	79	95
rc_strow_g	67	95	78	95	85	95	79	95
urban	98	98	98	98	98	98	98	98
wood_p	45	95	66	95	77	95	87	95
sg_strow	63	95	75	95	83	95	87	95

Table 24:

Key parameters for SWAT+ plant growth, their default and used values, and reference for adaption

Parameter	Adapted value							Reference
	Default	oa	be	spru	doug	pine	mixed*	
Radiation use efficiency [Kg biomass/ ha/(MJ/m^2)]	15	18	18	18	18	18	18	Gower et al. 1999; Garbulsky et al. 2010; Bartelink et al. 1997
Fraction of biomass removed in harvest [unitless]	0.76	0.75	0.75	0.7	0.71	0.61	0.75	Matyssek et al. (2010:283)
Maximum potential leaf area index [m^2/m^2]	5	5.2	6.7	6	8	3.5	6.1	FAWF monitoring data (2020)
Maximum canopy height [m]	6-10	34	38	40	44	32	37.6	Dong Yield charts
Maximum stomatal conductance [m*s-1]	0.002	0.01	0.009	0.005	0.01	0.01	0.008	Hayes & Bangor 2017, p.35, transformation formular: Matyssek & Herrpich 2019, p. 202 (9)
Vapor pressure deficit [kPa]	4	3.1	3.1	3	3	3	3	Hayes & Bangor 2017: 35
Minimum leaf area index [m^2/m^2]	0.75	0	0	5	7	2.5	2.9	FAWF monitoring data (Dr. Greve)
Fraction of biomass converted to residue [unitless]	0.3	0.05	0.05	0.05	0.05	0.05	0.05	Estimation by Dr. Greve from FAWF monitoring data (2020)
Maximum biomass on a stand [tons/ha]	10	185	289	215	215**	113	150	Bartsch & Röhrig 2016, p. 264
Initial root to shoot ration [unitless]	0-0.4	0.29	0.24	0.2	0.2	0.2	0.22	Mokany et al. 2006, p. 91

Table 25:

Comparison between statistical indices for the Hargreaves-Samani method and the Penman-Monteith method, indicating a better model performance in case of Hargreaves-Samani with respect to the objective target issue.

Objective function	Sub-catchment Bobenthal			
	Hargreaves-Samani	**Penman-Monteith**	**Optimum value**	**Description**
KGE	0.86	0.7	1	Goodness of fit measure index, that the bias and variability ratios are not cross-correlated
NSE	0.73	0.51	> 0.8	Goodness of fit between observed and simulated data
PBIAS	-0.3	22.8	0	Average tendency of the simulated values to be larger or smaller than their observed ones
RSR	0.51	0.69	0	Ratio between simulated and observed values to the standard deviation of the observation

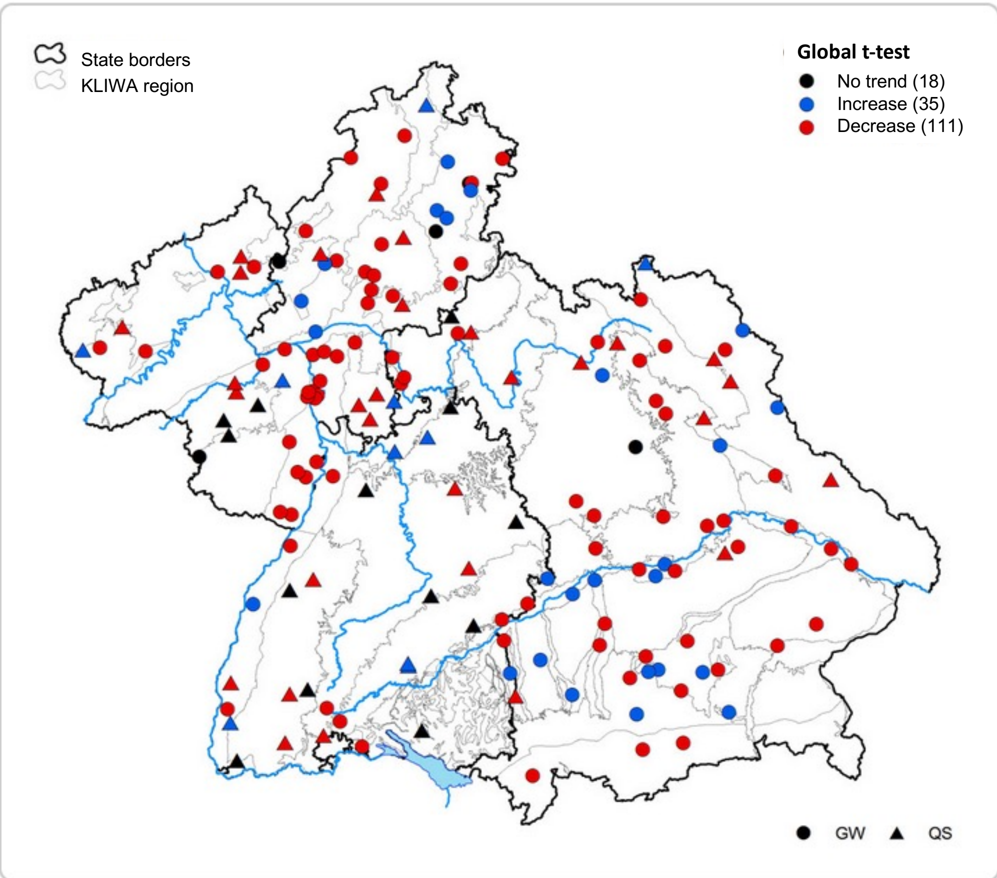

Figure 83: Long-term tendency for decrease in mean groundwater (GW) levels and spring discharges (QS) in the KLIWA region: Rhineland-Palatinate, Hesse, Baden-Württemberg and Bavaria (modified after www.kliwa.de).

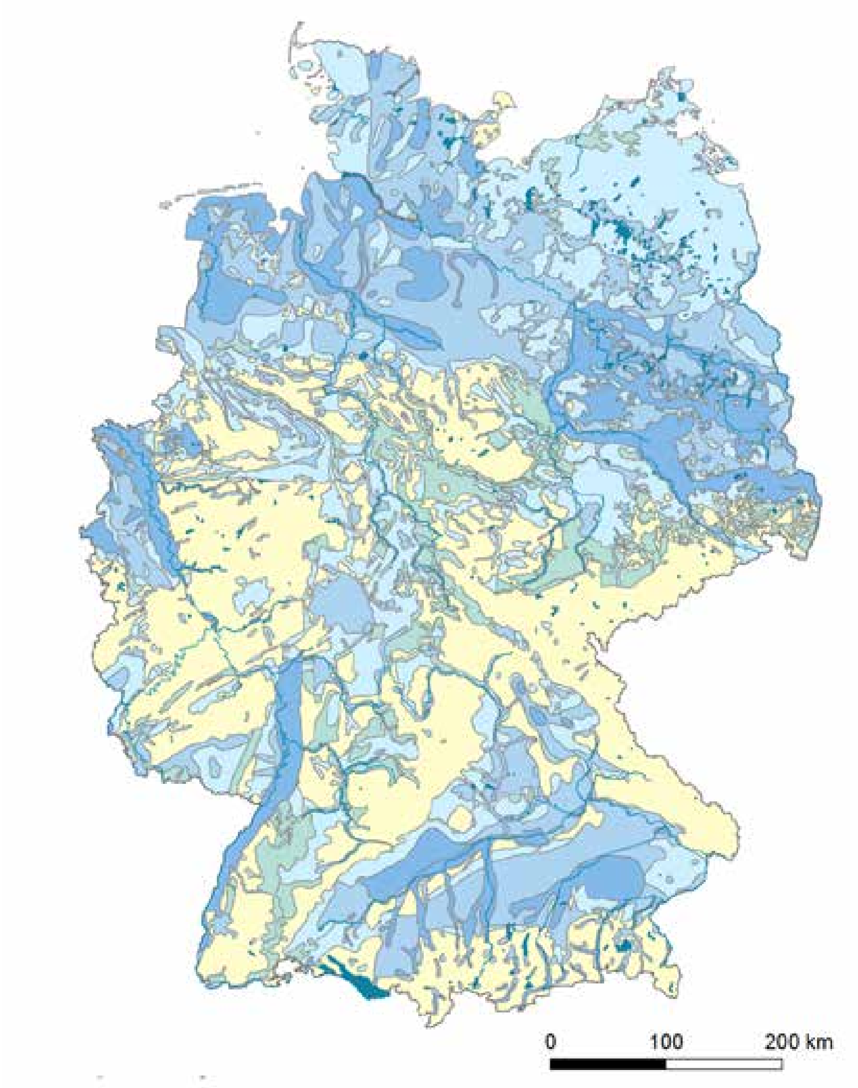

> 40 l/s, 15 – 40 l/s, 5- 15 l/s, > 5 l/s, < 2 l/s (Source: BGR[1], Topography: BKG)

Figure 84: Field of the groundwater resources in Germany.

[1] https://www.bgr.bund.de/DE/Themen/Wasser/grundwasser_deutschland.html

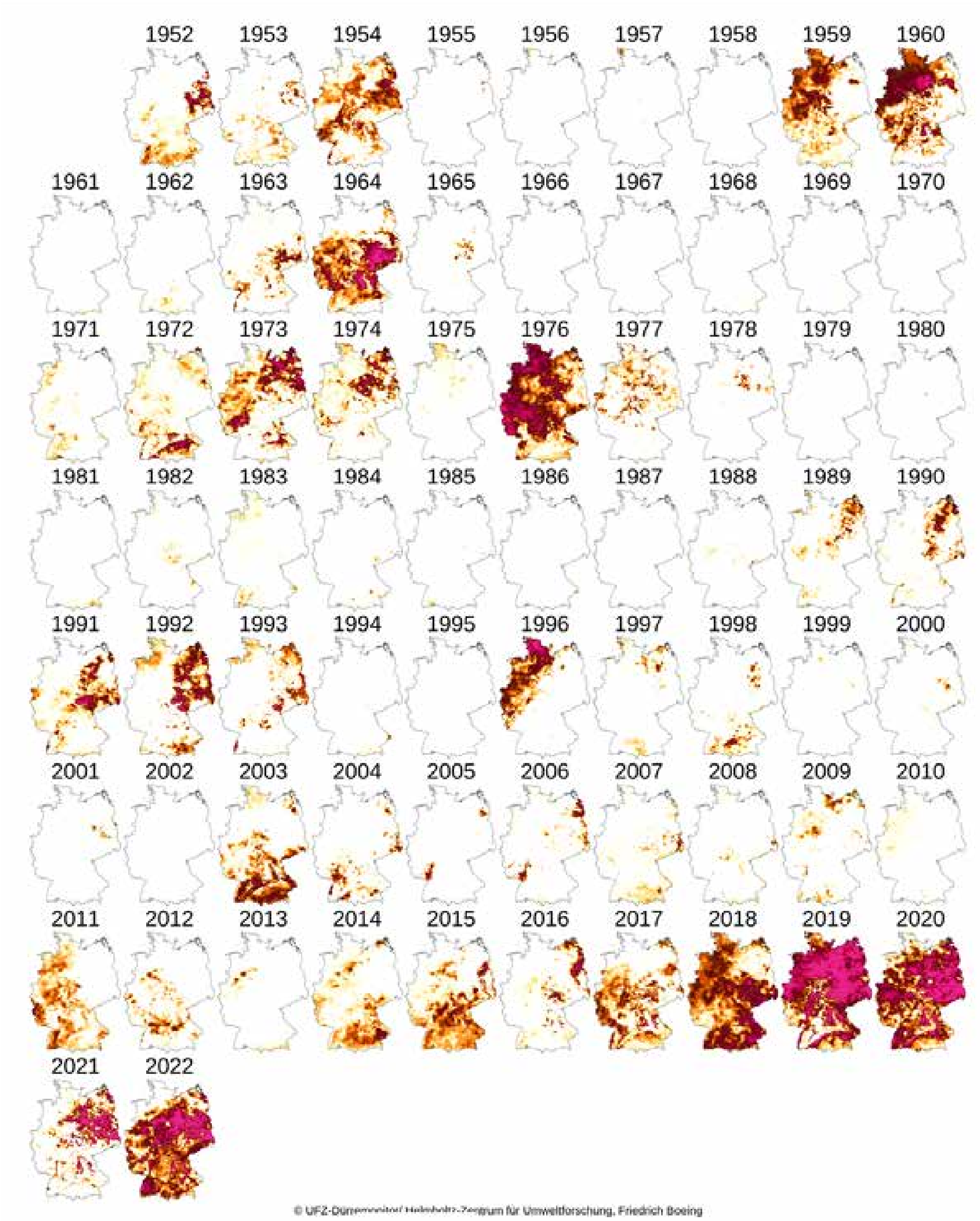

Figure 85: Development of soil moisture conditions in Germany from 1952 to 2020 according to the UFZ drought monitoring program of the Helmholtz Centre of environmental research (Source:, https://www.ufz.de/index.php?de=37937).

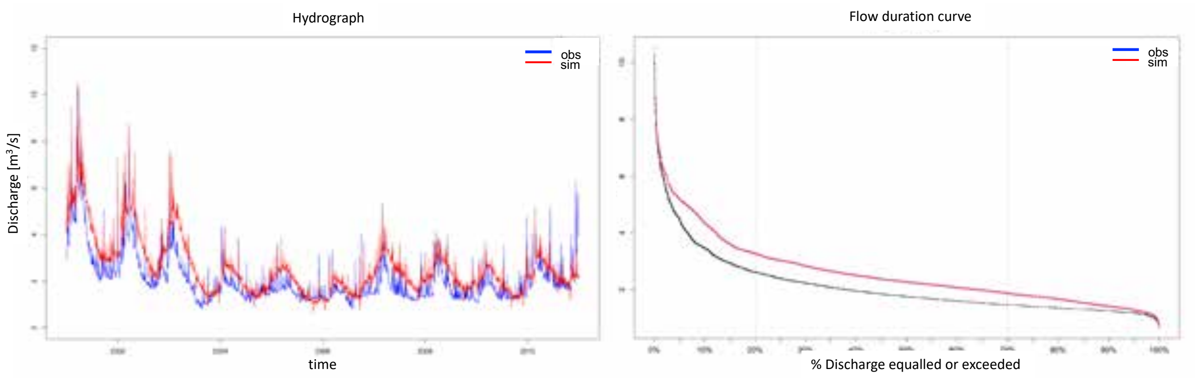

Figure 86: Daily discharge hydrograph (right) and flow duration curve (left) for the best parameter fit using the Penman-Monteith method for calculating evapotranspiration in the sub-catchment Bobenthal. Observed values (obs, blue/black), and simulated values (sim, red) do not match sufficiently enough compared to the Hargreaves method.

Eva Verena Müller
Master of Science *Umweltschutz*
Master of Arts *Darstellende Kunst*

CURRICULUM VITAE

Eva Verena Müller
* 1979 in Darmstadt
Primary School
Schillerschule Darmstadt 1986-1990
Abitur/High School graduation 1999
Justus-Liebig-Gymnasium Darmstadt
Academic studies:
Folkwang Hochschule Essen 2000 - 2004:
Performing art, degree: Diploma
M.A. Perfroming Arts
University of Rostock 2014 - 2017:
Masters correspondence course environmental science
Degree: *Master of Science (M.Sc.)*
University of Trier 2019-2022:
Doctoral Studies. Institute of spatial and environmental science. Degree: *Doctor of Natural Science (Dr. rer. nat)*

Work history

2001 - 2017	**Actress**. Engagements at different theatres in Germany: Düsseldorf, Bonn, Leipzig, Berlin, Dortmund. Engagements at cinema and television productions and radio. For further information visit: www.thomas-wernicke.eu. Different national and international Moderations.
2017	**Graduation Master of Science** at the University of Rostock, department landscape planning and ecology, title: „holistic assessment of ecosystem services of suspended peatlands in the example of Hunsrück-Moore".
2018	**Practical training** at the environmental planning office ecotone Dortmund. Specialized direction: Faunistic mapping for environmental assessments.
2019 -2021	**Doctoral Position** at the research institute of forest ecology and forestry (FAWF) in Trippstadt/Germany appointed to the EU-Project Ecoserv
2022	**Graduation Doctor of Natural Science** (Dr. rer. nat.) at the University of Trier, department of environmental science, title: "Analysis of forest-specific ecosystem services with regard to water balance components: runoff and groundwater recharge in the forest".
2022	**Permanent Employment** at the research institute of forest ecology and forestry (FAWF) in Trippstadt/Germany, department Environmental Precaution – Forest and Water.

Publications

2018	„Holistische Bewertung der Ökosystemleistungen renaturierter Hangmoore - Eine Analyse am Beispiel der Hunsrück- Moore", scientific journal Natur- und Landschaftsplanung (NuL) 08-2018, p. 278.285